Diffusion and Advection of Radionuclides through a Cementitious Backfill with Potential to be used in the Deep Disposal of Nuclear Waste

by

John Hinchliff

Doctoral Thesis

Submitted in partial fulfillment of the requirements
for the award of

Doctor of Philosophy of Loughborough University

March 2015

ABSTRACT

This work focuses on diffusion and advection through cementitious media, the work arises from two research contracts undertaken at Loughborough University: “Experiments to Demonstrate Chemical Containment” funded by UK NDA and the “SKIN” project, funded by the European Atomic Energy Community's Seventh Framework Programme.

Diffusion will be one of the most significant mechanisms controlling any radionuclide migration from a nuclear waste, deep geological disposal facility. Advection may also occur, particularly as the immediate post closure groundwater rebound and equilibration proceeds but is expected to be limited by effective siting and management during the operational phase of the facility. In this work advection is investigated at laboratory scale as a possible shorter timescale technique for providing insight into the much slower process of diffusion.

Radial techniques for diffusion and advection have been developed and the developmental process is presented in some detail. Both techniques use a cylindrical sample geometry that allows the radionuclide of interest to be introduced into a core drilled through the centre of the test material. For diffusion the core is sealed and submerged in a container of receiving solution which is sampled and analysed as the radionuclide diffuses into it. For advection, a cell has been designed that allows inflow via the central core to pass through the sample in a radial manner and be collected as it exits from the outer surface. The radionuclide of interest can be injected directly into the central core without significant disturbance to the advective flow. Minor improvements continue to be made but both techniques have provided good quality, reproducible results.

The majority of the work is concentrated on a potential cemetitious backfill known as NRVB (Nirex Reference Vault Backfill) this is a high porosity, high calcium carbonate content cementitious material. The radioisotopes used in this work are ^{3}H (in tritiated water), ^{137}Cs, ^{125}I, ^{90}Sr, ^{45}Ca, ^{63}Ni, ^{152}Eu, ^{241}Am along with U and Th salts. In addition the effect of cellulose degradation products (CDP) on radioisotope mobility was investigated by manufacturing solutions where paper tissues were degraded in water, at 80ºC, in the absence of air and at high pH due to the presence of the components of NRVB. All diffusion experiments were carried out under a nitrogen

atmosphere. All advection experiments were undertaken using an eluent reservoir pressurised with nitrogen where the system remained closed up to the point of final sample collection.

Results for tritiated water and the monovalent ions of Cs and I were produced on a timescale of weeks to months for both diffusion and advection. The divalent ions of Sr, Ca and Ni produced results on a timescale of months to years.

Variations of the experiments were undertaken using the CDP solutions. The effects of CDP were much more apparent at radiotracer concentration than the much higher radiotracer with non-active carrier, concentration. In the presence of CDP Cs, I and Ni were found to migrate more quickly; Sr and Ca were found to migrate more slowly. Additional Sr experiments were undertaken at elevated ionic strength to evaluate the effect of the higher dissolved solids content of the CDP solutions.

Some of the results for HTO, Cs, I and Sr have been modelled using a simple numerical representation of the system in GoldSim to estimate effective diffusivity and partition coefficient. The diffusion model successfully produced outputs that were comparable to literature values. The advection model is not yet producing good matches with the observed data but it continues to be developed and more processes will be added as new results become available.

Autoradiography has been used to visualise the radionuclide migration and several images are reproduced that show the fate of the radiotracers retained on the NRVB at the end of the experiments.

As the experimental programme progressed it was clear that results could not be produced in a suitable timescale for Eu, Am U and Th. These experiments have been retained and will be monitored every six months until either diffusion is detected or the volume of receiving liquid is inadequate to ensure the NRVB is saturated.

Acknowledgements

First and foremost I want to thank my beautiful wife Julie for support not only when I needed it most but all of the time, I could not have completed this without her and I love her with all my heart. Also, to our lovely daughters, Jemma and Janna whose lives have brought me immense pleasure and pride.

I must also express my gratitude to my Mum and late Father for bringing me into the world and encouraging me to be the person I wanted to be. A special thank you to my little sister Christine, who helped in her own special way at the time when I became concerned about how I might make this whole endeavour a reality.

I feel indebted to Peter Warwick and Nick Evans for having sufficient faith in me to believe that I could make a success of returning to a research environment for the first time in over 25 years. Once I got started Nick was a great supervisor along with our “new Prof” David Read who proved to be a valuable source of support and intelligent intervention.

My most important friend and colleague, in the laboratory and office was Monica Felipe-Sotelo, I remain very grateful for her help, advice and ideas. My old friend, David Drury from Golder Associates must be mentioned as he provided the horsepower for the modelling, making it look easy whilst working very hard.

I’ve had some great times in the laboratory with a bunch of new and for the most part, much younger friends, including Mei Chew, Amy Young, Stephen Pendleton, Larry Anjolaya, Hanna Tuovinen, Joan Sutherland, Julie Turner, Sneh Jain, James Holt, Ollie Preedy, Hayley Gillings, Matt Isaacs, Darren Huxtable, Frank Dal Molin and of course Ricky Hallam who coaxed me into the laboratory to get me started. When I think back, I will remember smiling a lot.

I want to acknowledge the help, input and cheerful support of Steve Williams and Rebecca Beard at the NDA, Tony Milodowski from BGS and Felix Brandt from Jeulich who looked after my contributions to the SKIN project. Finally, I’m grateful to Jan Tits of PSI whose comments caused me to look more critically at some aspects of the work and improved my overall understanding as a consequence.

Contents

List of Figures

List of Tables Appearing in the Main Text

1.0 Introduction

This work arises from two research contracts:

> Experiments to Demonstrate Chemical Containment – (UK NDA contract number NPO004404).

And:

> Slow Processes in Close to Equilibrium Conditions for Radionuclides in Water/Solid Systems of Relevance to Nuclear Waste Management (the "SKIN" project), as part of the European Atomic Energy Community's Seventh Framework Programme (FP7/2007-2011).

Both of the contracts seek in part, to address the practicality, functionality and reliability of cementitious chemical barriers in the development of geological disposal facilities (GDF) for nuclear industry waste. In addition the associated experimental programmes are expected to provide useful data for GDF performance assessment models and calculations.

The technical and political background to this research is detailed in sections 2.0 to 4.0. It is important to recognise that the development of radial diffusion and advection techniques to study radionuclide mobility in cementitious media was a significant component of this research. Sections 5.0 and 6.0 describe the development and early trials in detail. Section 7.0 provides information about the conceptualisation of the radial systems in preparation for numerical modelling and gives details of the diffusion and advection models used. Section 8.0 describes the autoradiography technique used to visualise the migration and fate of the radionuclides. Useful background data is gathered together and reported in section 9.0. Individual sections are then dedicated to each radionuclide where results could be obtained on a timescale of a few months to a few years. The nature of the research meant that an iterative and oppportunistic approach to the experimentation was adopted to provide an adequate range of interesting results. The disadvantage with this type of approach was that some experiments were missed out and complete datasets are not always available.

The research reported herein is best envisaged as a short term window on a long term experimental programme. It is clear that some experiments can only produce results on timescales exceeding the duration of a PhD study and that the extended duration of the experimental programme must be acknowledged when reading this work. The full set will be completed over time. Where experiments remain ongoing, they are detailed in section 16.0. Conclusions are presented in section 17.0 and recommendations for future work are given in section 18.0.

2.0 Background

The UK nuclear industry has generated radioactive waste since the 1940s, initially from defence sector activities associated with developing a nuclear deterrent and subsequently from the generation of electricity using nuclear reactors. It should be remembered that until the late twentieth century the nuclear industry in the UK was almost totally confined to the public sector and attempts to deal with the waste generated by the industry somewhat subject to political influence. Governments have come and gone and various initiatives to give the industry a future and deal with the legacy of accumulated waste and outdated infrastructure have failed to successfully address the problems.[1]

The last serious attempt to develop a long term solution, the Nirex (Nuclear Industry Research Executive) Sellafield site investigations of the late 1980 and 1990s was terminated in 1997. The termination was assured when an appeal against the planning application refusal for an underground laboratory (also known as a rock characterisation facility or RCF) was dismissed following a Public Inquiry [2].

The detailed reasons for refusal will not be reproduced here but after linking the RCF development to any future GDF development, several technical issues pertinent to the GDF were highlighted in the conclusions of the Planning Inspector's report. The concept of "chemical containment" is mentioned twice:

"…I consider that Nirex's emphasis on the relatively novel chemical containment concept in the mixed artificial and natural barrier suggests a lack of confidence in the geosphere."

And,

"The last assessment published in 1995 assumes that the artificial chemical barrier would have a very significant retarding effect on release of the longer-lived radionuclides from the repository, and yet the barrier is new and untried and the assumptions in the assessment entail great simplifications and may be non-conservative."

One of the proposed components of the artificial chemical barrier to which the above statements refer is a cementitious backfill material known as NRVB (Nirex Reference Vault Backfill).[3] Effective testing of this backfill and its containment capability for a series of radionuclides are together the focus of the majority of this PhD thesis.

The Inspector's comments provided impetus for research into the potential function of chemical barriers and whether they could be practically realised. These points are stressed here because they articulate a significant part of the motivation for the detailed research activities and results presented herein and initiated the current UK research effort in this area.

It is important to be aware of the political dimension and its impact when undertaking any technical or scientific work in the nuclear sector. This was keenly observed by the technical assessor for the previously mentioned Public Inquiry; Colin Knipe, who belatedly made the following comment which is clear in its inference that the political considerations outweighed the financial and technical issues:[4]

"Early in 1997 John Gummer, Secretary of State for the Environment, formally rejected the Appeal. More than 10 years of work and several hundred million pounds of research, investigations and planning by Nirex were frustrated and the future of nuclear waste disposal in the UK thrown into confusion."

Whatever the reality of the situation it was clear that a new approach able to bring on board politicians and the public would be needed if an effective solution was to be successfully developed.

The House of Lord's Review in 1999 acknowledged the technical and scientific shortcomings of the previous attempts to deal with radioactive waste disposal and stated that the absence of stakeholder engagement as a major consideration must be addressed if any future plans were to succeed.[5] Or perhaps more bluntly, the failure to engage the wider public in a positive (or at least not a negative) way, has resulted in politicians being unable to support their own or their predecessors' initiatives.[6]

In 2001 a new programme of policies – Managing Radioactive Waste Safely (MRWS) – was launched by the government. [7] The aims were stated as:

"…*provide long term protection to people and the environment; based on sound science, value for money and above all an approach which would be open and transparent to inspire public confidence*."

The use of the term *"sound science"* should be viewed as a government commitment to undertaking the required research and development and moving to a technically viable solution. It also implied that previous attempts to deal with the issue may not have been entirely based on sound science.

This was followed in July 2002 by a Department of Trade and Industry (DTI) White Paper entitled Managing the Nuclear Legacy which laid out a strategy for action with suggested timescales.[8]

The following year (July 2003), as part of the MRWS programme, what remained of Nirex published a technical note recommending that GDF site selection and investigations progress in a stepwise and iterative manner.[9] In the same year the Committee on Radioactive Waste Management (CoRWM) was established with a wide ranging brief to review and make preliminary assessments of all nuclear industry waste management options. Within two years of commencement, CoRWM was being criticised by the House of Lords Science and Technology Committee noting that: [10]

"…we are astonished that the Committee [CoRWM} should have been told to set about this task with a blank sheet of paper"

And in relation to the scientific, technical and engineering skills possessed by members of CoRWM,

"With the greatest respect to the members of CoRWM, who possess expertise in many areas, we do not feel that these essential skills are adequately represented within CoRWM".

Despite this criticism which reflected the ever present desire to revert to the tried and failed methods of the past, CoRWM set about delivering its remit.

All management options for radioactive waste were considered and there was successful engagement of the public and interested parties. In 2004 (prior to the criticism highlighted above), CoRWM published a “Long List of Options” [11] and commenced an extensive programme of consultation including public meetings throughout the country to arrive at the following short list of four options, presented to government in July 2006.[12]

- long-term interim storage.
- near-surface disposal of short-lived wastes.
- deep geological disposal.
- phased deep geological disposal.

An important feature of the long list was the consideration and dismissal of options such as disposal in space and disposal at sea, that were considered technically unacceptable but widely believed to be realistic in the wider community accustomed to reading scare stories in the media. These issues of perception and stakeholder interest have been the subject of much discussion in the relevant literature and their importance was eventually recognised by Nirex in 2002 [13] and further expanded upon by CoRWM in 2011 as a result of the experience gained from the public consultations.[14]

In October 2006 the government accepted CoRWM’s recommendation that geological disposal coupled with safe and secure interim storage should be the long-term management option for the UK’s higher activity wastes.[15]

It is worth noting that the current (2014) membership of CoRWM has significantly greater scientific, technical and engineering representation than its original incarnation. The change of emphasis reflecting the shift to assessment and evaluation of the selected option.[16]

The Nuclear Decommissioning Authority (NDA) was created in 2005 [17] to take responsibility for legacy issues including infrastructure decommissioning and was also given responsibility for funding, planning and implementing geological disposal. The current government, as did its predecessor, remains committed to the NDA and an approach based on stakeholder willingness to participate.

Bringing this summary up to date; in 2007 the government held a public consultation on a framework for implementing geological disposal and in June 2008 published, Managing Radioactive Waste Safely: A framework for implementing geological disposal.[1] This was supported by CoRWM in its review published in June 2008.[18] In October 2009, the Joint Research Centre of the European Commission published its report "Geological Disposal of Radioactive Waste: Moving Towards Implementation". It concluded; "Our scientific understanding of the processes relevant for geological disposal is developed well enough to proceed with step-wise implementation."[19]

Questions about the concept, practicality, functionality and reliability of a chemical barrier remained and additional research was required. Consequently, in 2009 Loughborough University was commissioned by NDA as part of its research programme, [20] to undertake a series of experiments to demonstrate chemical containment. The results of several of the experiments investigating the migration behaviour of Cs, I, Th, U, Ni and Eu through the potential backfill material NRVB form a significant part of this thesis. The EU, using funding from the SKIN project, as part of the European Atomic Energy Community's Seventh Framework Programme (FP7/2007-2011) also commissioned Loughborough University to undertake a series of similar experiments investigating the migration behaviour and slow kinetics of Sr, Am, Ca, Eu and Se in cementitious media. The currently available results from the SKIN experiments make up the remainder of this thesis.

In the course of this research NRVB samples have been subjected to diffusion and advective flows similar to and exceeding those likely to be experienced within the GDF near field under hydrogeologically equilibrated and equilibrating conditions. Individual processes including solubility, sorption, precipitation and incorporation have also been considered. The behaviour of the range of radionuclides was observed, increasing the understanding and predictability of migration rates and mechanisms. It is recognised that some of the experiments will require extended timescales, inevitably exceeding the duration of a PhD study.

The NDA is currently engaged in the preparatory work and planning the work programme whilst setting up the management infrastructure to deliver it. [12] In March 2010 it published "Geological Disposal: Steps Towards Implementation" which provides information about the variants of geological disposal available to the UK and likely developmental scenarios.

The political process in which the NDA is engaged is not the subject of this thesis but it continues to be a significant influence on overall timescales and direction. Most recently, the Cumbria County Council decision (January 2013) to reject plans to find a suitable site within the County only served to reiterate the point.[21]

3.0 Geological Disposal Facilities

The section provides a brief description of GDFs, outlining the main issues and criteria requiring consideration, from initial concepts to realisation. As stated in section 2.0, political considerations and stakeholder issues are major concerns but they are not the focus of this thesis and will not be discussed further.

When considering the technical aspects of GDFs the important issues are the: [22] [23]

- amount of radioactive waste requiring geological disposal;
- types of rock that potentially could host a facility; and
- potential geological disposal concepts.

These three issues are discussed in more detail below.

3.1 The Waste Requiring Disposal

3.1.1 Waste types

The following are the relevant UK definitions: [24] [25]

Very low level waste (VLLW): is a subset of LLW, formally defined such that each 0.1 m^3 contains less than 400 kBq of beta/gamma activity or single items contain less than 40kBq of beta/gamma activity enabling it to be safely disposed with ordinary refuse. No alpha emitting waste is permitted to be disposed as VLLW.
Low level Waste (LLW): is higher than VLLW but below 4 kBq g^{-1} of alpha or 12 kBq g^{-1} of beta/gamma nuclides**.**
Intermediate level waste (ILW): is more active than the LLW limits but does not meet the heat generating criteria required to be classified as high level waste.
High level waste (HLW): generates heat so that it must be cooled, spent nuclear fuel is HLW.

3.1.2 Waste quantities

The current NDA estimate of the inventory of radioactive waste eventually requiring disposal is shown in table 3.1 below and is usually referred to as “the baseline inventory as at 1 April 2007 comprising the following radioactive wastes and materials”.[26]

Materials	Notes	Packaged volume		Radioactivity (1.4.2040)	
		m^3	%	TBq	%
High Level Waste (HLW)	1, 2, 3, 5	1,400	0.30%	36,000,000	41.30%
Intermediate Level Waste (ILW)	1, 2, 5	364,000	76.30%	2,200,000	2.50%
Low Level Waste (not for Low Level Waste Repository) (LLW)	1, 2, 5	17,000	3.60%	<100	0.00%
Spent nuclear fuel	1, 4, 5	11,200	2.30%	45,000,000	51.60%
Plutonium	1, 4, 5	3,300	0.70%	4,000,000	4.60%
Uranium	1, 4, 5	80,000	16.80%	3,000	0.00%
Total		**476,900**	100%	**87,200,000**	100%

Table 3.1 Estimate of radioactive waste eventually requiring disposal

Notes to Table 3.1

1. Quantities of radioactive materials and wastes are consistent with the 2007 UK Radioactive Waste Inventory (UKRWI).

2. Packaging assumptions for HLW, ILW and LLW not suitable for disposal at the existing national LLWR are taken from the 2007 UKRWI. Note that they may change in the future.

3. The HLW packaged volume may increase when the facility for disposing the canisters, in which the vitrified HLW is currently stored, has been implemented.

4. Packaging assumptions for plutonium, uranium and spent nuclear fuels are taken from the 2005 CoRWM Baseline Inventory. Note that they may change in the future.

5. Radioactivity data for wastes and materials was derived using the 2007 UK Radioactive Waste Inventory. 2040 is the assumed start date for the geological disposal facility.

6. It should be noted that at present the Baseline Inventory is based on UK Inventory figures, and as such, currently contains waste expected to be managed under the Scottish Executive's policy of interim near-surface, near-site storage as announced on 25 June 2007.

The figures in table 3.1 should be seen as estimates based on current assumptions about existing waste quantities. If a new generation of nuclear power stations were to be constructed in the UK additional waste to that documented above would result. The current UK NDA plans for a GDF concentrate on disposal of the comparatively large volume of ILW.

3.1.3 The Presence of Cellulose and its Degradation Products in the Waste

UK radioactive waste inventory [26] estimates that current mass of cellulosic material within ILW is 2000 tonnes and within LLW, between 100,000 and 125,000 tonnes. The w/w content of cellulosic materials in ILW and LLW were given as 0.7 % and 2 - 2.5%, respectively. The total load of other organics for both ILW and LLW was estimated at 36,200 tonnes within a total of some 5,000,000 tonnes requiring disposal. The cellulose will degrade under GDF conditions [27] and previous work has shown that the cellulose degradation products (CDP) have the potential to affect cementitious materials and the mobility of some species present in the waste.

These effects include solubility enhancement by complexation, influence on the sorption to the cement and rate of incorporation; [28] modification of the ionic strength of the pore water by complexing metals from the cement and the consequent acceleration of its structural degradation.[29]

In the current literature much of the attention regarding the effect of CDP has been focussed on iso-saccharinic acid even though other short chain carboxylic acids in the mixture are often present at higher concentrations. Moreover, in previous work carried out by the Loughborough group [30] when the effect on the solubility of Th was compared for CDP mixtures and solutions of ISA of equivalent concentration, the effect of the CDP mixture was almost 50 times higher than ISA. This suggests that mobilisation is dependent on more than one component of the CDP mixture. Reference is made, where relevant, to more specific literature in later sections.

NDA, being familiar with the work already undertaken on ISA wanted to investigate more realistic scenarios as the formulation and selection of a suitable backfill medium must progress. NDA requested that the study of the effect of CDP on diffusion should be carried out in organic mixtures that reflect in a realistic way the compositions of the cellulose degradation products in solution, instead of focussing on only one of them, i.e. ISA. The amount of cellulosic material used in these studies (see section 9.2) is a realistic representation of the load expected in the UK inventory.

3.2 The Rock Types

Even if generous allowance was made for the spacing of waste packages, the volumes of waste for disposal detailed in the table are not significant in construction terms. A UK GDF, assuming no disposal of HLW or spent fuel, will be to all intents and purposes, a small underground mining and backfilling operation. Technologies to mine all rock types are highly developed and available now.

The rock types under consideration fall into 3 generic categories: [16 31]

Higher strength or crystalline rocks: e.g. basalt and granite, having low matrix permeability and any water flow that occurs is via fractures in the rock mass. The Finnish and Swedish disposal programmes plan to construct GDFs in this type of host rock.

Lower strength sedimentary rocks: e.g. clays and mudstones having physically uniform structures, low permeability and low fracture frequency, water flow occurs through the whole structure. The Swiss GDF design will utilise this type of rock.

Evaporites: e.g. Halite, having no available water except that trapped in the structure at formation and saturated with respect to the composition of the rock mass, water flow is undetectable. Evaporite mines exhibit “creep” where the rock appears to flow and close mine openings on a timescale of decades. This property could be useful in ensuring a “natural closure” of a GDF. It is important to note that evaporites are usually very soluble in water so hydrogeological and hydrological isolation is a prerequisite if this rock type is to be used. The Waste Isolation Pilot Plant in New Mexico, US where waste has been disposed for more than a decade is constructed in this type of rock.

In the absence of a selected site it is not currently possible to assign a rock type for the UK GDF. It is worth noting that the Nirex site investigations at Sellafield in the 1990s targeted the high strength, crystalline Borrowdale Volcanic geological sequence.

3.3 Geological Disposal Concepts – The Multi Barrier Approach

A range of disposal concepts or ideas needs to be considered in relation to the potential geological settings. However it is anticipated that all concepts will utilise a multi barrier approach and the UK is no exception as it develops its GDF concept.[18] The multi barrier approach uses natural and engineered barriers to prevent radioactive releases to the environment in amounts that could cause harm.

The individual barriers under consideration in the UK disposal concept are summarised below: [23 24 32 33]

The waste form: The waste is conditioned into a chemical and/or physical form to make it suitable for disposal; examples of conditioning include super-compaction of low density wastes and vitrification of high-level waste.

The waste container: The conditioned waste (conditioning is often simply mixing and sealing with cemetitious grouts) is located in the waste container to form the waste package which must have sufficient strength and corrosion resistance to safely contain the waste during its storage and transit to the GDF. The material and design of the container must also provide reliable long term physical containment within the GDF.

The buffer or backfill: When waste packages have been placed underground in a disposal facility, they will eventually be surrounded with buffer or backfill materials which will provide physical support and chemical protection of the waste container, and chemical containment of the long lived radionuclides.

Mass backfill: Access tunnels and shafts will be filled in with mass backfill which is required to ensure the integrity of the engineered barriers, prevent collapse of the access ways and potentially control groundwater flow.

Sealing systems: Engineered seals could be used to prevent or control the flow of fluids through more permeable zones within the rock.

Geology: The barriers outlined above are all engineered but the geology must also be correctly selected to act as a barrier. It may limit liquid and gas flow through and around the GDF which will in turn limit the movement of radionuclides towards the

ground surface. The nature of the cover rocks and near surface hydrogeology will be important over the very long term affording protection from human intrusion and dilution and dispersion of any leakage that may occur.

A number of descriptive terms for the zones of the GDF are in general use and will be used in this report:

Near Field: is the zone within the confines of the GDF and includes all areas where waste is stored.

Excavation disturbed zone: is defined as the region beyond the excavation boundary where the physical, mechanical and hydraulic properties of the rock mass have been significantly affected as result of the excavation and redistribution of stresses.

Alkaline disturbed zone: applies to GDFs that use cementitious packaging and backfills and is the zone where pH is raised due to leaching from highly alkaline cements.

Far Field – Is the zone beyond the alkaline disturbed zone which is within the theoretical range of potential impact of migration from the GDF but where “normal” environmental conditions are expected to prevail.

The research presented here concentrates on the GDF near field, excavation disturbed zone and alkali disturbed zone. Specifically, the potential backfill and buffer material NRVB: that may also be used as the mass backfill is investigated. Occasional reference will be made to similar experiments using a 3:1, PFA:OPC packaging grout also being undertaken in the Loughborough laboratory.

4.0 Cement and Concrete

4.1 History

This section provides a brief summary of the history and chemistry of cement and concrete, it concludes with a more detailed description of NRVB noting how its components are intended to create a cementitious material potentially suitable for use as a GDF backfill.

Concrete has been manufactured and used in construction since at least 2500 BC and there is evidence that it was extensively used by the Greeks and early Romans. The concretes developed by these civilizations used either roasted limestone or gypsum as a starting material which could be mixed with sand and water to create mortars to fix stonework or act as cheap structural fillers in conjunction with coarse rocks. Concrete was to become the dominant technology in Roman buildings due to a number of developments including the discovery that the addition of volcanic ash created a material that would continue to harden in wet conditions and even underwater. This simple addition to the basic “recipe” allowed concrete to be used in wet ground to construct the foundations for bridges, aqueducts, harbours and large scale buildings.[34]

The main cement used in the modern construction industry is Ordinary Portland Cement (OPC) which is made by roasting a mixture of limestone and clay at temperatures between 1400-1500°C. The resulting material is known as clinker which is ground to a fine dust with the addition of small amounts of gypsum (to control the speed of setting) prior to sale and use.[35]

It is important to differentiate between the two terms cement and concrete. Cement is the binder and concrete is the result of mixing cement with other materials including rocks, stones and pebbles and/or fillers such as various grades of sand (from coarse to fine), blast furnace slag (BFS), pulverized fuel ash (PFA) or calcium carbonate. These materials are collectively referred to as aggregates.[36] [37] Modern concretes may also utilize a range of additives developed to affect the speed of setting, chemical resistance and strength, dependent upon specific applications.

The term “grout” in the context of this research is applied to concretes that are made using fine particle size fillers, including but not limited to fine sand, limestone flour, PFA or ground BFS.

It is important to be aware that the composition of OPC will vary dependent on the sources of limestone, clay and gypsum and the type of fuel used in its manufacture. It should also be noted that since 2004 cement manufacturers have been permitted by implementation of European Standard EN197-1 to add up to 5% “minor constituents” which can include PFA, to the clinker in an effort to reduce overall energy consumption. In addition Sn II salts can be added to chemically reduce the hazardous content of Cr VI to Cr III. [38]

4.2 Chemistry

Whilst it is true that cements and concretes have been used as construction materials for thousands of years, the chemistry involved is complex and despite the attention of many scientists it remains a subject of current research. This is partly because of the continuous flow of new uses and formulations and partly because small variations in the chemistry can have significant consequences on the physico-chemical properties and quality of the final product. [34 36]

It is clear from the number of textbooks and scientific literature available that a great deal of chemical knowledge about what happens when water is added to OPC has already been accumulated.

The relatively complex nature of the individual chemical compounds present in OPC has resulted in a notation convention being developed to simplify equations and communication, in addition the method of expressing elements as oxides used in geochemistry is often adopted. Tables 4.1 and 4.2 below provide the keys to the notation and the main compounds of interest expressed in the available conventions. It is common to refer to the hydrated calcium silicates as CSH gels or gel phases providing both a simplification of the overall composition and inference that the waters of crystallisation may be loosely bound.[34]

Oxide form	Notation
CaO	C
SiO_2	S
Al_2O_3	A
Fe_2O_3	F
SO_3/SO_4	$\bar{S}$
H_2O	H

Table 4.1 Cement nomenclature [36]

Chemical Name	Chemical Formula	Oxide Formula	Cement Notation	Mineral Name
Tricalcium Silicate	Ca_3SiO_5	$3CaO.SiO_2$	C_3S	Alite
Dicalcium Silicate	Ca_2SiO_4	$2CaO.SiO_2$	C_2S	Belite
Tricalcium Aluminate	$Ca_3Al_2O_6$	$3CaO.Al_2O_3$	C_3A	Aluminate
Tetracalcium Aluminoferrite	Ca_4AlFeO_5	$4CaO.Al_2O_3.Fe_2O_3$	C_4AF	Ferrite
Calcium hydroxide	$Ca(OH)_2$	$CaO.H_2O$	CH	Portlandite
Calcium oxide	CaO	CaO	C	Lime

Table 4.2 Main mineral phases of interest [36]

In addition oxides of magnesium are abbreviated to M and oxides of sodium to N. Clearly the miscellany of expressions used to clarify communication is not entirely successful; in particular, care must be taken not to confuse calcium and carbon, hydrogen and water, silicon and sulphur, iron and fluorine.

The main reaction occurring is hydration of the metal oxide silicates formed in the roasting stage of production. The solid particles are finely divided and the solubility of individual particles ranges from highly soluble alkali metal hydroxides to sparingly soluble calcium sulphate. The majority of the mass usually comprises four anhydrous metal oxide silicates (the first four entries in table 4.2 above) which begin to hydrate on contact with water. The hydration of the mixture gives rise to a series of significantly hydrated compounds often termed gels, phases or even gel phases with structures identical to minerals found in geology. Indeed the mineral names are often

used to describe individual phases and as a consequence, these have also been provided in table 4.2 above.

About 90-95% of an OPC comprises the four compounds, C_3S, C_2S, C_3A, and C_4AF, with the remainder being calcium sulphate, alkali sulphates, CaO and MgO; trace metal concentrations will vary dependent upon the source of raw materials. The four most prevalent compounds exhibit different behaviour during the hydration process. C_3S and C_2S generate the main beneficial hydration product, C-S-H gel. C_3S hydrates more quickly than C_2S and contributes most significantly to early strength development. C_3A and C_4AF also hydrate, but the products formed are not significant in short or long term development of strength or chemical resistance. It is uneconomic to separate C_3A and C_4AF.[34]

Tricalcium Silicate (C_3S)

C_3S is the most abundant compound in OPC, occupying 40–70 wt% of the cement; it is also the most important. Pure C_3S has three possible crystal structures. Below 980˚C the equilibrium structure is triclinic, between 980˚C – 1070˚C the structure is monoclinic, and above 1070˚C it is rhombohedral. The high temperatures of production mean that these structures can all be present in OPC but variation of the composition does not lead to significant differences in reactivity with water. The important feature of the structure and cause of the rapid reaction with water is the asymmetric packing of the calcium and oxygen ions which leaves holes in the crystal lattice.

The C_3S also contains about 3-4% of oxides other than CaO and SiO_2 making it very similar in composition and structure to the mineral alite. In a typical OPC the C_3S contains about 1 wt% each of MgO, Al_2O_3, and Fe_2O_3, along with trace amounts of Na_2O, K_2O, P_2O_5, and SO_3.

The impurities Mg and Fe are able to replace Ca and stabilize the monoclinic structure, preventing loss of strength due to the structural transformation from monoclinic to triclinic that would occur on cooling. [35 39]

Dicalcium Silicate (C_2S)

C_2S also occurs in different crystal structures. The β belite structure predominates in OPC it is also irregular but less so than C_3S. This accounts for the slower reactivity of C_2S with water and its importance in the development of long term strength. The C_2S in cement also contains higher levels of impurities than C_3S. [35 39]

Tricalcium Aluminate (C_3A)

C_3A comprises anywhere from zero to 14% of OPC. Like C_3S, it reacts readily and exothermically with water. The hydration products of C_3A contribute little to the strength or engineering properties but in the presence of sulphate can participate in expansive reactions causing cracking. [35]

Tetracalcium Aluminoferrite (C_4AF)

A stable compound with any composition between C_2A and C_2F can be formed, and the cement mineral termed C_4AF is an approximation that represents the series midpoint. The crystal structure is complex, mainly due to the enrichment of Mn, Ti and Zn during roasting which can reach percentage concentrations dependent upon the source of raw materials. It is often termed simply as ferrite though this does not convey any of the complexity. The hydration C_4AF does not contribute to the strength or engineering properties. [39]

4.3 Relevance to this Research

The hydrated phases of the compounds above make up the “cement gel” it is important to note that hydration is non-stoichiometric and may continue to occur over many decades in finished cement products. The gels have a high surface area enabling significant and strong sorption of a wide variety of chemical species, in particular many of the positively charged radionuclide ions likely to be present in a GDF. The hydrating cement also has small amounts of Na and K hydroxides present which cause the pH to be above 13 in young cements, these alkali metals are leached readily because of their high solubility.[39] Also, the significant presence of Portlandite (CH or calcium hydroxide) can maintain the pore solution at a pH of 12.5 for times in excess of 1000 years. [40 41] The reaction of these pore solutions with atmospheric carbon dioxide and precipitation of calcium carbonate is another aspect of how the long term chemistry of cements develop. There is clearly an element of

kinetic control which must be considered when assessing how radionuclides will be taken up and retained by cementitious media or how the process of incorporation of radionuclides into the structures could limit availability for migration. [34 42]

The chemical changes occurring with time also cause changes to physical properties; changes to porosity and permeability are important in the context of this research as they will be the physical controls on migration into, through and from the cement.[43]

The hydrated or hydrating cement has two types of porosity; a non-interconnected gel porosity due to the presence of poorly crystallised C-S-H and capillary porosity due to micro pores that were initially water filled and the water has been used up by cement hydration. The capillary porosity persists despite the increase in total volume due to the formation of hydration products. [35]

Structural quality construction concretes exhibit low permeability, typically in the range 10^{-13} – 10^{-11} ms^{-1} and diffusion is the most significant mechanism of migration through the matrix. [35 44] In addition, the long term volume increase associated with hydrate formation will fill the micro pores and decrease permeability. This research is not concerned with construction quality concrete and focusses on materials that are commonly termed grouts and used as backfills, fillers, barriers or buffers in applications where structural properties are not the main requirement. NRVB, a potential backfill material is the main subject of this research and it is described in more detail below.

4.4 NRVB

NRVB is composed of a mixture of OPC, limestone flour, hydrated lime and water in the following proportions:

OPC 450 kg m^{-3}
Hydrated lime aggregate 170 kg m^{-3}
Limestone flour 495 kg m^{-3}
Water 615 kg m^{-3}

This produces a high porosity (~50%) relatively homogeneous grout that allows gas migration. It has high alkalinity for long-lived chemical conditioning i.e. low solubility and precipitation of many species will be favoured. It is low bleed and high fluidity providing very good void filling capability. Organic additives are not used so soluble and mobile metal-organic complexes cannot form and it is low strength so waste packages can be retrieved if required. The high calcium carbonate content is unusual and its presence explained by the need for a high calcium content after GDF closure to condition any inflowing groundwater to a pH greater than 10. This is expected to enable additional cementation in waste-forms where lack of calcium may have limited the formation of CSH gels. It is anticipated that the integrity of the packages will be preserved by preventing the packaging grout from dissolving in unconditioned groundwater. At the same time, the initial corrosion of the wastes and the metallic waste packages would rapidly remove any oxygen remaining from the operational phase. The establishment and long term maintenance of high pH, almost anaerobic conditions is expected to preserve the integrity of the waste containers well into the post-closure period. [3 45] It was appreciated when NRVB was formulated that it may not be effective for chemical containment of alkali metal and halide ions but there is inference in the published documents that sorption due to the high surface area of NRVB, will be a significant factor inhibiting migration.

In chemical terms NRVB is complex and it will contain: [22 45 46]

- Calcium hydroxide; from the lime added and as a product of calcium silicate hydration.
- CSH gel; from calcium silicate hydration. This can be present in several forms, but is usually poorly crystalline or amorphous.
- Aluminate phases; from tricalcium aluminate and calcium aluminoferrite.
- Ettringite produced from the gypsum (calcium sulphate) added during cement manufacture.
- Monocarboaluminate; from interaction of aluminate cement phases with carbonate from the added limestone.
- Calcium carbonate as the majority (80-90%) of the added limestone remains unreacted during NRVB hydration.

The trace chemistry of water equilibrated with NRVB is detailed in section 9.0.

The rationale for including NRVB in this research is simple; it has potential to be used as an engineered, major control or barrier in the overall GDF multi barrier concept to be implemented by the NDA in the UK. As such the effectiveness with which it is able to arrest or control the migration of radionuclides is of fundamental importance to the long term integrity of the UK GDF.

5.0 Diffusion Experiments

5.1 Background: Diffusion, Partition and Ionic Strength

One of the primary aims of this research is to understand how a range of elements associated with radioactive wastes diffuse through and interact with NRVB. Diffusion will be one of the most significant processes driving the migration of isotopes from the GDF to the wider environment.[23 24]

Diffusion is the movement of particles from regions of higher concentration to regions of lower concentration. For a porous solid Fick's first diffusion equation relates diffusion flux to the concentration across a path length as follows: [47 48]

$$J = -D_e \frac{\partial C}{\partial x}$$

Where:

- J is the diffusion flux with dimensions g m^{-2} s^{-1}, flux is the amount of substance flowing through an area during a time interval, expressed per unit cross sectional area and per unit time, perpendicular to the direction of flow.
- D_e is the effective diffusion coefficient or effective diffusivity (see below) with dimensions m^2 s^{-1}.
- C is the concentration with dimensions of g m^{-3} or mol m^{-3}.
- x is the position with dimension m.

Fick's Second Law predicts how the concentration will change with time when diffusion is occurring; it is presented below in the one dimensional, radial form: [47 48]

$$\frac{\partial C}{\partial t} = \frac{1}{r} \frac{\partial}{\partial r}\left(r D_e \frac{\partial C}{\partial r}\right)$$

Where, t is time and r is radial distance.

The effective diffusivity D_e incorporates the physical properties of the solid porous medium and is defined as:

$$D_e = \frac{\delta n}{\tau^2} D_w$$

Where:

- D_w is the diffusivity in the fluid with dimensions $m^2\ s^{-1}$, in the absence of the solid medium.
- n is the available porosity expressed as a fraction of the total sample volume
- τ is the tortuosity – a dimensionless factor to account for elongation of the diffusion path length arising from the "tortuous" nature of the connected porosity in a solid medium.
- δ is the constrictivity – a dimensionless factor associated with pore narrowing (see below).

Decreasing effective diffusivity due to constrictivity becomes important when pore diameters are close in size to those of the diffusing particles.[49]

The dimensionless tortuosity and constrictivity factors are conventionally expressed on the "top line" of the equation as numbers ≤ 1, so the relationship between D_e and D_w can also be represented:

$$D_e = D_w f(\tau\delta n)$$

Some texts [50] also use expressions of the form:

$$D_e = D_w G n$$

Where, G is termed a "geometric factor" which can be used to aggregate the relevant parameters into a single value.

Partition of the dissolved species between the solid and liquid phases will also be significant and modifications of the diffusion equations to account for this are available in the literature.[51] [52] [53] [54] An alternative diffusivity coefficient; D_a the sorption retarded diffusivity (or apparent diffusivity) is used and is defined as:

$$D_a = \frac{D_e}{\alpha}$$

Where, α is the rock capacity factor for the diffusing species and is defined as:

$$\alpha = n + \rho . K_d$$

Where, n is the porosity, ρ is the dry bulk density (g m^{-3}) and K_d is the partition coefficient ($m^3\ g^{-1}$).

The equation below [54] incorporates the significant parameters affecting diffusion in porous media, including K_d and is a revised version of a previously reported equation.[53]

$$D_a = \frac{nD_w}{(1-n)\rho K_d + n} f(\tau, \delta)$$

K_d is formally defined as the ratio of the quantity of the adsorbate, adsorbed per mass of solid to the amount of the adsorbate remaining in solution at equilibrium. For the reaction:

$$A + C_i = A_i$$

The expression for K_d is:

$$K_d = \frac{mass\ of\ adsorbate\ sorbed}{mass\ of\ adsorbate\ in\ solution} = \frac{A_i}{C_i}$$

Where:

- *A* = free or unoccupied surface adsorption sites
- C_i = total dissolved adsorbate remaining in solution at equilibrium
- A_i = amount of adsorbate on the solid at equilibrium.

K_d is given in units of volume mass^{-1} e.g. m^3 g^{-1} or dm^3 kg^{-1},

The key assumptions are that A is present in excess with respect to C_i, so sites are always readily available and that the sorption process is fully reversible. [55]

The significant quantity of K_d data available in the literature for a variety of cements and elements have been summarised by SKI in a single report. [56] This report also provides an indicative range of values to be used in performance assessment and was used as a comparative data source for the present work.

In some cases, when there is a linear relationship between the concentration in solution and on the solid; the proportionality constant that relates them is known as the distribution ratio (R_d) which can be calculated from the concentration initially added and that remaining in solution as follows:

$$R_d = \frac{[RN]_{initial} - [RN]_{solution}}{[RN]_{solution}} . \frac{solution\ volume\ (dm^3)}{solid\ mass(g)}$$

This equation does not imply any specific sorption process and clearly sorption isotherms may deviate from linearity due to saturation of the solid surface or precipitation of the radionuclide of interest.[57 58 59]

In practice and because experimentally determined values are similar, the K_d and R_d terms are often used interchangeably despite the implied standard conditions and reversibility in the former and pre requisite linearity in the latter.

In addition the ionic nature of the systems studied mean it is necessary to acknowledge the electrostatic interactions. The movement of an ion in solution will be restricted by the electrostatic field created by other ions present in solution. Therefore, from a theoretical point of view it is necessary to be aware of Nernst and electrical double layer theories to understand the migration of an ion. Accordingly, *D* for an ionic species will depend on the molar conductance of the ion (Λ_i), which is empirically associated to the concentration by a relationship of the type:

$$\Lambda_c = \Lambda_0 - kc^n$$

Where, c is the concentration of the ionic species.[60] It is possible to express the dependence of the diffusivity upon the concentration of the diffusing ion by a similar empirical equation;

$$D_c = D_0 - k_c c^n$$

Where, k_c is a constant that includes the pore characteristics of the matrix and for monovalent species *n* is usually 0.5.[61 62] Experimentally, the consequence of these relationships is that diffusivity will decrease with increasing concentration and ionic strength.

The equations above provide an insight into the effects likely to be observed as ionic strength increases but the complexity of the solutions and cementitious solids being studied negates the possibility of fully quantitative analysis.

Diffusion experiments provide fundamental information to support the performance assessment of a GDF. Diffusion can be observed and studied by many means. Initial conditions and whether or not determination is under steady state or non-steady state are important. Steady state diffusion can be determined by studying the mass transport from one solution to another separated by a slice of the solid and non-

steady state diffusion can be determined by studying the concentration profile in a solid after contact with a solution containing the species of interest.

Several studies have been devoted to investigating the mobility of ions in cementitious materials using diverse experimental approaches: (i) in-diffusion, where the diffusive penetration of a sample is measured;[54 63 64] (ii) through-diffusion, where a sample, often disc shaped or cylindrical is sealed between two reservoirs containing different concentrations of the diffusant [65 66 67 68 69 70] and most commonly, (iii) out-diffusion or leaching where samples of known diffusant concentration or samples doped with a known concentration of diffusant are placed in contact with a fluid into which diffusion can occur. The subsequent increase of diffusant concentration in the fluid is the parameter that is usually measured. [71 72 73 74 75 79]

A literature search also revealed relevant papers on radioisotope movement through hardened cement pastes, [77 78] disaggregated rocks, [79 80] structural concrete, [54 64] and intact rocks, [81 82 83] the rock beaker and diffusion in the geosphere experiments undertaken by Nirex being of particular interest. [84 85 86] A substantial overview of the techniques used to investigate radionuclide migration in groundwater and rocks was commissioned by NDA RWMD and the resulting 2008 report was used to provide up to date insight into many of the previous references for the current work.[87]

This research also investigates variation in radionuclide mobility associated with the presence of organics and in particular cellulose degradation products (CDP). Previous work has demonstrated that isosaccharinic acid, gluconic acid and other low molecular weight organics are able to affect the solubility and mobility of radionuclides in sandstone, calcite and NRVB systems. [83 88 89 90] These studies amongst others generally indicate a probable enhancement of radionuclide mobility in the presence of organics.

When developing any dynamic experimental method it is necessary to be aware of the general engineering references regarding the physical responses of test equipment and materials to changes in temperature, pressure, effective stress, abrasion, etc. Information relating to these properties of cementitious media is readily accessible in the literature. [91 92 93]

There are also references that collect and collate values for a range of properties of cementitious media and rocks including K_d, porosity, permeability solubility and interaction with solvents [56] [94] [95] which proved useful for scoping the experiments included in the research. The papers mentioned above provided significant insights into the issues and problems that might be encountered when developing dynamic techniques for observing diffusion. However, it was noted that there were no experiments investigating radial diffusion of radioisotopes through intact samples of cementitious media in the presence and absence of organics.

5.2 Development of Experimental Methodology for Diffusion

It was realised, at an early stage in this research, that setting up experiments aimed at accurately quantifying diffusion coefficients was unlikely to deliver the quick and generalised information desired. This is particularly true of the radionuclides likely to have low solubility at high pH e.g. Eu, Ni and in particular the actinides U, Th and Am.[96]

A cheap and reproducible method for comparing isotope diffusion and retention in various cementitious media was required to enable a significant number of experiments to be carried out on “identical” samples. After some discussion in the research group it was decided that developing a radial diffusion method was the most likely way to generate readily comparable and understandable results.

The experimental approach used in the present work is based on a through-diffusion set-up in a radial configuration. This approach had been used successfully to study migration of uranium through granite. [97] This methodology combines the advantages of through-diffusion experiments, where breakthrough is determined by monitoring the solution in contact with the solid and the simplicity of out- and in-diffusion approaches where the use of specially constructed diffusion cells that are prone to leakage, is avoided.

The main theoretical disadvantage for these radial diffusion experiments is the lack of effective analytical solution with time-dependent boundary conditions for the relevant diffusion equation. An analytical solution for hollow cylinders is available [47] but it requires maintenance of a steady state gradient and zero tracer concentration at the outer edge of the cylinder. This in turn, requires constant removal of the tracer (presumably without causing mixing or advection). Work published in 2004, [48]

describes a successful experiment with a rig capable of maintaining the boundary conditions but it required regular management interventions. It would not be practical to maintain the boundary conditions over the long time periods requested by NDA. Also, any model or simulation will have to assume uniform radial diffusion from the central core over relatively long path lengths compared to the thin disc methods. [77 78] More generally, the relevance of the geometry could be questioned as it only simulates a small cavity in the NRVB.

A method was developed based on the simplification of an advection technique being trialled in the research group (see section 6.0). The main issues encountered during the development of the diffusion and advection techniques were, the design of effective seals and establishing a geometry where the path length could be fixed and reproducible to obtain results quickly and faciltate modelling. The experimental set up is shown schematically in fig. 5.1 and photographed as fig. 5.2.

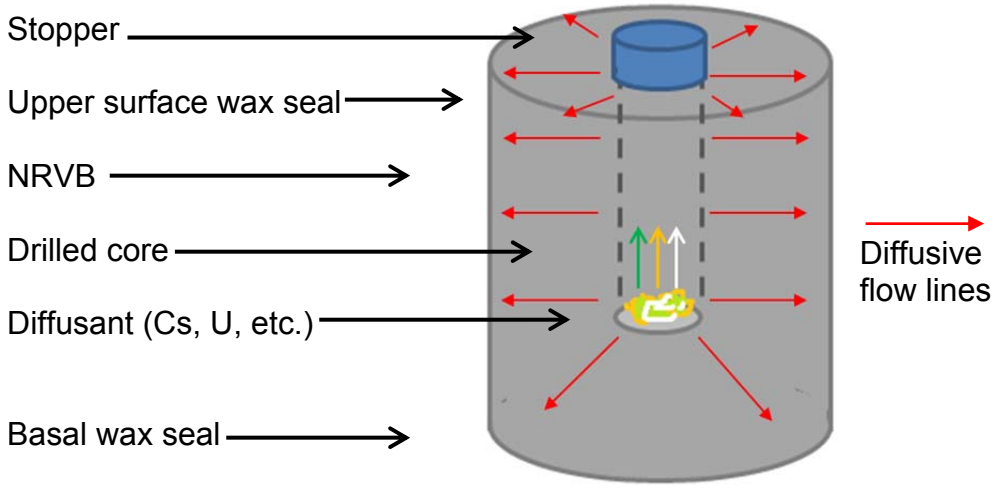

Fig. 5.1 Schematic of diffusion apparatus

Fig. 5.2 Photographs of experimental set up

The feasibility of the method was initially tested by filling the core with 5% potassium permanganate solution, immersing it upside down in a plastic container of water and leaving for several weeks to establish that the seals functioned appropriately. The result of one of these experiments is shown in fig. 5.3 below. Although the brown colour suggests that the permanganate has been reduced to manganese dioxide (probably by iron (II) or tin (II) salts added to the OPC to reduce the hazard caused by the presence of Cr(VI) [98 99 100 101]) a clear and regular pattern of radial diffusion can be seen.

Fig. 5.3 Photograph of permanganate trial

5.3 Radial Diffusion Experiment – Detailed General Procedure for NRVB

The three ingredients of NRVB were purchased in sufficient quantity to ensure that all samples required for this research could be made from the same starting materials.

40 mm diameter x 40 – 45mm height NRVB cylinders were manufactured using the recipe available in the literature [3] using polyethylene 50 cm^3 sample containers as moulds.

A batch of approximately 100 cylinders was manufactured to ensure consistency.

After 24 hours the blocks were demoulded and cured under water in a sealed container for at least 30 days.[102]

A 10 mm diameter hole was then drilled in the centre of the cylinder using a sequential set of drills starting at 2 mm to avoid cracking the cylinder. The hole was stopped at least 15 mm from the base of the block.

The surface of the block was then allowed to dry for 1 - 2 hours and dipped top and bottom in melted paraffin wax until a good seal was made.

The block was then returned to the curing water for at least 7 days.

The experiment was commenced by adding the species of interest at the desired concentration or activity to the central port and topping up with the curing water or water previously equilibrated with NRVB. Solids and mixtures of solids and solutions can be added, tracer and tracer carrier experiments can be undertaken in the same manner.

The core was then plugged using a 10 mm diameter polyethylene tube stopper wrapped in “parafilm” and washed quickly with water to remove any surface contamination that may have occurred during the addition of the radionuclide (the washings were collected and monitored prior to disposal)

The block was then placed in a 250ml Nalgene wide mouth screw top container and 200 cm^3 of water previously equilibrated with NRVB added.

A sample of the water was taken after 3-4 hours and a further sample after 24 hours to establish that the contents remained sealed in the block.

Samples were taken daily for 4 days and then the sampling frequency adjusted to a rate that facilitated detection of breakthrough and stabilisation.

The undrilled cylinders continued to be stored under water in the sealed container until required.

It is common practice to exclude carbon dioxide from experiments on cementitious materials that may be used in a GDF application. This measure aims to exclude the possibility of continuous carbonation and consequent precipitaion of calcium carbonate during the experiment. The measure is taken to mimic the GDF environment where carbonation is likely be very slow.[103 104 105]

It was not possible to undertake all operations in carbon dioxide free conditions due to practical problems. In particular it was decided that dispensing open sources and dosing the blocks in the glove box represented too high a risk of spills and contamination. In addition drilling the holes in the blocks is an activity more easily accomplished on a laboratory bench. However once the experiment was underway it was possible to move all operations to a glove box.

A small number of issues were noted as the experimental programme progressed and although no significant problems appear to have arisen, solutions have been proposed and are currently being evaluated. The main issues and proposed solutions are as follows:

- Verticality of central hole – holes will be bored using a pedestal drilled and fixed mount.
- Damage and potential for preferential diffusion pathways caused by drilling the central hole – holes will be drilled sequencially starting at 1 mm diameter using professional grade drill bits.
- Detachment of upper surface and basal wax seals – other sealing materials are being investigated including polyurethane and epoxy coatings. Wax was chosen originally because of its perceived inertness.
- Ingress of carbon dioxide – a larger glove box is required to enable more of the procedure to be undertaken in a carbon dioxide free atmosphere.

- When a large number of samples are taken there is a potential impact on partition because the 1 cm^3 sample that is removed during the early part of an experiment contains a disproportionately small amount of radioactivity. A correction calculation has been developed for use on the observations and models (see section 11.2).
- It was also noted that the experiment as it stands could not be undertaken at increased pressures to reflect potential GDF conditions.

The issues of scale seen when producing small cores to make rock beakers were not encountered.[106]

6.0 Advection Experiments

6.1 Background

Advection is a transport mechanism of a substance, or a conserved property, by a fluid, due to the bulk motion of the fluid in a particular direction. An example of advection is the transport of a contaminant through rocks or soil in groundwater. The motion of the water carries the substance down an hydraulic gradient. Any dissolved or suspended substance or conserved property can be advected in any fluid.[43 107]

The fluid motion in advection can be expressed mathematically as a vector field, and the material transported is typically described by the spatial coordinates and concentration present in the fluid. Advection requires the movement of a fluid and cannot happen in solids. Advection does not include diffusion but diffusion and dispersion perpendicular to flow will be present in most of the advection experiments undertaken in this research.

In aqueous solute transport systems advection and dispersion are usually dealt with together and expressed in the form of the advection dispersion equation below:

$$\frac{\partial C}{\partial t} = -v\frac{\partial C}{\partial x} + Đ\frac{\partial^2 C}{\partial x^2}$$

Where: C is solute concentration, v is the average linear velocity, x is the spatial domain, t is time, and $Đ$ is the dispersion coefficient.[108 109]

The advection experiments reported in the present work should be regarded as trials and the numerical transport model developed for this research does not use the advection dispersion equation explicitly (see section 7.0 for details).

6.2 Background to the Radial Advection Technique

Initially a series of advection trials were undertaken using packed columns of crushed and sieved NRVB.[110] These trials are not presented herein as they were only partially successful, further emphasising the need to work on more representative intact samples.

Advection of intact samples is usually studied in an axial format where the fluid is pushed through a cylinder of the test material from bottom to top, a comparative

study of the types of equipment used is available in the literature.[111] For porous solids the side wall leakage can be eliminated or reduced by sealing the sample in a heat shrink plastic jacket.

The first axial advection trials were undertaken on NRVB cylinders sealed using a tubular heat shrunk PTFE side wall seal. The cylinder was clamped in a simple rig and the NRVB equilibrated water eluent delivered using a Waters HPLC pump. The experiment was carried out under a nitrogen atmosphere.

The experiment ran for three months at constant flow (1.5 cm^3 hr^{-1}) and a steadily increasing pressure was observed until the sample and seal failed. When the rig was opened, see fig. 6.1, the inlet was clear but a hard crystalline deposit had formed on the outlet surface. This deposit was identified as Portlandite ($Ca(OH)_2$) using XRD and EDX.

Fig. 6.1 First axial advection experiment showing the clear inlet (left) and crystalline portlandite deposit on the outlet (right)

The SEM image and EDX output are shown as fig. 6.2, the hexagonal plates of Portlandite are clearly visible.

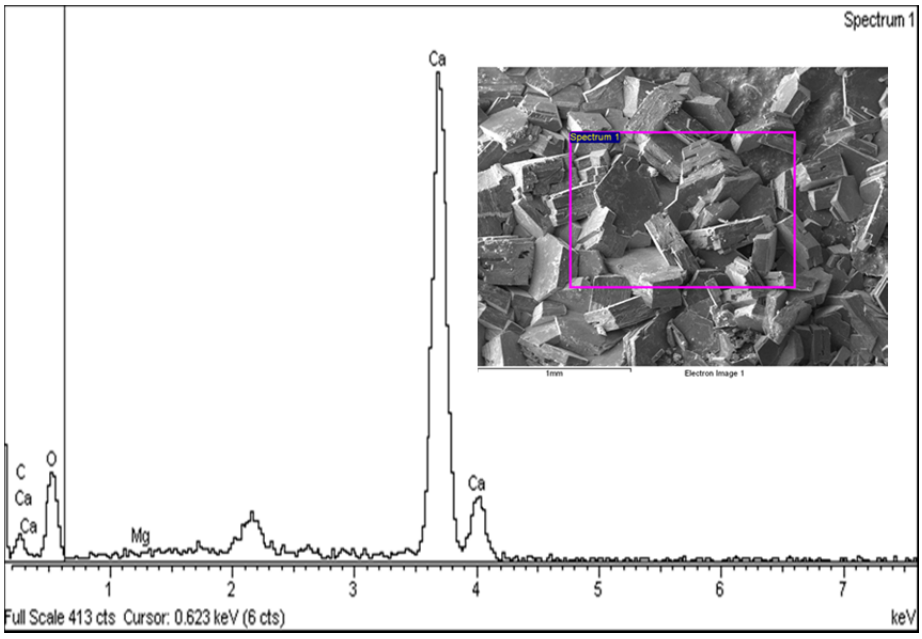

Fig. 6.2 SEM image of the Portlandite deposit from the outlet and EDX output

The cores were examined in greater detail and found to contain an area around the inlet where Portlandite had beeen depleted and areas (specifically air bubbles in the NRVB matrix) where it had been deposited, these features increased in frequency towards the outlet.[112] This experiment indicated that the path length was too long to operate the experiments over very long durations without the application of very high pressures to overcome the porosity reduction associated with the Portlandite deposition.

A system capable of operating at high pressure was made available by British Geological Survey, Keyworth, Nottingham, UK and trialled with intact NRVB samples. The side seal arrangement can subjected to an externally applied confining water pressure, similar to a triaxial clay permeability cell.[111] A schematic of the apparatus is shown in fig 6.3 below. The axial advection equipment is expensive as it is engineered to withstand significant pressures and it also proved difficult to operate. Photographs of the system used are included in figs. 6.4 and 6.5.

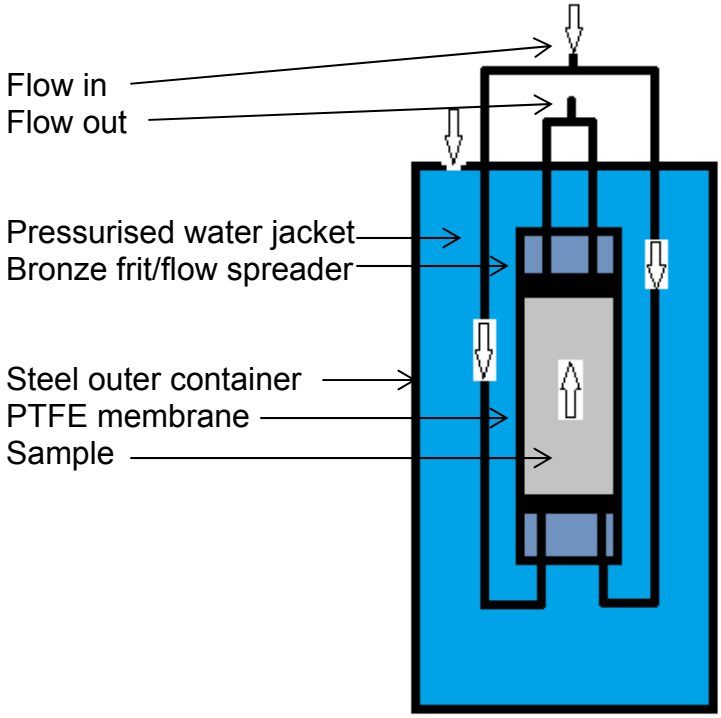

Fig. 6.3 Schematic of typical axial advection apparatus

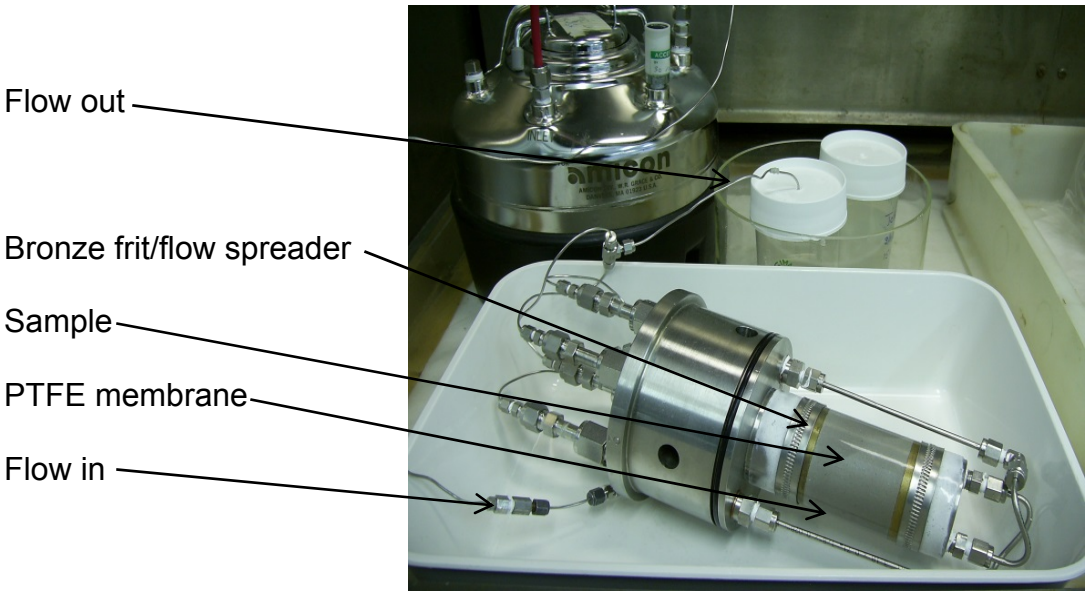

Fig. 6.4 Photograph of axial advection apparatus without outer steel jacket

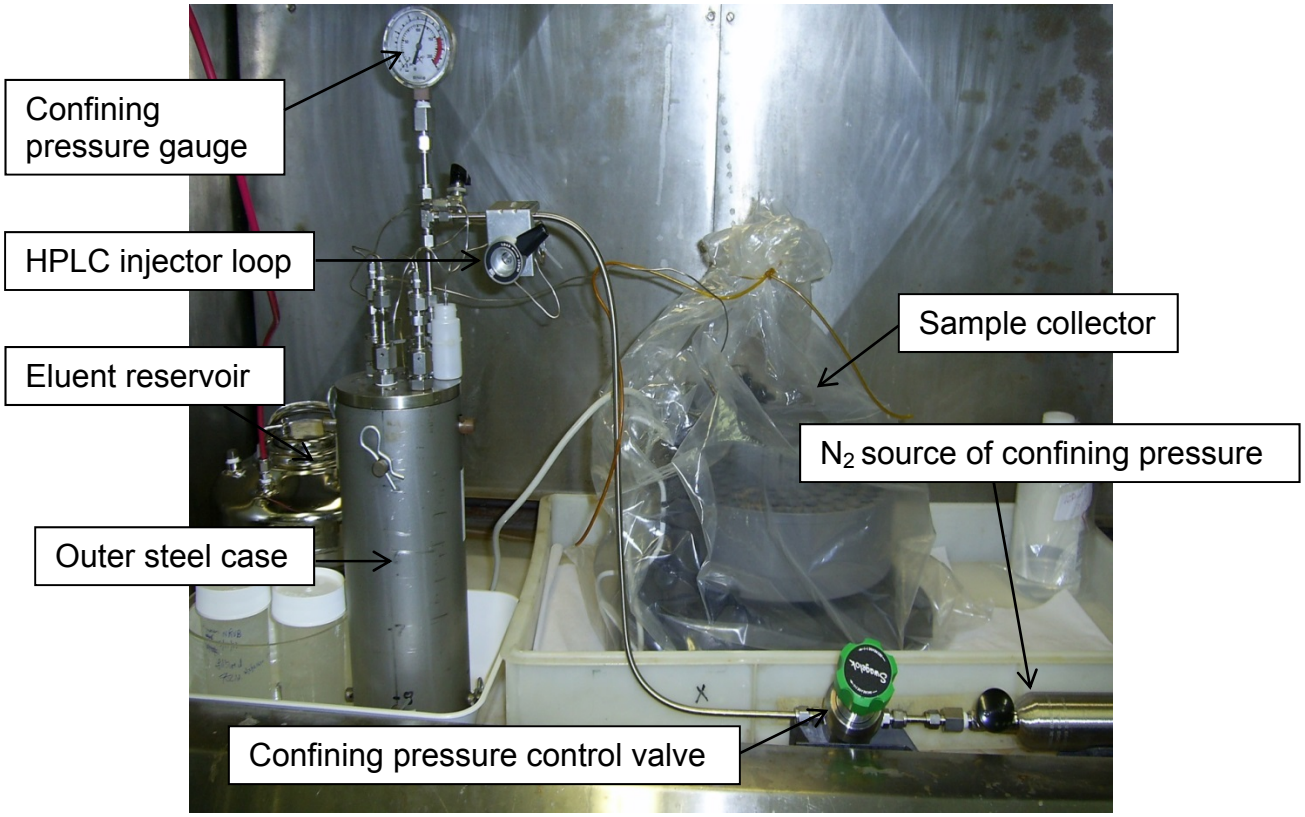

Fig. 6.5 Photograph of fully assembled axial advection apparatus with outer steel jacket, injector loop and applied confining pressure

Sample injection was via an HPLC injection loop. During trialling of the axial advection equipment some of the problems that were encountered could not be easily resolved. Specifically, unanticipated side wall leakage caused unpredictable short circuiting around the sample which was discovered during experiments when using HTO as a tracer. This continued to occur despite stepping up the confining pressure until the differential pressure across the sample exceeded its compressive strength and caused the mechanical failure. As a consequence the axial advection experiments were abandoned.

6.3 Radial Advection Trial Experimental Set Up

It is possible to use a radial arrangement similar to the diffusion experiments described in section 5.0. The Rowe and Barden cell, used to assess consolidation properties of soils, clays and concretes can be configured radially to allow collection of consolidation water at the perimeter of the cylindrical samples. [113] [48] A similar approach on a smaller scale was employed when developing the radial advection technique. The main advantages of exploiting radial flow are that the problem of side wall leakage is eliminated and the seals are simple. The main disadvantage is that

the applied pressure cannot exceed the strength of the sample because it is effectively in tension. A schematic of the arrangement is shown in fig. 6.6.

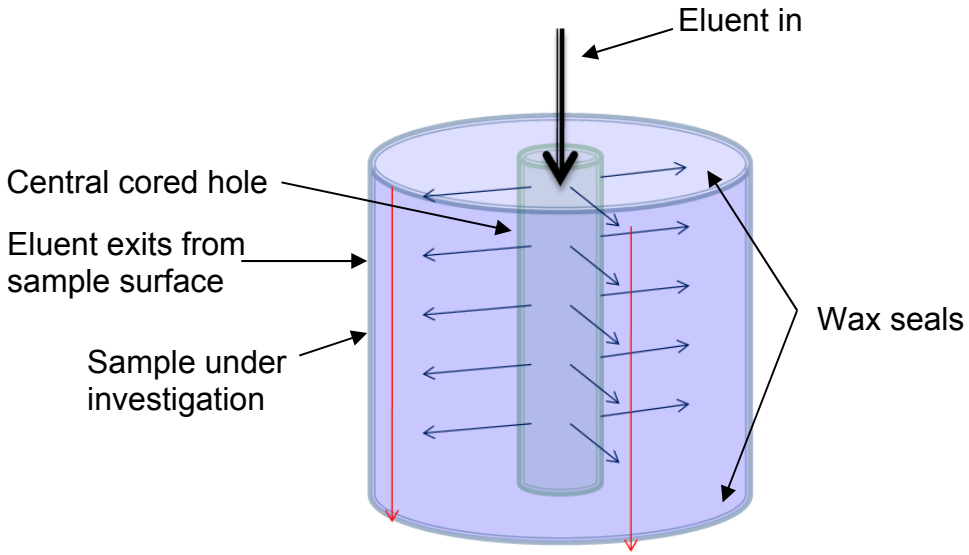

Fig. 6.6 Schematic of the radial advection set up

The fluid is introduced under nitrogen pressure from a stainless steel reservoir into the central core and provided the block is correctly securely clamped in place and sealed, flow can only occur in a radial manner. The fluid exits from the sides of the block and is collected in a tray. The actual trial set up is shown in fig 6.7 below.

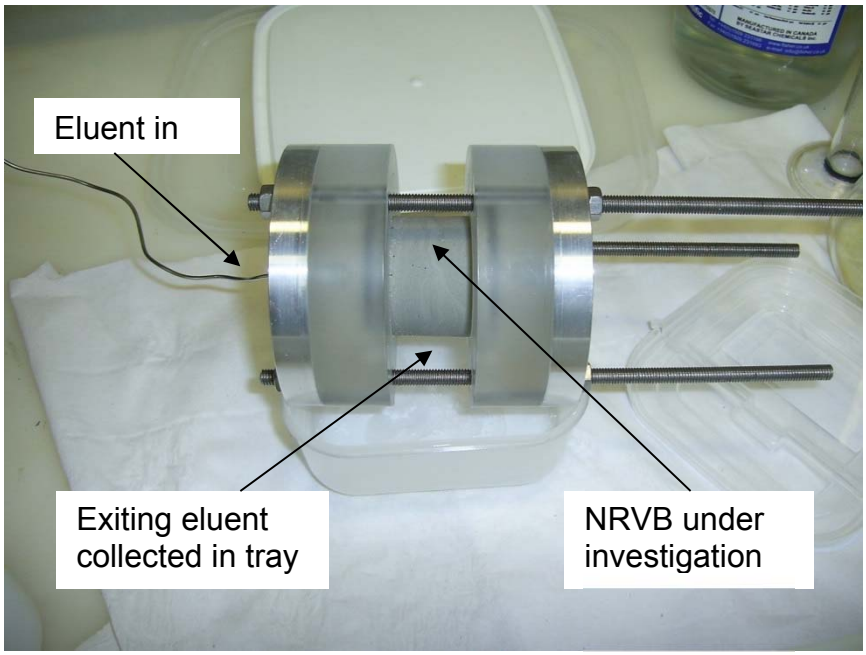

Fig. 6.7 Photograph of prototype radial advection cell

6.4 Permanganate Advection Trial

The initial trial for the technique was undertaken using a 1% potassium permanganate solution. The objectives were to produce radial flow only (i.e. no leaks through the ends of the block), ascertain whether a consistent flow could be maintained and show that the fluid had contacted all parts of the block.

The results are demonstrated by the photographs in figs. 6.8 and 6.9 below:

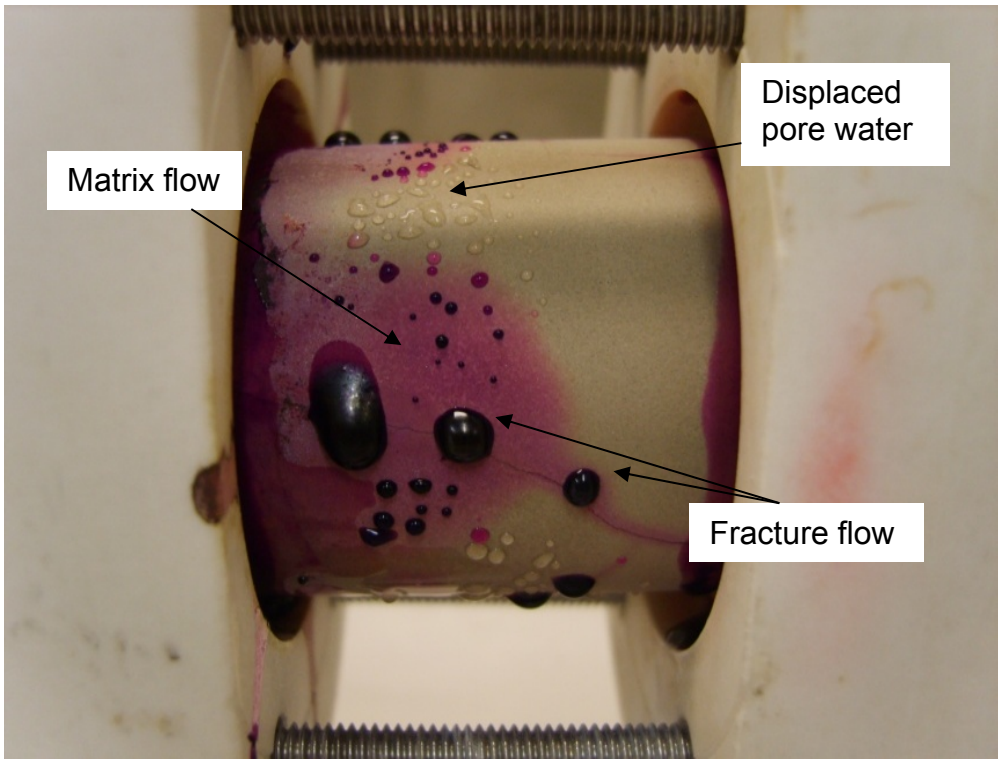

Fig. 6.8 Photograph of permanganate advection showing flow mechanisms and pore water displacement

Fig. 6.9 Photograph showing extent of permanganate contact

6.5 Trial Results and Discussion

The photographs show that the technique is feasible with leakage appearing to be negligible and contact with all internal surfaces demonstrated by the broken block shown in fig. 6.9.

The photograph (fig. 6.8) of the experiment in progress shows that flow is occurring through fractures and the matrix, there is also evidence of residual pore water being displaced (the clear droplets on the surface). This may indicate that the technique could be modified to run very slowly and collect pore water as it evolves, which is known to be difficult to achieve in practice.[114]

As the experiment progressed the outer surface of the block eventually became completely purple. The main visible fracture was most likely caused by over tightening the rig but the photograph is included here because it demonstrates both the modes of transport occurring together on one picture. The fracture was obviously a major feature and not likely to have been “autogenousy healed” (self-healed) [115 116] with extended experimental duration. Self-healing is very similar in nature to the portlandite deposition that had been observed in some of the early axial advection trials, where it had been associated with the steady pressure increases required to maintain constant flow. Subsequent advection experiments were undertaken using

soft compressible seals on the ends of the block and the fracturing was successfully avoided.

The final trial experiment was undertaken with a 13.5 KBq ^{90}Sr tracer introduced into the central core. This experiment identified a significant deficiency (~30%) in the mass balance, which was attributed to co-precipitation of radioisotope with calcite on the external surface of the block and more leakage than noted in the previous trials.

The main design issues encountered and needing to be addressed during the trials were:

- leakage caused by ineffective seals,
- uneven upper surfaces on the NRVB cylinders causing difficulty clamping the samples consistently,
- NRVB is very weak and the clamps apply load unevenly,
- atmospheric carbon dioxide causing excessive precipitation of calcite,
- the requirement to dismantle the rig to insert the radioisotope tracer.

6.6 New Equipment and Design Issues Addressed

The issues identified above were addressed by purpose designing a radial advection cell. The sample under investigation is enclosed to prevent carbon dioxide ingress and the clamping rods and screws are replaced by manually tightened acrylic components. Photographs of the rig are shown below as fig 6.10 and fig.6.11. O-ring seals were incorporated and screw fit closures included top and bottom to enable smooth tightening onto the seals. Dead space in the system was minimised by reducing the internal diameter of the cell to 41 mm, a “good fit” for a 40 mm diameter block. A gas chromatography injector was fitted to allow radioisotope injection into the central core without interrupting the flow. Fluid can be driven through the block by inert gas (nitrogen) pressure or a pump. As the fluid exits the block it is piped to a fraction collector via narrow diameter PTFE pipework.

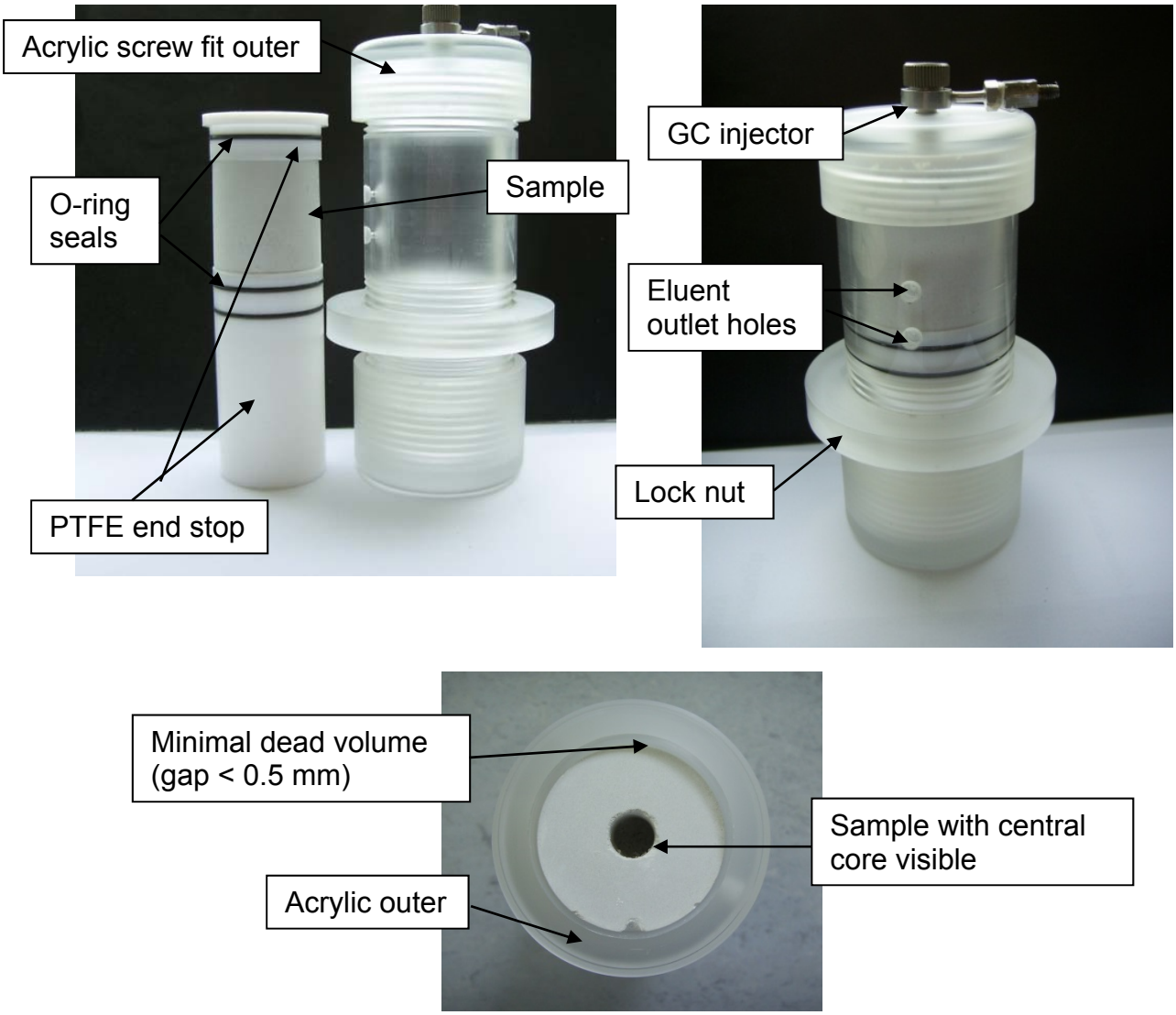

Fig. 6.10 Photographs of advection cell components

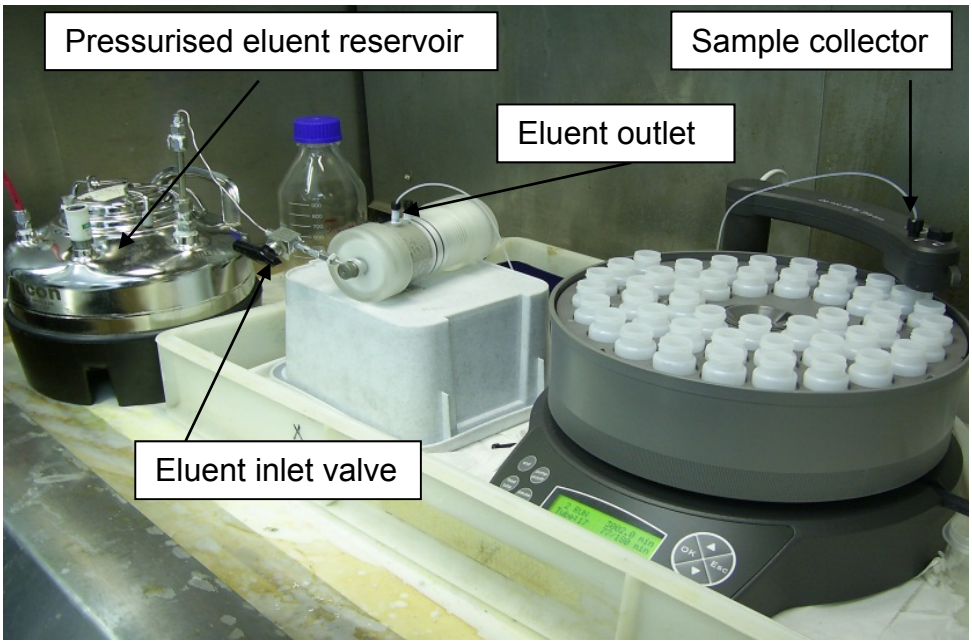

Fig. 6.11 Advection cell in operation

The purpose designed radial advection equipment proved relatively easy to operate. The path length for advection is less than the diameter of the sample, the deposition of Portlandite or Calcite on the outer surfaces was not observed and low pressure operation could be maintained for many weeks. After trials using tritiated water and ^{90}Sr tracer (see results in sections 10 and 13) it was decided to use the set-up for the advection experiments undertaken for this research.

7.0 Transport Modelling

Whilst accepting that the overall objective of the NDA (and to some extent, the funders of the SKIN research) is to understand the migration processes at a fundamental level. It was felt that the available results could be suitable for preliminary transport modelling. The experimental setup used in the present work was designed to allow observation of the radial migration of radiotracers through NRVB cylinders. The configuration was simplified and conceptualised as a hollow cylinder and then treated as one-dimensional for modelling purposes. The modelling approach detailed below was discussed and agreed with NDA representatives prior to go ahead.

7.1 Goldsim

As an initial approach, GoldSim [117] was selected for the transport modelling. It is an internationally accepted code for simulating radionuclide migration from waste facilities and is the platform considered most suitable for use by the Environment Agency for England and Wales, to carry out performance assessments for shallow disposal facilities for radioactive waste.[118] This modelling tool has been used to produce preliminary simulations of the HTO, Cs, I and Sr diffusion and advection experiments. Estimates of the partition coefficients and effective diffusivity values have been made.

GoldSim is a platform that provides access to a variety of tools that can be employed to create simulations. It is used commercially to carry out dynamic simulations to support management and decision-making in business, engineering and science. Its mixing cell capability can explicitly represent mass transfer, partition and solubility constraints.

Provided the geometry and physical features of the system being modelled are known or can be estimated, the processes and properties controlling the rate at which mass moves between cells can be represented for both diffusive and advective transport mechanisms. The mixing cells can be “filled” with porous media and the transferred mass partitioned between the solid and liquid components present using partition coefficients.

When multiple cells are linked together via advective and diffusive mechanisms, the behaviour of the cell network is mathematically described using a coupled system of differential equations (GoldSim uses implicit Euler integration to control numerical error propagation). In effect, a network of cells is mathematically equivalent to a finite difference network of nodes. GoldSim numerically solves the coupled system of equations to compute the mass present in each cell (and the mass fluxes between cells) as a function of time. [119]

7.2 NRVB Radial Diffusion Simulation

The complexity and heterogeneity of NRVB may have significant effects on the diffusion of species. However, the absence of a large particle size aggregate and obvious crystalline assemblages suggests that it is isotropic at the scale of the experiments and that it can be modelled as a uniformly porous medium.

The model simulates the radial experiments using the Goldsim capability to create mixing cells that are concentric cylinders, where mass transfer by diffusion takes place through the defined areas between the cells. The schematic diagram showing the conceptual basis of the model is given below. [54]

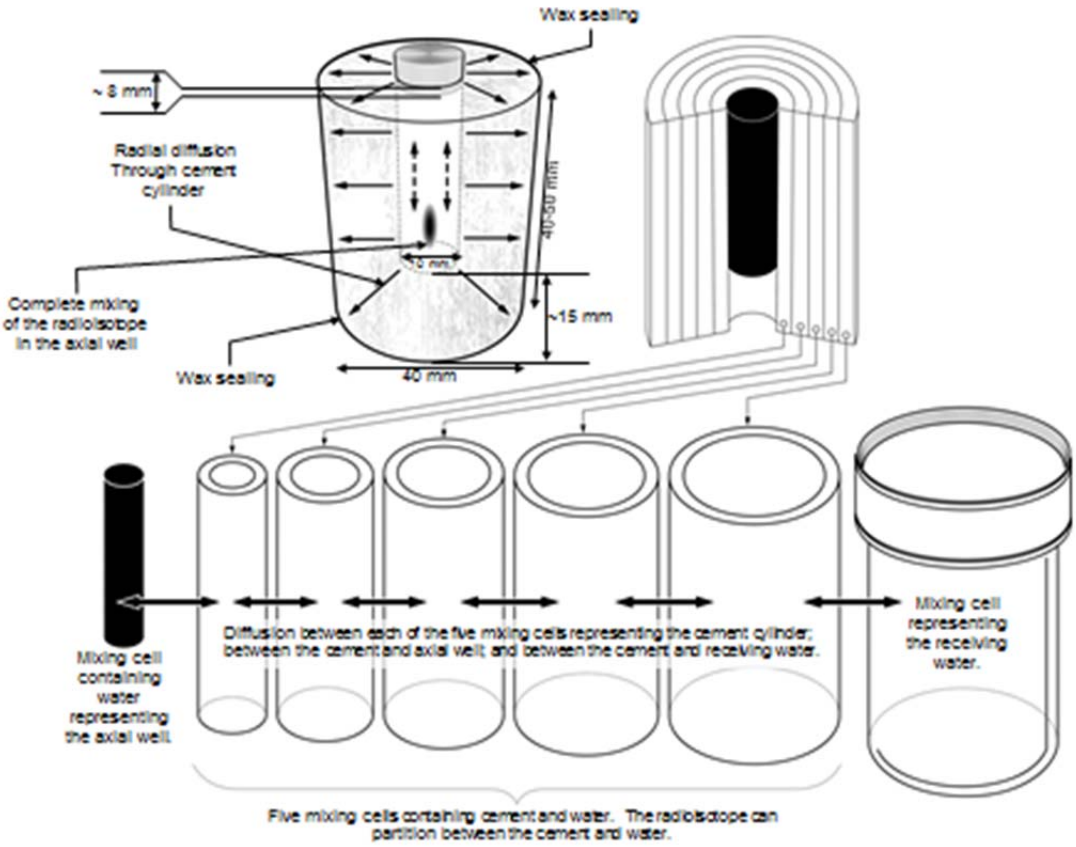

Fig. 7.1 Conceptual basis of the GoldSim model

The NRVB cylinder was discretised into five concentric cylinders each with the same wall thickness. Each of the seven parts (5 NRVB cylinders, the central core and the receiving water) of the experimental system was represented in the modelling as a perfectly mixed cell containing a volume of solution. The masses of NRVB, water occupied porosity and receiving water were calculated using the porosity value and bulk dry density from the literature (0.5 and 1095 kg m^{-3} respectively).

The seven part model was recommended by the GoldSim development team because when run in advection mode it would be capable of numerically simulating ~10% dispersion.[119]

7.3 Calculational Basis of the GoldSim Model

The main sources for the following discussion [50] [120] [121] specify the general cases available on the GoldSim platform for calculating mass transfer and partition along with two functions not used in the present work; solubility limited control and radioactive decay; as they are applied to multiple geometries, fluids and solids.

The current radial diffusion experiments are a simpler case, with a single fluid, solid and diffusant and the equations that follow have been modified accordingly. It should also be noted that the relevant literature uses the engineering terminology of mass flow, mass transfer and diffusive conductance.

The calculational basis for the numerical model is the mass transfer equation (Fick's first law, see also section 5) below:

$$J = -D_e \frac{\partial C}{\partial x}$$

The flux term can also be stated as:

$$J = \frac{1}{A} . \frac{\partial m}{\partial t}$$

Showing that when diffusive area (A) is fixed, a relatively simple relationship between mass transfer rate $\frac{\partial m}{\partial t}$ and concentration gradient results.

$$\frac{\partial m}{\partial t} = -D_e A \frac{\partial C}{\partial x}$$

Integrating the above expression for the 2-dimensional system (i.e. diffusion through an area) it is necessary to introduce a gradient operator, transforming the above equation into a surface integral. The formalism is also changed to include $\dot{m}$, the time differential of mass (mass flow rate, g s^{-1}) and $\vec{n}$ the normal vector of the surface, S as follows:

$$\dot{m} = -\int_S D_e \nabla C \cdot \vec{n} dS$$

This formal fluid dynamics double integral is the integration that the model approximates numerically.

The diffusive mass flow between neighbouring cells must be considered so that the diffusion can be discretised. The diffusive mass flow from cell *i* to cell *j* is given by:

$$\dot{m}_{d,i\to j} = Q_{i\to j}(c_i - c_j)$$

c_i and c_j are the diffusant concentrations in the fluid in cells *i* and *j* respectively.

The Q term is known as diffusive conductance (m^3 s^{-1}) and gathers together the quantities that will remain constant in each time-step:

$$Q_{i\to j} = \frac{D_e A_j}{L}$$

Where:

$$D_e = D_w G n$$

And:

- G is the geometric factor (note: GoldSim does not have separate tortuosity and constrictivity inputs, it uses a single factor which it calls tortuosity that can be used to estimate some of the physical parameters).
- A_j is the inner surface area of cell *j*,
- L is the diffusive length (cell thickness). Using cell thickness here averages the mass transferred throughout the volume of available porosity in cell *j*.

Each time-step can now be computed and is represented by:

$$\frac{m_{d,i\to j}}{\Delta t} = Q_{i\to j}(c_i - c_j)$$

The time step is known (user defined) and the mass transferred between the adjacent mixing cells is calculated. The mass added to a cell is instantaneously partitioned amongst the user specified media present in that cell. For the current experiments the partitioning is controlled by the user defined partition coefficient (K_d). New cell concentrations in the fluid are calculated and the next step commences.

The numerical method used by GoldSim is implicit Euler integration [122] [123] and requires only that the differential form of the equation being integrated satisfies:

$$\frac{dm}{dt} = f(m,t)$$

The key assumption of the Euler integration method is that the rate remains constant over a time-step. The validity of this assumption is a function of the length of the time-step and the timescale over which the rate is changing. The assumption is reasonable if the time-step is sufficiently small.

In the simulation of the advective experiments, the diffusive mass flow rate of a radionuclide between cells is supplemented with an advective mass flow rate. The advective mass flow rate is calculated as the product of the concentration of the radionuclide in the fluid in the cell and the fluid flow rate. The fluid flow rate between cells is kept equal to the measured rate of flow from the cement block and there is therefore conservation of fluid mass. Dispersion occurs in advective flow regimes and a good first approximation for one dimensional transport through a relatively homogeneous medium is that the dispersivity is 10% of the total length of the pathway.[124] Much of the relevant literature is concerned with large scale geological features or industrial processes but the equations used by GoldSim are conventional in engineering laboratories and scalable. The linked cells in the model exhibit a degree of numerical dispersion that is a function of the number of cells. In particular, the equivalent numerical dispersivity is equal to half the length of one cell. By representing the cement block with five cells numerical dispersivity has been introduced to the model that is equivalent to 10% of the radius of the cement block.

The diffusion and advection simulation methods described above are mass conservative and assume that NRVB is homogenous and isotropic with regard to transport properties.

Finally, the criterion utilised throughout for the fitting of experimental observations to modelled output curves is minimisation of the lack of fit (LOF) calculated as:

$$LOF = \sqrt[2]{\frac{\sum(x_{observed} - x_{modelled})^2}{\sum x_{observed}^2}}$$

This statistical method generates an output which can be expressed as a "percentage lack of fit" where, the lower the value; the better the fit.

7.4 Modelling Procedure

The model requires the following inputs:

- The initial radiotracer concentrations in the seven mixing cells
- Dimensions of the sample (including the inner core)
- Volume of receiving water
- Bulk dry density of the NRVB
- Diffusion available porosity
- Tortuosity or geometric factor
- Time step

The tracer concentration and fluid mass in the inner core at t_0 are known. The sample dimensions are easily measured. The radiotracer concentration in the 5 cylinders and receiving water at t_0 is zero. The volume of receiving water is 200 cm^3 plus 25 cm^3 of water within the porosity. The porosity value and bulk dry density are 0.5 and 1095 kg m^{-3} respectively. Whilst methods for estimating the geometric correction factor have been proposed [107] [121] [124] the appropriateness of their use for NRVB has not been demonstrated. The geometric correction factor was therefore set to unity.

Time step lengths were trialled at 0.1 days and 0.01 days and no differences in output were noted. The shorter time step was favoured for the modelling because the data files were limited to several thousand data points instead of tens of thousands.

The user is able to input values for the variables K_d and D_w to obtain model output curves. In this case the relationship between D_w and D_e is simple (the former is

double the latter as the porosity value is 0.5 and geometric factor is set to unity) and henceforth for clarity, only D_e values will be used in this text.

Fick's second law indicates a correlation between D_e and the rock capacity factor (α) (see section 5.1) and therefore also between D_e and K_d. As a consequence, two independent observations are necessary to determine D_e and K_d from each radial diffusion experiment. The evolution of the diffusion experiments is such that there is later, flat part to the curve. K_d can be independently determined from this part of the curve as net diffusion has ceased and the concentration of the tracer in the receiving water is dependent only on partition.

The first stage of fitting the data was to run a series of either 3 or 5 attempts (at 0.2 $dm^3\ kg^{-1}$ or 0.3 $m^3\ kg^{-1}$ intervals) to find the best LOF, K_d value for the flat part of the curve. This value was then fixed for the model simulation runs and D_w varied (at $0.2x10^{-10}$ or $0.3x10^{-10}\ m^2\ s^{-1}$ intervals) to find the best LOF for the entire dataset. The approach was manually checked by undertaking a mass balance on several of the observed points to check that K_d was being determined satisfactorily (example results of the mass balances are provided in appendix 2.

Each sample taken represents a reduction in the mass of receiving water present and when radionuclide migration is occurring, a reduction in the mass of the radionuclides in the system; both were simulated in the diffusion model.

7.4.1 Degree of Discretisation

The degree of discretisation used (5 concentric cells) was tested to see whether a finer discretisation (50 concentric cells) would significantly change the modelling outcome. Insufficient discretisation, like too large a time step can adversely affect error propagation in the initial calculation steps, creating numerical instability and lack of convergence.

GoldSim has a mesh generator capable of automatically increasing the number of elements (in this case mixing cells) in a simulation. The original model was set up manually so a parallel 5 cell model was created using the mesh generator as a cross check. Both models produced identical outputs.

Subsequently, a 50 cell model was produced using the mesh generator. The effective diffusivity and partition coefficient previously used to fit the CDP ^{137}Cs tracer only experiment from section 11.3.2 ($2.8x10^{-10}$ m^2 s^{-1} and 0.7 m^3 kg^{-1}) were inputted to produce the model curve. The outputs for the 5 and 50 cell models along with the (5 cell) curves for 2.5 and $3.0x10^{-10}$ m^2 s^{-1} and the relevant experimental data points are provided in appendix 2. A very small difference between the two curves can be seen over the first 4 - 5 days of the simulation but this did not have a significant effect on the data fit.

As a further check the same procedure was performed on the data from the NRVB ^{137}Cs tracer only experiment (see section 11.3.1; the inputs were $2.0x10^{-10}$ m^2 s^{-1} and 2.3 m^3 kg^{-1}). The small difference between the curves persists over the first 10 – 12 days of the simulation but once again this did not have a significant effect on the data fit. The relevant graphs and data fits for the discretisation trials outlined above are provided in appendix 2.

7.5 Important Limitations of the GoldSim Radial Diffusion Model

The model has important shortcomings, primarily because diffusion below the base of the inner core is not accurately described using the basic ID radial concept. Ideally, the experiments should be simulated by a 3D model which accounts for the diffusion in directions other than horizontal which occurs due to the inner core stopping at ~15 mm from the base of the block. An alternative practical approach would be to drill the hole all the way through the cylinder and use a seal at each end. This was not done initially because the seal was perceived to be a potential source of leaks.

The model generates the first diffusion surface area using the shorter length of the inner core and applies the relevant concentration gradient across that area to generate the mass transferred. In effect, the model assumes that none of the radiotracer diffuses vertically through the base of the inner core. The likely effect of this shortcoming is overestimation of the radiotracer concentration for the very early observations followed by underestimation as the radiotracer taking the extended pathway through the lower part of the cylinder eventually reaches the receiving water. The first of the two examples provided in appendix 2 behaves as anticipated but the second behaves in the opposite manner, suggesting that the situation is

more complex. This complexity is also likely to be causing some inaccuracy in the simulated effective diffusivity determination. Reference is made to this issue at several points in the following sections where it could be a factor responsible for poor data fits or anomalous results.

The initial approach to the modelling described in this section proved to be adequate for the NDA and EU funders of this work. The initial outputs were close enough to NRVB literature values [3] to provide confidence that the model could be used for the current work and further developed into a 3D simulation at a later date, if required.

8.0 Autoradiography

Fuji BAS MP 2025 autoradiography image plates were used for this work. The plates are flexible 20 cm x 25 cm radiation sensors with a linear response over at least five orders of magnitude. They comprise a backing coated with a layer of phosphor crystals embedded in an organic polymer binder which is sealed with a thin protective layer against humidity and mechanical wear. The photostimulable phosphor is a barium fluorohalide activated (doped) with divalent europium ions ($BaFBr:Eu^{2+}$). [125]

Exposure is achieved by placing the radioactive sample material directly onto the plate for a time largely determined by trial and error. The image plate absorbs radiation emitted from the sample, causing Eu^{2+} to oxidise to Eu^{3+} and the liberated electron can subsequently be trapped at a Br or F vacancy. This results in a density pattern of filled electron traps, corresponding and proportional to the distribution and intensity of radiation emitted by the sample. [126]

The plate is developed using a scanning laser-beam in the red part of the spectrum to excite the trapped electrons and allow relaxation to the ground state in turn generating the emission of 390 nm blue light (in the case of $BaFBr:Eu^{2+}$). The stimulated as well as the incident light are collected by a light guide, routed through a filter to block the red parts of the spectrum and then funnelled into a high-sensitivity photomultiplier tube. The signal is amplified, filtered to reduce signal noise and digitized into a greyscale image. The greyscale images can be manipulated/colourised etc., using the freely available software package “ImageJ” [127] [128]

The technique originally used photographic plates and remains in frequent use in biomedical science for imaging of radio-labelled proteins.[129] It has also found application in the geosciences field to trace and identify radioactive mineral phases in rock samples.[130] [131] In this and similar work[132] [133] it is used to study the fate of radiotracers added to cement systems.

9.0 Additional Information

9.1 Preamble to Sections 10 – 15

The results of the diffusion and advection experiments are presented in sections 10 - 15. The first results presented are those for the tritiated water. There are results for diffusion and advection experiments with NRVB equilibrated water and an advection experiment using CDP solution. In addtion, GoldSim transport modelling of the data has been provided. Autoradiographs have not been produced for tritiated water because the low energy of the tritium emission requires specialist uncoated plates.

The experiments were undertaken initially according to the requirements of either the NDA chemical containment or SKIN work programme. The SKIN work did not require the effect of organics to be assessed so experiments with CDP solutions were not planned. However, where interesting results were obtained in the initial diffusion experiments further “opportunistic” experiments were undertaken. For example, the NRVB diffusion experiment using ^{45}Ca yielded good evidence from the autoradiographs that diffusion was occurring. As a consequence when the opportunity arose to run an advection experiment with the CDP solution, the experiment was undertaken (see section 14.4). This iterative and oppportunistic approach to the experimentation continued throughout the research and has provided some interesting results. The disadvantage with the approach was that some experiments were not undertaken and complete datasets are not available. It is hoped to complete the full set experiments over time but it is also important that the necessarily extended duration of such an experimental programme is acknowledged.

Results demonstrating migration have been obtained for Cs, Sr, I, Ca and Ni in addition to tritiated water. The results are presented in separate sections along with a short precis of why the element and its respective radioisotope were chosen as subjects of this research. In addition there are a number of longer term radial diffusion experiments which have been started using U, Th, Am, Eu and Se. These experiments are not anticipated to yield results within the timescale of the PhD programme. Finally the NDA chemical containment programme also included under and over saturation solubility experiments for Cs, I, Eu, Ni, U, Th and mixed isotope NRVB diffusion experiments.[134] Results from these experiments will be referred to when appropriate in the following sections.

For Cs and Sr, tracer only and tracer carrier, diffusion experiments in the presence and absence of CDP have been undertaken. The advection experiments were undertaken at tracer concentration only. Autoradiographs have been produced to visualise the fate of the radioisotopes. GoldSim transport models are also presented. In addition the Sr experiments were extended to include high ionic strength and gluconate surrogate for CDP.

The I experiments were affected by the short half live (60 days) and low gamma energy (35 keV) of the ^{125}I isotope being used. Good results were obtained for the tracer carrier diffusion experiments but long duration experiments could not be undertaken satisfactorily and the autoradiographs were indistinct. In addtion the experiments without KI carrier were ineffective.

The Ca diffusion experiments yielded results only after stopping one of the duplicate experiments and producing the autoradiographs. The radiographs indicated that diffusion was occurring and consequently advection experiments with and without CDP were undertaken.

The Ni diffusion experiments indicated that Ni was only mobile in NRVB when CDP was present but that progress to a stable concentration was very slow. The CDP advection experiment was also undertaken.

Finally, the SKIN programme required investigation of a 3:1, PFA:OPC waste packaging grout and parallel diffusion experiments were started. These experiments (with the exception of tritiated water) are not expected to yield results within the PhD timeframe.

9.2 NRVB Equilibrated Water and CDP Solution

The experiments were undertaken using one of two solutions, NRVB equilibrated water and CDP solution. This section provides details about the solutions.

The NRVB equilibrated water used was the curing water from the sealed containers where the NRVB cylinders were stored. The water in the sealed container was topped up periodically with nitrogen sparged tap water. Several storage containers were in use and water was assumed to be equilibrated with the NRVB after 28 days.

The preparation of CDP solution followed a modification of the previously reported procedure and related material [135] [136] as follows:

750 cm^3 deionised water were placed in a stainless steel can and sparged for one hour with N_2. 30 g of Kimwipe ® tissues were cut into small pieces (ca. 2 cm^2) and added to the steel canister, followed by 270 g of powdered NRVB. After mixing and sparging for a further 30 minutes, the container was closed tightly, weighed and placed in an oven at 80^oC for 30 days. A variation on the method using 3 g of tissues and 297 g of NRVB was also undertaken; analysis revealed that this yielded a weaker solution of organics. The two methods were used in an attempt to reflect the potential heterogeneity of w/w cellulosic waste content in different parts of the GDF. The CDP solutions used in the experiments were 50/50 mixtures of the two products. This represented a cellulose loading of 1.6% of the total mass in the stainless steel cans, adequately reflecting the cellulose loading estimated in the UK inventory (see section 3.1.3). Several batches of the CDP solutions were prepared and mixed prior to their use in the diffusion experiments in an effort to ensure that all the blocks were subjected to the similar conditions.

All solutions were filtered under CO_2-free conditions before use in the diffusion and advection experiments. Trace metals were determined by ICP-MS [137] [138] in semi-quantitative mode (7700x series, Agilent) and major cations (Na^+, K^+ and Ca^{2+}) and anions (Cl^-, NO_3^- and SO_4^{2-}) by ion chromatography (DX-100, Dionex), using IonPac® AS4A-SC and CS12A (both Dionex) columns,[139] respectively. In addition to analysis of total organic carbon (TOC) determined by wet oxidation (Sievers InnovOx, GE),[140] the main organic constituents of the CDP liquor were separated and quantified by capillary ion exchange chromatography (AS11-HC capillary column, Dionex). The main characteristics of the NRVB-equilibrated water and CDP mixture are summarised in Table 9.1 below.

Technique (units)	Species	NRVB equilibrated water			CDP solution		
		Average ± SD	Min	Max	Average ± SD	Min	Max
IC (mg dm^{-3})	Ca^{+2}	462 ± 222	123	847	627 ± 110	513	809
	K^{+}	358 ± 228	138	868	974 ± 184	791	1204
	Na^{+}	102 ± 53	49.4	228	326 ± 112	214	484
IC (mg dm^{-3})	Cl^{-}	23 ±8	15.7	44	44 ± 26	22	88
	NO_3^{-}	10 ±12	1.4	42	9.0 ± 8.1	2.0	23
	SO_4^{2-}	29 ±20	5.6	65	173 ± 220	13	546
ICP-MS (µg dm^{-3})	Al	268 ± 215	35.6	872	208 ± 131	72	413
	Cs	4768 ± 14854	26.3	51741	12609 ± 27681	175	74506
	Eu	0.61 ± 0.41	0.096	1.4	0.42 ± 0.37	0.06	0.99
	Li	1642 ± 1196	327	4606	5983 ± 1696	4083	9527
	Mg	127 ± 163	11.8	443	46 ± 28	11.1	101
	Ni	8.3 ± 4.7	1.1	15.2	504 ± 373	13.3	1158
	Se	2.3 ± 0.74	1.4	3.5	5.6 ± 0.8	4.2	6.6
	Sr	6495 ± 5795	1028	16471	12607 ± 4866	2462	17060
	Th	0.06 ±0.03	0.03	0.13	0.11 ± 0.05	0.04	0.16
	U	0.04 ± 0.05	0.008	0.2	0.20 ± 0.19	0.014	0.58
TOC (mg dm^{-3})	TIC (as CO_3^{2-})	2.5 ±2.4	<0.5*	6.4	4.8 ± 4.9	<0.5*	13
	TOC (as C)	3.4 ±4.0	<0.5*	12	187 ± 113	63	374
pH		-	12.4	13.0	-	12.8	12.9

Analysis of organics in CDP

IC (Anions, mmol dm^{-3})	Species	Average ± SD	Min	Max
	ISA	0.41 ±0.24	<0.15*	0.77
	Lactate	2.0 ±1.6	0.22	5.7
	Formate	1.9 ± 1.2	0.4	4.6
	Acetate	0.66 ± 0.34	0.17	1.5

* LOD

Table 9.1 Composition of NRVB equilibrated water and CDP solution

Table 9.1 indicates that there are variations in the solutions used in the experiments. There are clear differences in ionic concentrations between the NRVB equilibrated water and CDP solution with the latter having a higher ionic strength. There are three potential reasons for this increase;

- The high temperature at which the CDP solution is produced dissolves more of the NRVB components
- The organic components are increasing solubility of some minor components by complexation.
- The CDP solution is made in contact with the components of NRVB and not pre formed NRVB.

There is potential for the higher ionic strength to affect diffusivity [60] and competition for sorption sites (see section 5) in the diffusion experiments. This is dealt with in the individual experimental sections where relevant.

Table 9.1 also indicates that there is significant variation between individual batches of NRVB equilibrated water used in the experiments. This was not anticipated and was most likely due to insufficient equilibration time in the presence of the NRVB and/or the removal of soluble components in the initial batches. These concentration variations also had the potential to affect diffusivity and competition for sorption sites. As a consequence and where possible, experiments requiring comparative data for an individual element, were undertaken with a single batch of NRVB equilibrated water.

The variation in organic content and specifically the low iso-saccharinic acid (ISA) content of the CDP solutions is potentially more significant. The reason for the low ISA content is likely to be sorption to one or more components of the NRVB.[141 142 29]

The potential for NRVB to sorb (or precipitate) ISA was briefly investigated at the start of the CDP advection experiments. The CDP advection experiments typically commence with a three day equilibration with the CDP solution. This equilibration period provided an opportunity to investigate whether ISA in the CDP solution would be retained on the NRVB cylinder.

Consequently samples were collected throughout the equilibration period and a selection from the beginning, middle and end of two runs were sent to Manchester University for analysis. The results along with the concentrations in the initial solution are shown in table 9.2 below:

	Sample	ISA (mM)	Lactate (mM)	Acetate (mM)	Propionate (mM)	Cl (mM)	SO_4 (mM)	NO_3 (mM)
	CDP initial	0.051	1.51	1.10	0.00	0.76	5.14	0.07
Run 1	4	nd	0.01	0.02	0.00	0.74	0.15	0.10
	7	nd	0.01	0.02	0.00	0.68	0.15	0.08
	10	nd	0.01	0.07	0.01	0.73	0.15	0.09
	12	nd	0.01	0.15	0.00	0.79	0.15	0.10
	14	nd	0.01	0.29	0.01	0.85	0.16	0.12
	18	nd	0.01	0.52	0.11	0.85	0.16	0.11
	23	nd	0.01	0.69	0.20	0.94	0.16	0.12
	31	0.002	0.85	0.79	0.33	0.93	0.16	0.11
	42	0.004	1.42	0.85	0.41	0.97	0.17	0.11
	50	nd	1.60	0.84	0.48	0.89	0.16	0.10
Run 2	3	nd	0.02	0.15	0.00	1.73	0.12	0.09
	4	nd	0.01	0.22	0.01	1.95	0.13	0.09
	6	nd	0.01	0.39	0.04	2.17	0.13	0.10
	7	nd	0.11	0.42	0.07	2.11	0.13	0.09
	8	nd	0.18	0.46	0.10	2.15	0.13	0.10
	10	nd	0.38	0.50	0.19	2.14	0.13	0.10
	12	nd	0.56	0.52	0.22	2.06	0.14	0.10
	16	nd	0.69	0.54	0.26	1.93	0.13	0.10
	20	nd	0.77	0.56	0.27	1.83	0.20	0.10
	24	nd	0.87	0.60	0.32	1.88	0.14	0.10

Table 9.2 Concentrations of CDP components during the equilibration phase of two advection experiments

The concentration of ISA for both runs is reduced below the quantitation limit (0.05 mM) after passing through the NRVB cylinder. This confirmed that ISA is being sorbed to the NRVB. The concentrations of lactate, acetate and chloride in the CDP solution fall initially as residual pore water is displaced from the NRVB and begin to rise back to their initial concentrations. Sulphate concentration is reduced significantly suggesting precipitation (this may eventually reduce porosity and flow rate). The propionate concentration rises from below detection to a maximum of 0.48 mM during the runs. Propionate is known to be generated late (~180 days) in the evolution of CDP. [28] [142] The results above suggest that advection through NRVB initiated the production of propionate.

This research is not focussed on the nature of the organics present in CDP but clearly the results in table 9.2 suggest that there is a significant and dynamic interaction between the CDP components and NRVB.

9.3 Diffusion and Elution Profiles.

The form of the majority of the diffusion and elution profiles obtained in this research initially showed rapid diffusion with a steep slope, followed by a smooth reduction in rate until the concentration in the solution in contact with the solid reached a stable condition. This kind of profile is certainly not unique and it has been previously described for the migration of Cs in cementitious material. [48] [70] [143] [144] [145] This kind of profile has been explained [143] by considering two diffusion paths for the migrating ion; fast migration through pathways of few microns and slower movement through the network of submicron pores. A similar explanation [145] proposed that, as the initial phase of the migration commences, the larger pores are filling relatively quickly with the migrating ions and in the later stage the rate of migration slows down as it moves through the smaller pores. Consequently, the rate of migration does not only depend on the overall porosity of the material but also the pore size distribution and connectivity. For NRVB specifically it has been argued [146] that the distribution of pore sizes (from 800 to 0.16 nm) could explain the two phases observed in the elution profiles.

10.0 Tritiated Water (HTO)

10.1 Background

Tritiated water contains the radioactive hydrogen isotope tritium ($^{3}_{1}\mathrm{H}$ or T) which is a β emitter. The maximum energy of the β electron is low at 18.6 keV and tritium decays to $^{3}_{2}\mathrm{He}$ with a half-life of 12.32 years,[147] an electron anti-neutrino is also released. The decay equation is:

$$^{3}_{1}\mathrm{H} \rightarrow {}^{3}_{2}\mathrm{He} + {}^{0}_{-1}e + \bar{\nu}_{e}$$

Tritium in the environment arises from three sources; natural occurence due to the interaction of oxygen and nitrogen with cosmic radiation, from historic nuclear weapons testing and from operational nuclear reactors.[148] [149] In the past tritium has not been regarded as a serious pollutant. However as the worldwide inventory of tritium falls, attention focusses on the environmental emissions, current and historic from nuclear power plants and risk based assessments and clean ups are being demanded by regulators.[150]

Tritiated water is chemically very similar to water and consequently it is an effective tracer for water in aqueous systems.

The HTO experiments were undertaken to provide confidence that the diffusion and advection techniques worked satisfactorily and reproducibly. There was also an assumption that tritiated water represented the most conservative species available to check that the GoldSim transport model was working correctly at a physical level i.e. without incorporating partition.

The experiments undertaken were as follows

- Diffusion with NRVB equilibrated water
- Advection with NRVB equilibrated water
- Advection with CDP solution.

In addition a parallel experiment using a 3:1, PFA:OPC waste packaging grout was commenced but this is not referred to further in this section.

10.2 Additional Experimental Details for HTO Diffusion Experiments

The diffusion experiment utilised a 1.8 cm^3 addition of $1.7x10^{-9}$ mol dm^{-3} HTO to the central core of duplicate NRVB cylinders equivalent to 3317 Bq (or 199035 d min^{-1} where d = disintegrations). The addition was made in the "dispensing area" of the laboratory not in the nitrogen glove box, the cylinder was sealed, submerged in 200 cm^3 NRVB equilibrated water and returned to the glove box over a period of less than two minutes. The total volume of equilibrated water in the system is assumed to be 225 cm^3 (the additional 25 cm^3 being an estimate of the pore water volume in the NRVB cylinder). HTO activity concentrations were determined using liquid scintillation counting [151] [152] on a Packard 2100 TR liquid scintillation counter with GoldStar Multi-purpose liquid scintillation cocktail. Samples were taken throughout the experimental duration but all determined on one day when the experiment was completed to negate the need to correct for radioactive decay. In addition "control" samples were made at the start of the experiment to enable recovery graphs to be made. The control samples and appropriate blanks were also determined on the same day as the samples from the experiments. All determinations were subject to the 2 σ criterion available on the Packard counter to provide confidence that the results were statistically valid.

10.3 Results HTO NRVB Diffusion with NRVB equilibrated water

Figs. 10.1 and 10.2 below show the complete data and early data for the diffusion experiments, the plots are presented as the average of two duplicate samples. The vertical error bars denote the 90% confidence limits assuming a two tailed t distribution and horizontal error bars are set at +/- 0.25 days. Tabulated results are presented as table 10.1 in appendix 1. Fig 10.3 presents the recovery of HTO from the NRVB cylinder as the experiment progressed. The maximum achievable activity concentration (C_{max}) was 885 d min^{-1} cm^{-3} (=199035/225). A value of 1.00 implies that 885 d min^{-1} cm^{-3} was achieved and all the HTO was distributed evenly throughout the system, a value of zero implies that all the HTO remains within the cylinder.

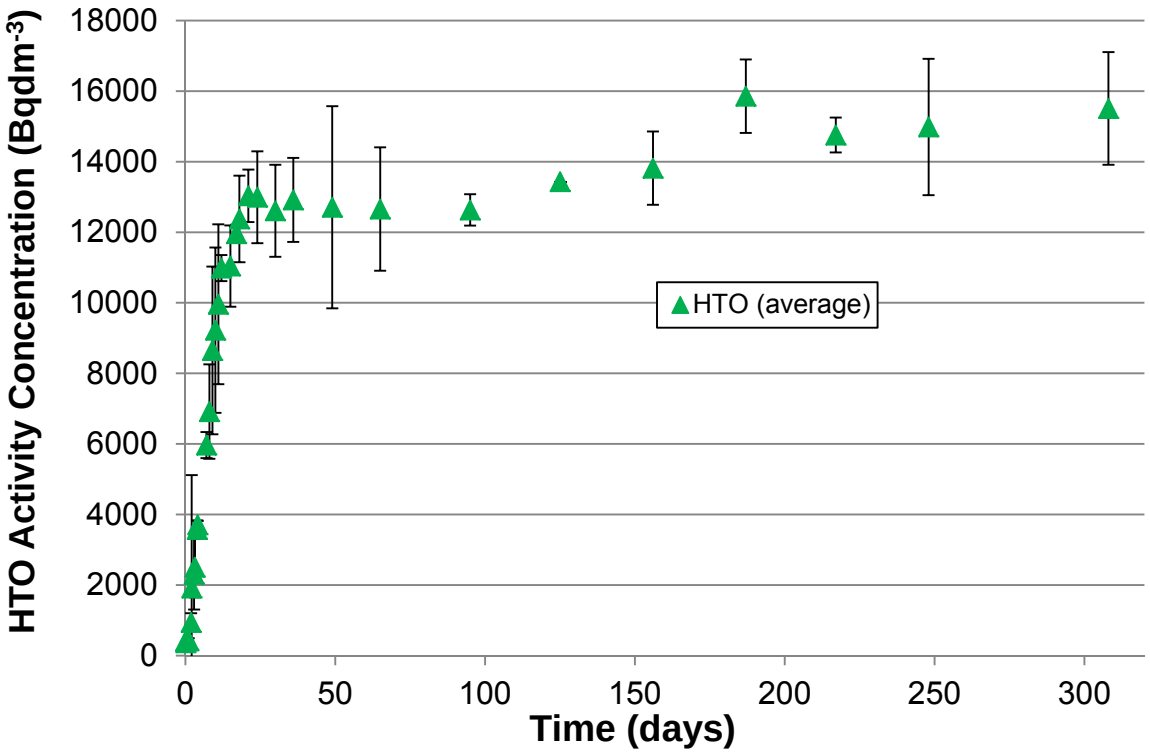

Fig. 10.1 Plot of HTO activity concentration vs time for the NRVB equilibrated water diffusion experiment

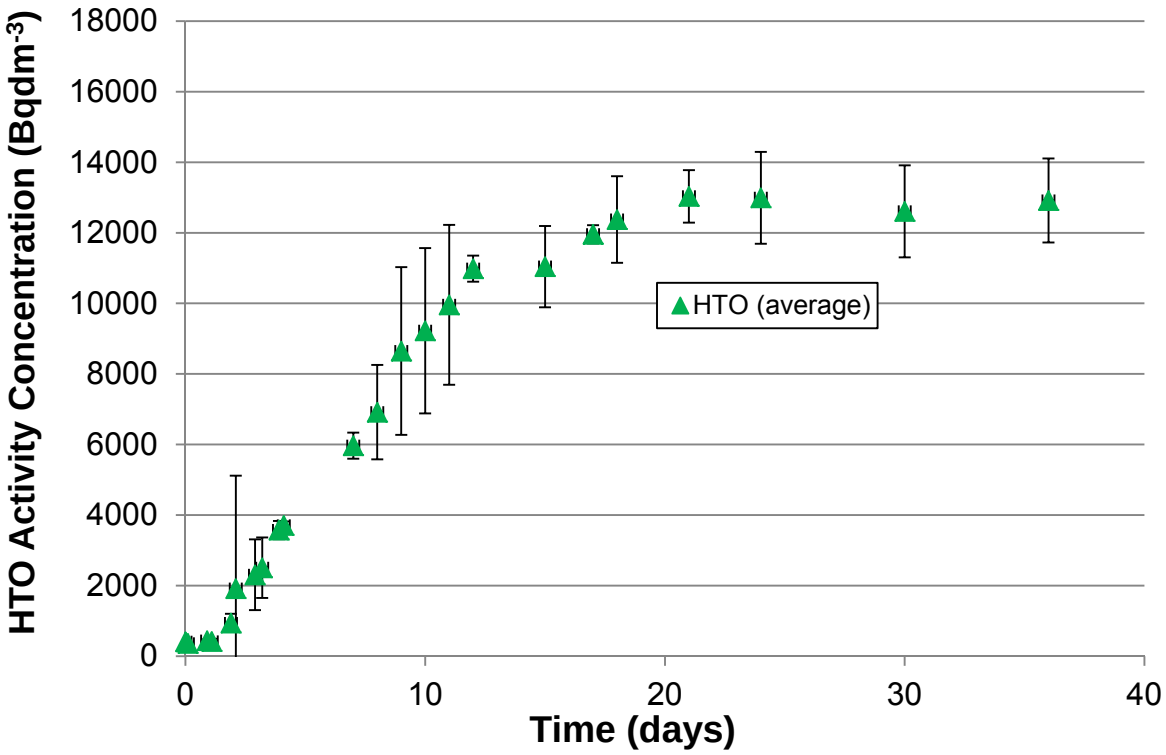

Fig. 10.2 Early data plot of HTO activity concentration vs time for the NRVB equilibrated water diffusion experiment

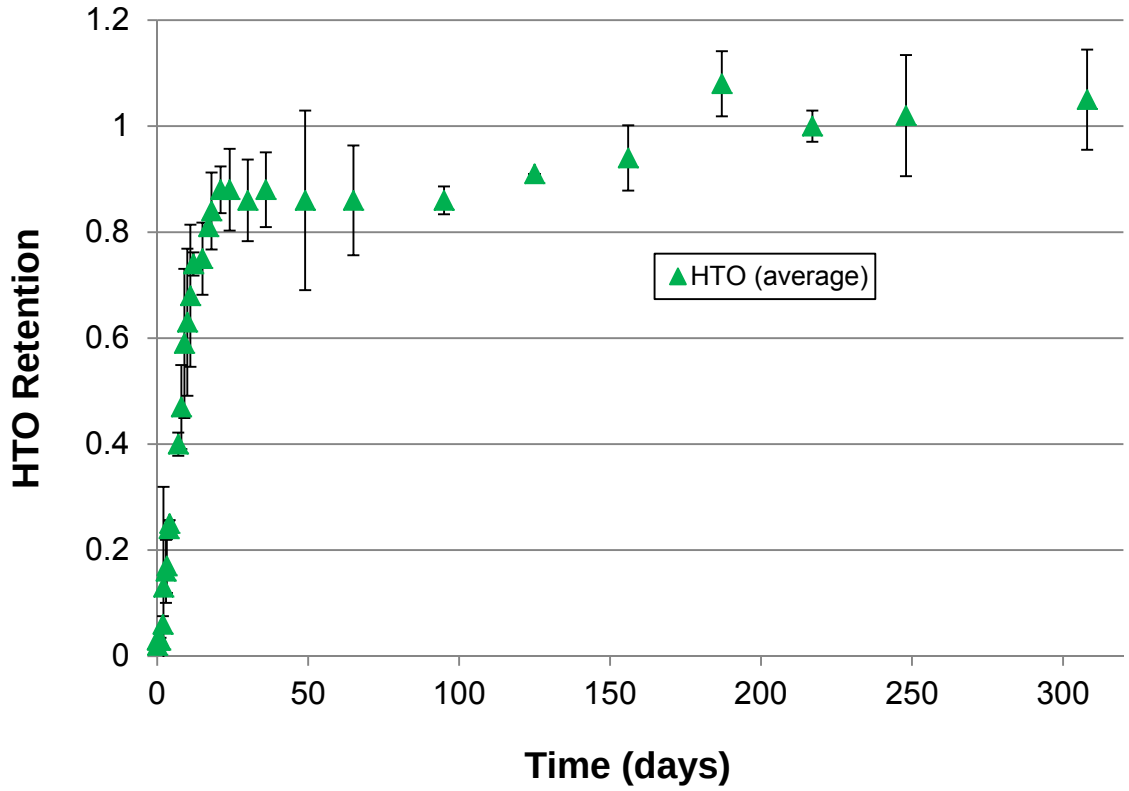

Fig. 10.3 HTO Retention vs time for the NRVB equilibrated water diffusion experiment

The plots show breakthrough at just less than 2 days followed by a smooth almost linear initial increase in concentration which can be seen in more detail on the early data graph, fig. 10.2. The rate of diffusion then slows at around 20 days and remains stable until almost 100 days. Recovery during this period is around 0.85 i.e. about 85% of the total HTO inventory is in solution. The HTO concentration in solution then continues to rise slowly up to 187 days when recovery reaches 1.08, significantly exceeding 1.00. The trend of the later data on the recovery plot suggests that the 187 day data point is anomalous even though the high result was repeated in both samples. The rising trend shows recovery in the later part of the experiment consistently exceeding 1.00, suggesting that more HTO has been recovered than was originally added to the experiment.

The suggestion that HTO recovery might exceed 1.00 implies that a mass balance should be undertaken to check that the liquid scintillation technique used to determine HTO activity concentration was functioning reasonably.

The control sample activity concentration of 199035 d min^{-1} (realistically 199000 d min^{-1}) represents the start activity at 308 days into the experiment.

By day 308, a total of 32 x 1 cm^3 samples had been taken from each experiment leaving 193 cm^3 (225-32) in each container.

The activity concentrations of samples 1 and 2 at day 308 were 909 and 952 Bq min^{-1} cm^{-3} respectively.

The total number of d min^{-1} in sample 1 and sample 2 were 175473 (909x193) and 183736 (952x193) respectively.

The activity in d min^{-1} removed during sampling is provided in table 10.1 in appendix 1 and is 16696 for sample 1 and 17092 for sample 2.

Adding the inventory in the sample containers to the amount removed by sampling should equal the original inventory represented by the control sample.

Sample 1 = (175473+16696) = 191679 d min^{-1}
Sample 2 = (183736+17092) = 200364 d min^{-1}
Average = (191679+200364)/2 = 196022 d min^{-1}

The average for samples 1 and 2 compares well with the control sample being smaller by only 1.5%.

Control samples at three different activity concentrations were tried due to concerns about reproducibility caused by chemiluminescence at high pH, quenching, detector efficiency across the concentration range and old HTO stocks. The control sample detailed in the mass balance above was made using 200 µL of the original HTO with 10 cm^3 of the scintillation cocktail. The result was multiplied by 9 to provide the equivalent result for 1.8 cm^3 of HTO addition. A control sample was also made using 1.8 cm^3 of the original HTO and 10 cm^3 of the scintillation cocktail produced erroneously low result of 143729 d min^{-1} suggesting the detector may have been saturated [ref]. Finally a series of 10x10 µL samples were made with 1 cm^3 of NRVB equilibrated water and 10 cm^3 of scintillation cocktail added. The results had an

average of 995 d min^{-1} with a high of 1100 d min^{-1}, a low of 908 d min^{-1} and a standard deviation of 73 d min^{-1}. The results were multiplied by 180 to enable comparison, yielding an average of 179100 d min^{-1} with a low of 163440 d min^{-1} and a high of 198000 d min^{-1}.

It is clear that there was a lack of precision in the control samples used for the tritium analyses. This cast doubt on the use of retention plots because the start concentration needs to be stated accurately. A further problem arises because C_{max} will change each time a sample is taken (because activity and volume are removed in different proportions). In later experiments a correction is applied to ensure C_{max} is correctly evaluated. These issues are revisited in the HTO modelling section (section 10.6) where the concept of a data envelope is developed and used.

10.4 HTO Advection Experiments

10.4.1 Additional Experimental Details for HTO NRVB Advection Experiments

A 50 µL injection of tritiated water was used for this experiment, delivering 1765 Bq or 105900 d min^{-1} into the central core of the NRVB cylinder, the nitrogen pressure driving the NRVB equilibrated water through the cylinder was fixed at 12 psi but rose to 16 psi throughout the duration of the experiment.

The results below have been subjected to a correction for evaporative losses during the collection of the samples. This was done using a blank tube containing a known weight of deionised water and monitoring it throughout the experiment. Evaporation rates were calculated per hour and corrections applied accordingly. The rate of evaporation of HTO and non tritiated water were assumed to be equal.

The results are shown as figs. 10.4 and 10.5 and presented in table 10.2. The control samples were made by taking 50 µL of the same HTO and diluting it with 50 cm^3 of deionised water. Two control samples were made each using 1 cm^3 of the diluted solution and 10 cm^3 of scintillation cocktail. The results were 2104 and 2132 d min^{-1} cm^{-3}, the average of the two results was multiplied by 50 to give the 105900 d min^{-1} estimate of HTO activity in the injection. Blanks were prepared and all results have been corrected accordingly.

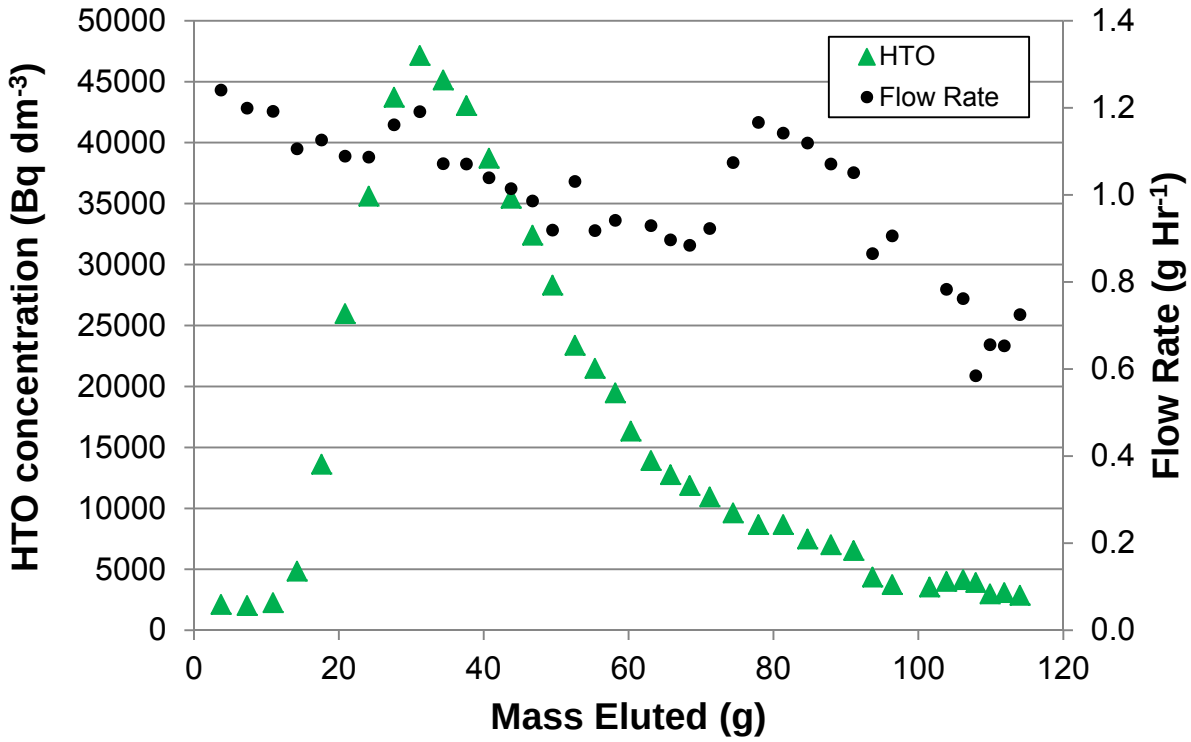

Fig. 10.4 Plot of HTO NRVB advection results using NRVB equilibrated water

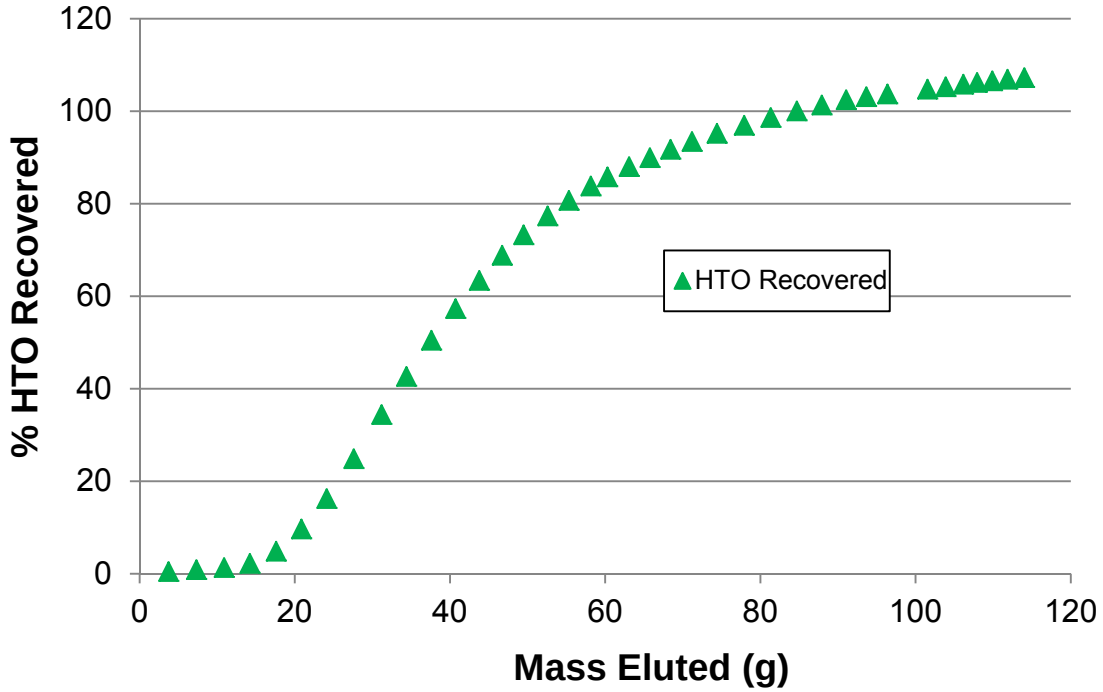

Fig. 10.5 Plot of recovered HTO from the NRVB advection experiment using NRVB equilibrated water

10.4.2 Results

The results are shown with mass eluted on the x axis; this parameter was selected as it appeared to be a better way of comparing data for the different dissolved ions being investigated. It would be more conventional to show time on the x axis but the variation in flow rate seen across the range of advection experiments means that time is not the best comparator. Nevertheless, flow rates and time have been recorded because they are needed for the GoldSim modelling (see section 10.6).

It can be seen from figs. 10.4 and 10.5 that the advection experiment progressed smoothly and the HTO peak broke through between 11 and 14 g of eluted mass (between 9 and 12 hours into the experiment). Porosity of the NRVB cylinder can be roughly estimated using the value at 50% of the upslope [153] which is approximately 21 g, the nominal volume of the cylinders is 48 cm^3 (50 cm^3 - 2 cm^3 for the central hole), the experimental estimate of porosity is therefore 21/48 = 0.44, which compares reasonably to the published porosity of 0.5. The flow rate can be seen to be generally falling over the course of the experiment. Also, the driving pressure though initially low, increased throughout the experiment (from 12 to 16 psi) suggesting that blocking could be occurring.

The recovery plot suggests that over 100% of the HTO has been recovered. The recovered amount is 107% of the amount added and whilst the discrepancy is not overly large and accepting the “wet and dirty” nature of the experiments, it must be regarded as significant. It is also noticeable that the discrepancy is very similar to that seen in the HTO NRVB diffusion experiments even though a different HTO source was used and extra care was taken to produce control samples in the anticipated eluent concentration range. It is known that the vapour pressure of HTO in an enclosed system (containing only HTO and water) is approximately 20% lower than that of water at ambient temperatures. [154] This implies that the mass of HTO evaporated is likely to have been over estimated. An accurate correction cannot be made because the advection experimental sample collection equipment is not enclosed and the relative rates of evaporation for HTO and water are also dependent on other variables including, ionic strength of the solution (intermolecular forces) and relative humidity of the atmosphere.

10.5 HTO CDP Advection Experiment Results

10.5.1 Additional Experimental Detail for the HTO CDP Advection Experiments

Prior to injection of HTO the NRVB cylinder was "run in" with the CDP solution for a period of 3 days at the anticipated experimental flow rate (1.0 cm^3 hr). As a consequence approximately 3 pore volumes (70 - 75 cm^3) of the CDP solution had passed through the cylinder prior to the experiment commencing.

A 50 µL injection of HTO water was used for this experiment, delivering 2100 Bq or 126000 d min^{-1} into the central core of the NRVB cylinder, the nitrogen pressure driving the NRVB equilibrated water through the cylinder was fixed at 20 psi throughout the duration of the experiment. The results are presented as figs. 10.6 and 10.7 and table 10.3.

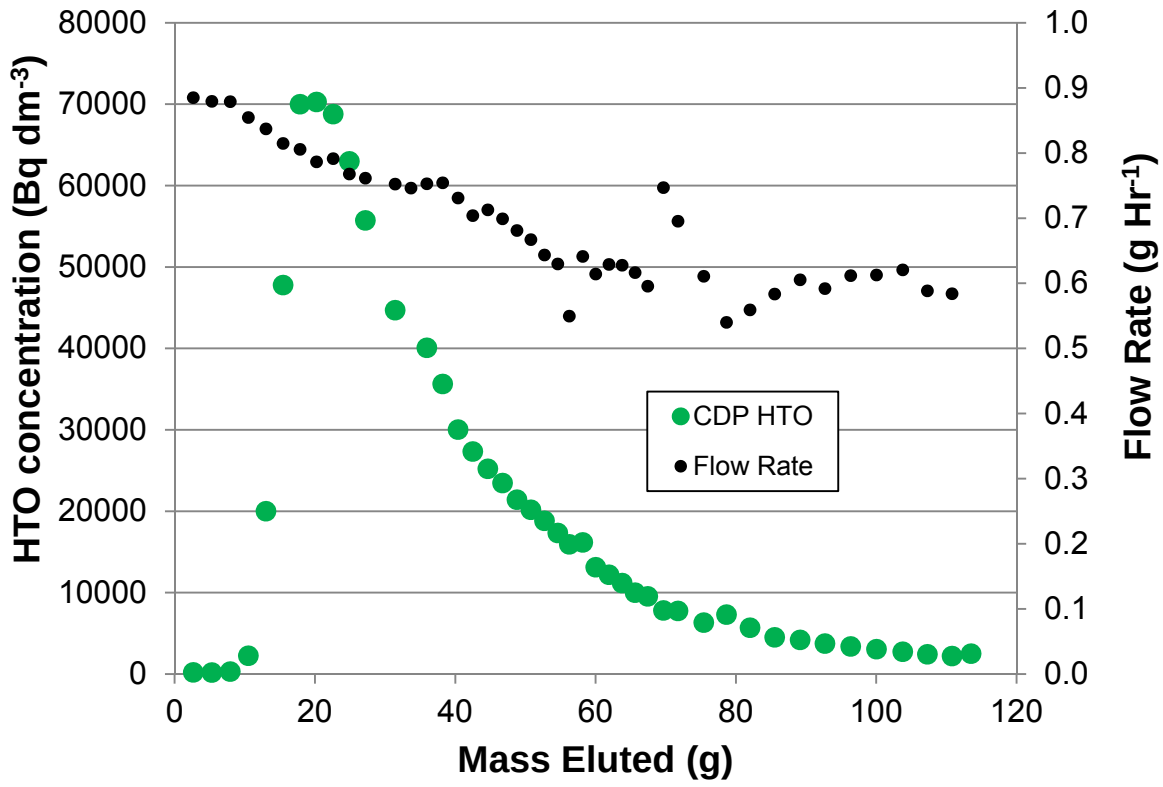

Fig. 10.6 Plot of HTO NRVB advection results using CDP solution

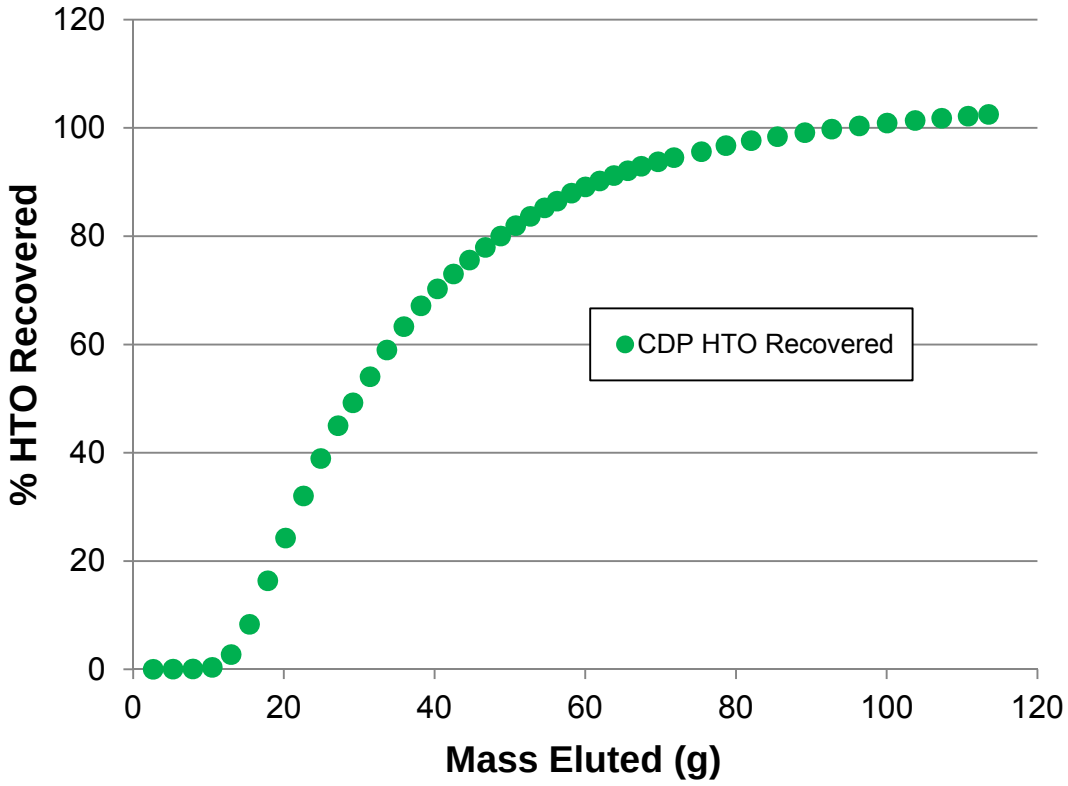

Fig. 10.7 Plot of recovered HTO from the NRVB advection experiment using CDP solution

10.5.2 Results

It can be seen from figs. 10.6 and 10.7 that the advection experiment progressed smoothly and the HTO peak broke through between 8 and 10 g of eluted mass (between 7 and 10 hours into the experiment), quicker than the equivalent NRVB equilibrated water experiment. The flow rate can be seen to be falling over the course of the experiment and the driving pressure was maintained 20 psi. The steady decrease in flow rate at constant pressure suggests blocking may be occurring.

The recovery plot suggests that over 100% of the HTO has been recovered. The recovered amount is 102% of the amount added. The discrepancy is small and accepting the “messy” nature of the experiments, it is not significant (see comments regarding HTO evaporation at the end of section 10.4.2). The same HTO source was used as used in the NRVB equilibrated water advection experiment and again care was taken to produce control samples in the anticipated eluent concentration range.

10.6 GoldSim Transport Modelling of HTO Diffusion and Advection Results

The construction of the GoldSim models used is described in section 8. The output files from the models are very large (typically several thousand data points) and as a consequence the data are presented graphically only and not in tabular form.

10.6.1 HTO NRVB Diffusion Model

The model results and observed data for the HTO diffusion experiments are presented as figs. 10.8 and 10.9; the second figure shows the early data from the experiment.

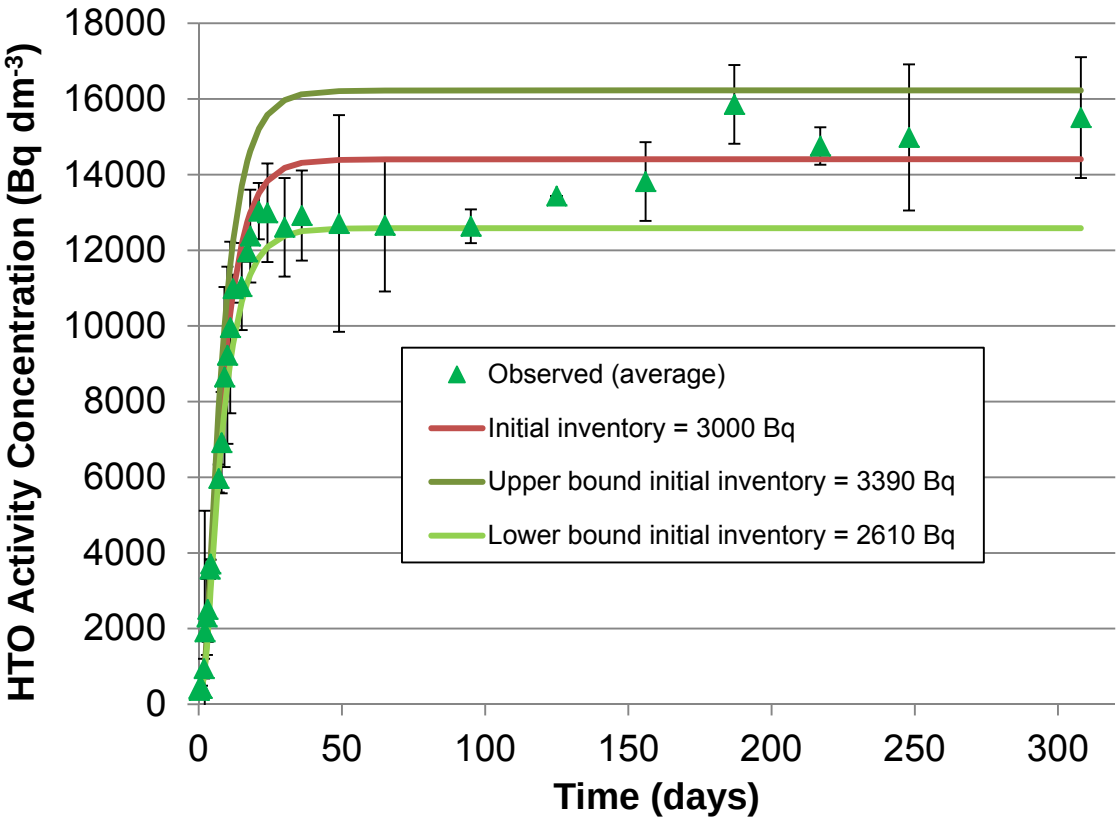

Fig. 10.8 GoldSim model of HTO NRVB diffusion experiments

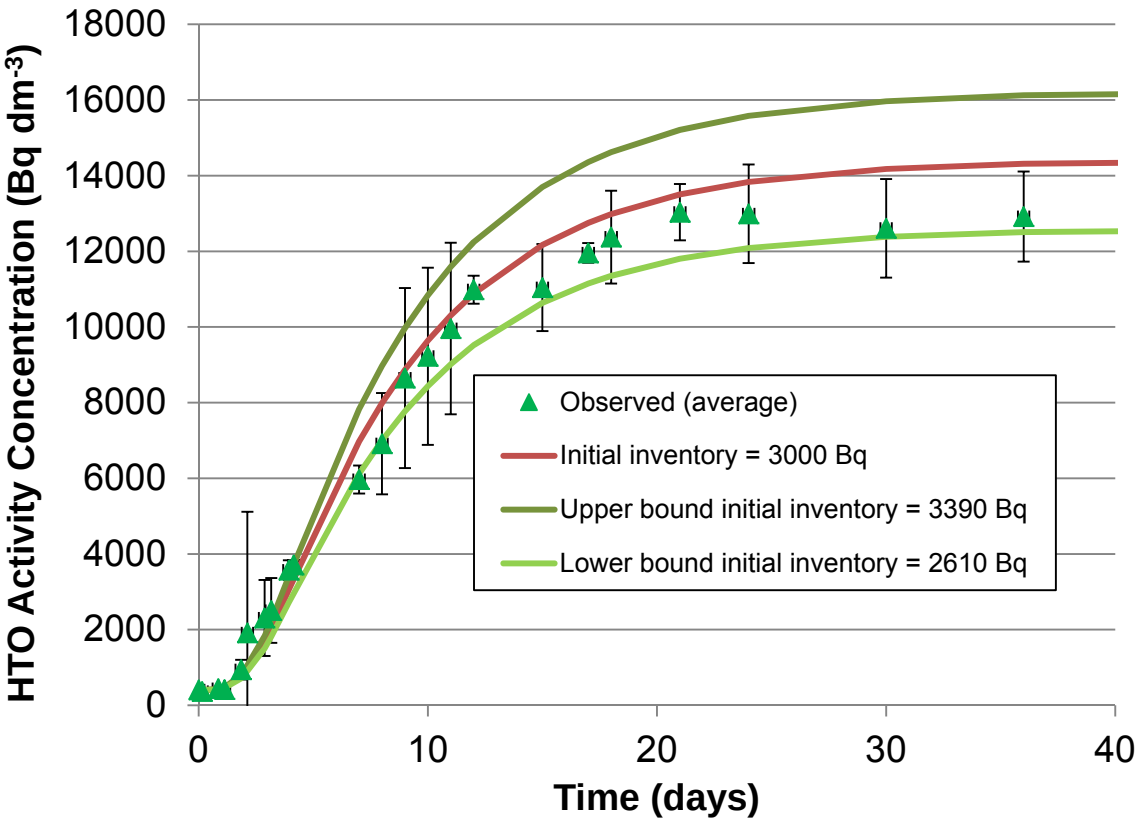

Fig. 10.9 Early data from GoldSim model of HTO NRVB diffusion experiments

The uncertainty over the starting HTO concentration for the diffusion experiments led to an approach for the modelling where a "data envelope" was created between 2610 Bq (156600 d min^{-1}) and 3390 Bq (203400 d min^{-1}). These are the lower and upper values determined in the 10 µL control samples (see section 10.3) with a +/- sampling error of 50 µL on the 1.8 cm^3 addition (made with a graduated glass pipette). The upper boundary also encompasses the 199035 d min^{-1} control sample. The average of the two values is 3000 Bq and an LOF analysis was undertaken to determine the effective diffusivity at which the minimum LOF would be achieved for the 3000 Bq curve. The full dataset from the analysis is not reproduced here but the early straight line part gave a minimum LOF of 9.1% at a D_e of 0.75x10^{-10} m^2 s^{-1} and the whole data set gave a minimum LOF of 8.4% also at the same D_e of 0.75x10^{-10} m^2 s^{-1}. Consequently, the model curves shown in figs. 10.8 and 10.9 have D_e set at 0.75x10^{-10} m^2 s^{-1} and use no partition.

The majority of the observed data fits inside the envelope apart from a few results during the first 8 days as can be seen on fig 10.10 below.

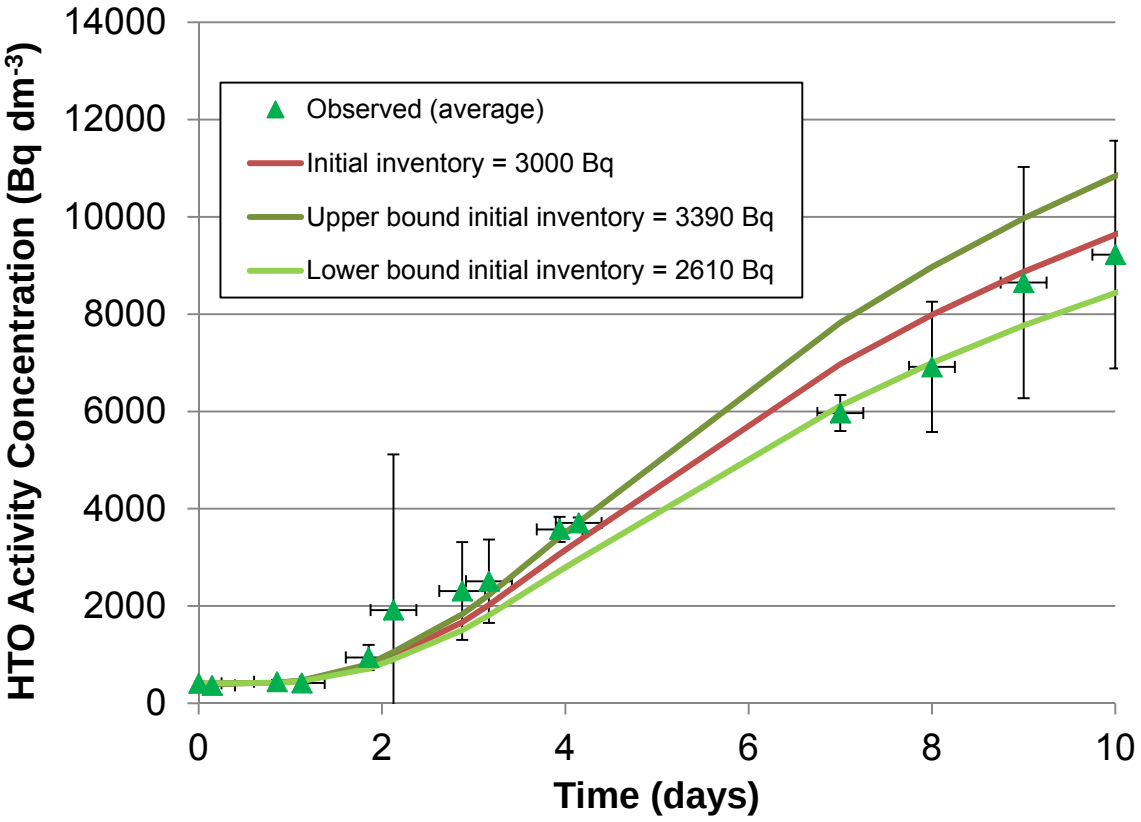

Fig. 10.10 Early data showing minor deviations from GoldSim model of HTO NRVB diffusion experiments

10.6.2 HTO Advection Models

The model results and observed data for the HTO diffusion experiments are presented as figs. 10.11, 10.12 and 10.13. The parameters used to generate the model curves are presented immediately below the respective figures. The stepped appearance of the observed data curves occurs because each data point extends over a period of time (and mass of eluent). Time is presented on the x axis and not eluted mass because the GoldSim model is easier to manipulate and was found to produce better results against a time base. The statistical approach used in the diffusion modelling was not considered appropriate with the advection data because the experimental methodology is still in the trial stage.

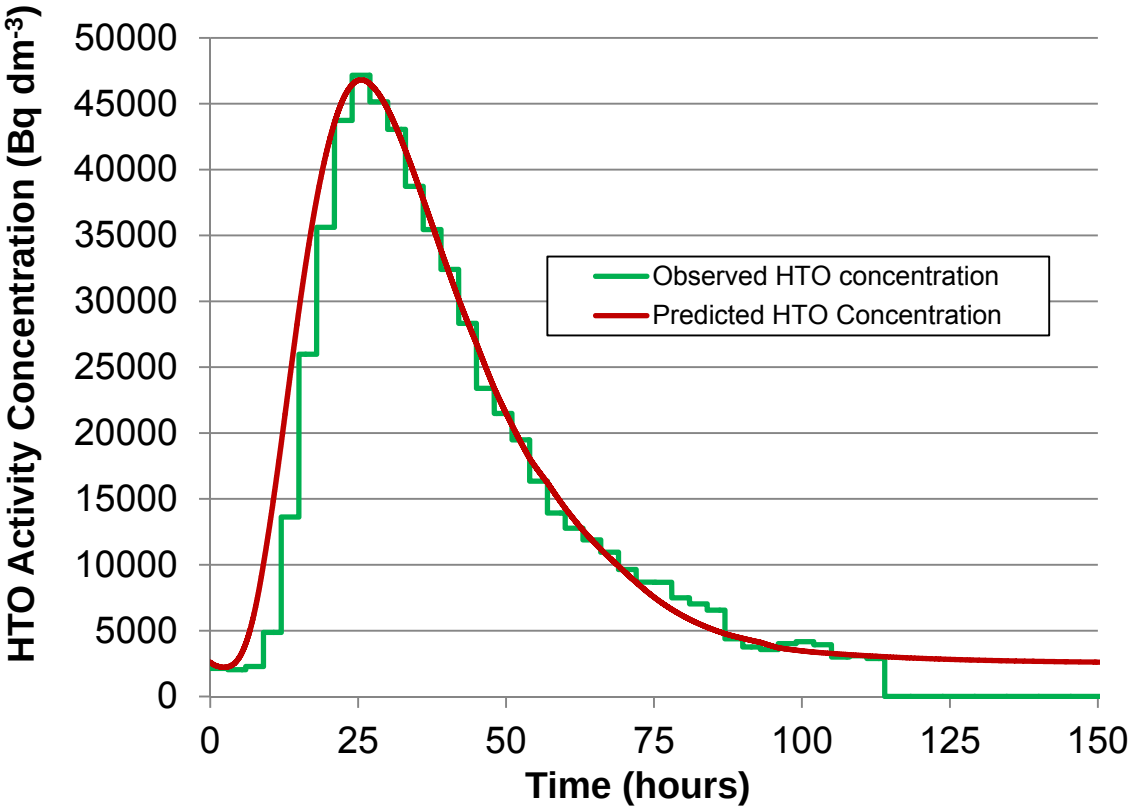

Fig. 10.11 Observed and GoldSim predicted data for the advection of HTO in NRVB equilibrated water

Model Parameters

- porosity = 0.5
- start inventory = 1765 Bq HTO
- D_e = 0.75x10^{-10} m^2 s^{-1}
- background = 2500 Bq dm^{-3}
- K_d = 0.18x10^{-3} m^3 kg^{-1}

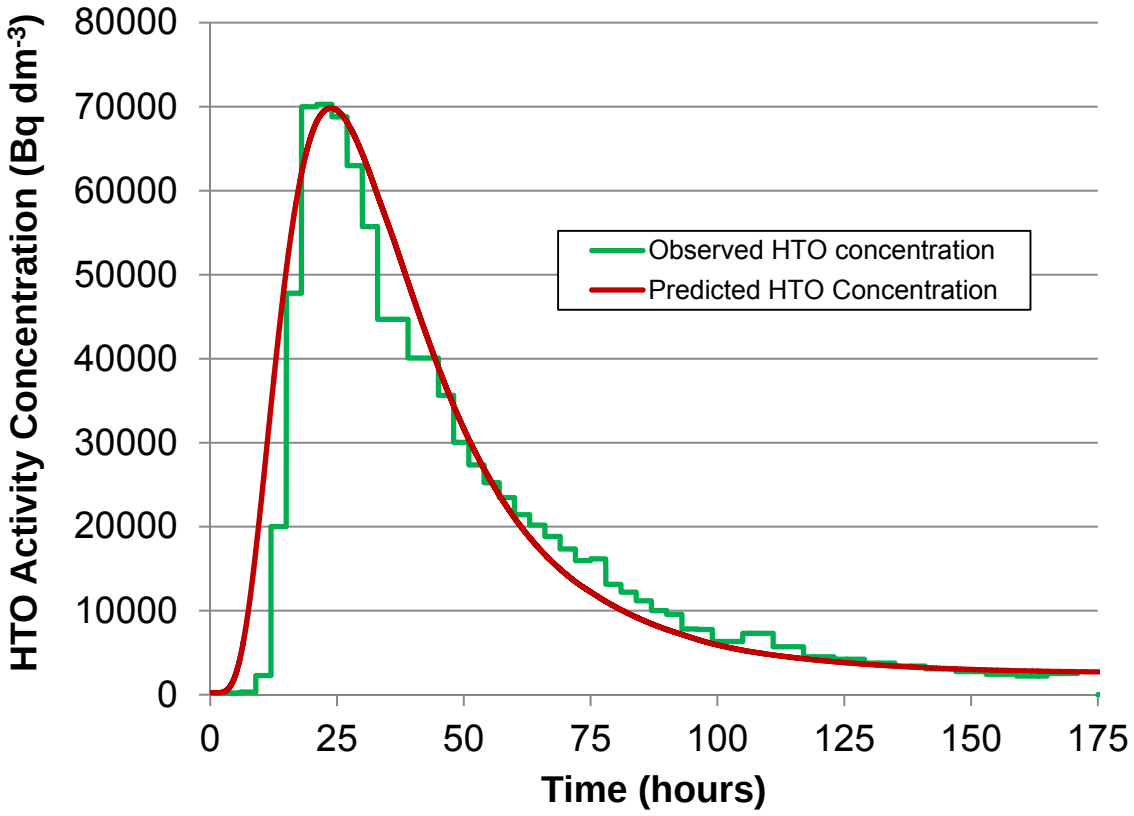

Fig. 10.12 Observed and GoldSim predicted data for the advection of HTO in CDP solution

Model Parameters

- porosity = 0.5
- start inventory = 2100 Bq HTO
- D_e = 0.75x10^{-10} m^2 s^{-1}
- background = 2500 Bq dm^{-3}
- no partition

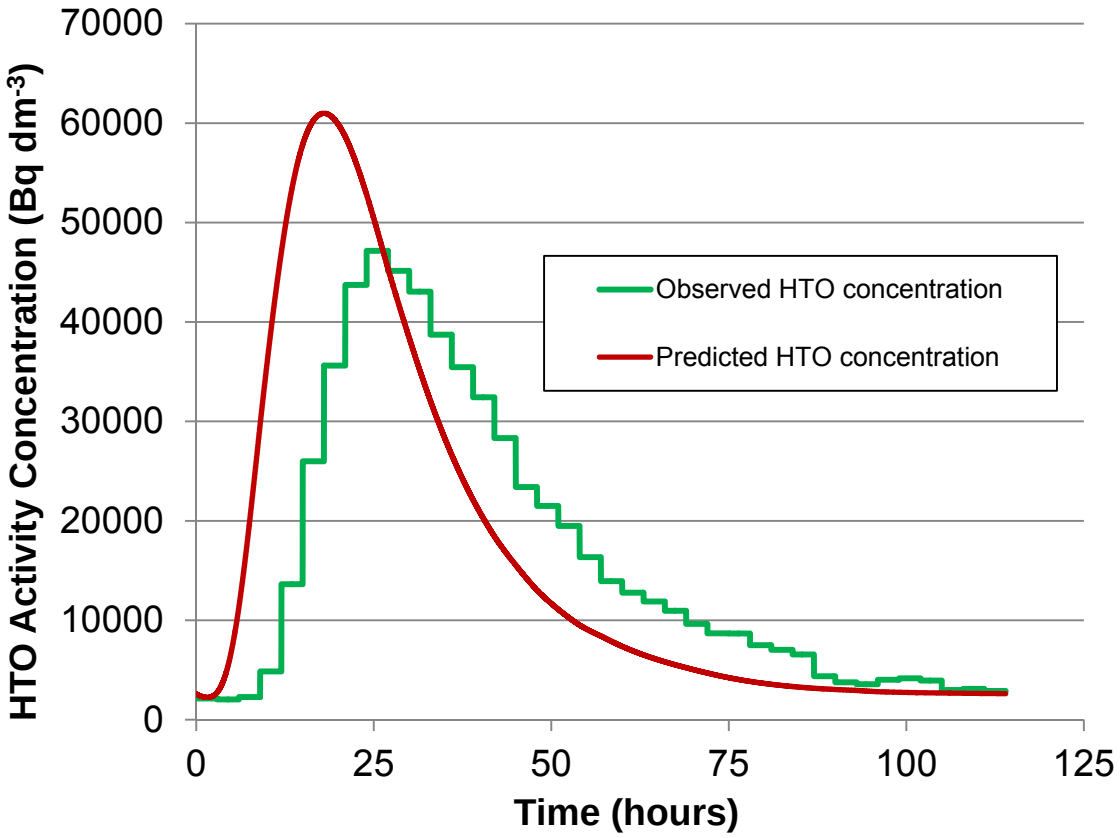

Fig. 10.13 Observed and GoldSim predicted data for the advection of HTO in NRVB equilibrated water

Model Parameters

- porosity = 0.5
- start inventory = 1765 Bq HTO
- D_e = 0.75x10^{-10} m^2 s^{-1}
- background = 2500 Bq dm^{-3}
- no Partition

Commentary

Fig. 10.11 shows that the elution curve for HTO in NRVB equilibrated water can be readily modelled. The main point of interest is that a small amount of partition was required to produce an accurate match. This suggests that HTO is sorbed preferentially over water. This behaviour has been observed on silica gels in other studies [155] [156] and was shown to be dilution of the adsorbed HTO by isotopic exchange with non-tritiated water and hydroxyl groups present in the matrix. A similar mechanism involving CSH waters of crystallisation [70] could be responsible for the behaviour observed in the NRVB advection experiments.

Fig. 10.12 shows the elution curve for HTO in the CDP solution is also readily modelled. The main points of interest are that the advection is faster in the presence

of CDP and that partition is not required to produce an accurate match. The difference between the two plots is small but noticeable. The effective diffusivity used for both diffusion and advection models, is comparable, [157] if a little lower than literature values (see table 17.1). For comparison, fig. 10.13 shows the effect of modelling the advection results of HTO in NRVB equilibrated water without partition and it can be seen that there is a clear mismatch. The limitations of the GoldSim model mentioned in section 7.5 are also relevant.

There are a number of potential explanations for the results:

- One or more of the CDP components is chemically interacting with the NRVB preventing access to the exchangeable water in the NRVB matrix.
- Some tritium is exchanged into the CDP components which have different sorption characteristics (see section 9) and its migration behaviour is changed as a consequence.
- The physical nature of the NRVB is changed by the process of advection and/or exposure to CDP and that the experiments have been undertaken at different stages of the physical evolution of the NRVB.
- The results simply exhibit the range of possible outcomes and the presence of CDP is not having an effect i.e. the results are a reflection of the reproducibility of the experiments.

In addition to the silica gel studies referred to above this non-conservative behaviour of HTO has also been observed in cementitious matrices. Some authors,[66] [156] attributed the deviation mainly to isotope exchange of tritium for hydrogen in the cement. It has also been proposed [77] that if isotopic exchange was indeed the main process affecting HTO migration, the R_d for HTO should correspond to the fraction of water bound to the cement. However, the expected R_d values obtained from ignition of the cement samples were between 2.5 and 4 times higher than the values determined from batch sorption or through-diffusion experiments. This suggests that there are other factors in addition to isotopic exchange that could affect HTO migration. These could include occluded or variably accessible pore space (see section 9.3 for additional information).

It was realised before starting the experimental programme that prolonged advection could have a physical effect on the NRVB cylinders and consequently new blocks were used for each experiment. The reproducibility of the advection experiments has not been investigated and in particular the effect of running many consecutive experiments on the same NRVB cylinders.

More confirmatory data may be gathered from the diffusion experiment for HTO using CDP solution which has yet to be undertaken.

The information provided by these experiments is interesting and the successful application of a type of model usually used on a much larger scale suggests that the techniques can be used to compare the migration of radionuclides in porous solids.

11.0 Caesium

11.1 Background

The main Cs isotope of interest is ^{137}Cs, it is an important component of the UK radioactive waste inventory and is mentioned along with ^{135}Cs and ^{134}Cs in the latest estimate at 01/04/2010 [26], table 11.1 below reproduces the relevant activities.

Isotope	HLW	ILW	LLW	units
^{137}Cs/^{137m}Ba	4.2x10^{7}	1.1x10^{6}	8.0	T Bq
^{135}Cs	1.9x10^{2}	6.8	1.5x10^{-4}	T Bq
^{134}Cs	2.5x10^{5}	4.8x10^{3}	4.4x10^{-2}	T Bq

Table 11.1 Radioisotopes of Cs in the UK waste inventory at 01/04/2010

^{137}Cs has a half live of 30.17 years, about 95% of the decays are by beta emission to ^{137m}Ba a metastable isomer; ^{137m}Ba decays to the ground state with gamma emission and has a half-life of about 153 seconds.[147] It is this decay product that makes ^{137}Cs an external hazard, it is also the emission commonly used to quantify ^{137}Cs as is the case in the Cs advection and diffusion experiments described in the following sections. The specific activity of ^{137}Cs is 3.22x10^{12} Bq g^{-1} and the decay equation is:

$$^{137}_{55}Cs \rightarrow {}^{137m}_{56}Ba + {}^{0}_{-1}e \rightarrow {}^{137}_{56}Ba + \gamma$$

The maximum energy (E_{max}) of the main beta emission is 0.51MeV (95%) and the energy of the main gamma emission from ^{137m}Ba is 0.66MeV (85%).[158]

^{137}Cs can be formed in nuclear reactors when an atom of ^{235}U splits asymmetrically into two large fragments generating fission products with mass numbers between 90 and 140, additional neutrons are also generated by this fission. ^{135}Cs and ^{137}Cs are produced with relatively high yields of about 7% and 6%, respectively. ^{137}Cs is present in spent nuclear fuel, high level radioactive wastes resulting from the processing of spent nuclear fuel, and radioactive wastes associated with the operation of nuclear reactors and fuel reprocessing plants. ^{137}Cs is an isotope of concern from an environmental management perspective; it is an alkali metal and can be very mobile in the groundwater environment. ^{137}Cs is present in soil around the world largely as a result of fallout from past atmospheric nuclear weapons tests it

is also present as a contaminant at locations such as nuclear reactors and facilities that process spent nuclear fuel.[159] As a consequence the potential migration of Cs through and beyond a GDF is significant to researchers in the area.

The experiments undertaken were as follows:

- Diffusion with NRVB equilibrated water using ^{137}Cs tracer only and ^{137}Cs tracer plus $CsNO_3$ carrier
- Diffusion with CDP solution with ^{137}Cs tracer and with ^{137}Cs tracer plus $CsNO_3$ carrier
- Mixed element diffusion experiments (NRVB equilibrated water and CDP solution) where Cs diffusion is evaluated in the presence salts containing Ni, Eu, U, Th and I.
- Advection with NRVB equilibrated water and ^{137}Cs tracer only

Autoradiographs for the diffusion experiments have also been produced along with gamma spectroscopy of the residual ^{137}Cs in the NRVB cylinders to complete a mass balance. Environmental SEM micrographs and EDX analyses are also included. GoldSim transport models have been generated for the ^{137}Cs diffusion experiments. Reference is also made to a series of solubility experiments (under and over-saturation) underway in the Loughborough Radiochemistry laboroatory as part of the NDA chemical containment research.

11.2 Additional Experimental Details for ^{137}Cs Diffusion Experiments

The diffusion experiment utilised a 50 µl addition of ^{137}Cs (produced as the nitrate in nitric acid by Perkin Elmer) to the central cores of duplicate NRVB cylinders, equivalent to:

- C_{max} of 2661 d min^{-1} (9979 Bq per cylinder and an initial concentration in the inner core = $1.5x10^{-8}$ mol dm^{-3}) for NRVB equilibrated water with ^{137}Cs tracer only.
- C_{max} of 2631 d min^{-1} (9866 Bq per cylinder and an initial concentration in the inner core = $1.5x10^{-8}$ mol dm^{-3}) for CDP solution with ^{137}Cs tracer only.
- C_{max} of 3088 d min^{-1} (11580 Bq per cylinder and an initial concentration in the inner core = $1.8x10^{-8}$ mol dm^{-3}) for both the NRVB equilibrated water and CDP solution ^{137}Cs tracer with $CsNO_3$ carrier

C_{max} is the maximum possible number of disintegrations per minute in the 1 cm^3 sample if the ^{137}Cs was to equilibrate completely with the liquid in the system. The results figures and tables also utilise a calculation to account for the effect on C_{max} caused by the removal of volume and activity during sampling. A disproportionately small amount of activity is removed during sampling compared to volume, the overall effect is to increase C_{max} each time a sample is taken. C_{max} is used to prepare the relative retention plots to enable visualisation of a range of diffusion experiments on the same axes.

The solubility "chemical containment" research [134] did not identify any potential effects on Cs solubility due to high pH, presence of NRVB, presence of CDP or reducing agents. Consequently fast breakthrough, equilibration or at least movement to a stable condition and limited retention of Cs were anticipated.

The mass of Cs added to each of the carrier experiments was 32.9 mg in the form of (Aldrich) $CsNO_3$. The amount of carrier added was agreed after discussion with NDA and was calculated so that the maximum concentration in the system, assuming no sorption would be 10^{-3} mol dm^{-3}. The initial concentration of the carrier in the inner cores was 0.15 mol dm^{-3} The mass of ^{137}Cs (~3.6 ng) added was considered to be negligible. Initially NDA wanted to investigate a low concentration (the tracer only) and a high concentration with the option of undertaking further experiments above the background concentrations (~$4x10^{-5}$ and 10^{-4} mol dm^{-3} for the NRVB and CDP solutions respectively) and below the present carrier experiments. These additional experiments have not been requested by NDA.

The NRVB cylinders used for the experiments were equilibrated in the CDP solution in sealed containers, in a nitrogen glovebox for 43 days prior to commencement. The radioisotope addition was made outside the nitrogen glove box, the cylinder was sealed, submerged in 200 cm^3 NRVB equilibrated water and returned to the glove box over a period of less than two minutes. The total volume of equilibrated water in the system at the start is assumed to be 225 cm^3 (the additional 25 cm^3 being an estimate of the pore water volume in the NRVB cylinder). ^{137}Cs activity concentrations were determined by counting the peak centred at 0.66 MeV on a NaI crystal detector, Packard Cobra II auto-gamma counter.[160] 1 cm^3 samples were taken throughout the experimental duration but all determined on one day when the experiment was completed to negate the need to correct for radioactive decay (the

total decay of ^{137}Cs across the duration of the longest experiment is less than 4% of the initial amount added). In addition 1 cm^3 "control" samples were made at the start of the experiment to enable retention graphs to be made. The control samples and appropriate blanks were also determined on the same day as the samples from the experiments. All determinations were subject to the 2 σ criterion available on the gamma counter to ensure results are statistically valid.

11.3 Results of ^{137}Cs diffusion experiments.

All results are presented as the average of duplicates along with with vertical error bars denoting the 90% confidence limits assuming a two tailed t distribution and horizontal error bars set at +/- 0.25 days. Three graphs are presented for each experiment; showing all results, early data and C/C_{max} relative retention. The data are presented in two tables for each experiment. A short commentary is provided after each set of graphs and before the tables.

11.3.1 Results of the 137Cs tracer NRVB diffusion experiment

The results of the ^{137}Cs tracer NRVB diffusion experiment are presented below as figs. 11.1 to 11.3 and tables 11.2 and 11.3 in appendix 1.

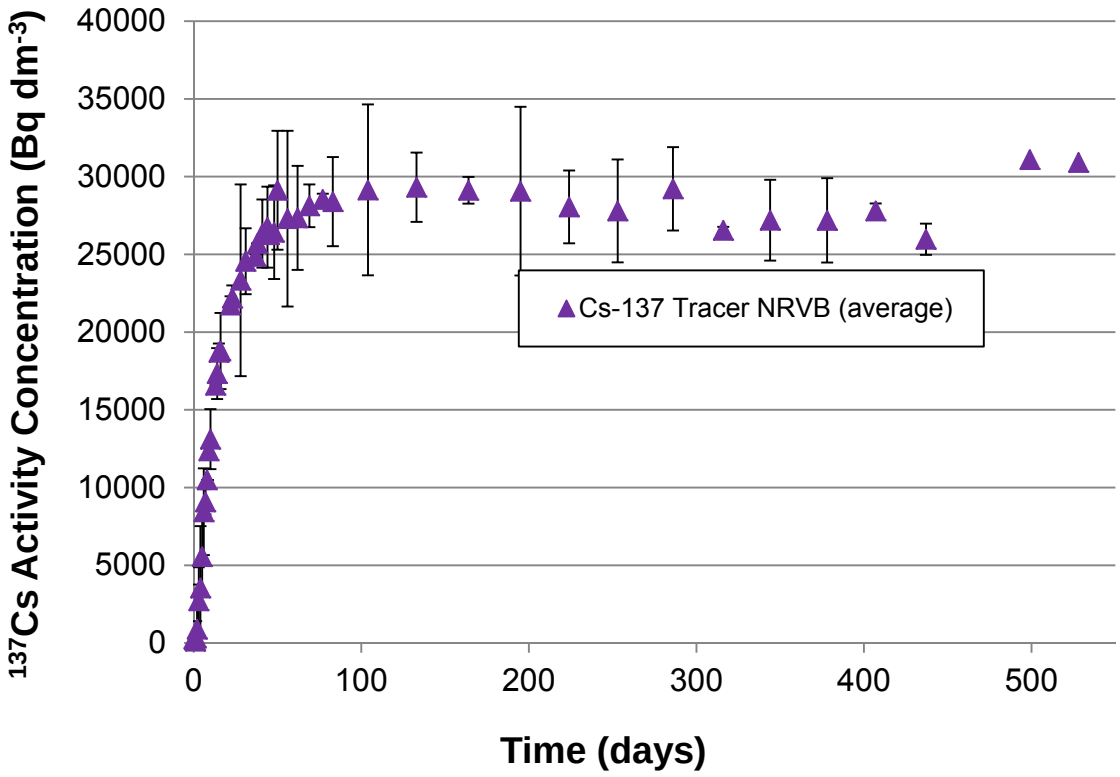

Fig. 11.1 Results of the NRVB ^{137}Cs tracer only diffusion experiment using NRVB equilibrated water

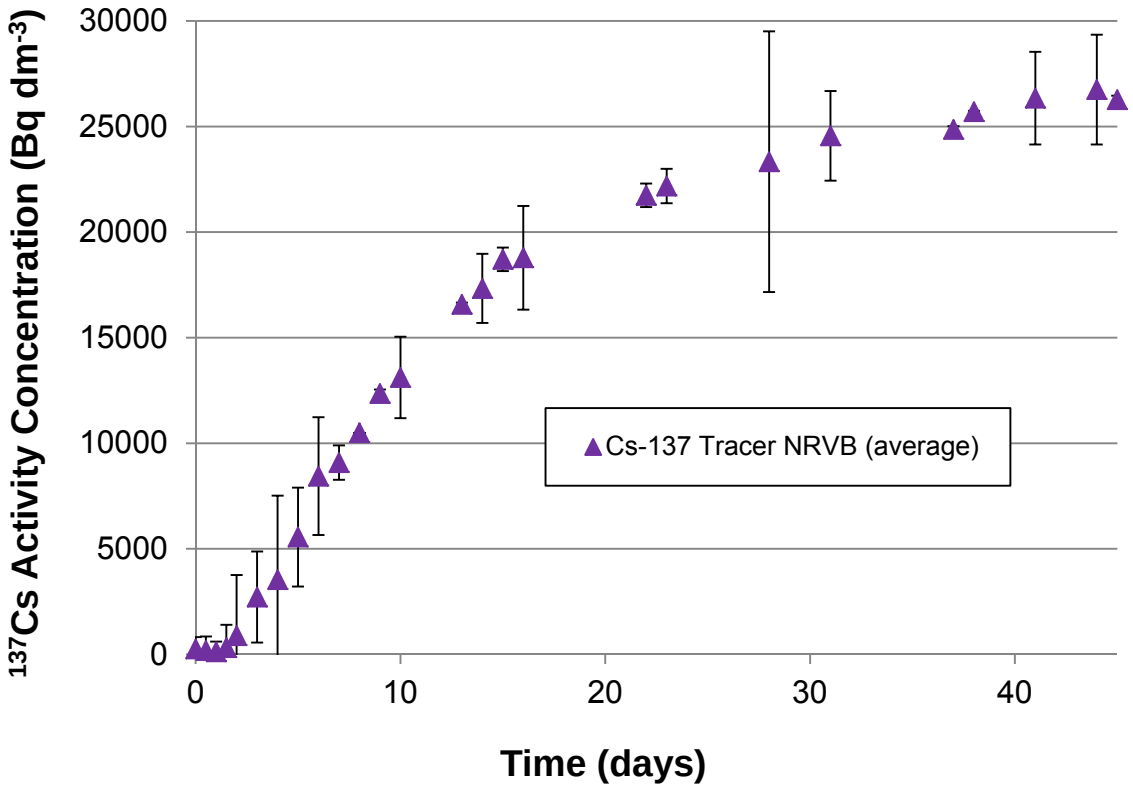

Fig. 11.2 Early data from the results of the NRVB ^{137}Cs tracer only diffusion experiment using NRVB equilibrated water

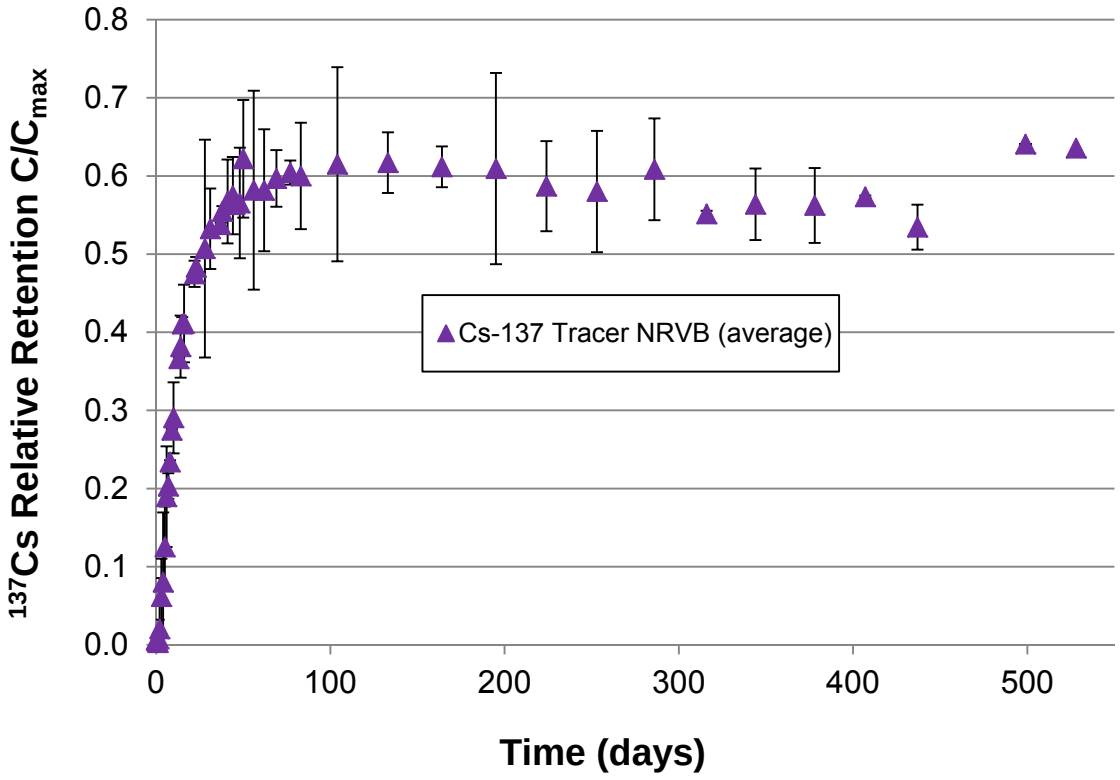

Fig. 11.3 C/C_{max} relative retention plot of the NRVB ^{137}Cs tracer only diffusion experiment using NRVB equilibrated water

Commentary

Significant breakthrough occurred in less than 2 days followed by an almost linear increase in concentration over the following 13 days. The concentration increase continued at a slower rate achieving an interim maximum concentration of 29317 Bq dm^{-3} at 133 days. The relative retention plot (where C_{max} = 2661 d min^{-1}) indicates that this corresponded to just over 40% of the tracer being retained on the NRVB cylinder. There was a significant spike in the dataset at 499 days. It should be noted the data from 499 days onward is less reliable as it originates from a single experiment due to one of the NRVB cylinders being sacrificed to produce autoradiographs.

11.3.2 Results of the ^{137}Cs tracer CDP diffusion experiment

The results of the ^{137}Cs tracer CDP diffusion experiment are presented below as figs. 11.4 to 11.6 and as tables 11.4 and 11.5 in appendix 1.

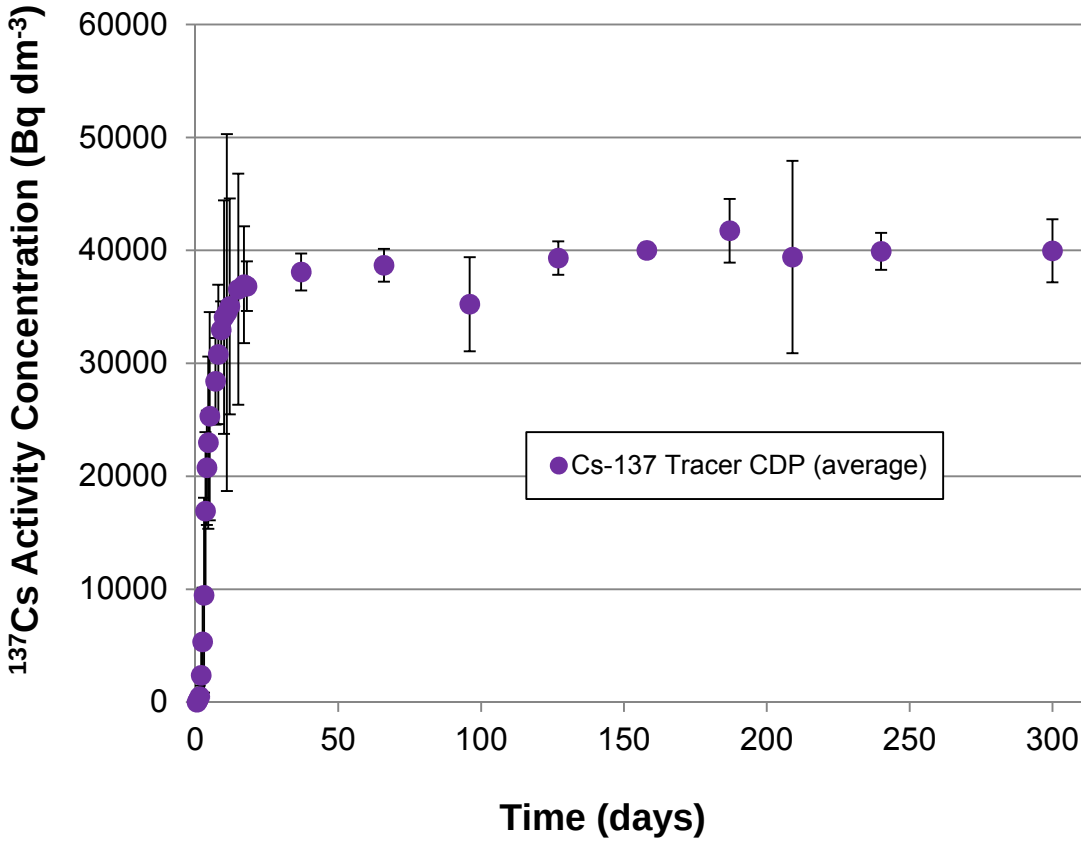

Fig. 11.4 Results of the NRVB ^{137}Cs tracer only diffusion experiment using CDP solution

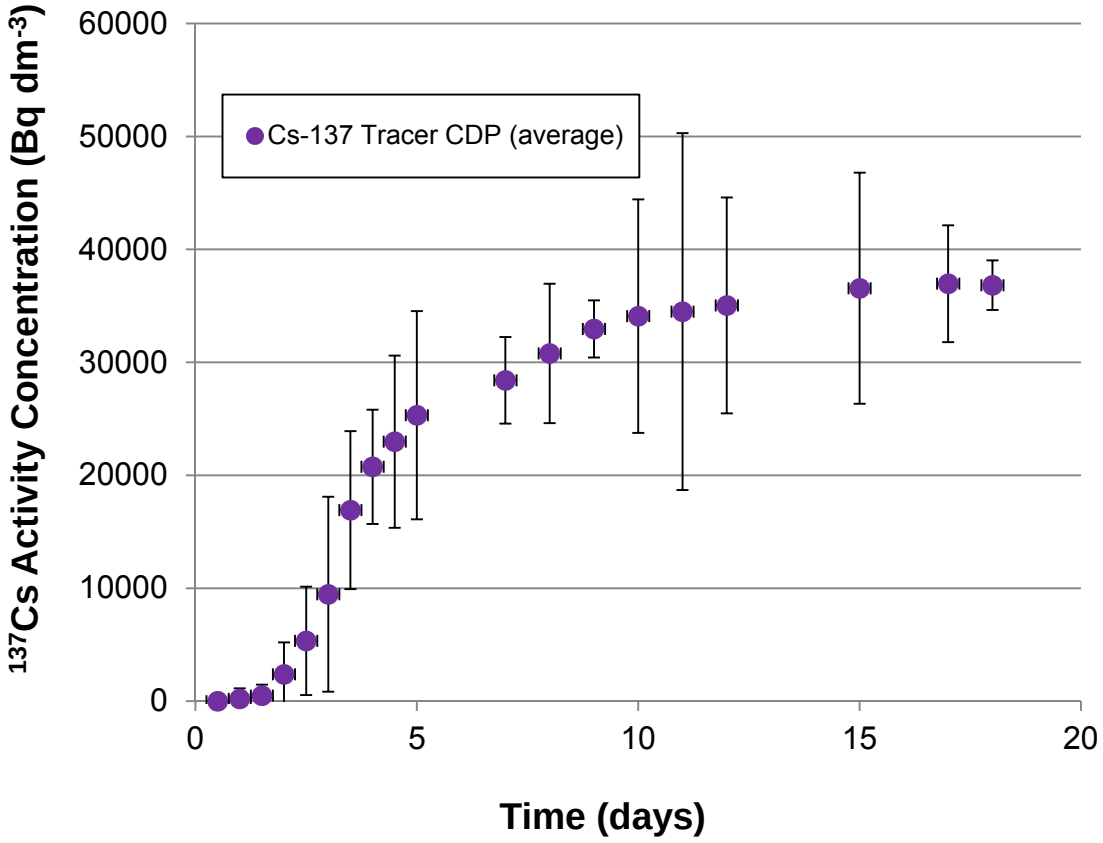

Fig. 11.5 Early data from the results of the NRVB ^{137}Cs tracer only diffusion experiment using CDP solution

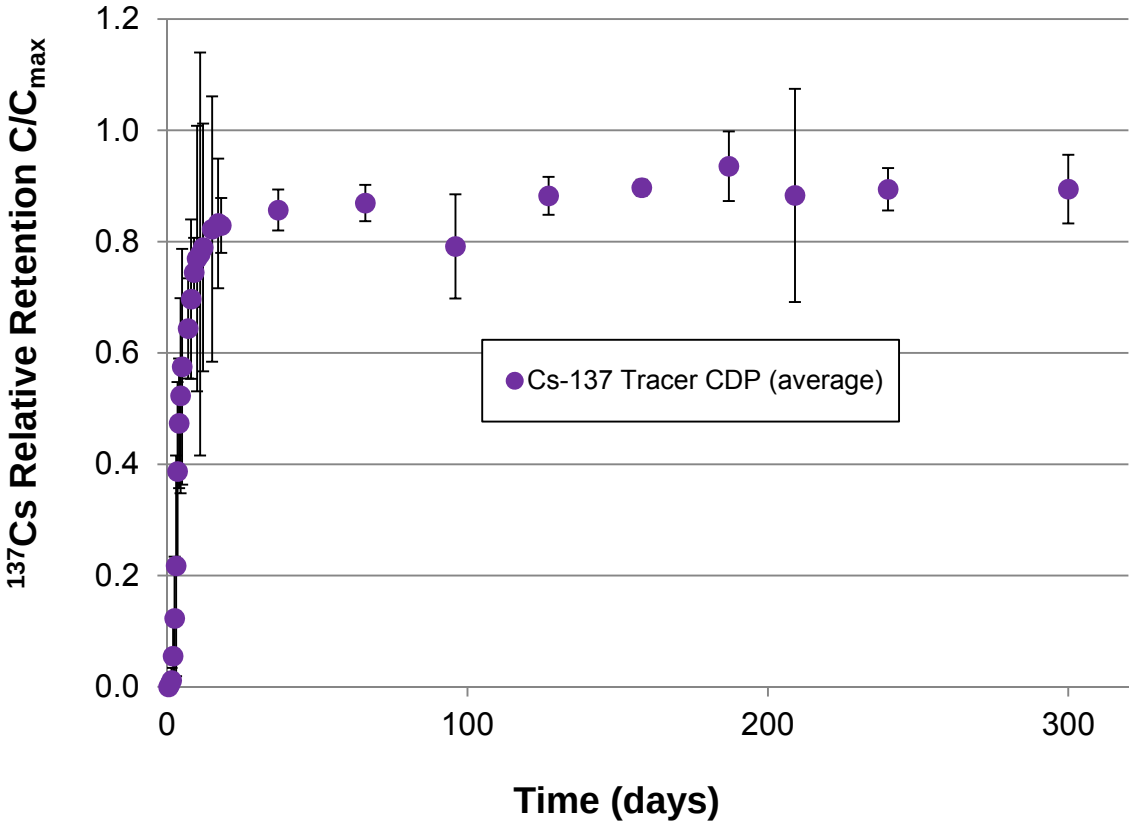

Fig. 11.6 C/C_{max} relative retention plot of the NRVB ^{137}Cs tracer only diffusion experiment using CDP solution

Commentary

Significant breakthrough occurred in less than 1.5 days followed by a sigmoidal increase in concentration over the following 10 days, significantly quicker than the experiment in the absence of CDP. The concentration continued to increase at a slower rate stabilising around 40000 Bq dm^{-3} and achieving a maximum activity concentration of 41733 Bq dm^{-3} at 187 days. The relative retention plot (where C_{max} = 2631 d min^{-1}) indicates that just over 10% of the tracer was retained on the NRVB cylinder i.e. 90% of the tracer was in solution. The data point at 15 days was considered anomalous as one of the duplicate samples was lost.

11.3.3 Results of the ^{137}Cs tracer; $CsNO_3$ carrier NRVB diffusion experiment

The results of the ^{137}Cs tracer; $CsNO_3$ Carrier NRVB diffusion experiment are presented below as figs. 11.7 to 11.9 and as tables 11.6 and 11.7 in appendix 1.

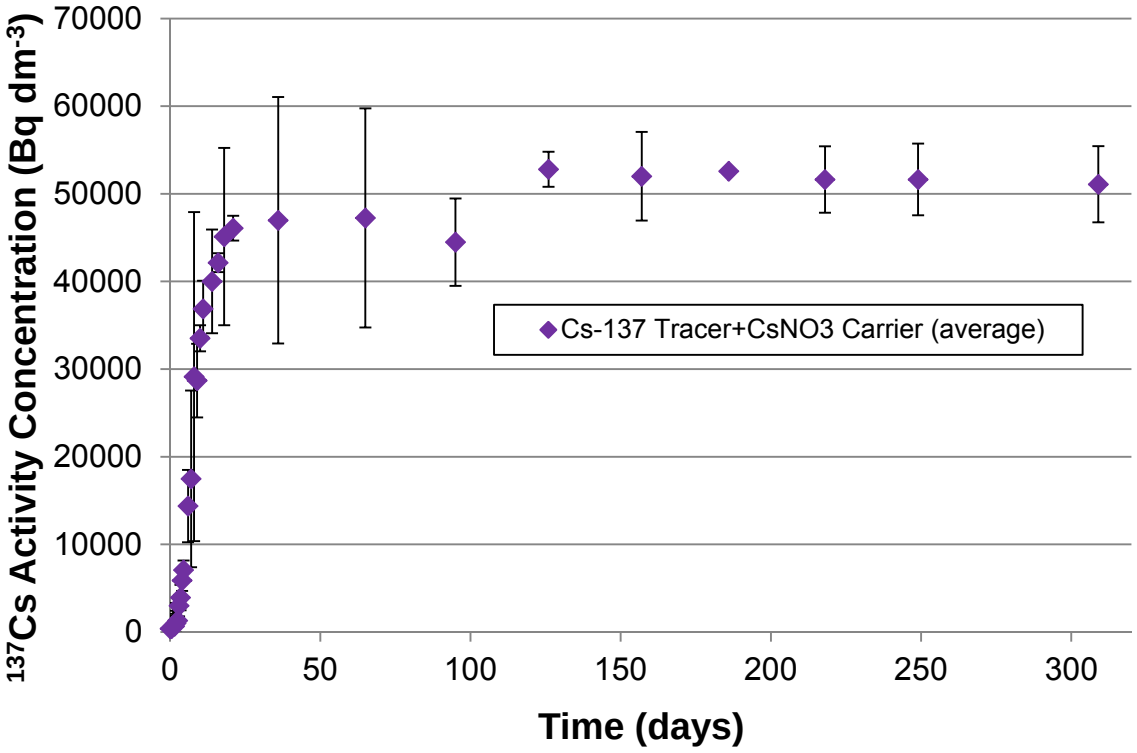

Fig. 11.7 Results of the NRVB ^{137}Cs tracer; $CsNO_3$ carrier diffusion experiment using NRVB equilibrated water

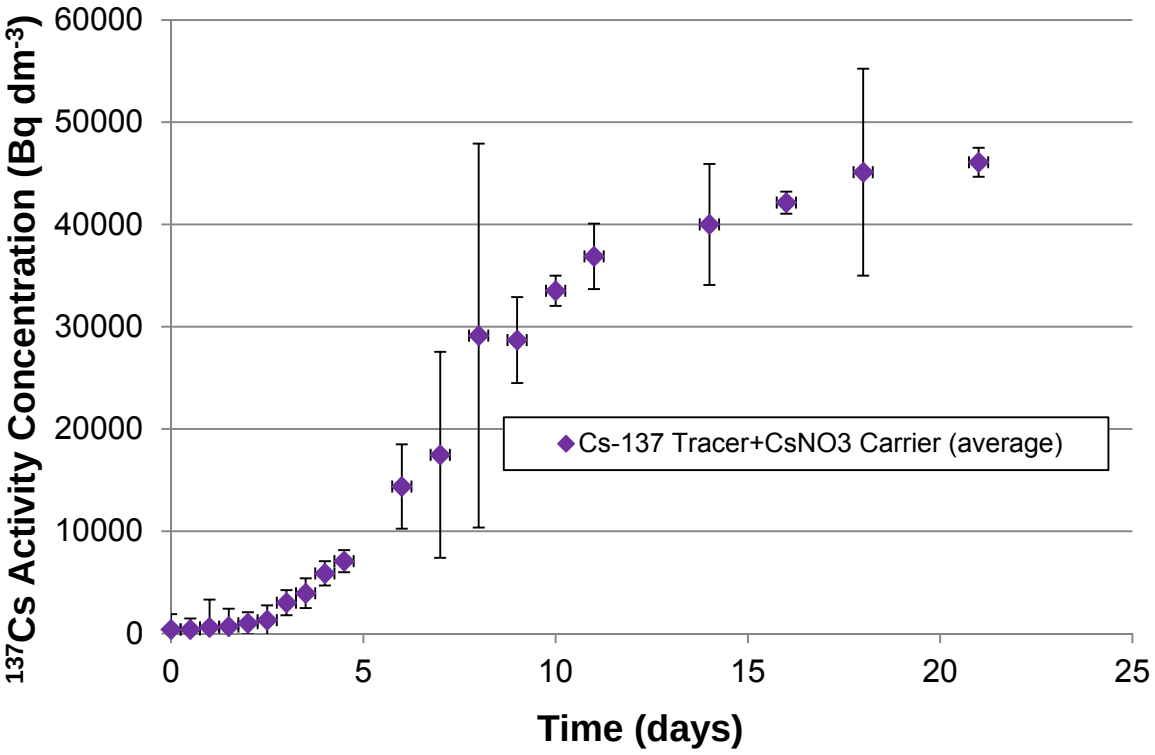

Fig. 11.8 Early data from the results of the NRVB ^{137}Cs tracer; $CsNO_3$ carrier diffusion experiment using NRVB equilibrated water

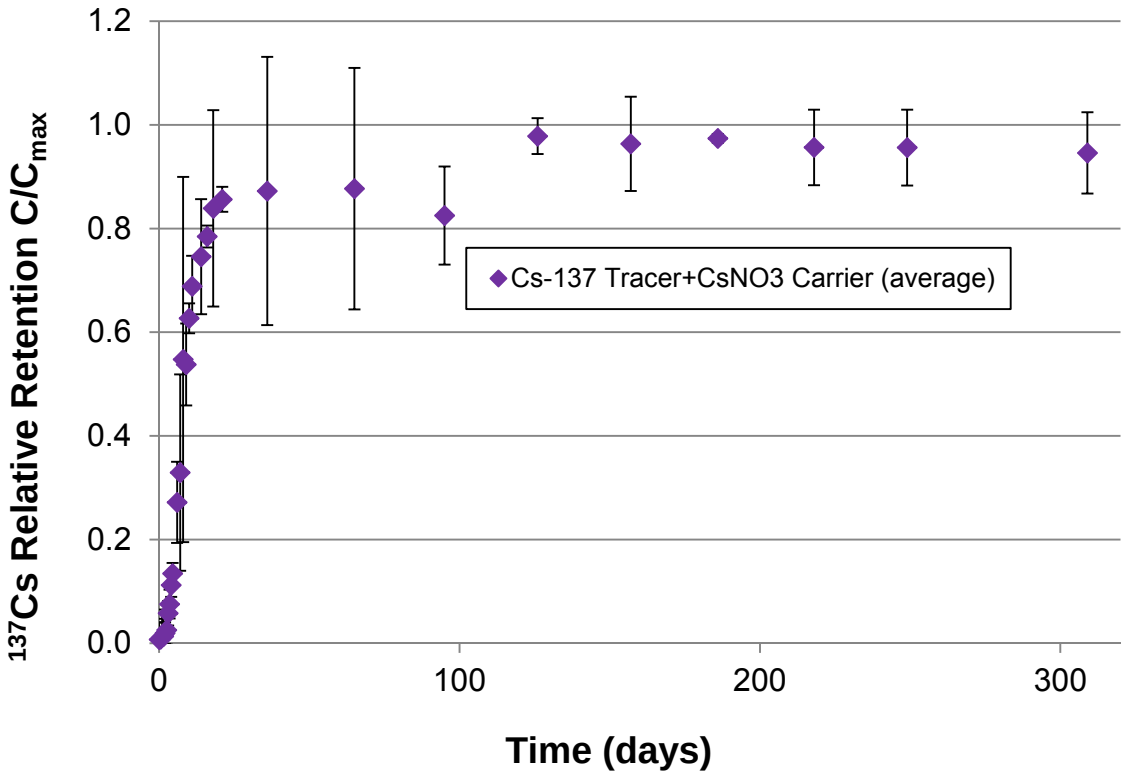

Fig. 11.9 C/C_{max} relative retention plot of the NRVB ^{137}Cs tracer; $CsNO_3$ carrier diffusion experiment using NRVB equilibrated water

Commentary

Breakthrough commenced in less than 2.0 days followed by an almost linear increase in concentration over the following 9 - 10 days, similar to the equivalent tracer only experiment. The concentration continued to increase at a slower rate stabilising between 50000 and 52000 Bq dm^{-3} but achieving a maximum activity concentration of 52800 Bq dm^{-3} at 186 days. This maximum is coincindent with an apparent spike in the dataset. It is not clear whether there is a spike in concentration or the previous point at 95 days is anomalously low. The relative retention plot (where C_{max} = 3088 d min^{-1}) indicates that only ~5% of the tracer was retained on the NRVB cylinder i.e. 95% of the tracer (and carrier) was in solution.

11.3.4 Results of the ^{137}Cs tracer; $CsNO_3$ carrier CDP diffusion experiment

The results of the ^{137}Cs tracer; $CsNO_3$ Carrier CDP diffusion experiment are presented below as figs. 11.10 to 11.12 and as tables 11.8 and 11.9 in appendix 1.

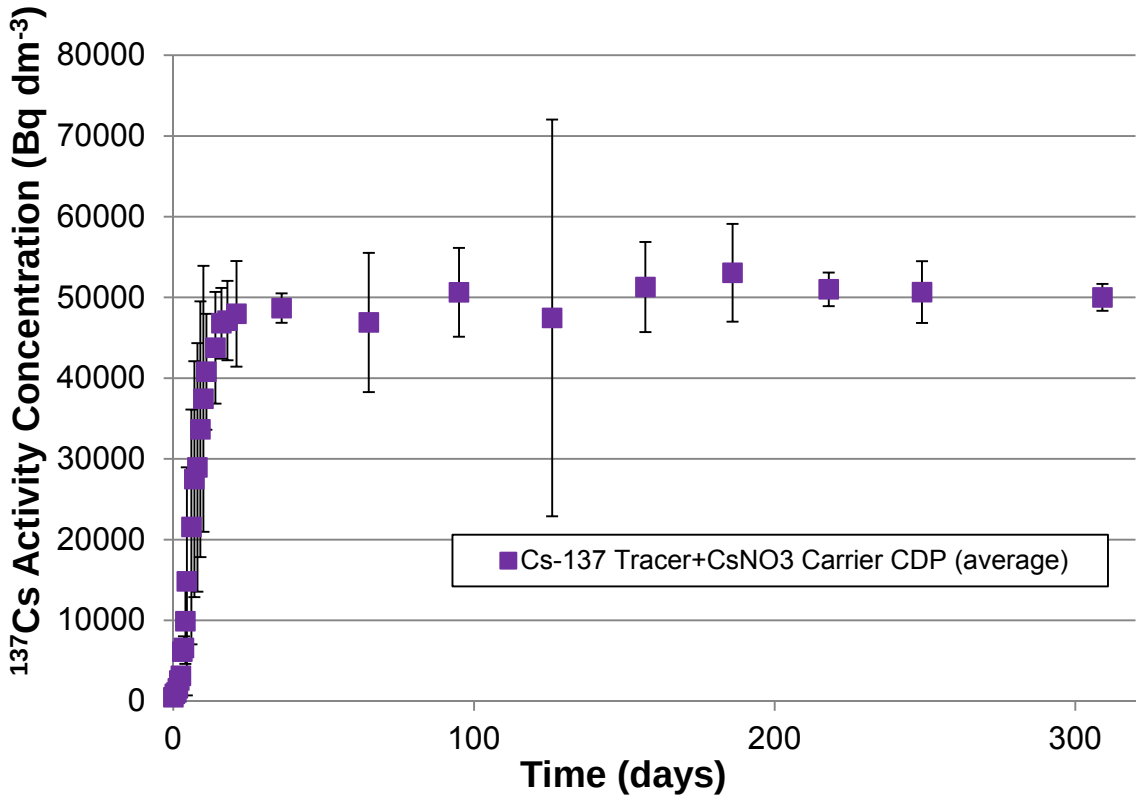

Fig. 11.10 Results of the NRVB ^{137}Cs tracer; $CsNO_3$ carrier diffusion experiment using CDP solution

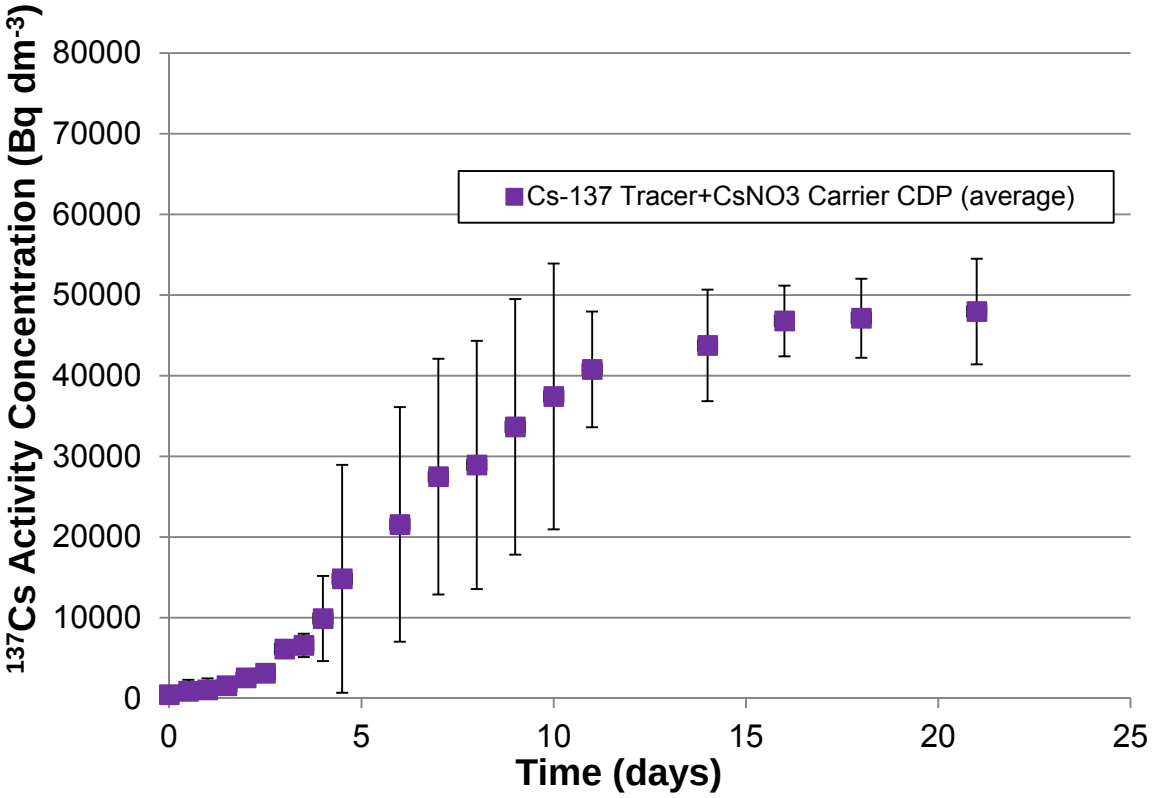

Fig. 11.11 Early data from the results of the NRVB ^{137}Cs tracer; $CsNO_3$ carrier diffusion experiment using CDP solution

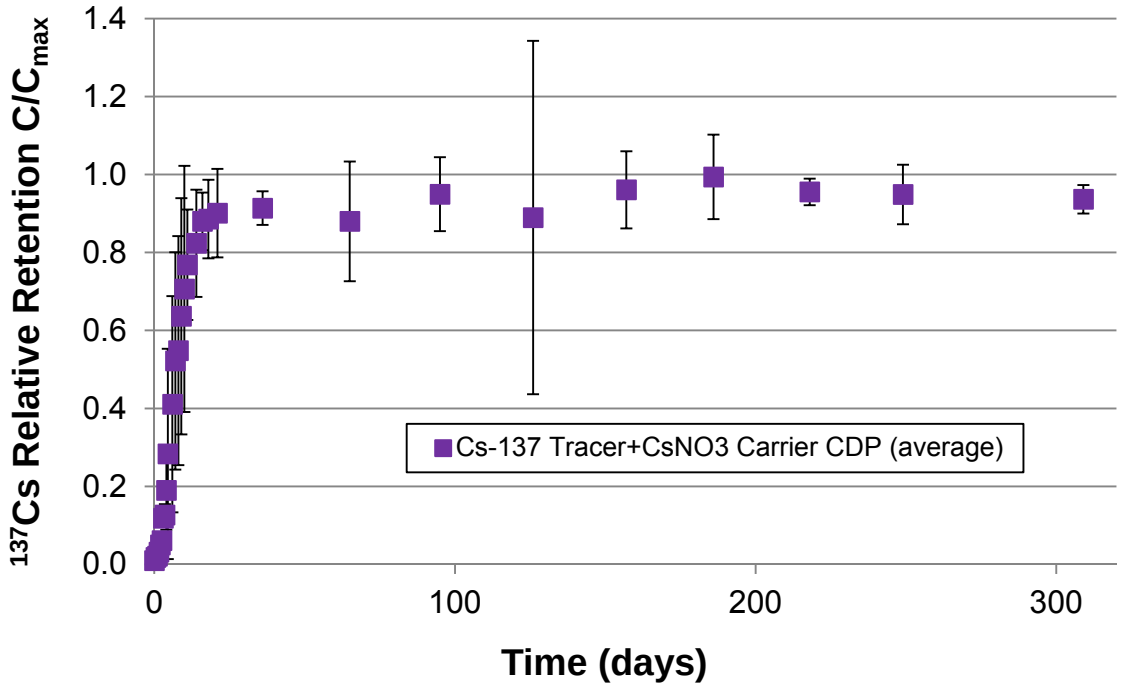

Fig. 11.12 C/C_{max} relative retention plot of the NRVB ^{137}Cs tracer; $CsNO_3$ carrier diffusion experiment using CDP solution

Commentary

Breakthrough commenced in less than 2.0 days followed by a sigmoidal increase in concentration over the following 10 days. The concentration continued to increase at a slower rate stabilising between 50000 and 53000 Bq dm^{-3} but achieving a maximum activity concentration of 53058 Bq dm^{-3} at 186 days. The relative retention plot (where C_{max} = 3088 d min^{-1}) indicates that only ~5% of the tracer was retained on the NRVB cylinder i.e. 95% of the tracer (and carrier) was in solution. The results were very similar to the tracer carrier experiment in the absence of CDP.

11.3.5 Comparison of ^{137}Cs tracer and tracer $CsNO_3$ carrier experiments

As stated earlier the relative retention or C/C_{max} plots allow for a quick visual comparison to be made of the similar experiments where there may be variation in the starting activities and concentrations. This section graphically presents the Cs data in a way that allows comparison of the tracer only experiments to the tracer carrier experiments. As a general rule, care is necessary when considering plots of this nature, particularly with diffusion experiments where initial concentrations and concentration gradients are crucially important to the evolution of the results.

Figs. 11.13 to 11.17 below show the Cs data comparatively as experimental pairs and a brief commentary is provided after each plot.

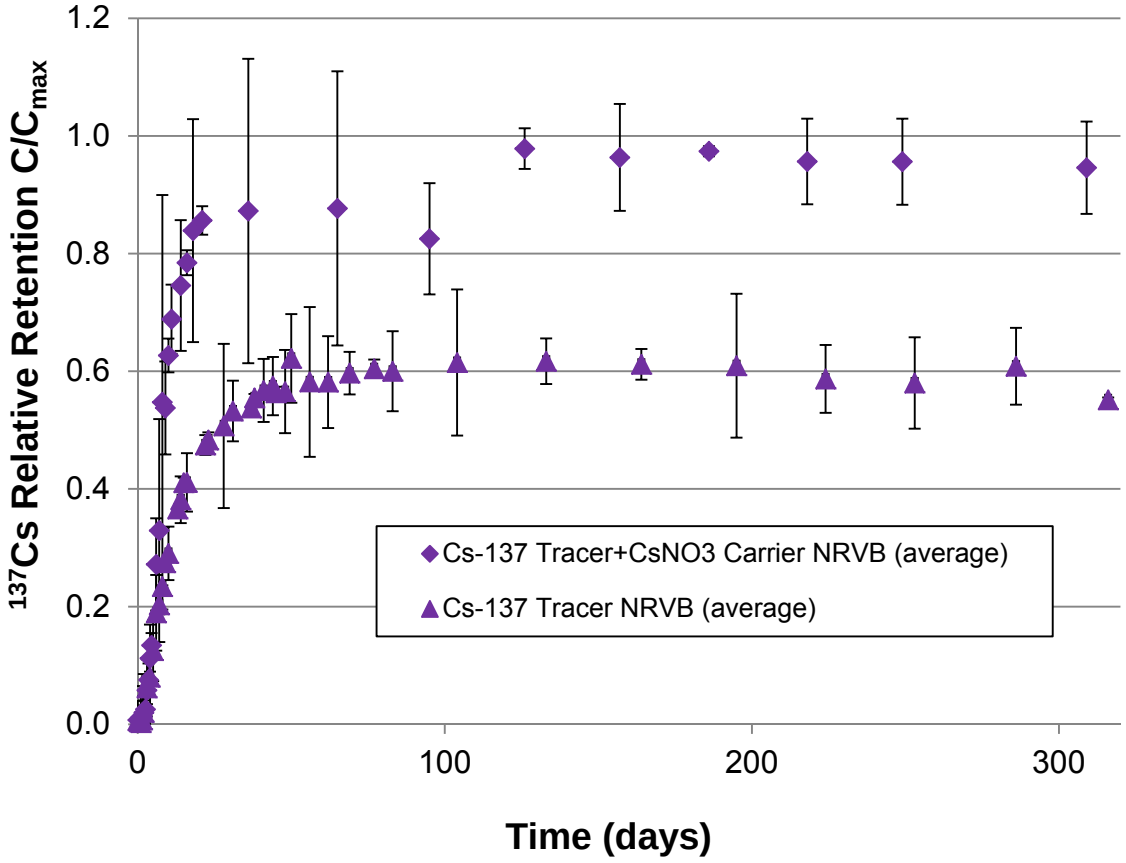

Fig. 11.13 Comparative relative retention plot of ^{137}Cs diffusion data for the NRVB equilibrated water experiments

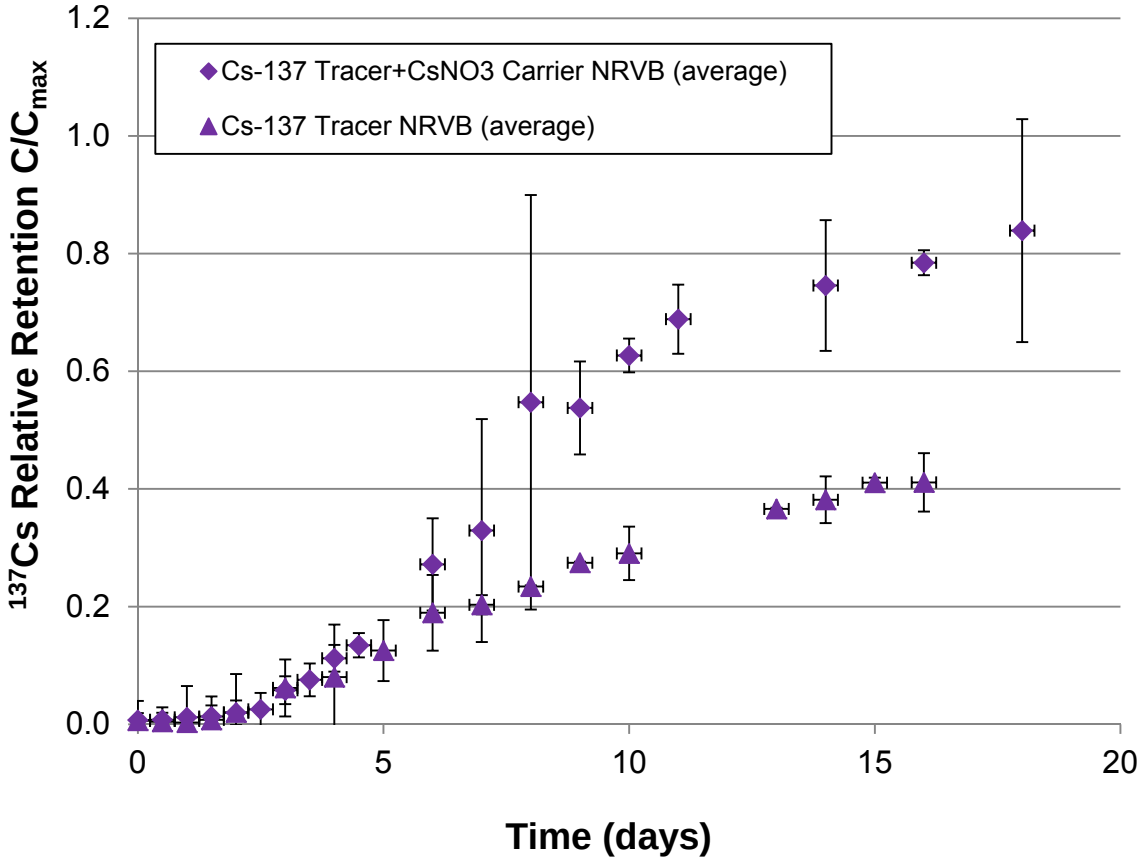

Fig. 11.14 Early data comparative relative retention plot of ^{137}Cs diffusion experiments using NRVB equilibrated water

There is a marked contrast between the two datasets for the NRVB equilibrated water experiments, the tracer only experiment was slower and retention on the NRVB was significant. The carrier experiment proceeds much more rapidly and the retention on the NRVB is less than 10%. The early data (Fig 11.14 above) confirms that the divergence begins in the initial stage of the experiments.

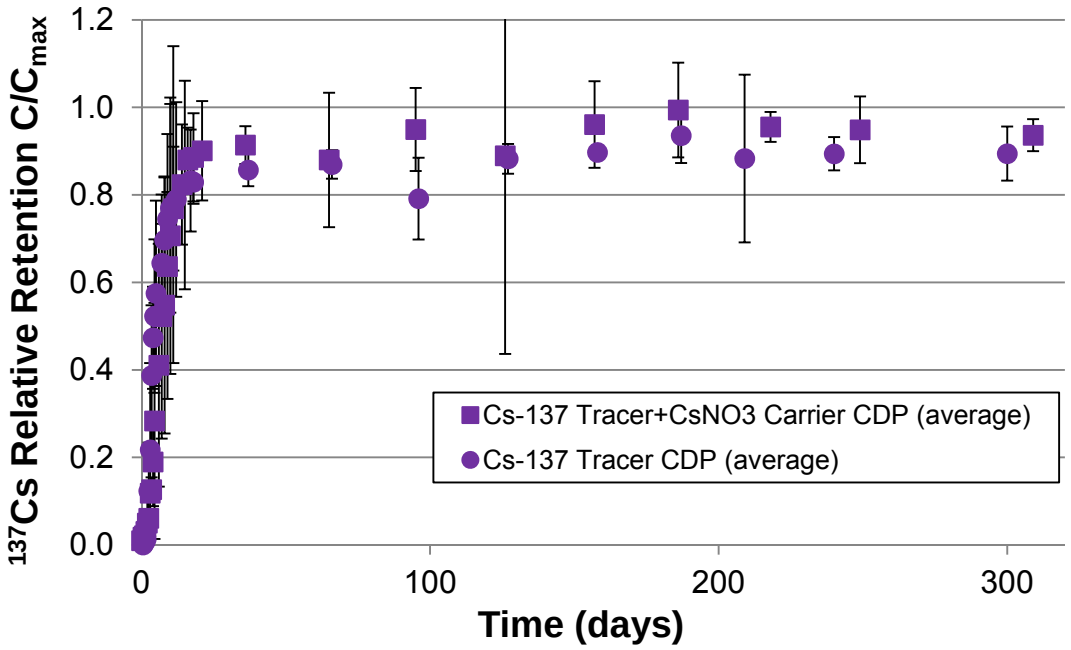

Fig. 11.15 Comparative relative retention plot of ^{137}Cs diffusion data for the CDP solution experiments

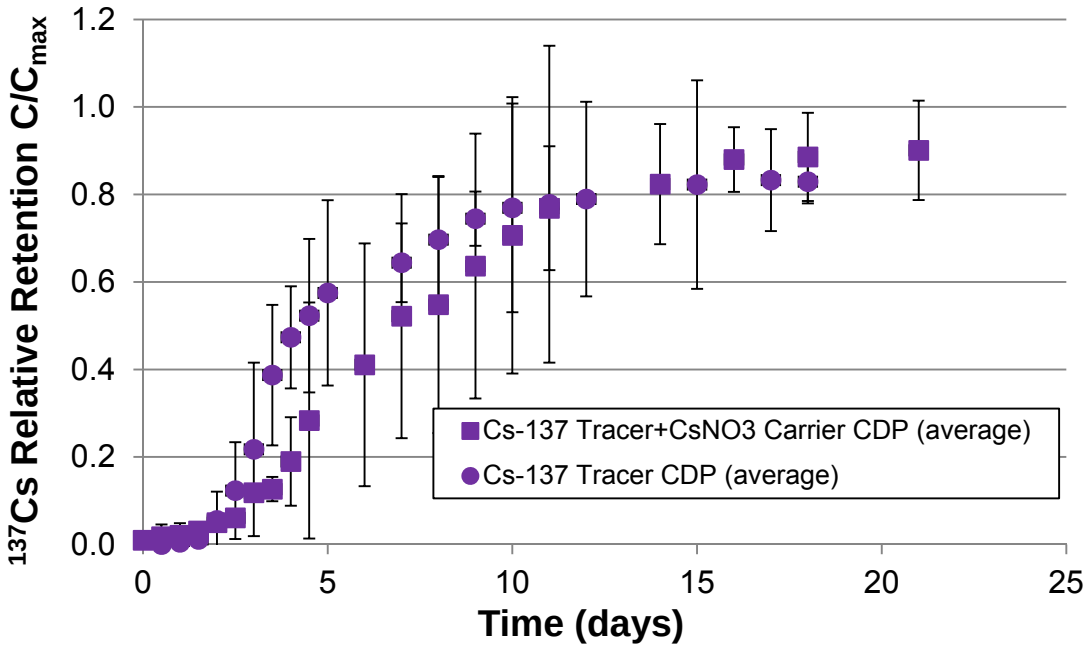

Fig. 11.16 Early data comparative relative retention plot of ^{137}Cs diffusion experiments using CDP solution

The CDP solution datasets appear very similar although the tracer only experiment stabilised with consistently higher retention of Cs. The early data exhibited different profiles and initial rates of concentration increase. The relative retention plot for the two carrier experiments (not reproduced here) shows them to be identical.

11.4 Cs in the Mixed Element Diffusion Experiments

11.4.1 Additional information relevant to the mixed element diffusion experiments

The mixed element diffusion experiments were set up to investigate the effect on the diffusion rates of Cs, I, U, Th. Eu and Ni when all were present.[134] The experiments, eleven of each type (NRVB equilibrated water and CDP solution), were the first to be undertaken using the radial approach. Sufficient $CsNO_3$ and KI were added to produce a 10^{-3} mol dm^{-3} solution in the event of complete equilibration. In addition precipitates from a neutralised solution containing $UO_2(NO_3)_2.6H_2O$, $Th(NO_3)_4.4H_2O$, $EuCl_3.6H_2O$ and $NiCl_2.6H_2O$ were mixed with the Cs and I solutions to produce a slurry which was added to the central cores of the NRVB cylinders. The NRVB cylinders used for the CDP experiments were equilibrated in a CDP solution for 30 days prior to commencement. The Cs determinations were performed by ICP-MS.

11.4.2 Cs Results for the mixed element diffusion experiments in NRVB equilibrated water and CDP solution

The average of eleven results for both types of experiment are presented below as fig. 11.17 and the data for all experiments provided as tables 11.10 and 11.11 in appendix 1.

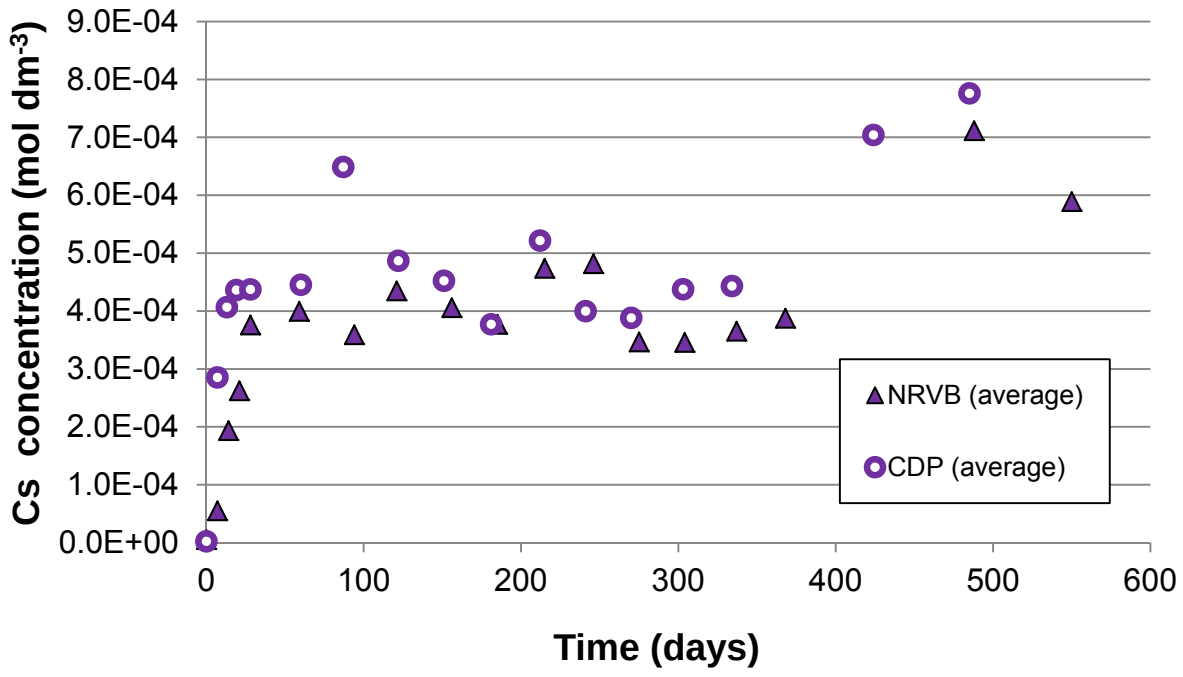

Fig. 11.17 Averaged Cs Results for the mixed element diffusion experiments in NRVB equilibrated water and CDP solution

The main points of interest arising from the Cs diffusion results in the mixed element experiments are:

- The overall behaviour was similar to the single element experiments; the presence of CDP appeared to cause faster breakthrough and stabilisation but retention is almost indistinguishable from the experiment in the absence of CDP
- The data are not as consistent as those generated by the single element versions of the experiments and whilst averaging has helped the visualisation, the raw data shows a large amount of variation (see figs. 11.18 to 11.21 for raw data plots). This variation commences early in the experiments, the extent of variation is less in the CDP experiments.
- There appears to be retention of Cs in the early part of the experiment but as time progresses the amount in solution is getting closer to the C_{max} of 10^{-3} mol dm^{-3}.
- The higher results at the end of the sequence are an average of nine results as two from each set were sacrificed for inspection and autoradiography.
- These experiments were very early attempts at the technique and modifications have been on-going, in particular handling time outside the glove box and dosing of the central cores have been speeded up and subject to more control.
- The slurry placed in the central core has not been fully characterised but it is a complex mixture of salts that could be affecting precipitation, solubility and subsequent migration.

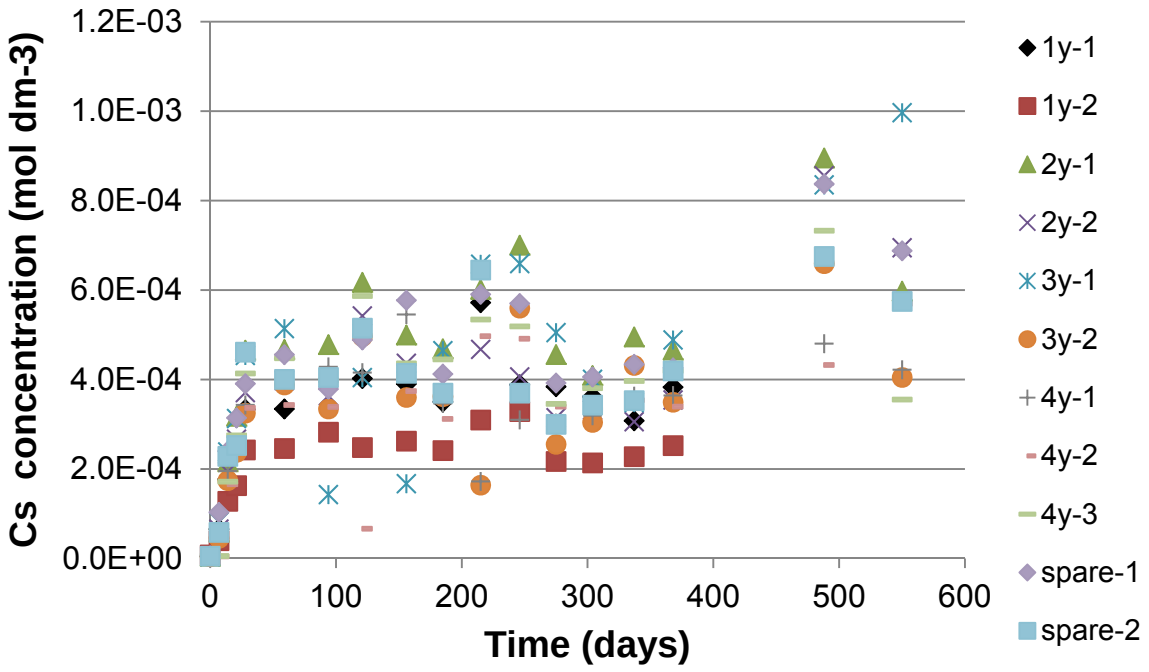

Fig. 11.18 Cs raw data from the mixed element diffusion experiments in NRVB equilibrated water[134]

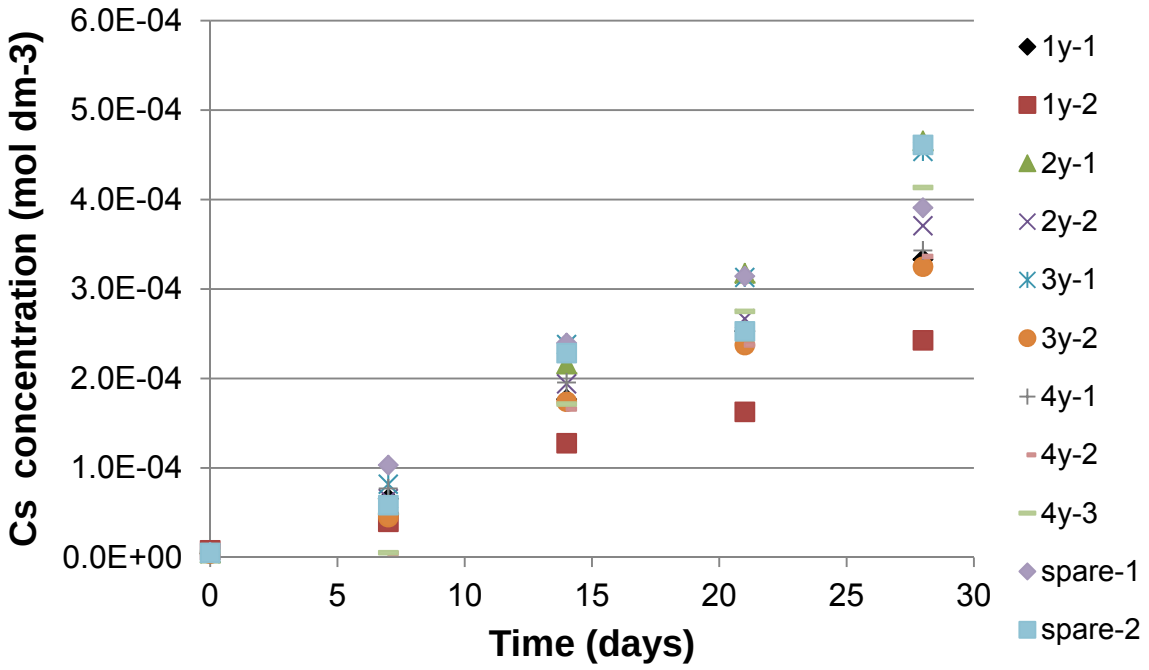

Fig. 11.19 Cs early raw data from the mixed element diffusion experiments in NRVB equilibrated water[134]

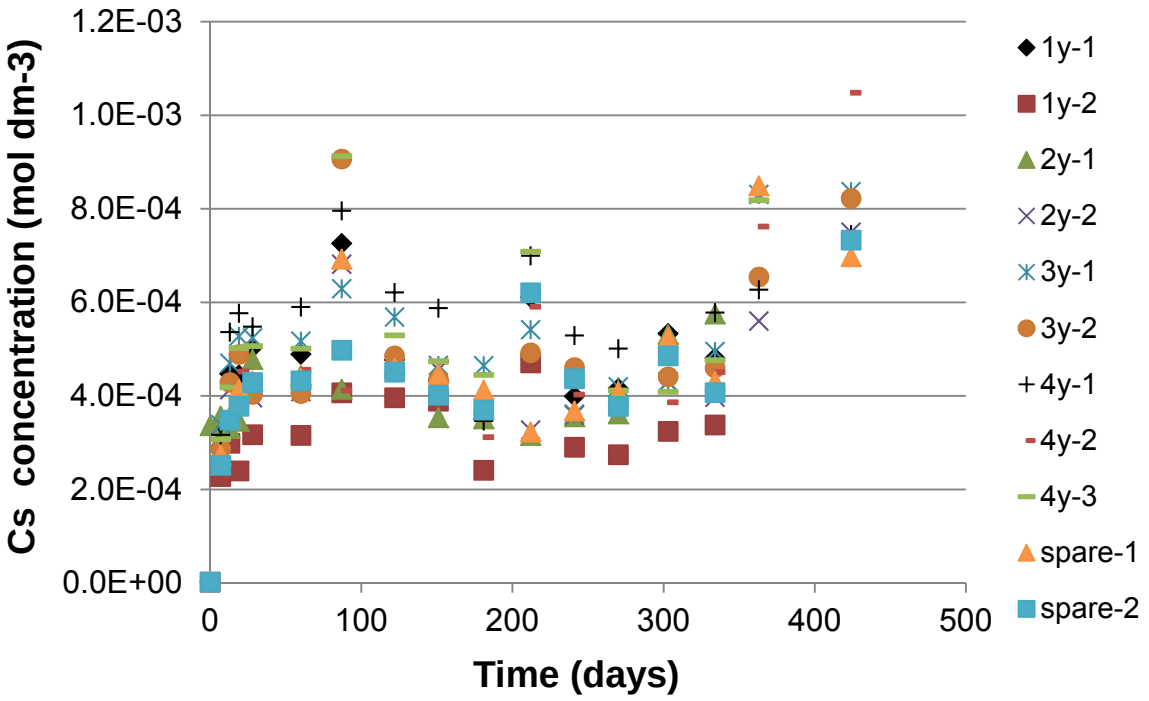

Fig. 11.20 Cs raw data from the mixed element diffusion experiments in NRVB equilibrated water [134]

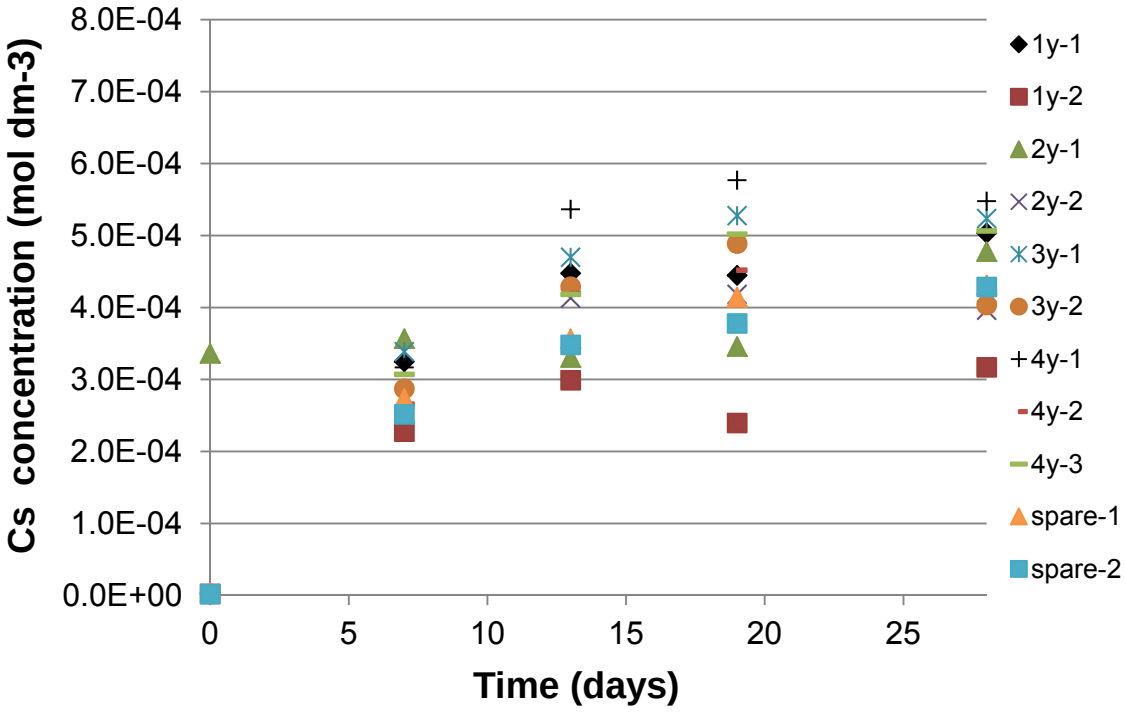

Fig. 11.21 Cs early raw data (unaveraged) from the mixed element diffusion experiments in CDP solution [134]

11.5 GoldSim Modelling

11.5.1 Additional information relevant to the Cs NRVB diffusion modelling

Details of the GoldSim model are discussed in section 8. The results from the modelling of the Cs NRVB diffusion experiments are presented as figs. 11.21 to 11.24. Initial concentrations are provided in section 11.2. It is important to be aware that activity concentrations were modelled and as a consequence a direct comparison cannot be made in the same manner as possible with the relative retention plots. Partition is referred to as K_d throughout, primarily because this term, rather than R_d is used in GoldSim. The LOF calculations are built into the model enabling it to determine the combination of D_e and K_d parameters that minimise LOF. Short commentaries explaining the data envelopes, diffusivity, partition coefficient and LOF outputs are also provided.

11.5.2 GoldSim models for ^{137}Cs tracer and tracer with carrier using NRVB equilibrated water

The GoldSim models for the ^{137}Cs tracer and tracer with carrier using NRVB equilibrated water are presented as figs. 11.22 and 11.23.

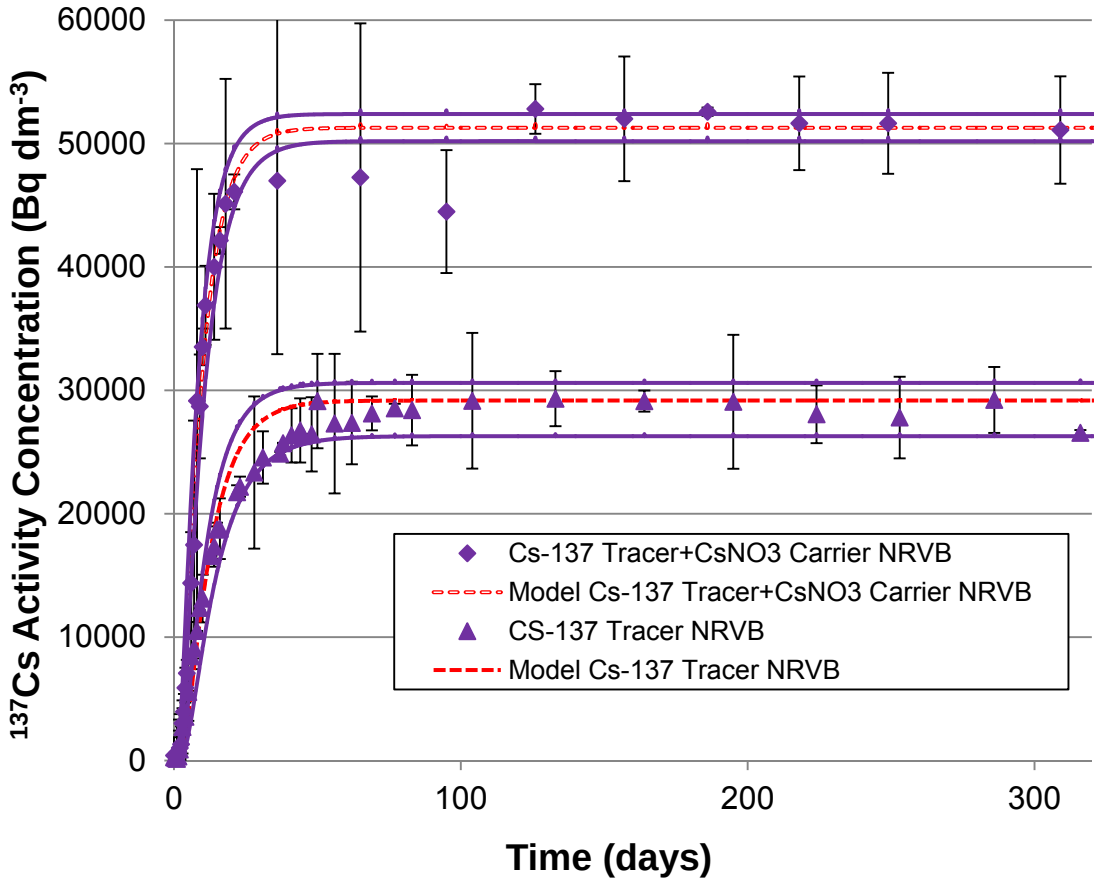

Fig. 11.22 Experimental and modelled NRVB diffusion curves for ^{137}Cs at tracer and tracer carrier ($CsNO_3$) concentrations in NRVB equilibrated water

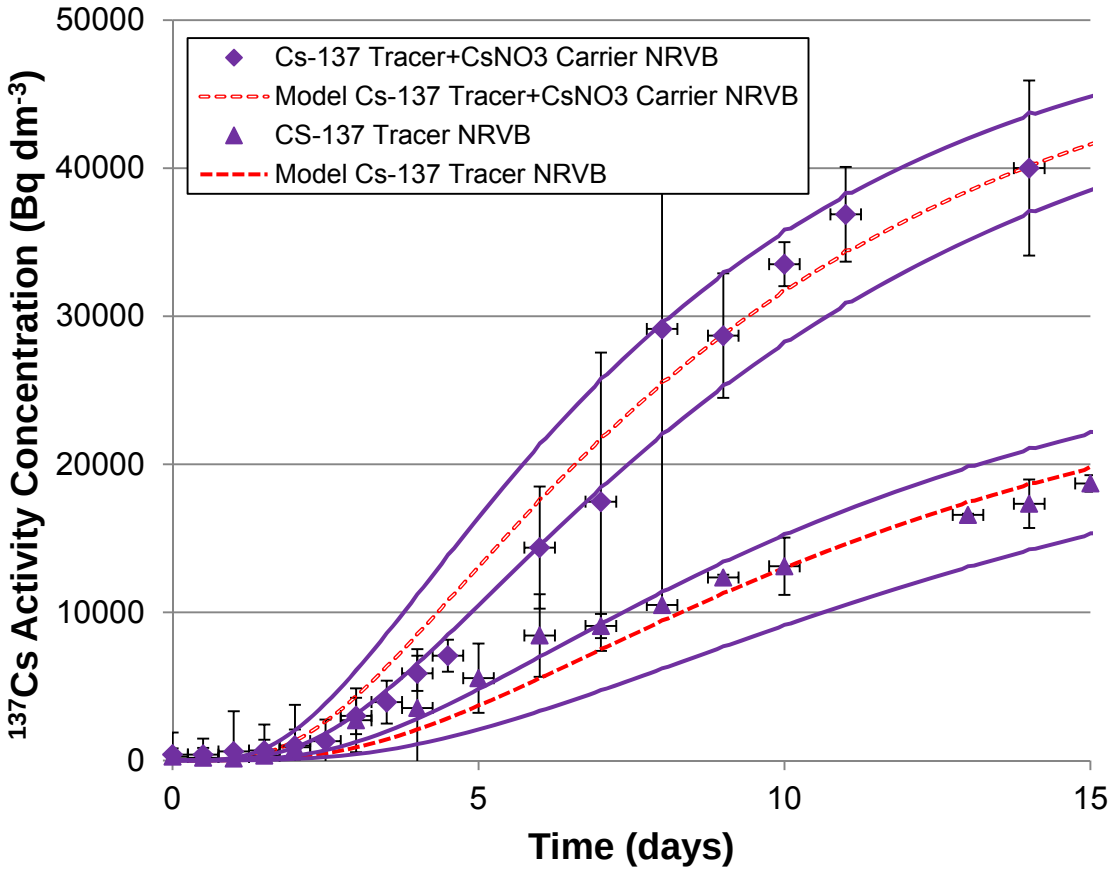

Fig. 11.23 Early experimental and modelled NRVB diffusion curves for ^{137}Cs at tracer and tracer carrier ($CsNO_3$) concentrations in NRVB equilibrated water

Commentary

The best fit D_e and K_d model results for the carrier experiments were 0.9x10^{-10} m^2 s^{-1} and 0.2x10^{-3} m^3 kg^{-1}, respectively (red long hashed line in fig. 11.22). The LOF for the best model result was 6.9%. The majority of the experimental data could be contained in the interval defined by setting D_e between 0.7x10^{-10} and 1.2x10^{-10} m^2 s^{-1} and K_d between 0.1x10^{-3} and 0.3x10^{-3} m^3 kg^{-1}, (upper pair of solid purple lines in fig. 11.21). The early data plot (fig. 11.23) has been provided to illustrate the difficulty of setting a suitable envelope. The results that fall outside the envelope can be clearly seen on the figures. It should be noted that all observed values are included in the LOF results even those outside the envelope.

The tracer experiments yielded higher best fit D_e and K_d model results than for the carrier experiments at 2.0x10^{-10} m^2 s^{-1} and 2.3x10^{-3} m^3 kg^{-1}, respectively (red short hashed lines in fig. 11.22). The LOF for the best model result was 8.5%. The intervals of D_e and K_d that encompass most of the experimental data were also wider

than for the carrier experiments with D_e between 1.8x10^{-10} – 2.8x10^{-10} m^2 s^{-1} and K_d between 2.0x10^{-3} – 3.0x10^{-3} m^3 kg^{-1}, (lower pair of purple solid lines in fig. 11.22 suggesting higher variability).

11.5.3 GoldSim models for ^{90}Cs tracer and tracer with carrier using CDP solution

The GoldSim models for the ^{137}Cs tracer and tracer with carrier using CDP solution are presented as figs. 11.24 and 11.25.

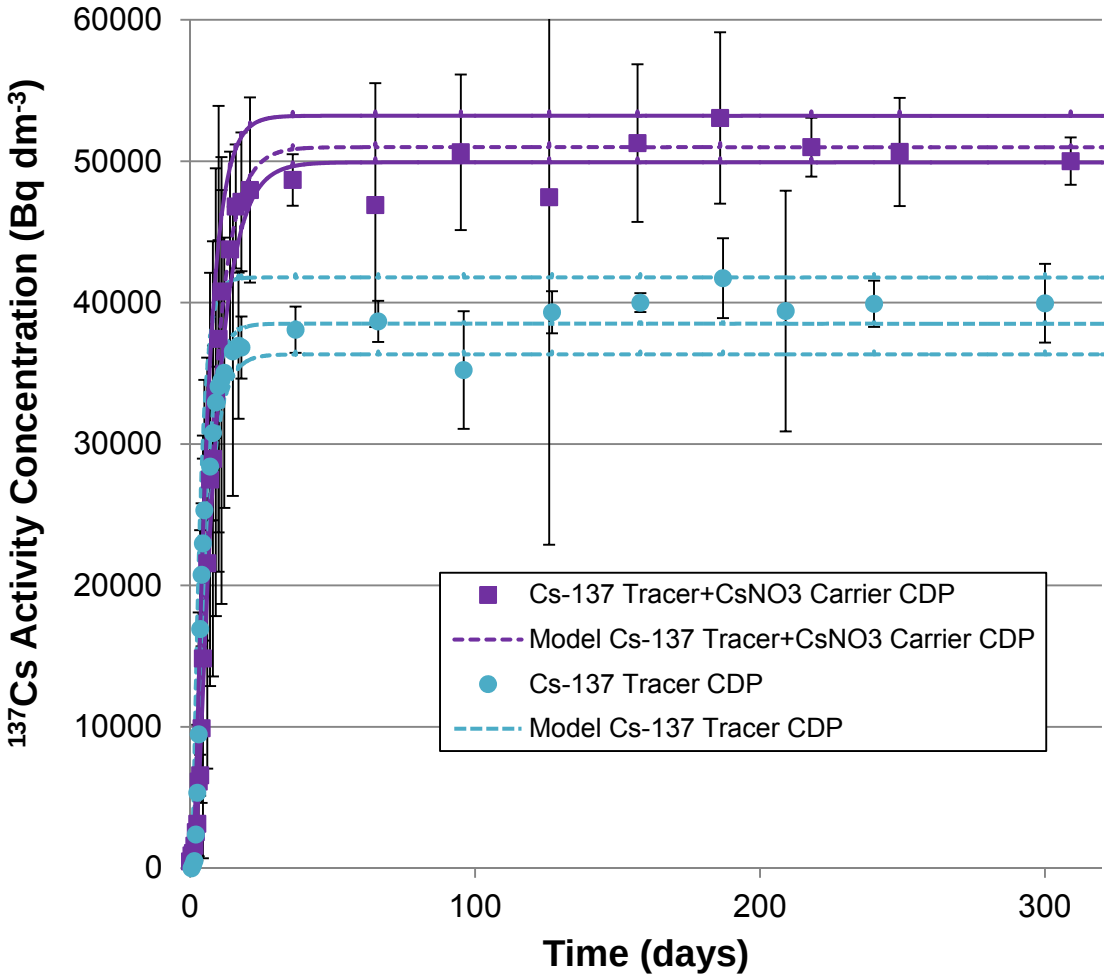

Fig. 11.24 Experimental and modelled NRVB diffusion curves for ^{137}Cs at tracer and tracer carrier ($CsNO_3$) concentrations in CDP solution

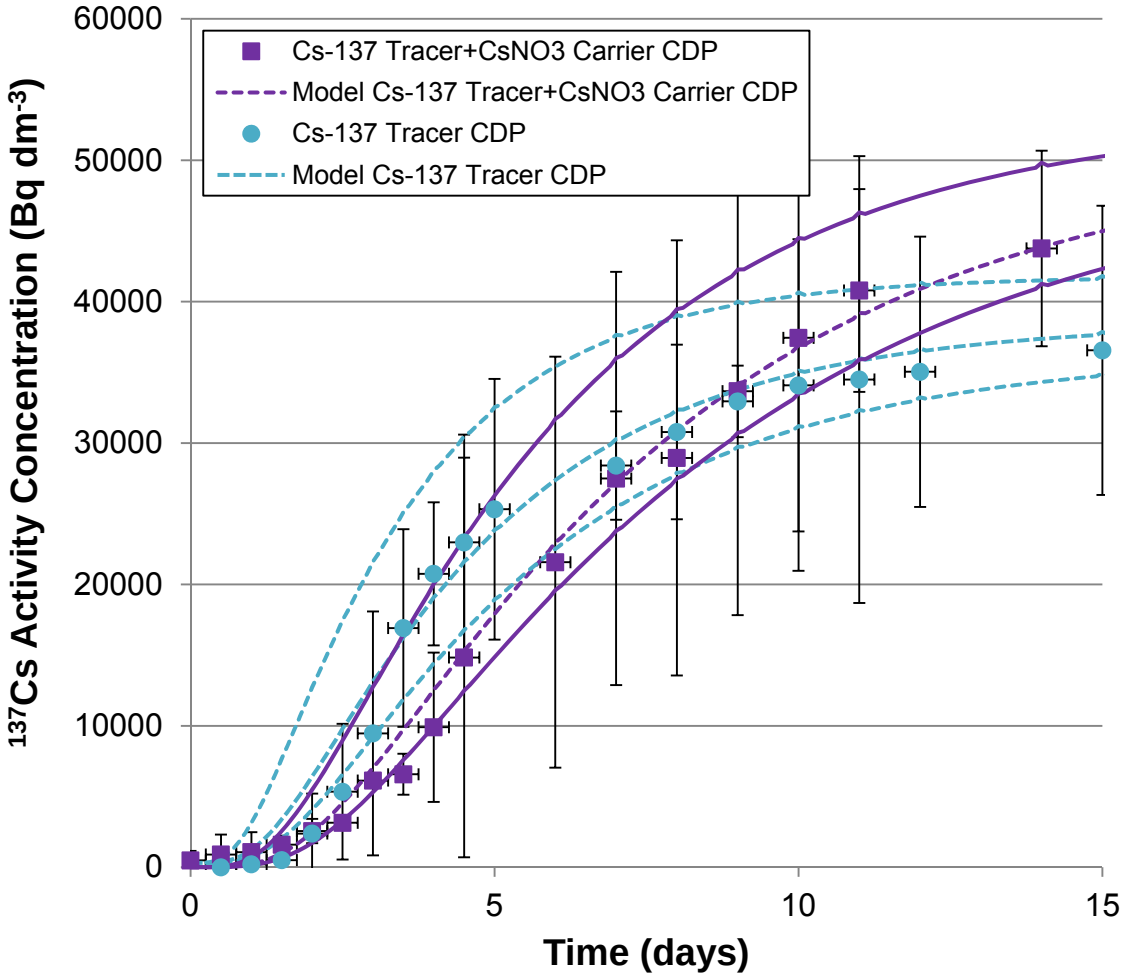

Fig. 11.25 Early experimental and modelled NRVB diffusion curves for ^{137}Cs at tracer and tracer carrier ($CsNO_3$) concentrations in CDP solution

Commentary

A change of colours has been used in figs. 11.24 and 11.25 above to enable easier consideration of the early data plots. The best fit D_e and K_d model results for the CDP carrier experiments were 1.1×10^{-10} m^2 s^{-1} and 0.2×10^{-3} m^3 kg^{-1}, respectively (purple hashed line in fig. 11.24). The LOF for the best model result was 4.5%. The majority of the experimental data could be contained in the interval defined by setting D_e between 0.7×10^{-10} and 1.2×10^{-10} m^2 s^{-1} and with K_d between zero and 0.3×10^{-3} m^3 kg^{-1}, (solid purple lines in fig. 11.24). The results that fall outside the envelope can be clearly seen on the figures. The early data plot (fig. 11.25) has been provided to illustrate the difficulty of setting a suitable envelope. It should be noted that all observed values are included in the LOF results even those outside the envelope.

The CDP tracer experiments yielded higher best fit D_e and K_d model results than for the carrier experiments at 2.8×10^{-10} m^2 s^{-1} and 2.3×10^{-3} m^3 kg^{-1}, respectively (turquoise hashed line in fig 11.24). The LOF for the best model result was 6.0%. The intervals of D_e and K_d that encompass most of the experimental data were also wider than for the CDP carrier experiments, suggesting higher variability with D_e between 2.6×10^{-10} – 3.6×10^{-10} m^2 s^{-1} and K_d =0.3×10^{-3} – 1.0×10^{-3} m^3 kg^{-1}, (solid turquoise lines in fig. 11.24).

11.6 Cs Diffusion Autoradiography

One of the duplicates from each diffusion experiment was removed from the container and sectioned longitudinally using a diamond rotary masonry saw. The pieces were placed flat face down on a Fuji BAS MP 20 cm x 25cm autoradiography image plate in darkness and exposed for a period of 4 hours. The sections were then removed, again in darkness and the plate taken to British Geological Survey, Nottingham to be developed. The resulting image is shown, unenhanced as fig. 11.26 below. A version of the image that has been enhanced using the software package ImageJ is shown as fig. 11.27.

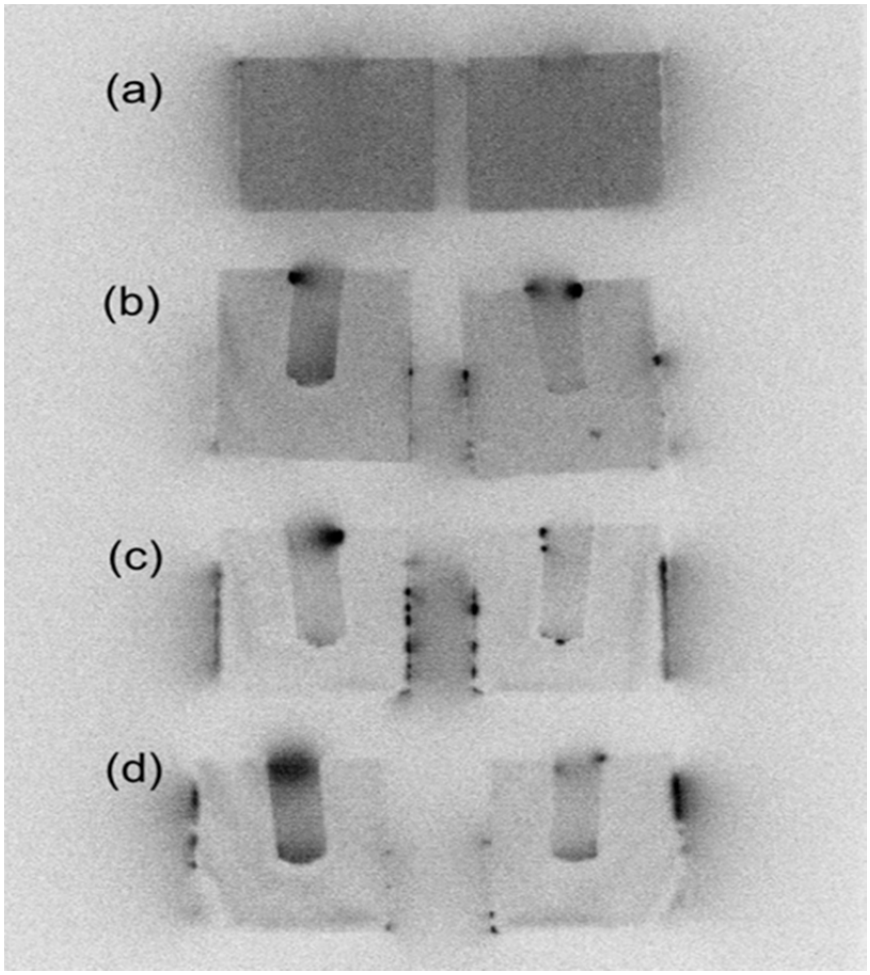

Fig. 11.26 Unenhanced digital autoradiograph of the distribution of ^{137}Cs in the NRVB cylinder used in the diffusion experiments

Key to fig. 11.26
(a) ^{137}Cs tracer only in NRVB equilibrated water
(b) ^{137}Cs tracer only in CDP solution
(c) ^{137}Cs tracer and $CsNO_3$ carrier in NRVB equilibrated water
(d) ^{137}Cs tracer and $CsNO_3$ carrier in CDP solution

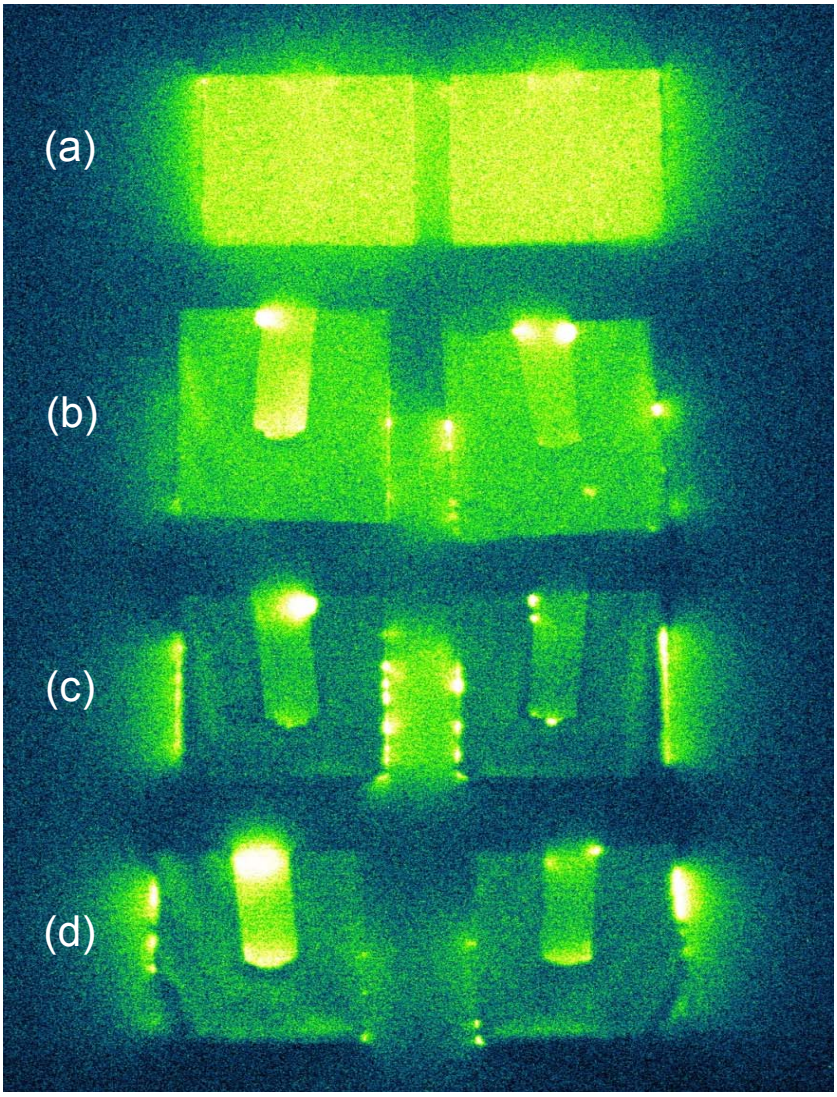

Fig. 11.27 ImageJ enhanced digital autoradiograph of the distribution of ^{137}Cs in the NRVB cylinder used in the diffusion experiments

Key to fig. 11.27
(a) ^{137}Cs tracer only in NRVB equilibrated water
(b) ^{137}Cs tracer only in CDP solution
(c) ^{137}Cs tracer and $CsNO_3$ carrier in NRVB equilibrated water
(d) ^{137}Cs tracer and $CsNO_3$ carrier in CDP solution

The autoradiography images (figs. 11.26 and 11.27) of the NRVB cylinders corroborated with the experimental observation and diffusion profiles. The darker areas of fig 11.26 indicate higher activity, these have been colourised to produce fig 11.27. The cylinders spiked only with tracer ^{137}Cs concentrations (a and b) showed higher retention of activity than those with $CsNO_3$ carrier (c and d). Cylinders from the experiments in the presence and absence of CDP were very similar when carrier was present. At tracer concentrations the CDP reduced the retention of ^{137}Cs in the NRVB. The profiles within the blocks were very homogeneous, especially in the case

of the tracer experiment in absence of CDP. There were several other interesting features noticeable on the autoradiographs including; high intensity spots around the area where the central core is sealed and on the outer surfaces, the central core appears brighter in three of the four images and non-verticality of the central cores is evident.

11.7 Cs Diffusion Scanning Electron Microscopy

In an attempt to determine the possible mineral phases involved in the retention of Cs on the outer surface of the NRVB, the same sectioned cylinders were examined with a Scanning Electron Microscope (SEM) at BGS Nottingham. The imaging (see figs. 11.28 and 11.29 below) using environmental SEM conditions in combination with energy-dispersive X-ray analysis (EDX) indicated that most of the outer surface of the specimens was covered by amorphous forms of CSH. In some localised areas close to the sealed top of the specimens, calcium carbonate could be found in crystalline form as calcite and the presence of ettringite was noted. An accumulation of amorphous magnesium silicates was also evident. The areas at the edge of the specimens that showed high activity in the autoradiography images did not show an accumulation of any specific mineral phase. The most intense spots are in the area of the seal at the top of the NRVB cylinders and are most likely the result of trapping radiotracer between the stopper and the wax. Some of the spots on the external surfaces (but by no means all) were noted to be coincident with small voids or pores partially blocked by $Ca(OH)_2$ as well as Ca silicates which would have been water filled at the end of the experiment. Subsequent evaporation of the water would have left locally concentrated regions of radiotracer. This phenomenon needs further investigation as it challenges the assumption that all of the radiotracer reaching the NRVB surface is discharged into the receiving water. It could also be causing a delay in breakthrough and may indicate that a different type of sorption (or even incorporation) is occurring at the surface.

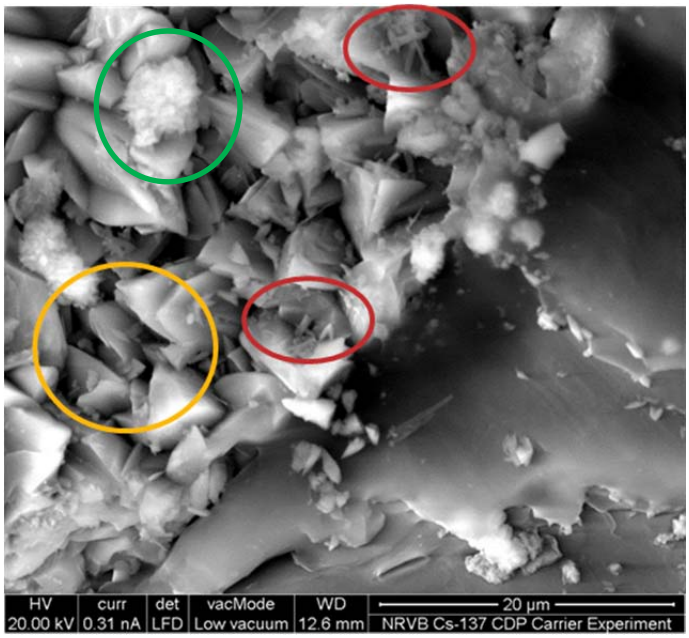

Fig. 11.28 Micrograph showing calcite (red) and possibly aragonite (yellow) in some localised areas and amorphous magnesium silicates (green), wax seal is the flat sheet lower left

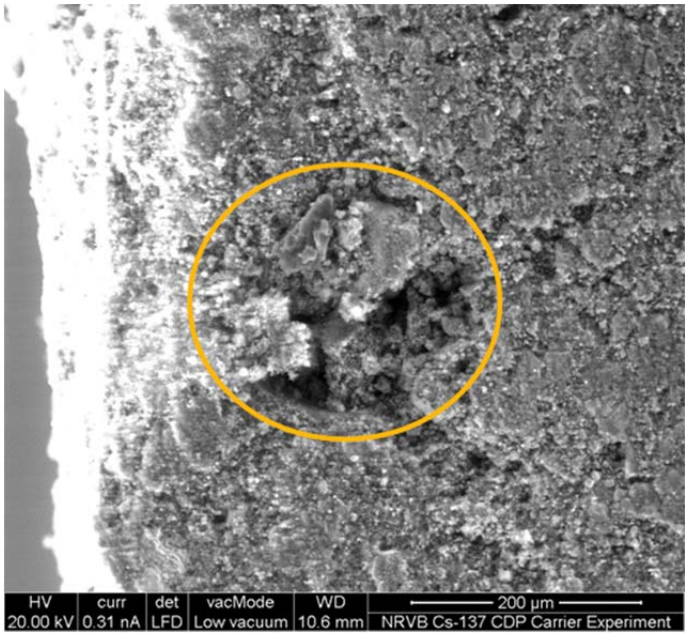

Fig. 11.29 Some of the "hot spots" at the edge of the solid corresponded to voids coated with $Ca(OH)_2$ (portlandite)

11.8 ^{137}Cs Tracer Advection with NRVB Equilibrated Water

11.8.1 Additional information relevant to the ^{137}Cs NRVB advection experiment

Only one ^{137}Cs advection experiment has been undertaken. The experimental procedure including 3 day “run in” for the NRVB cylinder was identical to that used in the HTO advection experiments (see section 10.6). The only exception being that the initial injection volume was 150 µL. The injection contained 2911 Bq or 174660 d min^{-1} of ^{137}Cs. All the eluent was collected and analysed for ^{137}Cs and the evaporation of the eluted mass corrected for by comparison with a weighed water blank left in the sample collector for the duration of the experiment. All ^{137}Cs determinations were performed by gamma counting in the same manner as the diffusion experiments.

The experiment was not completely successful as it was not always possible to maintain a steady driving pressure. In addition, clearing of blocked pipework caused an interruption soon after commencement and again near the end. The results are presented on fig. 11.30 and the interruptions are clearly visible as having caused step changes in the flow rate. A ^{137}Cs recovery plot is presented as fig.11.31 and the complete dataset as table 11.12. It is important to note that the x axis is mass eluted and not time.

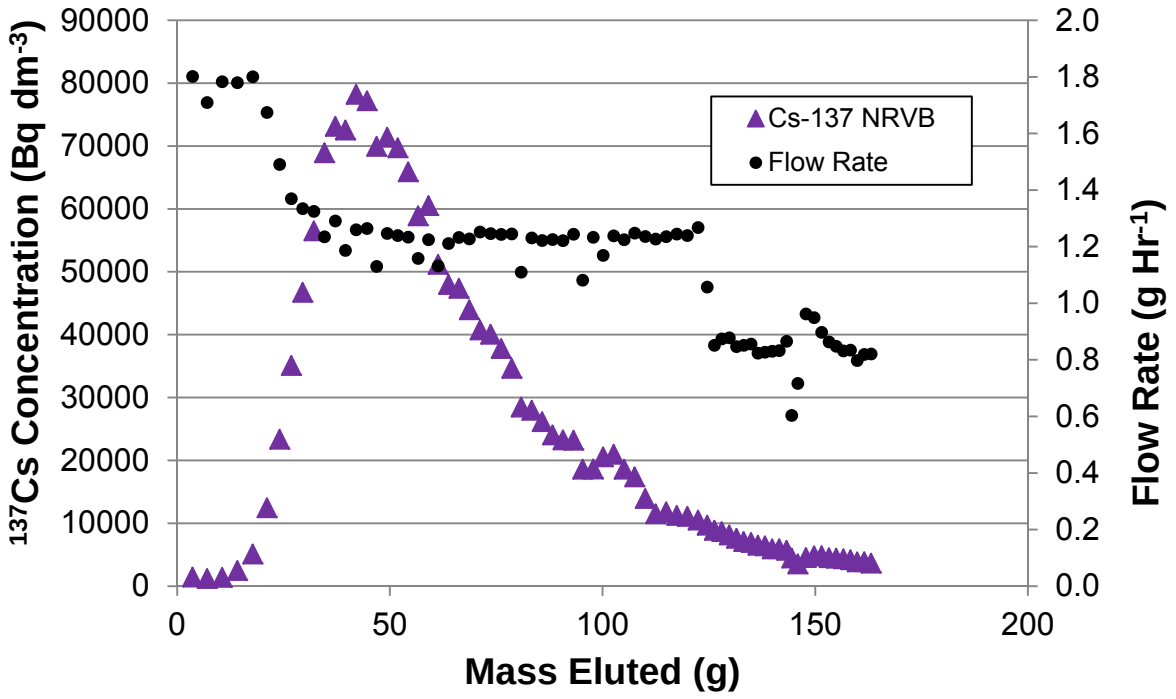

Fig. 11.30 Results of the ^{137}Cs tracer advection using NRVB equilibrated water

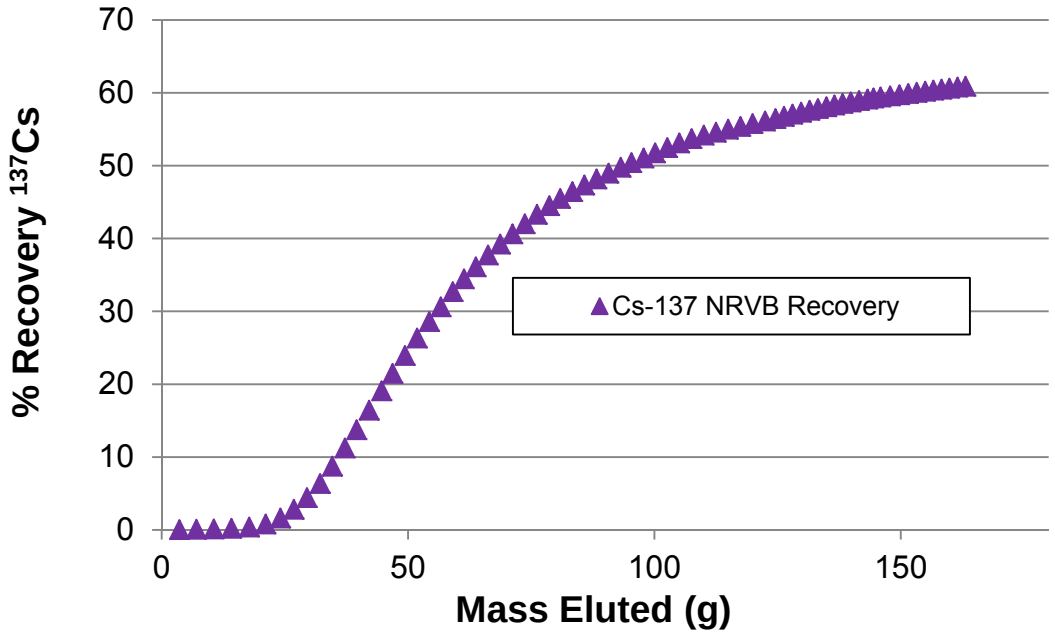

Fig. 11.31 Recovery plot of the ^{137}Cs tracer advection using NRVB equilibrated water

11.8.2 Results of the ^{137}Cs NRVB advection experiment

The plots resulting from the ^{137}Cs advection experiment appeared to be smooth despite the practical difficulties encountered. The breakthrough of ^{137}Cs occurred after 24 g of eluent had passed through the NRVB cylinder, approximately one pore volume and slower than the comparable HTO experiment. The peak top was sharp achieving a maximum activity concentration of 78217 at 42 g eluted. The peak was also asymmetric with significant tailing (this tailing is usually attributed to constricted porosity causing trapping of a proportion of the Cs [35]). The recovery plot indicates that only ~60% of the ^{137}Cs activity added to the system was recovered.

Autoradiographs of the cylinder were not produced because it went on to be used for the initial trial runs of HTO and ^{90}Sr. Consequently it was not possible to determine where the residual ^{137}Cs may have accumulated in the system. The possibilities are those seen in the diffusion experiments which included, distribution throughout the NRVB, deposition as hotspots on the outer edge of the cylinder or unmoved within the central core. Additional possibilities for the advection experiment include losses within the advection cell, pipework and seals, though monitoring washing and cleaning after completing the trial runs did not reveal any measureable amounts of ^{137}Cs.

11.9 Discussion of the Suite of ^{137}Cs Diffusion and Advection Results

The radial diffusion technique has been successfully used to investigate the migration of Cs through cylinders of the potential backfill NRVB. Experiments were performed using NRVB equilibrated water and a solution of cellulose degradation products (CDP) produced in the presence of the NRVB components.

The diffusion experimental results, notwithstanding the limitations of the GoldSim model mentioned in section 7.5, showed a decrease in the D_e and K_d in the presence and the absence of CDP for the carrier experiments when compared with the results at tracer concentrations. This may be attributable to restriction of ion mobility by the electrostatic field created by other ions present in solution. It is known that D_e for an ionic species can be dependent on the molar conductance of the ion (Λ_i), which is empirically associated to the concentration by a relationship of the type: $\Lambda_c = \Lambda_0 - kc^n$, where c is the concentration of the ionic species (see section 5).[60] It is possible to express the dependence of the diffusivity with the concentration of the

diffusing ion by a similar equation; $D_c = D_0 - k_c c^n$, where k_c is a constant that includes the pore characteristics of the matrix and for monovalent species n is usually 0.5.[62] In the present work a decrease of diffusivity with increasing concentration of Cs is observed. However, it would be necessary to carry out further investigations to confirm the relationship between diffusivity and the square root of the concentration. In the longer term it may be possible to combine Fick's second equation with previous empirical observations [61] to produce a better description and predictor of the movement of ^{137}Cs in these experiments. The main issues are the complexity of the ionic and dissolved organic solutions and the consequent difficulty assigning values for molar conductance or diffusivity. A further issue to consider is the initial addition of Cs for the carrier experiments which is at a relatively high concentration (~32,000 mg dm^{-3}, 0.25 mol dm^{-3}) that reduces as the experiment proceeds. This reduction in concentration should result in the electrostatic interaction having a decreasing effect on diffusivity throughout the experiment.

The reduction of the K_d values observed for the carrier experiments could be attributed to partial saturation of the solid and reduction of the sites available for retention of Cs. However, the background concentrations of Cs (see table 9.1) in the experiments, particularly in the CDP solutions is appreciable (10^{-5} ~10^{-4} mol dm^{-3}) and competing Na^+ and K^+ ions may provide a more reasonable explanation.

CDP reduced the retention of Cs onto NRVB under diffusive conditions. However, no effect had been reported in batch studies dealing with sorption of Cs onto ordinary portland cement (OPC) in contact with ISA [90] (at constant NaOH and KOH concentrations) or onto NRVB in the presence of CDP.[57] The diffusion of Cs through OPC in contact with a synthetic young pore water has been compared with and without ISA ($5x10^{-3}$ mol dm^{-3}), reporting no effect of the organic ligand on the diffusion rate of Cs. When comparing the composition of the NRVB and CDP solutions used in the present work (see table 9.1), it can be seen that the concentrations of Na^+, K^+ and Ca^{2+} in the CDP liqueur were between 2 and 3 times higher than in the NRVB equilibrated water. A further study [161] reported reduction of sorption to hydrated cement as a consequence of the increased concentration of concomitant ions Na^+ and K^+.

Consequently it remains possible that the differences observed in the present work are at least partially attributable to the concentration variation of the alkali metal ions and not solely due to the presence of CDP.

In the case of CDP solutions produced with the same methodology and comparable ionic strengths, the difference observed between previous batch studies [57] and the present experiments could be due to the increased surface area available for sorption as a result of the crushing of the material. The crushed material would necessarily offer more available sorption sites than intact cements potentially overcoming the increased concentration of the competing Na^+ and K^+.

It is difficult to draw any conclusions from the mixed element experiments except that the presence of other species in the original slurry in the central core appeared to increase the relative retention of Cs when compared to the carrier experiments. The low frequency of sampling during the first week of the experiments negated a meaningful comparison of breakthrough times and early concentration increase.

For the advection experiment it is tempting to link the results with the ^{137}Cs tracer only diffusion experiment in NRVB equilibrated water where retention of the radioisotope on the NRVB cylinder was comparable at ~60% of the total added. However at this early stage in the development of the radial advection technique and without autoradiographs or model results, it would be unwise to conclude that the results to have been generated by the same mechanisms.

12.0 Iodine

12.1 Background

The main iodine isotope of interest is ^{129}I, it is a component of the UK radioactive waste inventory and is mentioned in the latest estimate at 01/04/2010 [26] and table 12.1 below reproduces the relevant activities.

Isotope	HLW	ILW	LLW	units
^{129}I	9.0×10^{-2}	5.9×10^{-1}	3.4×10^{-4}	T Bq

Table 12.1 ^{I29}I in the UK waste inventory at 01/04/2010

The activities in the table above may not seem particularly high but ^{129}I has a half live of 1.57×10^{7} years [141] and this coupled with high mobility in the environment means that it will be a significant contributor to the long term inventory of a GDF. ^{129}I decays by beta emission and the decay equation is:

$$^{129}_{53}I \rightarrow {}^{129}_{54}Xe + {}^{0}_{-1}e + \bar{\nu}_e$$

Radioactive isotopes of iodine are produced by nuclear fission. ^{235}U in nuclear reactors fissions asymmetrically into two large fragments; ^{131}I can be produced in this manner with a yield close of 3% making it a significant product and problematic should releases occur. However, its short half-life of 8 days ensures that even very significant releases will decay in less than 3 months. ^{129}I is produced in the same manner with a yield of 0.67% and represents a more serious long term hazard. In terms of human health impact it should be noted that all iodine isotopes migrate preferentially to the thyroid gland and small exposures to radioactive iodine isotopes can have detrimental health effects[158 162]

The readily available isotope, ^{125}I has a 59.9 day half-life and will be used in this research. ^{125}I decays by electron capture to an excited state of ^{125}Te that immediately undergoes gamma emission with a maximum energy of 35 keV. This is the emission used to quantify ^{125}I in this research. The excess energy of the excited ^{125}Te is internally converted to eject electrons (also at 35 keV), produce Auger electrons and X-rays. Eventually, stable non-radioactive ground-state ^{125}Te is produced as the final decay product. The specific activity of ^{125}I is 6.45×10^{14} Bq g^{-1}.

The decay equation is:

$$^{125}_{53}I + {}^{0}_{-1}e \rightarrow {}^{125}_{52}Te + \bar{\nu}_e$$

The natural abundance of ^{125}I is effectively zero. It is created by electron capture decay of ^{125}Xe, a synthetic isotope of Xe that can be created by neutron activation of ^{124}Xe, it has a naturally occurring abundance of approximately 0.1%. The irradiation target is natural xenon gas containing ^{124}Xe which is loaded into capsules of zircaloy-2 (a nonreactive alloy, transparent to neutrons) to a pressure of about 100 bar prior to neutron activation. The relevant equations for the manufacture of ^{125}I are given below.[163 164]

$$^{124}_{54}Xe + {}^{1}_{0}n \rightarrow {}^{125}_{54}Xe$$

$$^{124}_{54}Xe + {}^{0}_{-1}e \rightarrow {}^{125}_{53}I$$

The diffusion and advection experiments undertaken were as follows:

- Diffusion with NRVB equilibrated water using ^{125}I tracer only and ^{125}I tracer plus KI carrier
- Diffusion with CDP solution with ^{125}I tracer plus KI carrier
- Mixed isotope diffusion experiments (NRVB equilibrated water and CDP solution) where I diffusion is evaluated in the presence of Cs, Ni, Eu, U and Th.
- Advection with CDP solution and ^{125}I tracer only

Autoradiographs have been produced where possible and GoldSim transport models have been generated for the diffusion experiments with the exception of the multi-element diffusions. Reference is also made to a series of solubility experiments (under and over-saturation) underway in the Loughborough Radiochemistry laboratory as part of the NDA chemical containment research.[134]

12.2 Additional Experimental Details for ^{125}I Diffusion Experiments

The diffusion experiment used a 50 µl addition of ^{125}I (produced as the iodide by Perkin Elmer) to the central cores of duplicate NRVB cylinders, equivalent to:

- C_{max} of 677 d min^{-1} (2538 Bq per cylinder and an initial concentration in the inner core = $2.1x10^{-11}$ mol dm^{-3}) at 133 days after commencement for NRVB equilibrated water with ^{125}I tracer and KI carrier.
- C_{max} of 1261 d min^{-1} (4727 Bq per cylinder and an initial concentration in the inner core = $3.9x10^{-11}$ mol dm^{-3}) at 67 days after commencement for CDP solution with ^{125}I tracer and KI carrier.
- C_{max} of 1381 d min^{-1} (5179 Bq per cylinder and an initial concentration in the inner core = $4.3x10^{-11}$ mol dm^{-3}) at 50 days after commencement for the NRVB equilibrated water with ^{125}I tracer only.

C_{max} is the maximum number of disintegrations per minute possible in the 1 cm^3 sample if the ^{125}I was to equilibrate completely into the liquid in the system. The measured activities are quoted at the time (in days) after commencement. The results, figures and tables also utilise a calculation to account for the effect on C_{max} caused by the removal of volume and activity during sampling. A disproportionately small amount of activity is removed during sampling compared to the total volume. The overall effect is to increase C_{max} each time a sample is taken. C_{max} is used to prepare the relative retention plots to enable visualisation of a range of diffusion experiments on the same axes.

The solubility research[134] did not identify any potential effects on I solubility due to high pH, presence of NRVB, presence of CDP or reducing agents. Consequently fast breakthrough, equilibration or at least movement to a stable condition and limited retention of ^{125}I were anticipated.

The mass of I as KI added to each of the carrier experiments was 32.8 mg for the NRVB equilibrated water and 31.8 mg for the CDP solution. This mass was calculated such that in the case of complete equilibration with the liquid in the system, the final concentration of I would be ~10^{-3} mol dm^{-3}. The initial concentration of the carrier in the inner cores was 0.15 mol dm^{-3} The mass of ^{125}I added was considered to be negligible.

The NRVB cylinders used for the experiments were equilibrated in the CDP solution in sealed containers, in a nitrogen glovebox for 43 days prior to commencement. The radioisotope addition was made outside the nitrogen glove box, the cylinder was sealed, submerged in 200 cm^3 NRVB equilibrated water and returned to the glove box over a period of less than two minutes. The total volume of equilibrated water in

the system at the start is assumed to be 225 cm^3 (the additional 25 cm^3 being an estimate of the pore water volume in the NRVB cylinder). ^{125}I activity concentrations were determined by counting the peak centred at 0.035 MeV on a Packard Cobra II auto-gamma counter. 1 cm^3 samples were taken throughout the experimental duration but all determined on one day when the experiment was completed to negate the need to correct for radioactive decay. In addition 1 cm^3 "control" samples were made at the start of the experiment to enable relative retention graphs to be made. The control samples and appropriate blanks were also determined on the same day as the samples from the experiments. All determinations were subject to the 2 σ criterion available on the gamma counter to ensure results are statistically valid.

12.3 Results of ^{125}I diffusion experiments

All results are presented as the average of duplicates along with vertical error bars denoting the 90% confidence limits assuming a two tailed t distribution and horizontal error bars set at +/- 0.25 days. Three graphs are presented for each experiment; showing all results, early data and C/C_{max} relative retention. The data are presented in two tables for each experiment. A short commentary is provided after each set of graphs and before the tables.

12.3.1 Results of the ^{125}I tracer KI carrier NRVB diffusion experiment with NRVB equilibrated water

The results of the ^{125}I tracer with KI carrier NRVB equilibrated water diffusion experiment are presented below as figs. 12.1 to 12.3 and as tables 12.2 and 12.3 in appendix 1.

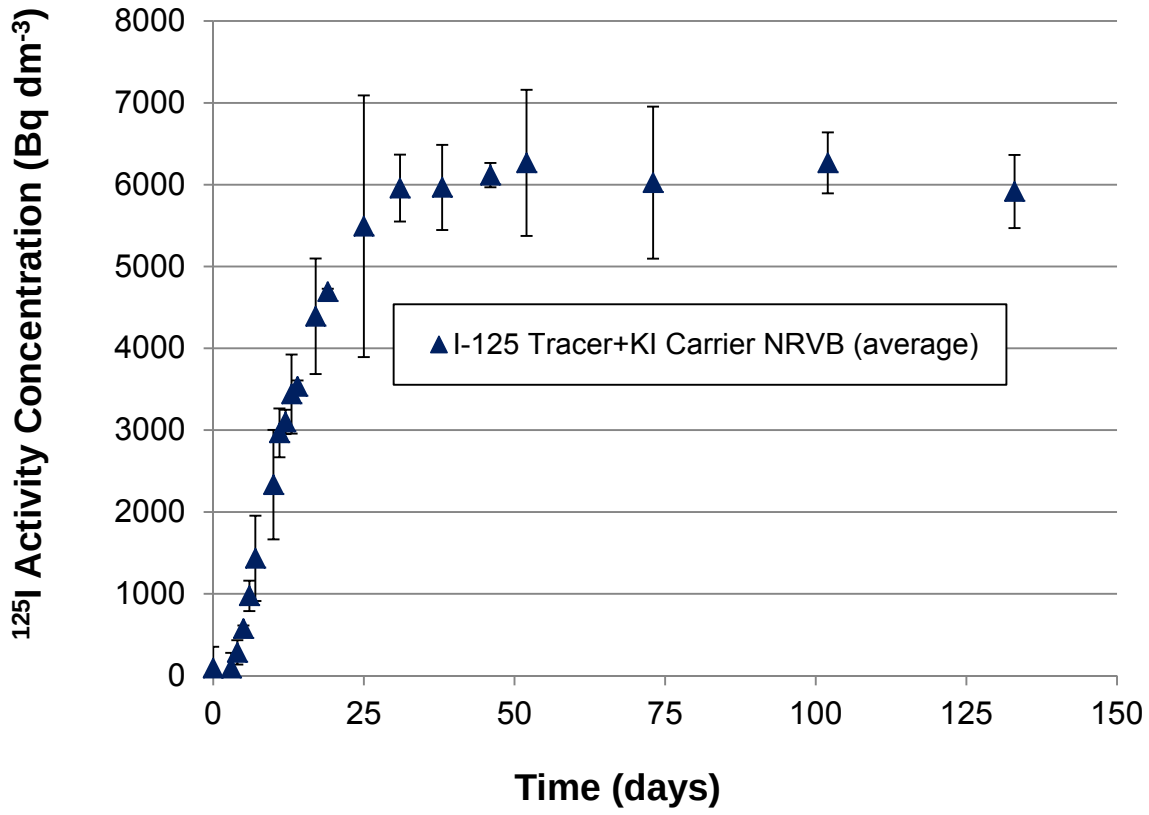

Fig. 12.1 Results of the NRVB ^{125}I tracer; KI carrier diffusion experiment using NRVB equilibrated water

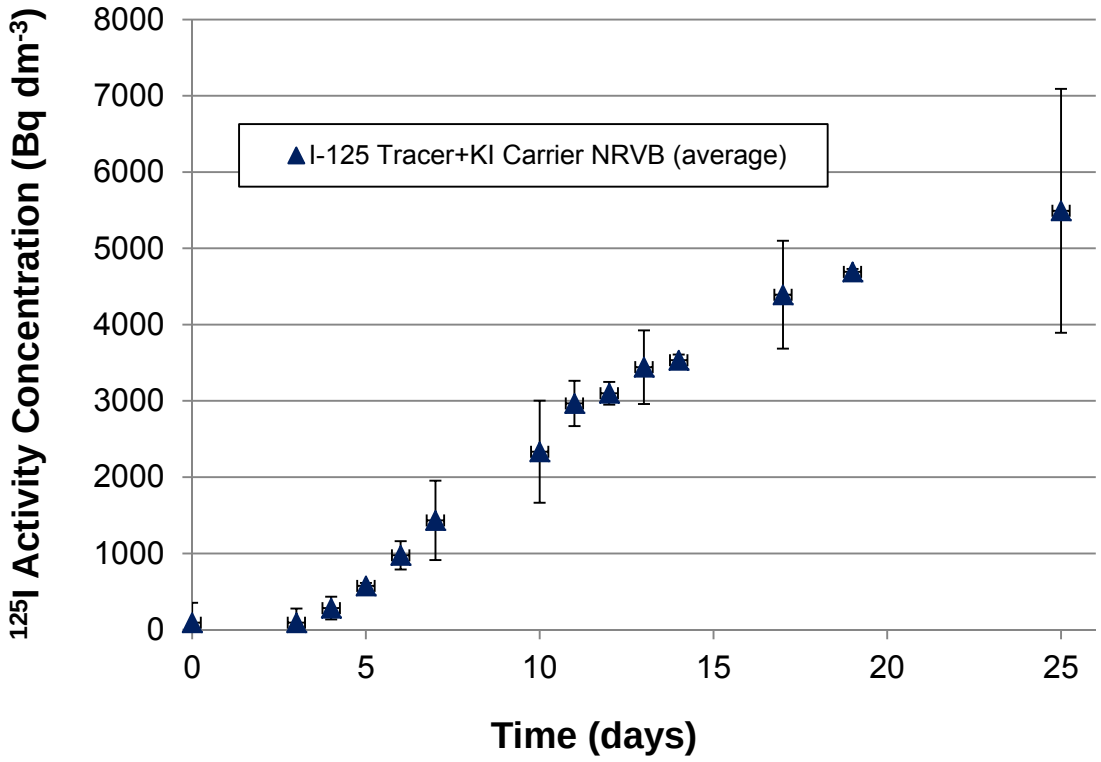

Fig. 12.2 Early data from the NRVB ^{125}I tracer; KI carrier diffusion experiment using NRVB equilibrated water

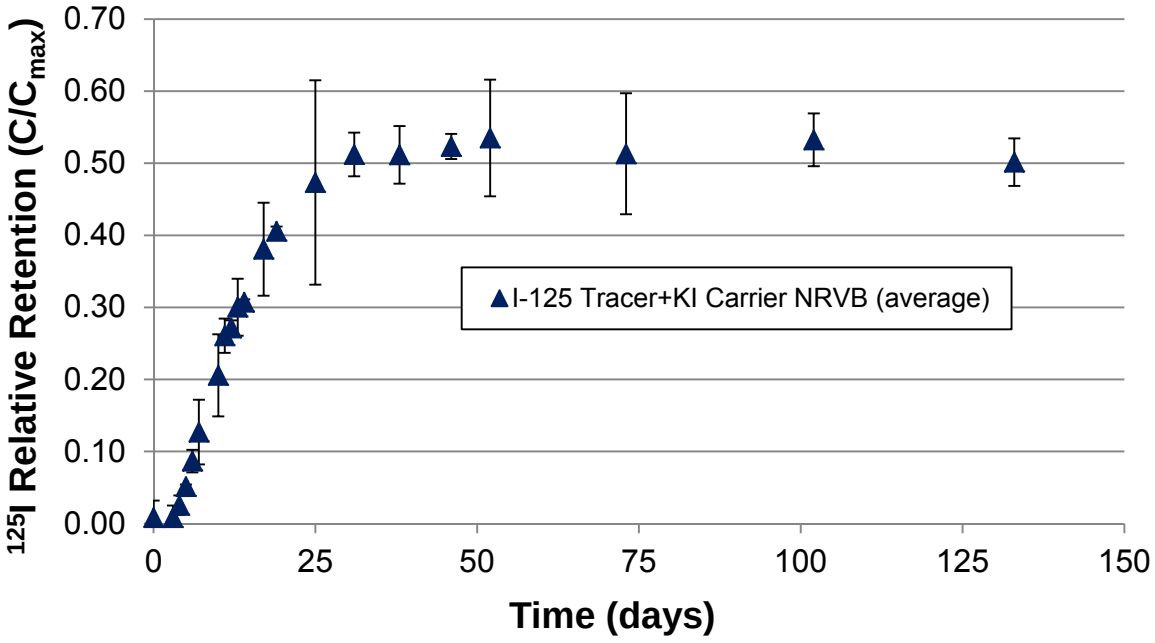

Fig. 12.3 C/C_{max} relative retention plot of the NRVB ^{125}I tracer; KI carrier diffusion experiment using NRVB equilibrated water

Commentary

The experiment was allowed to run for 133 days but it was clear by this time that the samples with lower activities were becoming difficult to determine due to radioactive decay of the ^{125}I. Breakthrough commenced at 3.0 days followed by an almost linear increase in concentration over the following 18 days. The concentration continued to increase at a slower rate stabilising at 6000 Bq dm^{-3} at 31 days. The maximum activity concentration of 6267 Bq dm^{-3} was achieved at 102 days. The relative retention plot (where C_{max} = 677 d min^{-1}) indicates that just over 50% of the tracer (and carrier) was retained on the NRVB cylinder, inferring that just under 50% of the tracer (and carrier) was in solution.

12.3.2 Results of the ^{125}I tracer with KI carrier CDP diffusion experiment

The results of the ^{125}I tracer with KI carrier using CDP solution, diffusion experiment are presented below as figs. 12.4 to 12.6 and as tables 12.4 and 12.5 in appendix 1.

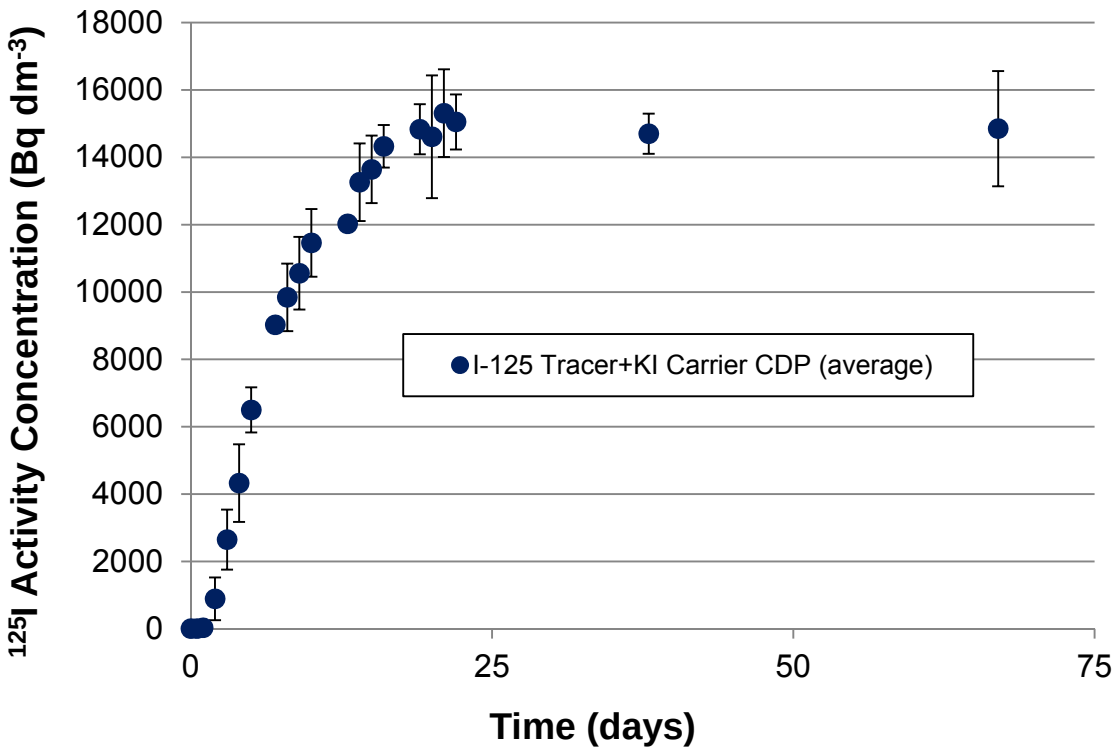

Fig. 12.4 Results of the NRVB ^{125}I tracer; KI carrier diffusion experiment using CDP solution

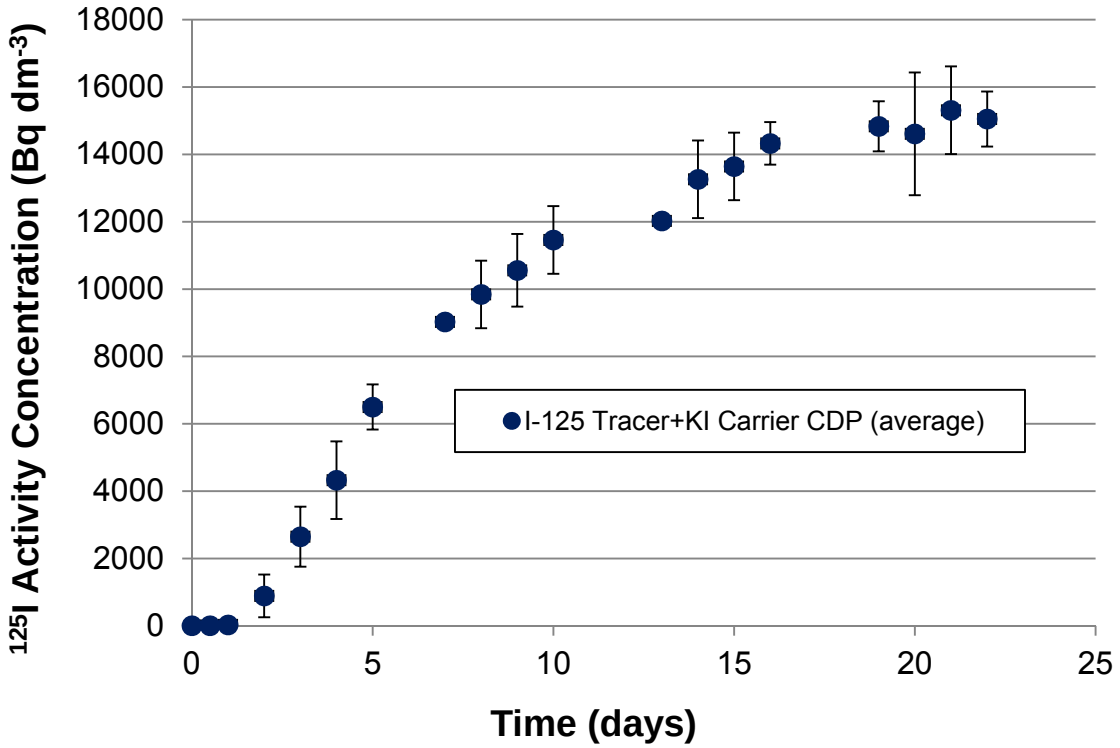

Fig. 12.5 Early data from the NRVB ^{125}I tracer; KI carrier diffusion experiment using CDP solution

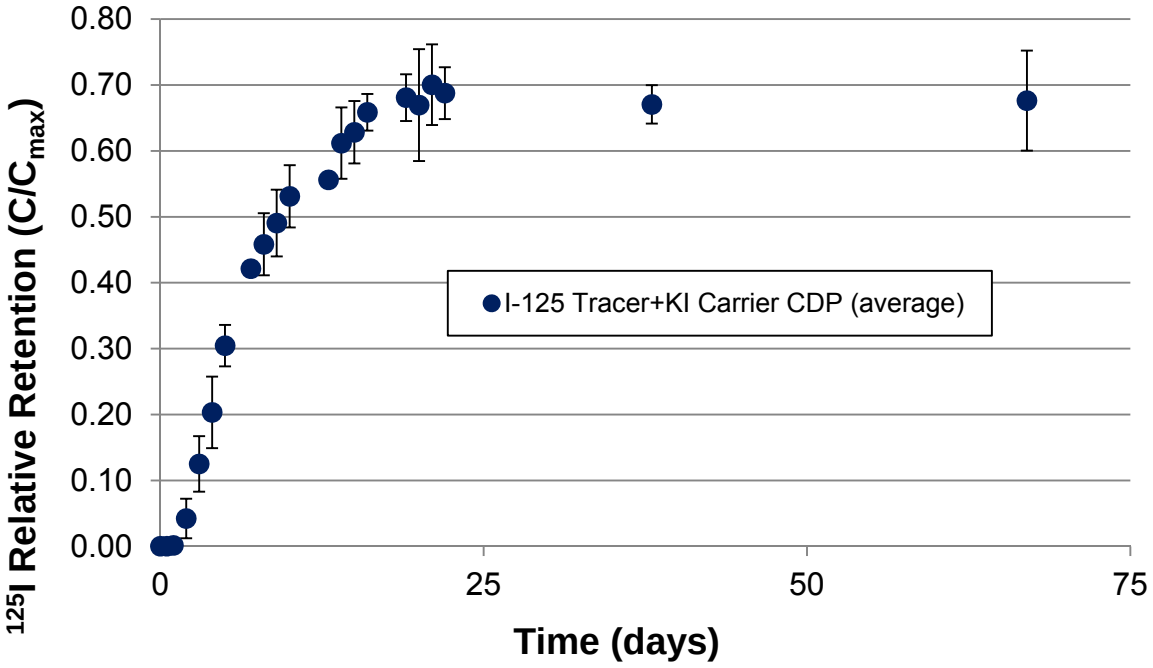

Fig. 12.6 C/C_{max} relative retention plot of the NRVB ^{125}I tracer; KI carrier diffusion experiment using CDP solution

Commentary

The experiment was allowed to run for 67 days to ensure the low activity determinations could be relied upon. It was clear that the activity concentration in solution had stabilised. Breakthrough commenced between 1 and 2 days followed by an almost linear increase in concentration over the following 3 days. The concentration continued to increase at a slower rate stabilising at 15000 Bq dm^{-3} at 22 days. The maximum activity concentration of 15308 Bq dm^{-3} was achieved at 21 days. The relative retention plot (where C_{max} = 1261 d min^{-1}) indicates that 30-35% of the tracer was retained on the NRVB cylinder, implying that 65-70% of the tracer (and carrier) was in solution.

There are clear differences in the diffusion profiles arising from the two experiments and it apparent that I is more mobile in the presence of CDP, exhibiting both faster diffusion and lower retention on the solid.

12.4 Iodine in Mixed Element Diffusion Experiments

12.4.1 Additional information relevant to the mixed element diffusion experiments

The mixed element diffusion experiments were set up to investigate the effect on the diffusion rates of Cs, I, U, Th, Eu and Ni when all were present. The experiments, eleven of each type (NRVB equilibrated water and CDP solution) were the first to be undertaken using the radial approach. Sufficient $CsNO_3$ and KI were added to produce a 10^{-3} mol dm^{-3} solution in the event of complete equilibration. In addition precipitates from a neutralised solution containing $UO_2(NO_3)_2.6H_2O$, $Th(NO_3)_4.4H_2O$, $EuCl_3.6H_2O$ and $NiCl_2.6H_2O$ were mixed with the Cs and I solutions to produce a slurry which was added to the central cores of the NRVB cylinders. The NRVB cylinders used for the CDP experiments were equilibrated in a CDP solution for 30 days prior to commencement. The iodine determinations were performed by ion chromatography using a Dionex DX 150 with AS4 anion exchange column and carbonate/bicarbonate eluent.

12.4.2 Iodine Results for the mixed element diffusion experiments in NRVB equilibrated water and CDP solution

The average of eleven results for both types of experiment is presented below as fig. 12.7. A graph comparing the breakthrough, concentration increase and relative retention of the NRVB and CDP single element active experiments is also presented

as fig. 12.8 on the same page. A brief commentary on figs. 12.7 and 12.8 is also provided. The data for the mixed element experiments are provided as tables 12.6 and 12.7 in appendix 1.

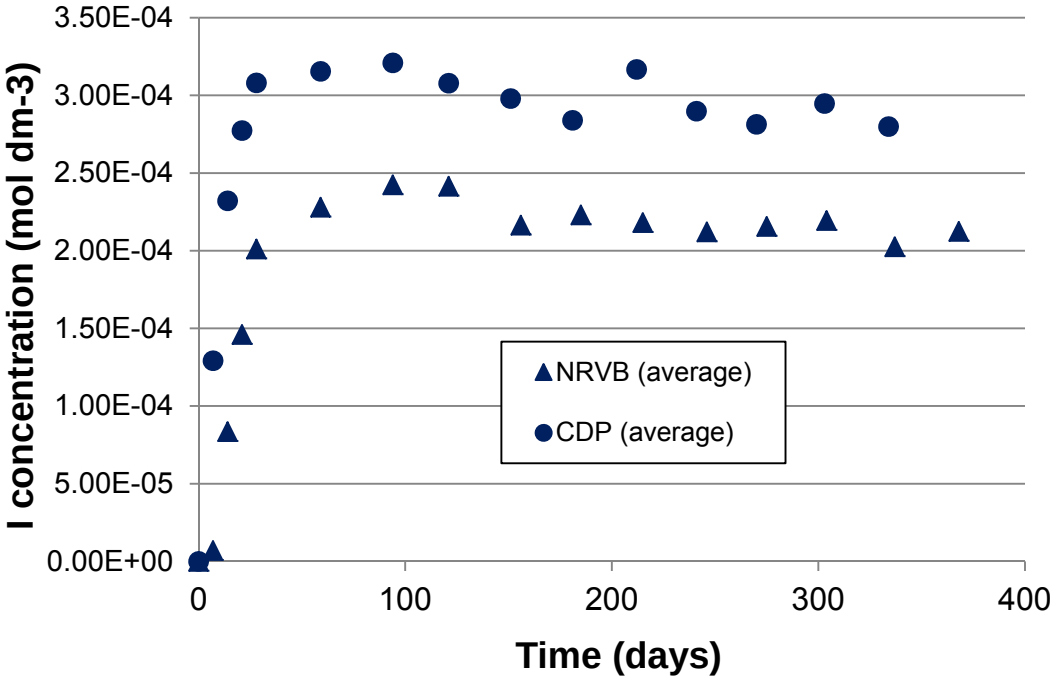

Fig 12.7 Averaged I Results for the mixed element diffusion experiments in NRVB equilibrated water and CDP solution

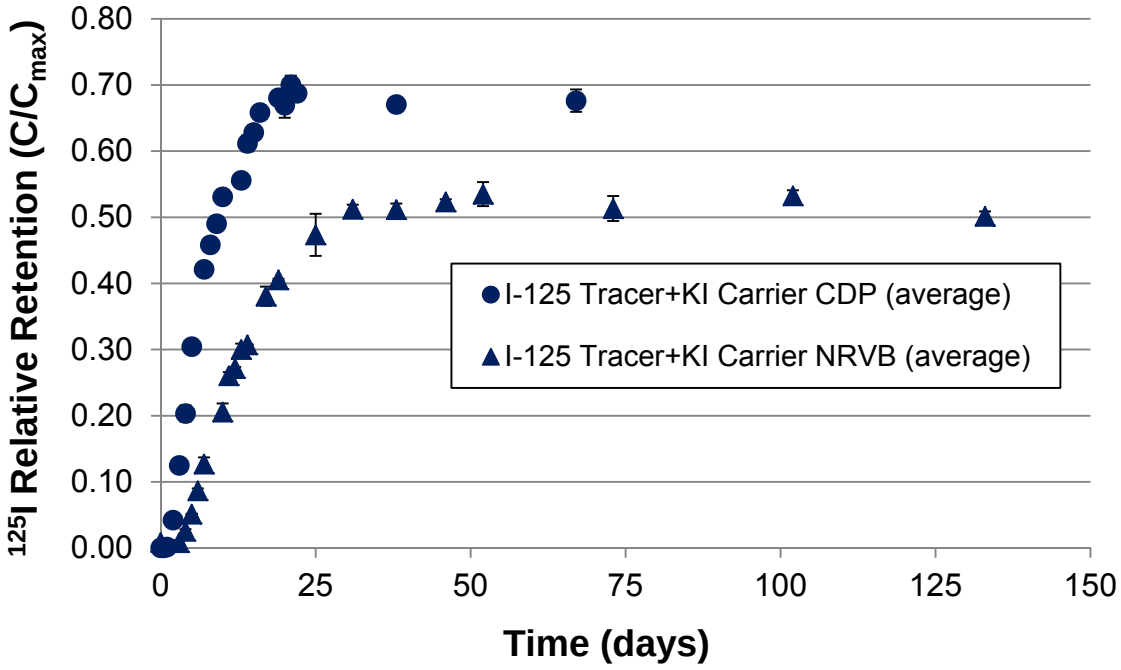

Fig. 12.8 C/C_{max} relative retention plots for the NRVB and CDP diffusions

Commentary

The main points of interest arising from the iodine diffusion results in the mixed element experiments are:

- The overall behaviour was similar to the single element experiments; the presence of CDP caused faster breakthrough and stabilisation and reduced retention.
- Retention of I was higher in the mixed element experiments than the single element experiments. C_{max} was 10^{-3} mol dm^{-3} and retention was ~30% and ~20% in the absence and presence of CDP, respectively.
- The mixed element data are not as consistent as those generated by the single element versions of the experiments and whilst averaging has helped the visualisation, the raw data shows a large amount of variation across the eleven replicates (see figs. 12.9 to 12.12 for raw data plots). This variation commences early in the experiments, the extent of variation is less pronounced in the CDP experiments.
- These experiments were very early attempts at the technique and modifications have been on-going, in particular handling time outside the glove box and dosing of the central cores have been speeded up and subject to more control.

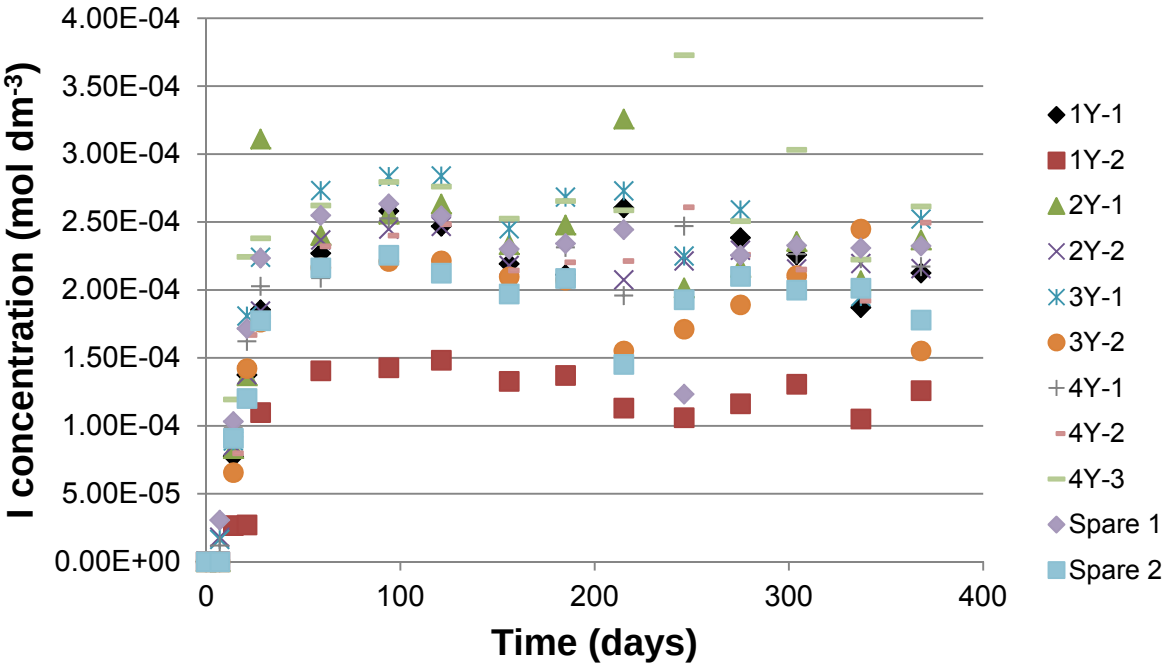

Fig. 12.9 I Raw data (un-averaged) for the mixed element diffusion experiments in NRVB equilibrated water [134]

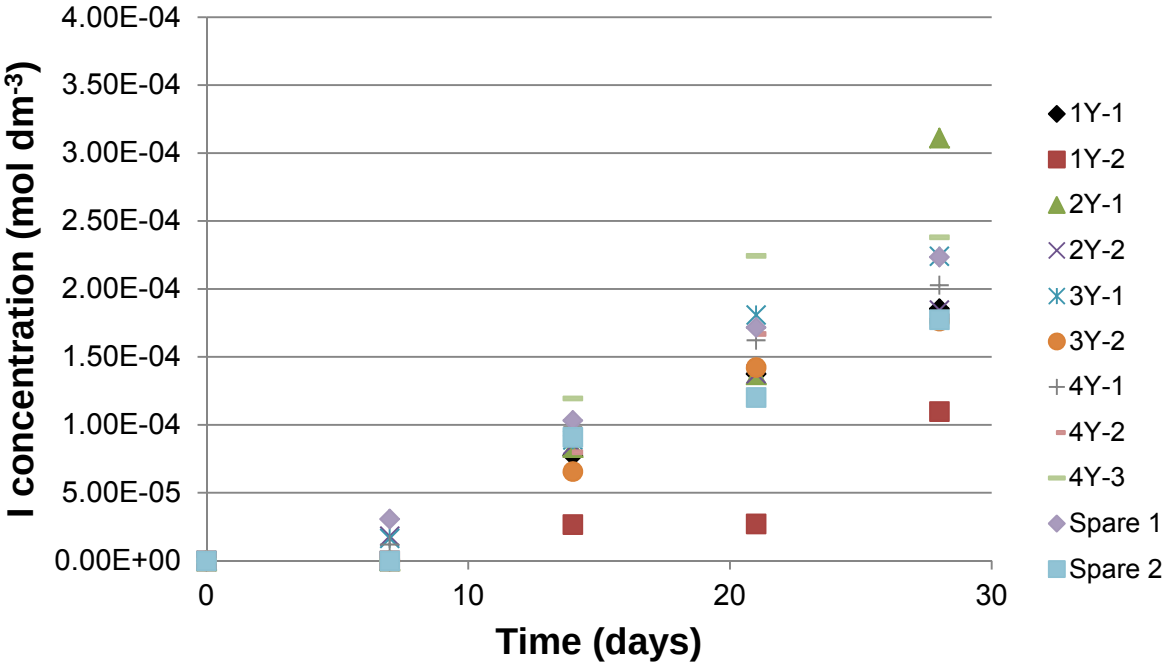

Fig. 12.10 I Early raw data (un-averaged) for the mixed element diffusion experiments in NRVB equilibrated water [134]

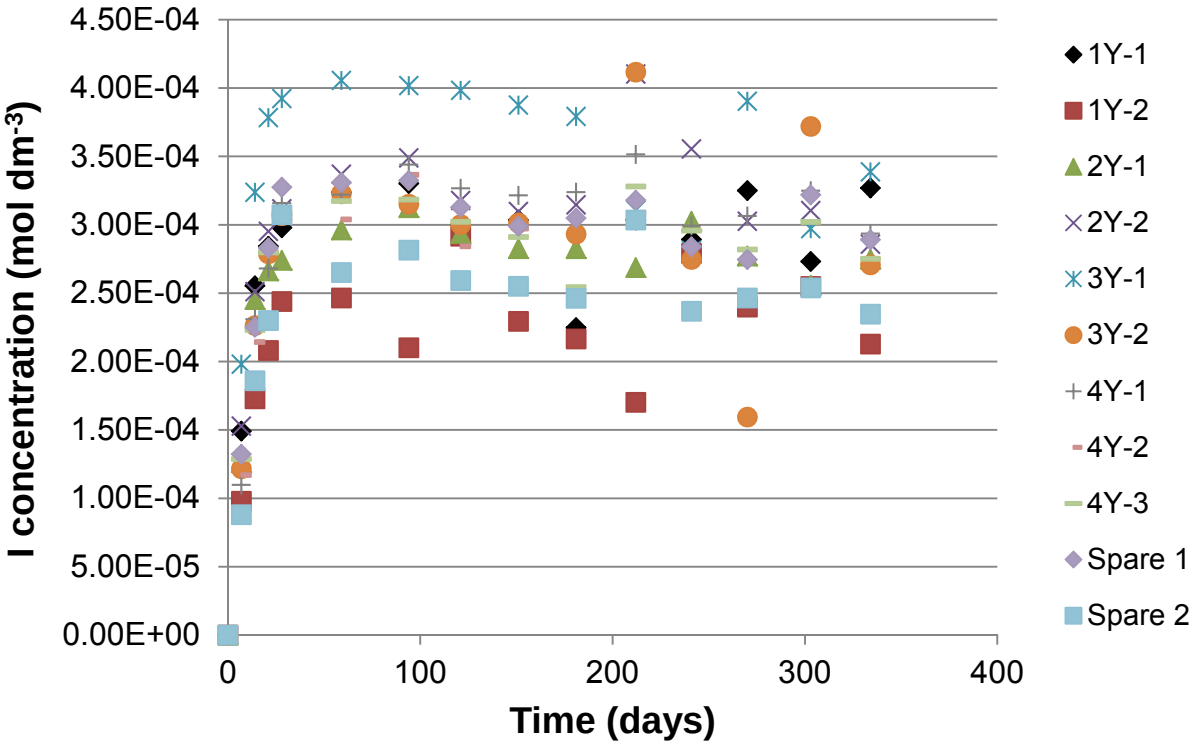

Fig. 12.11 I Raw Data (un-averaged) for the mixed element diffusion experiments in CDP solution [134]

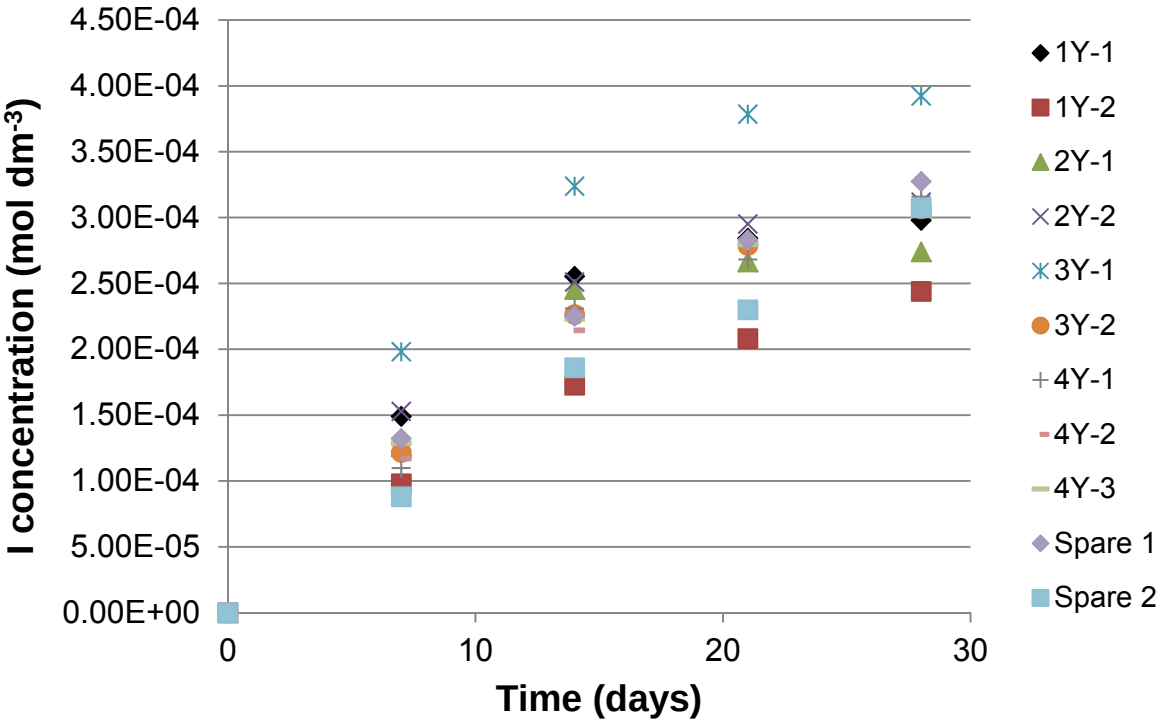

Fig. 12.12 I Early raw data (un-averaged) for the mixed element diffusion experiments in CDP solution [134]

12.5 ^{125}I Tracer Only NRVB Diffusion Experiment

12.5.1 Results of ^{125}I tracer only diffusion experiment

The results of the ^{125}I tracer only NRVB equilibrated water diffusion experiment are presented below as figs. 12.13 and 12.14 and as tables 12.8 and 12.9 in appendix 1.

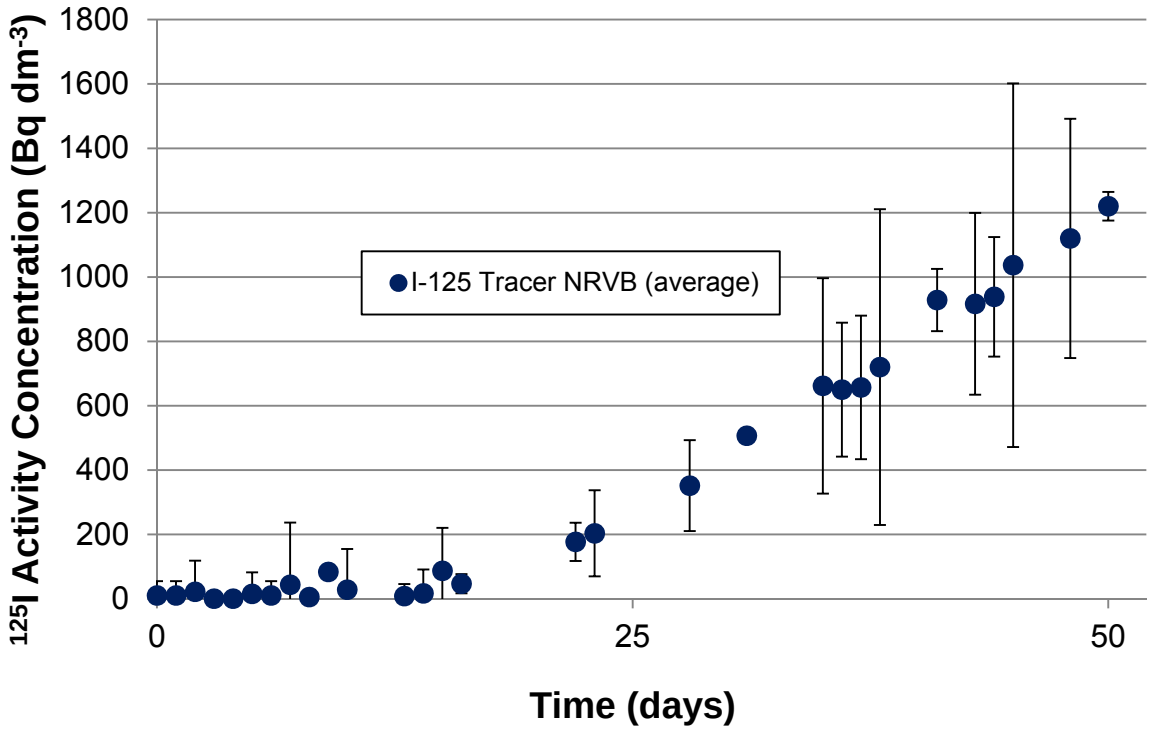

Fig. 12.13 Results from the NRVB ^{125}I tracer only diffusion experiment using NRVB equilibrated water

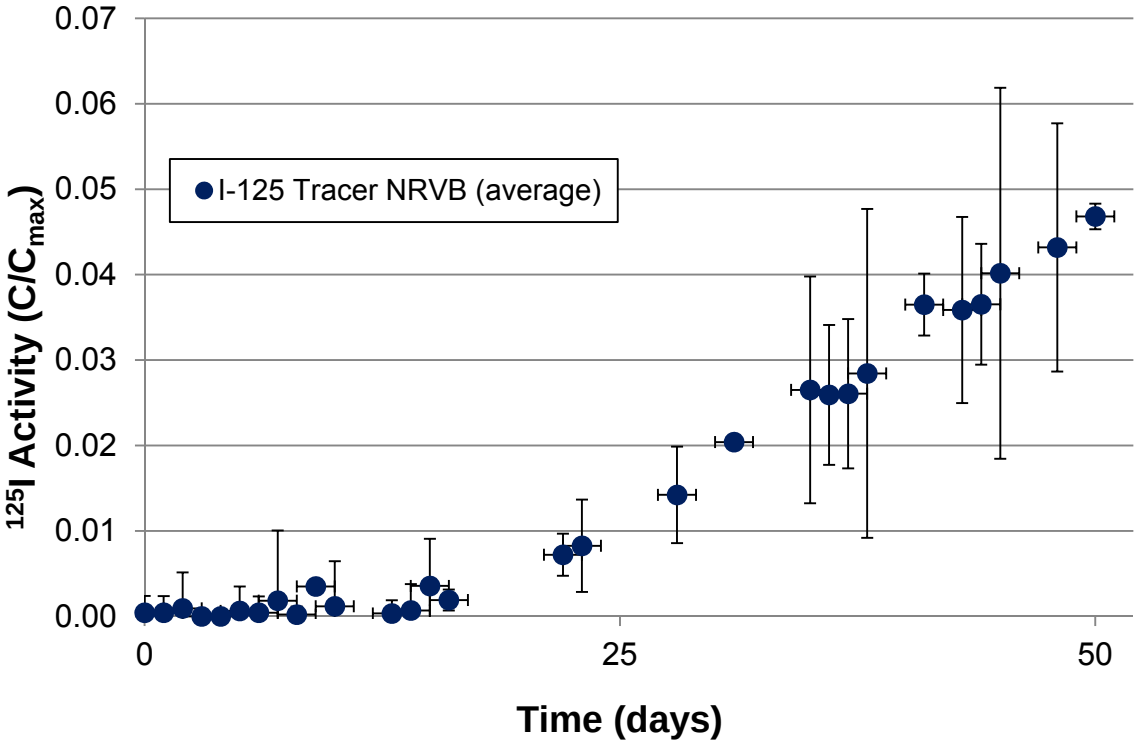

Fig. 12.14 C/C_{max} relative retention plot of the NRVB ^{125}I tracer experiment using NRVB equilibrated water

Commentary

The experiment was allowed to run for 50 days to ensure the low activity determinations could be relied upon. It was clear that the activity concentration in solution had not stabilised and that the concentration increase was proceeding very slowly in relation to the half-life of ^{125}I. Breakthrough commenced at around 15 days (in contrast to the 1-3 days in the carrier experiments), followed by an almost linear increase in concentration over the following 35 days. The relative retention plot (where C_{max} = 1381 d min^{-1}) indicated that 95% of the tracer was retained on the NRVB cylinder after 50 days. The mass of ^{125}I added was only ~8 pg and this coupled to the ability of NRVB to retain iodide as seen in the carrier experiments explain the observations. The tracer only experiment using CDP solution was not undertaken due to the same concerns arising about the ability to achieve results in a workable timeframe.

12.6 GoldSim Modelling

12.6.1 Additional information relevant to the ^{125}I NRVB diffusion modelling

Details of the GoldSim model are fully discussed in section 7. The results from the modelling of the single element ^{125}I with KI carrier, diffusion experiments are presented as fig. 12.15 and 12.16. Initial concentrations are provided in section 12.2. It is important to be aware that activity concentrations were modelled and as a consequence a direct comparison cannot be made in the same manner as possible with the relative retention plots. Partition is referred to as K_d throughout, primarily because this term, rather than R_d is used in GoldSim. The LOF calculations are built into the model enabling it to determine the combination of D_e and K_d parameters that minimise LOF. Short commentaries explaining the data envelopes, effective diffusivity, partition coefficient and LOF outputs are also provided.

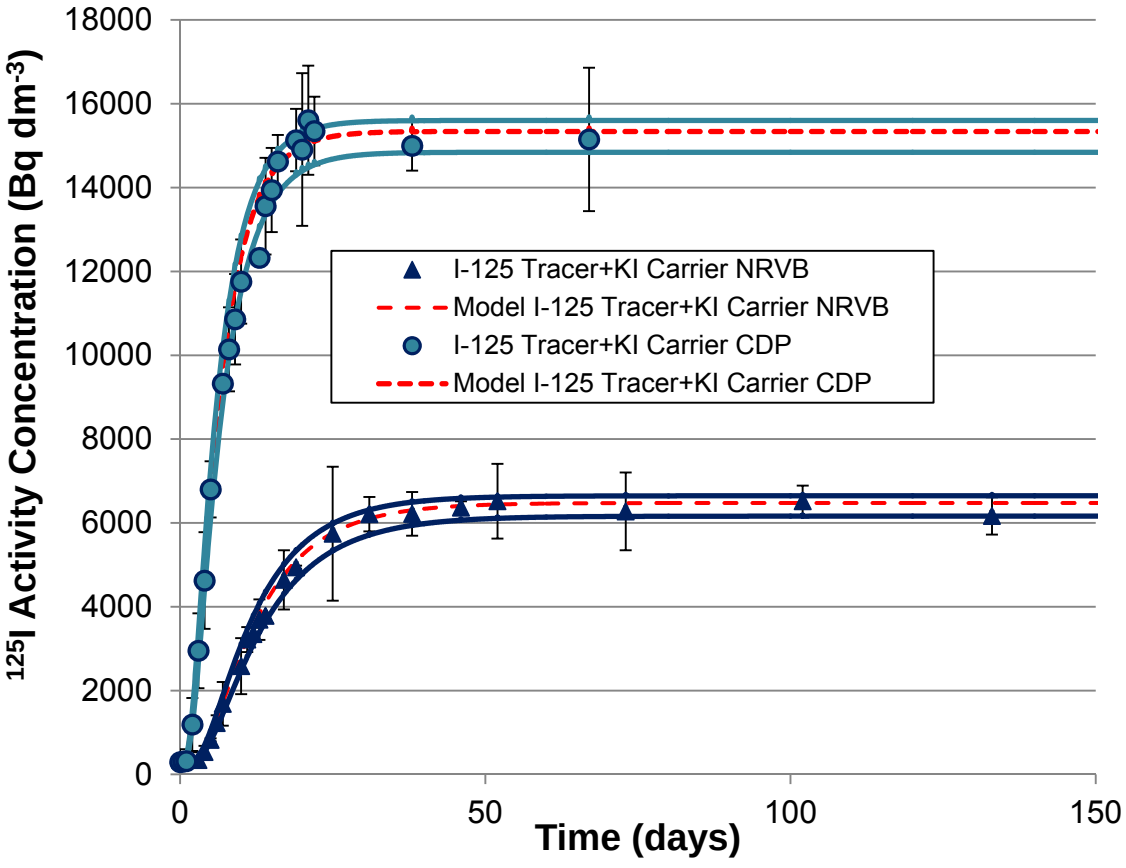

Fig. 12.15 Experimental and modelled diffusion curves for ^{125}I at tracer and tracer carrier (KI) concentrations in NRVB equilibrated water and CDP solution

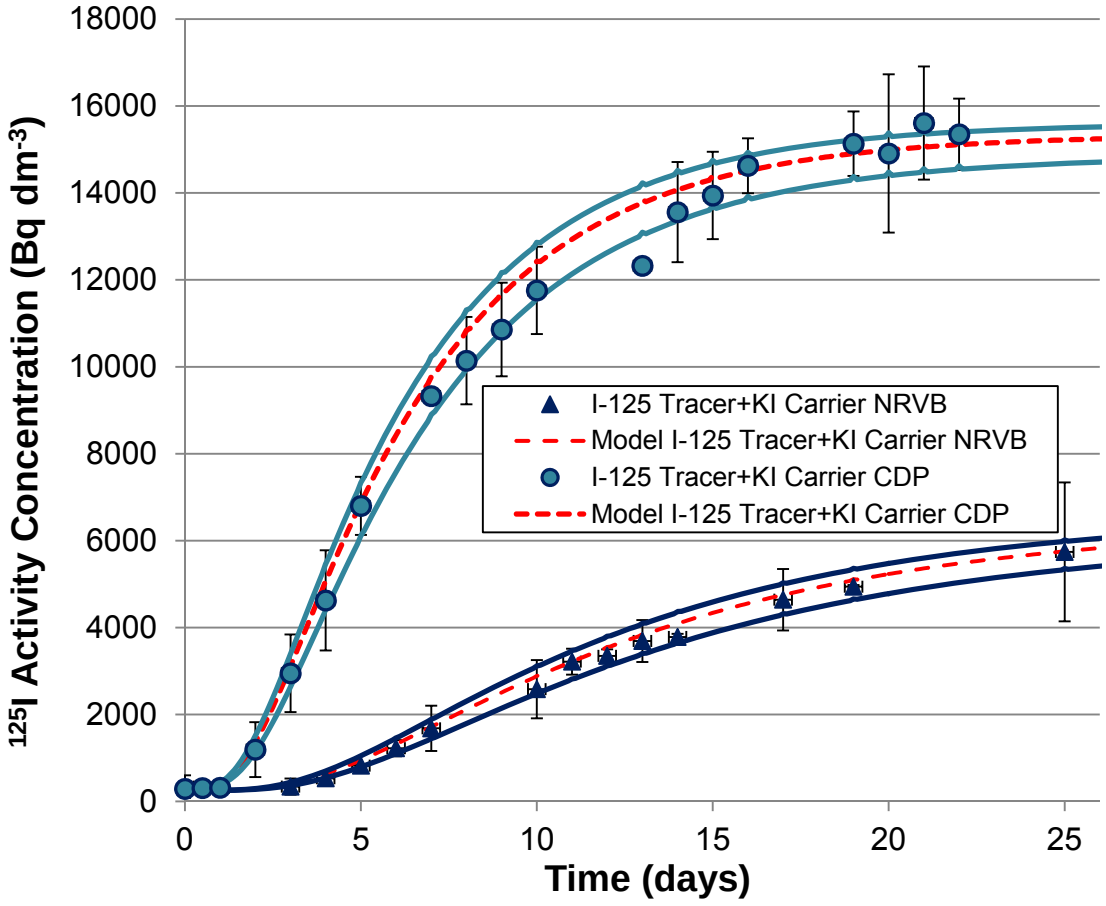

Fig. 12.16 Early experimental and modelled curves for ^{125}I at tracer and tracer carrier (KI) concentrations in NRVB equilibrated water and CDP solution

Commentary

A change of colours has been used in figs. 12.15 and 12.16 for clarity. It is important to note that figs. 12.15 and 12.16 are not relative retention plots and cannot be used to make comparisons between the NRVB and CDP experiments because of the different initial tracer concentrations and experimental durations (the relative retention plot is fig 12.8 earlier in this section).

The best fit D_e and K_d model results for the NRVB carrier experiments were 2.5x10^{-10} m^2 s^{-1} and 3.4x10^{-3} m^3 kg^{-1}, respectively (hashed red line in figs. 12.15 and 12.16). The LOF for the best model result was 3.6%. The majority of the experimental data could be contained in the interval defined by setting D_e in a range between 1.8x10^{-10} and 3.3x10^{-10} m^2 s^{-1} and K_d between 3.2x10^{-3} and 3.6x10^{-3} m^3 kg^{-1}, (solid turquoise lines on the figures). The results that fall outside the envelope can be clearly seen. The early data plot (fig. 12.16) has been provided to illustrate the fit is good even at

low concentrations. It should be noted that all observed values are included in the LOF results even those outside the envelope.

The carrier experiments using CDP solution yielded best fit D_e and K_d model results of 3.8×10^{-10} m^2 s^{-1} and 1.7×10^{-3} m^3 kg^{-1}, respectively (red dotted line on the figures). The LOF for the best model result was 4.5%. The majority of the experimental data could be contained in the interval defined by setting D_e between 2.3×10^{-10}- 4.0×10^{-10} m^2 s^{-1} and K_d between1.6×10^{-3}-1.9×10^{-3} m^3 kg^{-1}, (solid dark blue lines on the figures).

The effective diffusivity values for the NRVB and CDP experiments are close but the K_d value is significantly lower in the presence of CDP.

12.7 Iodine Diffusion Autoradiography

The autoradiography produced two usable images from the iodine diffusion experiments. These experiments were the first to be completed and attempts to manually hack-saw the blocks failed, resulting in broken and uneven pieces unsuitable for good images. A diamond rotary saw was purchased but the elapsed time, low energy of the ^{125}I emissions and its short half-life required long exposures to be made as soon as possible after the experiments were concluded. As a consequence of these issues further attempts to produce good images were abandoned. Fig 12.17 shows the two ImageJ enhanced images from the NRVB carrier experiment.

The images were produced using a Fuji BAS MP 20 cm x 25cm autoradiography image plate with an exposure duration of 5 days. The plate was developed at BGS, Nottingham.

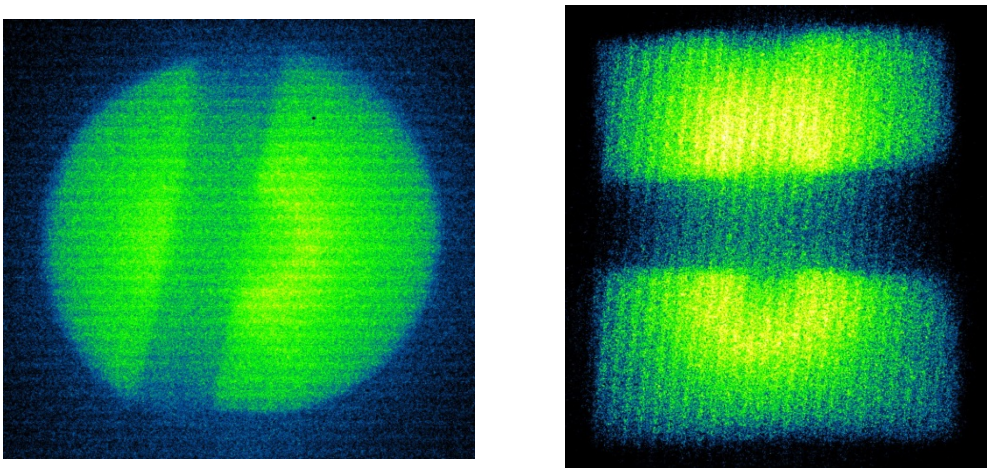

Fig. 12.17 ImageJ enhanced digital autoradiograph of the distribution of ^{125}I in the NRVB cylinder used in the carrier diffusion experiments

When compared with the images obtained for ^{137}Cs (see section 11.6), clear differences are observed in the behaviour of the two isotopes. In the case of ^{137}Cs, distribution of the isotope is homogeneous within the solid, for ^{125}I a gradient from the centre of the NRVB cylinder can be observed, with higher activity in the central area of the block. Preferential paths generated by micro-fissures in the cement are not observed.

12.8 ^{125}I Tracer Advection with CDP Solution

12.8.1 Additional information relevant to the ^{125}I CDP advection experiment

Only one ^{125}I advection experiment has been undertaken. The experimental procedure including 3 day “run in” for the NRVB cylinder was identical to that used in the HTO advection experiments (see section 10.6). The control samples indicated that the150 µL injection contained 1807 Bq or 108417 d min^{-1} of ^{125}I at the start of the 8 day experiment and1638 Bq or 98267 d min^{-1} at the conclusion. The latter value was used to determine recovery of the radionuclide as all samples (including relevant controls) were determined at the end of the experiment. All the eluent was collected and analysed for ^{125}I and the evaporation of the eluted mass corrected for by comparison with a weighed water blank left in the sample collector for the duration of the experiment. All determinations were performed by gamma counting in the same manner as the diffusion experiments.

Initially the experiment appeared to progress smoothly with no significant interruptions. It had been anticipated that the presence of CDP would cause relative retention to be low, even at tracer concentration and that rapid elution would occur.

However, it soon became evident that the radioisotope was being eluted from the NRVB cylinder much more slowly than expected. Consequently, the experiment was stopped at 8 days to try to get a good quality autoradiograph and ascertain the fate of the ^{125}I in the NRVB cylinder. The results up to 8 days are presented as fig. 12.18; the ^{125}I recovery plot as fig.12.19 and the complete dataset as table 12.10. A short commentary is provided after the figures. It is important to note that the x axis is mass eluted and not time.

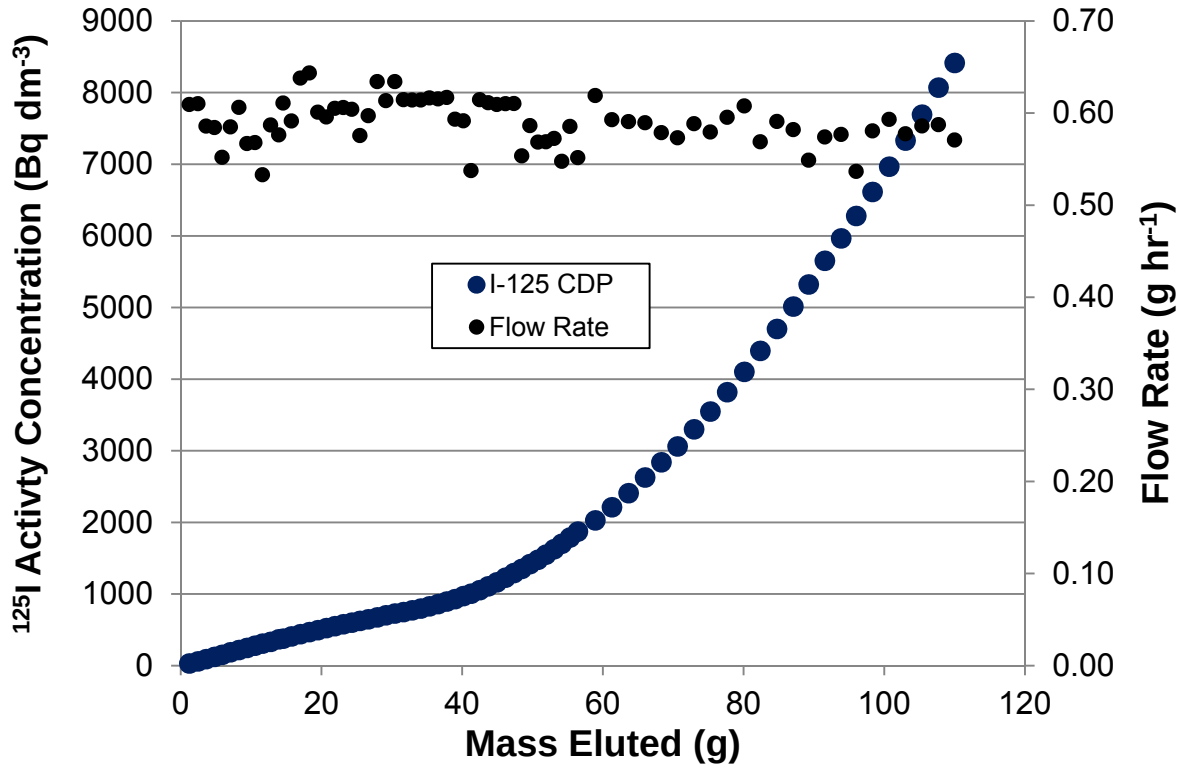

Fig. 12.18 Results of the ^{125}I tracer only advection using CDP solution

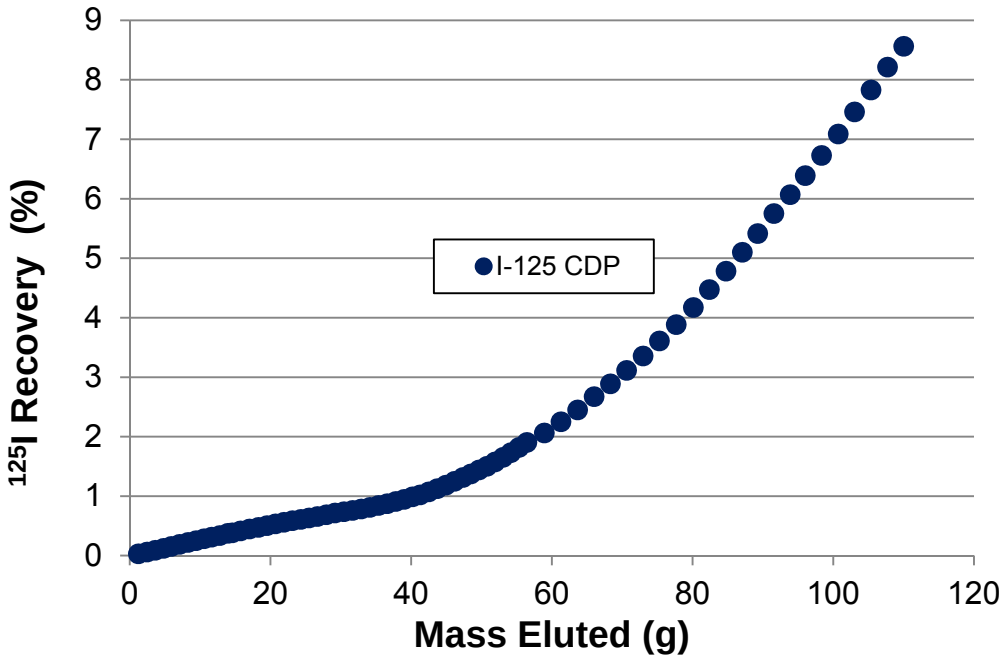

Fig. 12.19 Recovery plot of the ^{125}I tracer only advection using CDP solution

Commentary

The plots resulting from the ^{125}I advection experiment appeared to be smooth and a steady flow rate of ~0.6 g hr^{-1} was maintained throughout. The breakthrough of ^{125}I occurred after 40 g of eluent had passed through the NRVB cylinder, almost two pore volumes and somewhat slower than the comparable HTO and Cs experiments. The recovery plot indicates that less than 10% of the ^{125}I activity had been recovered after 125 g or five pore volumes had eluted. It was clear that the experiment could take a significant time to complete as almost 90% of the radionuclide remained on the NRVB after 8 days. The issues of short half-life and weak emissions created a choice between running to completion or using the opportunity to stop the experiment and produce an autoradiograph. The latter option was selected. The resulting autoradiograph is discussed in section 12.9 after table 12.10.

12.9 Autoradiograph from the ^{125}I CDP Solution Advection Experiment

The ^{125}I CDP advection NRVB cylinder was removed from the cell, dried and sectioned longitudinally and transversely using a diamond rotary masonry saw. The pieces were placed face down on a Fuji BAS MP 20 cm x 25cm autoradiography image plate in darkness and exposed for a period of 6 hours. The sections were then removed, again in darkness and the plate taken to British Geological Survey, Nottingham to be developed. The resulting ImageJ enhanced image is shown adjacent to a photograph of the same cylinder, as fig. 12.20 below. Alternative transverse images were produced but the one reproduced below was the best quality.

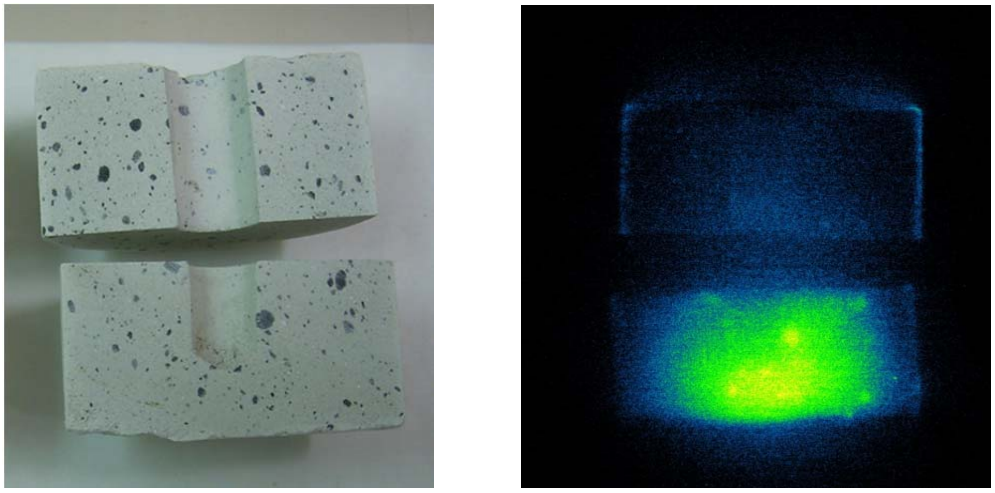

Fig. 12.20 Photograph and autoradiograph of ^{125}I advection using CDP solution

There are a number of points of interest arising from the images in fig. 12.20:

- The cylinder contains numerous black inclusions clearly visible on the photograph. The inclusions are ashy particles present in the OPC that sink to the bottom of the wet NRVB mix and accumulate in the final cylinders to be poured.
- The cylinder shows evidence of accumulations of radioactivity associated with the inclusions (see overlay fig. 12.21 below). This could be due simply to a change in surface area associated with the black inclusions or an increase in pozzolanic properties of the type seen when PFA is added to cements.[41 99]
- The ^{125}I is confined to the lower part of the cylinder suggesting that the radionuclide injection was not evenly distributed in the central core.

- There is evidence of ^{125}I on the outer edge of the upper section of the cylinder even though no activity moved in that direction. This raises the possibility that it was deposited there after elution through the cylinder.

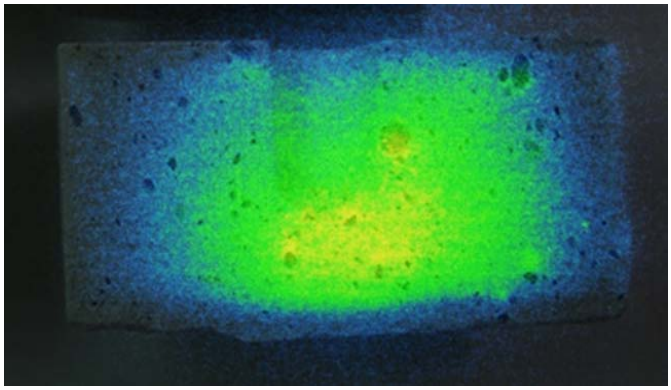

Fig. 12.21 Overlay of the photograph and autoradiographs from fig. 12.20

12.10 Discussion of the Suite of ^{125}I Diffusion and Advection Results

The radial diffusion technique has been successfully used to investigate the migration of I through cylinders of the cementitious backfill NRVB. Experiments were performed using NRVB equilibrated water and a solution of cellulose degradation products (CDP) produced in the presence of the NRVB components.

The diffusion experiments using ^{125}I with KI carrier showed a clear reduction in retention from 50% to 30% in the presence of CDP. In the mixed element experiments retention was ~30% and ~20% in the absence and presence of CDP, respectively.

Previous studies [165] have indicated that the uptake of I^- onto degraded and undegraded cement pastes is highly correlated with the concentration of Ca in solution and the consequent development of positive charges on the surface of the cement. This mechanism would enable the uptake of I^- onto the cement by electrostatic, non-specific interactions. At the pH of the cement solution (12.8-12.9 see table 9.1), the organic components of CDP are expected to be negatively charged ions. Under similar conditions the sorption of ISA (the main component of the CDP) onto cement has been reported [29] and more recently [165] where a decrease of the K_d values for the anionic species SeO_3^{2-} in presence of ISA was observed. It was suggested that the cause of the reduction of SeO_3^{2-} retention was the increase of repulsive electrostatic effects on the surface of the cement generated either by

sorption to the solid of the negatively charged H_4ISA^- or/and the removal of Ca^{2+} from the solid surface by formation of CaH_3ISA and CaH_4ISA^+ complexes. The same hypotheses could be also applied to the partition of I^- in presence of CDP seen in the present work.

The differences seen between the single element radioactive and the mixed element experiments could be due to a number of factors. Two of likely issues which were mentioned in section 11 when Cs behaviour in the experiments was discussed, are repeated below:

- The experiments were very early attempts at the technique and modifications have been on-going, in particular handling time outside the glove box and dosing of the central cores have been speeded up and subject to more control.
- The slurry placed in the central core has not been fully characterised but it is a complex mixture of salts that could be affecting precipitation, solubility and subsequent migration.

The comparatively slow evolution of the results for the ^{125}I tracer only experiment reflect the very small mass of ^{125}I added (~8 pg) in relation to the capacity of NRVB to retain I, as demonstrated by the carrier experiments.

Autoradiography imaging was used to determine the fate of the radionuclides in the NRVB. The concentration of ^{125}I in the solution in contact with the blocks was constant after a period of 30 days but the profile of ^{125}I in the block clearly showed accumulation of the radioisotope in the first 8 mm from the central well. This contrasted with the ^{137}Cs experiments where the distribution of the radionuclide was homogeneous. It is worth remembering that Cs and I will be singly charged cation and anion respectively under the experimental conditions and as a consequence unlikely to behave identically.

The GoldSim model simulated a good fit to the observed diffusion profiles and allowed determination of the diffusivity (D_e) and partition coefficient (K_d) values. The partition coefficients obtained for I^- were comparable with literature values [3] at 1.7 to 3.4×10^{-3} m^3 kg^{-1}. The diffusivity values for I^- ranged between 0.50 - 0.65×10^{-9} m^2 s^{-1}, significantly higher than those reported for high porosity cements. It is obvious from the results that many experimental factors may affect the D_e values, including

concentration of the diffusing species, ionic strength, and porosity of the media and also experimental setup (in-diffusion, leaching or through-diffusion) and caution must be taken when applying these values to make predictions.

Finally, the CDP advection experiment may have provided an insight into the location of I retention in the NRVB. There is a clear although maybe not wholly convincing association between the black inclusions seen in the NRVB and the accumulated presence of ^{125}I activity. The nature of the black inclusions is presently not known but they were assumed to be dense ashy particles accumulated at the bottom of the NRVB liquid mix. However, the photograph in fig. 12.20 shows the particles to be evenly distributed and not accumulated near the base.

13.0 Strontium

13.1 Background

The main strontium isotope of interest is ^{90}Sr, it is a component of the UK radioactive waste inventory and is mentioned in the latest estimate at 01/04/2010 [26] and table 13.1 below reproduces the relevant activities (note – it is common to report ^{90}Sr activity in conjunction with its short lived daughter ^{90}Y).

Isotope	HLW	ILW	LLW	units
^{90}Sr/^{90}Y	3.2x10^{7}	6.2x10^{5}	3.5	T Bq

Table 13.1 ^{90}Sr in the UK waste inventory at 01/04/2010

The activities in the table above are clearly significant but ^{90}Sr has a relatively short half-life of 29.1 years and this means that the inventory will have effectively decayed completely within 1000 years. [147] However, if a failure of the GDF engineering occurred within the operational phase or soon after closure, the migration of ^{90}Sr would be important and potentially diagnostic of the failure mechanism.

^{90}Sr is a potential hazard to humans as it can replace calcium in the solid tissues of the body preventing effective excretion. After entering the body, most often by ingestion of contaminated food or water, 20 – 30% of the dose may be absorbed and deposited in bones, bone marrow, teeth etc. Its presence in bones can cause bone cancer, cancer of nearby tissues, and leukaemia.[166]

^{90}Sr has a half-life of 29.1 years and decays by beta emission to ^{90}Y which in turn decays by beta emission to ^{90}Zr with a half-life of 64 days. The energy of the ^{90}Sr emission is 0.54 MeV whilst the energy of the ^{90}Y emission is much higher at 2.28 MeV. The ^{90}Y emission is the one usually measured when determining ^{90}Sr. The specific activities of ^{90}Sr and ^{90}Y are 5.21x10^{12} and 1.99x10^{16} Bq g^{-1} respectively.

$$^{90}_{38}Sr + {}^{0}_{-1}e \rightarrow {}^{90}_{39}Y + \bar{\nu}_e$$

$$^{90}_{39}Y + {}^{0}_{-1}e \rightarrow {}^{90}_{40}Zr + \bar{\nu}_e$$

Sixteen major radioactive isotopes of Sr exist, but only ^{90}Sr has a half-life sufficiently long to cause concern at nuclear facilities including GDFs. Similar to ^{137}Cs, ^{90}Sr can be produced when an atom of ^{235}U splits asymmetrically into two large fragments

with mass numbers between 90 and 140. In nuclear reactors it is produced with a yield of about 6% of fissions. ^{90}Sr is a significant component of spent nuclear fuel, high-level radioactive wastes resulting from processing spent nuclear fuel, and radioactive wastes associated with the operation of reactors and fuel reprocessing plants. It is also present in surface soil around the world as a result of fallout from past atmospheric nuclear weapons tests and contamination incidents of all scales at nuclear facilities. [158 166]

Sr is a Group II element like Ca and features in this research because it will be present in nuclear industry waste and has the potential to interact or exchange with the significant concentrations of Ca in cementitious media.

The experiments undertaken were as follows:

- Diffusion with NRVB equilibrated water using ^{90}Sr tracer only and ^{90}Sr tracer plus $Sr(NO_3)_2$ carrier
- Diffusion with CDP solution with ^{90}Sr tracer and with ^{90}Sr tracer only plus $Sr(NO_3)_2$ carrier
- Repeat of diffusion with CDP solution with ^{90}Sr tracer only with an extended pre-equilibration time.
- Diffusion with NRVB using ^{90}Sr tracer with gluconate as CDP surrogate in NRVB equilibrated water.
- Diffusion with NRVB using ^{90}Sr tracer with high ionic strength solution and gradient ionic strength.
- Advection with NRVB equilibrated water and CDP solution using ^{90}Sr tracer only.

Autoradiographs for most of the diffusion experiments have been produced. GoldSim transport models have been generated for the ^{90}Sr diffusion experiments. The GoldSim transport model has also been tested on the advection experiments. The results of the advection models suggest that there is still development work to do and consequently they are presented as GoldSim screenshots.

13.2 Additional Experimental Details for ^{90}Sr Diffusion Experiments

The diffusion experiment used a 50 µl or 100 µl addition of ^{90}Sr (produced as the nitrate by Perkin Elmer) to the central cores of duplicate NRVB cylinders, equivalent to:

- C_{max} of 3758 d min^{-1} (14092 Bq per cylinder and an initial concentration in the inner core = $1.9x10^{-8}$ mol dm^{-3}) for the ^{90}Sr tracer only, NRVB equilibrated water and CDP solution experiments.
- C_{max} of 6709 d min^{-1} (25159 Bq per cylinder and an initial concentration in the inner core = $3.4x10^{-8}$ mol dm^{-3}) for the ^{90}Sr tracer with $Sr(NO_2)_2$ carrier, NRVB equilibrated water and CDP solution experiments.
- C_{max} of 3380 d min^{-1} (12675 Bq per cylinder and an initial concentration in the inner core = $1.7x10^{-8}$ mol dm^{-3}) for the ^{90}Sr tracer with gluconate, NRVB equilibrated water experiment.
- C_{max} of 3279 d min^{-1} (12296 Bq per cylinder and an initial concentration in the inner core = $1.7x10^{-8}$ mol dm^{-3}) for the ^{90}Sr tracer high ionic strength and gradient ionic strength in NRVB equilibrated water experiment.
- C_{max} of 3279 d min^{-1} (12296 Bq per cylinder and an initial concentration in the inner core = $1.7x10^{-8}$ mol dm^{-3}) for the ^{90}Sr tracer (single cylinder) extended CDP equilibration repeat of the CDP solution experiment.

C_{max} is the maximum number of disintegrations per minute possible in the 1 cm^3 sample if the ^{90}Sr was to equilibrate completely into the liquid in the system. The results figures and tables use a calculation to account for the effect on C_{max} caused by the removal of volume and activity during sampling. A disproportionately small amount of activity is removed during sampling compared to the total volume, the overall effect is to increase C_{max} each time a sample is taken. C_{max} is used to prepare the relative retention plots to enable visualisation of a range of diffusion experiments on the same axes.

The NRVB cylinders used for the basic tracer and tracer carrier experiments were equilibrated in the CDP solution in sealed containers, in a nitrogen glovebox for 30 days prior to commencement. The radioisotope addition was made outside the nitrogen glove box, the cylinder was sealed, submerged in 200 cm^3 NRVB equilibrated water and returned to the glove box over a period of less than two minutes. The total volume of equilibrated water in the system at the start is assumed to be 225 cm^3 (the additional 25 cm^3 being an estimate of the pore water volume in the NRVB cylinder). The mass of Sr as $Sr(NO_3)_2$ added to each of the carrier experiments was 21.8 mg. This mass was calculated such that in the case of complete equilibration with the liquid in the system, the final concentration of Sr

would be ~10^{-3} mol dm^{-3}. The initial concentration of the carrier in the inner cores was 0.15 mol dm^{-3}. The mass of ^{90}Sr added was considered to be negligible.

The gluconate experiment was devised to ascertain whether a single organic substance could be used as a surrogate for the mixture of organics present in the CDP solution. This also enabled an experiment to be undertaken in the presence of a high concentration of a relevant organic but in the absence of the increased ionic strength seen in the CDP solution. The gluconate solution was made by adding an accurately weighed amount of gluconolactone ($C_6H_{12}O_7$, the lactone form of gluconic acid with no counter ions present) to the NRVB equilibrated water to produce a $2x10^{-3}$ mol dm^{-3} (400 ppm) solution, equivalent to a total organic carbon (TOC) of ~$0.75x10^{-3}$ mol dm^{-3} (147 ppm).

By the time these experiments commenced it was evident that equilibration time for the NRVB cylinder and solution was an important parameter for the experiments with organic components. Early trials that allowed a CDP solution to migrate into the central core, where it was sampled and the internal and external TOC results compared, suggested that 30 days would be sufficient. However, the first ^{90}Sr diffusion results showed that stable conditions for ^{90}Sr were not reached until in excess of 100 days had elapsed. It was not possible to determine whether equilibrating organics or equilibrating Sr concentrations (or both) were responsible. As a consequence the NRVB cylinders were allowed to equilibrate in the gluconate solution for 103 days before the addition of the ^{90}Sr tracer.

Two types of high ionic strength experiment were undertaken. The first, simply ran the experiment in NRVB equilibrated water with NaCl and KCl added at a concentration of 0.05 mol dm^{-3} each i.e. 0.1 mol dm^{-3} NaCl/KCl solution. The second added the same mass of NaCl/KCl (0.658g NaCl, 0.838g KCl and assumed 225 cm^{-3} liquid in system) in 1 cm^{-3} NRVB equilibrated water to the central core with the ^{90}Sr tracer. This represented a maximum start concentration of ~11 mol dm^{-3} each, for NaCl and KCl reducing to 0.1 mol dm^{-3} as the solution equilibrated with the contents of the central core i.e a gradient of ionic strength which should, at least initially decrease diffusivity (see section 5) . It should be noted that the two salts were added as a slurry immediately followed by the radiotracer.

One further diffusion experiment was undertaken which was a repeat of the ^{90}Sr tracer only in CDP solution with an extended equilibration time of 50 days, the

original experiment had used 30 days. Again this experiment was commenced prior to understanding that equilibration times were likely to be longer than originally anticipated. This experiment was not undertaken in duplicate as it was incorrectly assumed the results would be confirmatory of the earlier experiment.

^{90}Sr activity concentrations were determined by liquid scintillation counting using Goldstar multi-purpose scintillation cocktail and a Packard 2100TR liquid scintillation counter. 1 cm^3 samples were taken throughout the experimental duration but all determined on one day when the experiment was completed to negate the need to correct for radioactive decay. In addition 1 cm^3 control samples (the source of the C_{max} values above) were made at the start of the experiment to enable relative retention graphs to be made. The control samples and appropriate blanks were also determined on the same day as the samples from the experiments. All determinations were subject to the 2 σ criterion available on the counter to provide confidence of statistical validity.

13.3 Results of ^{90}Sr Diffusion Experiments

All results are presented as the average of duplicates (where undertaken) along with vertical error bars denoting the 90% confidence limits assuming a two tailed t distribution and horizontal error bars set at +/- 0.25 days. Three graphs are presented for each experiment; showing all results, early data and C/C_{max} relative retention. The data are tabulated in two tables for each experiment. A short commentary is provided after each set of graphs and before the tables.

13.3.1 Results of the ^{90}Sr tracer only NRVB diffusion experiment

The results of the ^{90}Sr tracer only NRVB equilibrated water diffusion experiment are presented below as figs. 13.1 to 13.3 and as tables 13.2 and 13.3 in appendix 1.

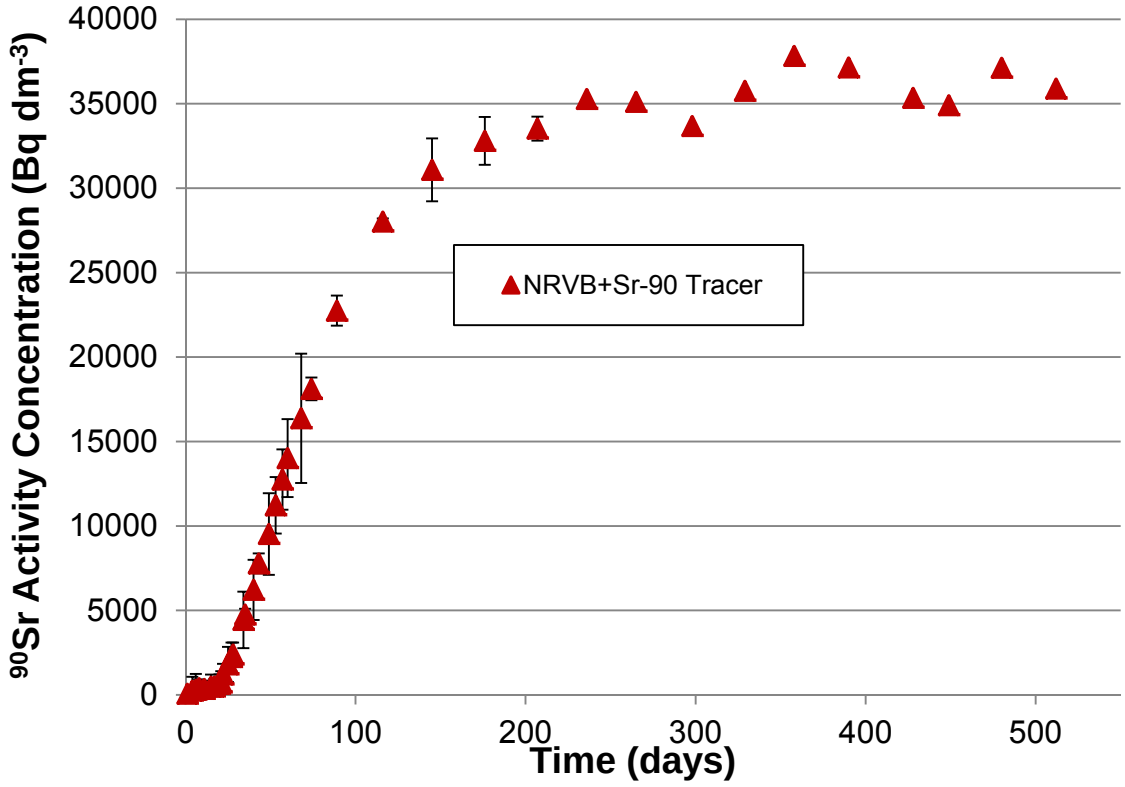

Fig. 13.1 Results of the NRVB ^{90}Sr tracer only diffusion experiment using NRVB equilibrated water

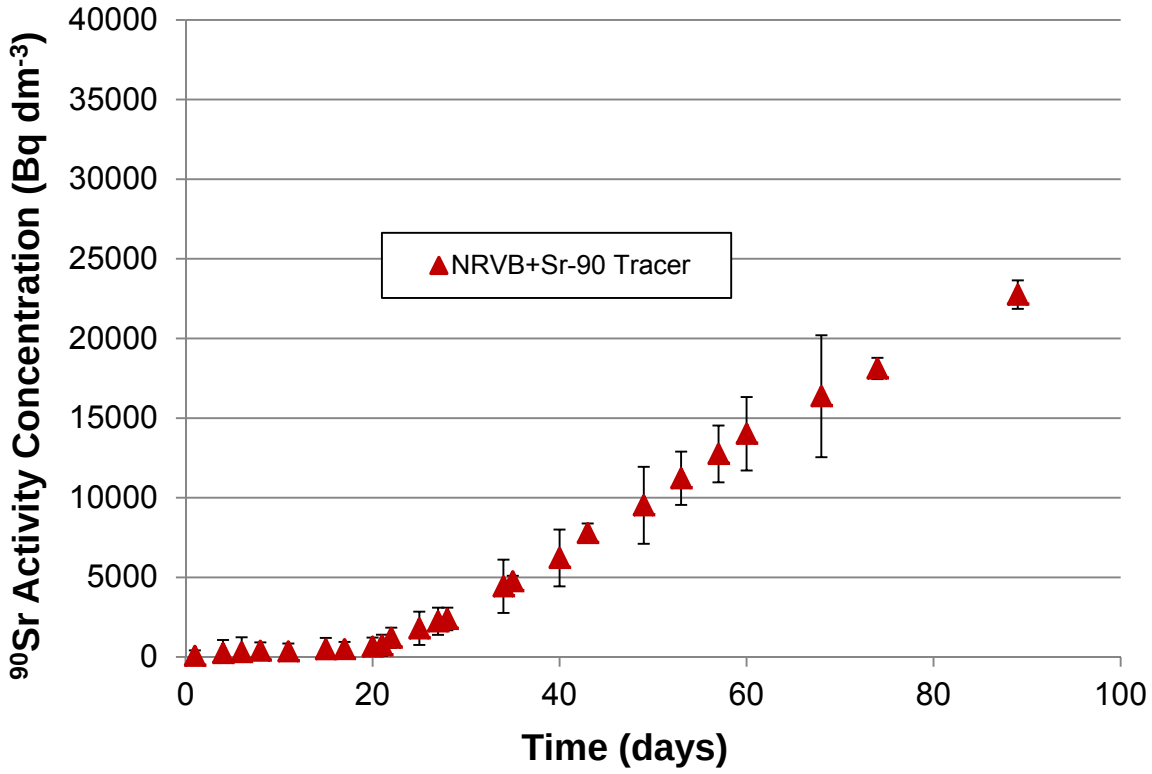

Fig. 13.2 Early data from the NRVB ^{90}Sr tracer only carrier diffusion experiment using NRVB equilibrated water

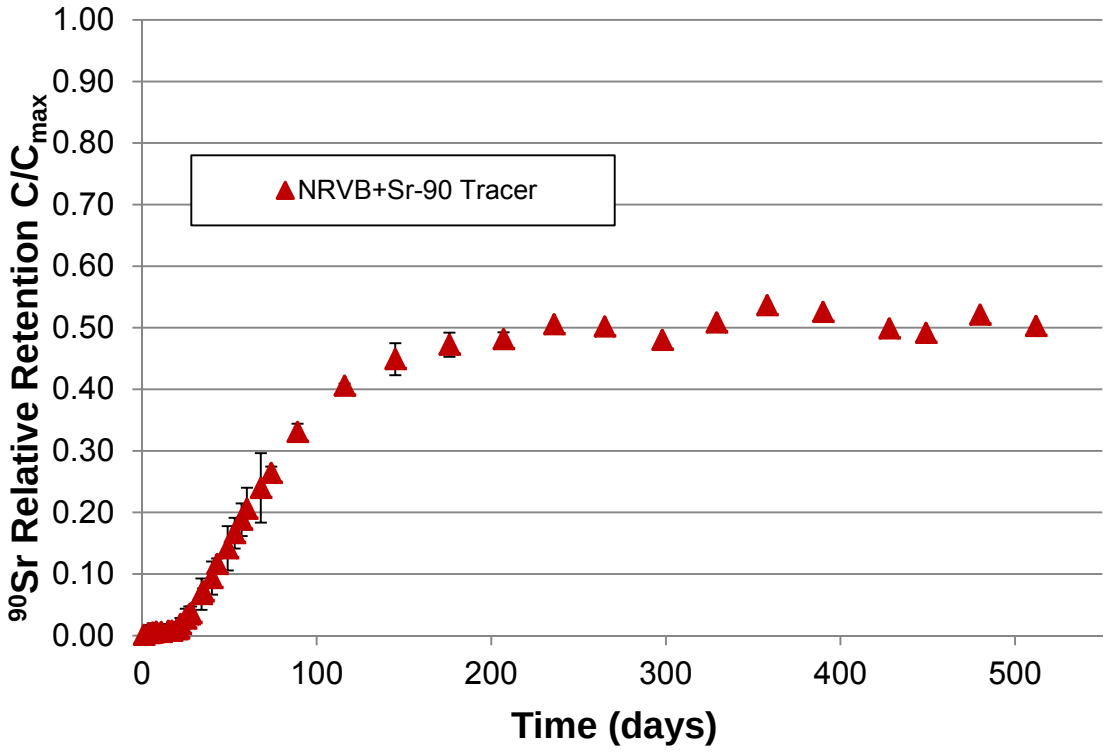

Fig. 13.3 C/Cmax relative retention plot of the NRVB ^{90}Sr tracer only diffusion experiment using NRVB equilibrated water

Commentary

Breakthrough of ^{90}Sr commenced at approximately 20 days, followed by a linear increase in concentration over the following 70 days, this is clearly shown on fig 13.2 the early data plot. The concentration continued to increase at a slower rate stabilising at 35000 Bq dm^{-3} at 250 days and achieving a maximum activity concentration of 37833 Bq dm^{-3} at 358 days. The relative retention plot (where initially C_{max} = 3758 d min^{-1}) indicates that ~50% of the tracer was retained on the NRVB cylinder i.e. 50% of the tracer was in solution. The effect of the steadily increasing C_{max} value can be seen in the later part of the results. The concentration plot fig. 13.1 exhibits much more variability than the somewhat flattened data shown in the relative retention plot, fig. 13.3.

It is important to be aware that the data points from 207 days onwards are not averages of duplicates. This is because one of the NRVB cylinders was removed to evaluate the autoradiography technique. The autoradiograph produced is presented in section 13.6 and clearly showed that a concentration gradient was present in the cylinder even though the results appeared to have stabilised.

13.3.2 Results of the ^{90}Sr tracer only diffusion experiment using CDP solution

The results of the ^{90}Sr tracer only CDP diffusion experiment are presented below as figs. 13.4 to 13.6 and as tables 13.4 and 13.5 in appendix 1.

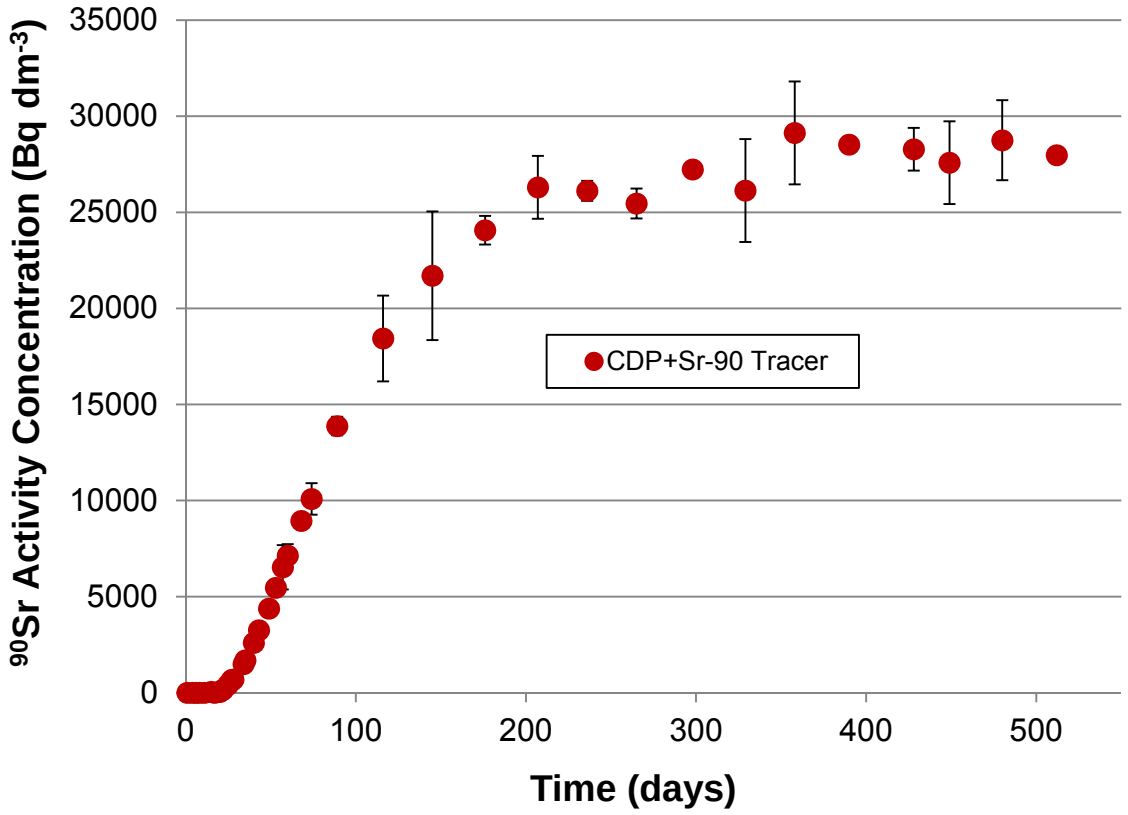

Fig. 13.4 Results of the NRVB ^{90}Sr tracer only diffusion experiment using CDP solution

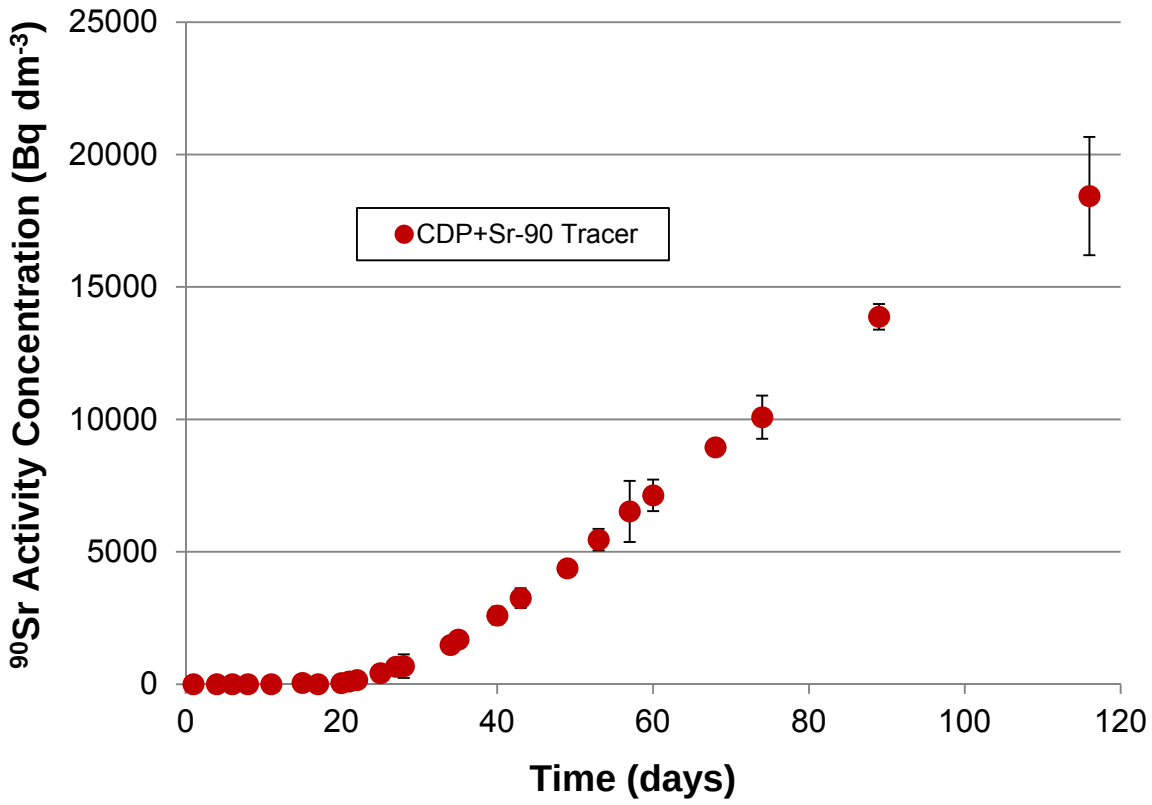

Fig. 13.5 Early data from the NRVB ^{90}Sr tracer only diffusion experiment using CDP solution

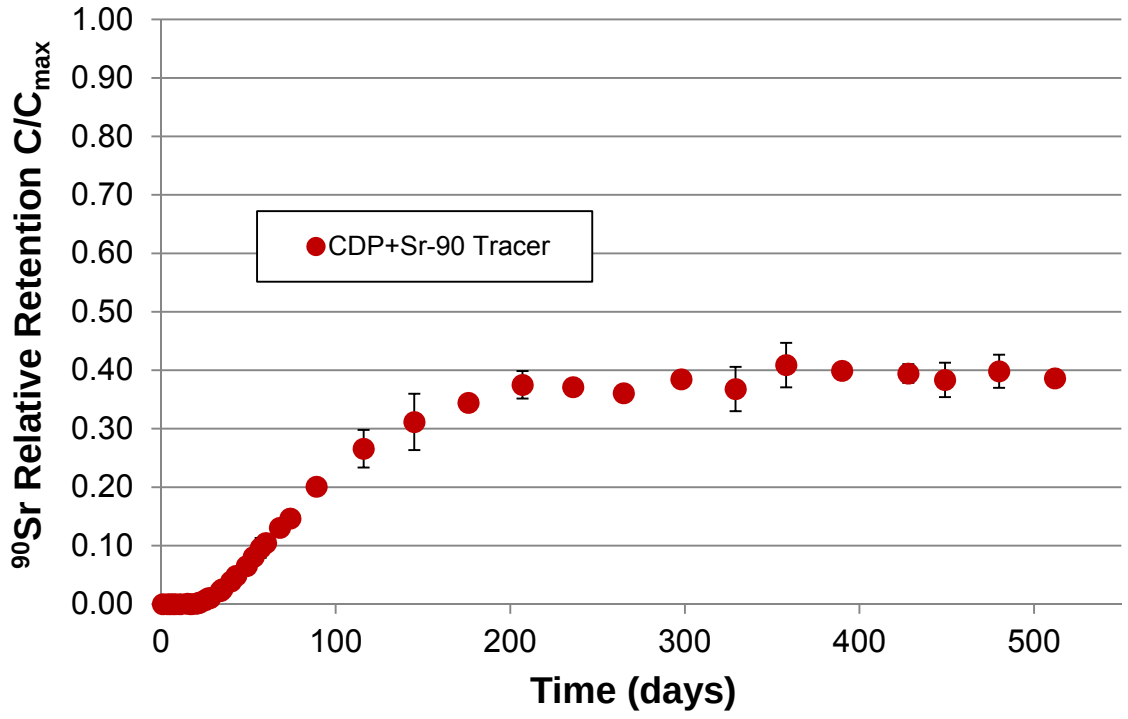

Fig. 13.6 C/C_{max} relative retention plot of the NRVB ^{90}Sr tracer only diffusion experiment using CDP solution

Commentary

Breakthrough of ^{90}Sr commenced at approximately 25 days, followed by a linear increase in concentration over the following 90 days, this is clearly shown on fig 13.5 the early data plot. The concentration continued to increase at a slower rate, initially stabilising at ~26000 Bq dm^{-3} after 236 days and then very slowly rising again to stabilise at ~28500 Bq dm^{-3} before achieving a maximum activity concentration of 29133 Bq dm^{-3} at 358 days. The relative retention plot (where initially C_{max} = 3758 d min^{-1}) indicates that ~60% of the tracer was retained on the NRVB cylinder i.e. 40% of the tracer was in solution. The effect of the steadily increasing C_{max} value can be seen in the later part of the results. The concentration plot fig. 13.4 exhibits much more variability than the somewhat flattened data shown in the relative retention plot, fig. 13.6.

The contrast between the experiments in the presence and absence of CDP was marked and contrary to the results seen for Cs and I, where the presence of CDP appeared to be responsible for an increase in the rate of migration and decrease in retention. The comparison can be seen on the composite plots (see section 13.4, figs. 13.21 and 13.22 These observations started an ongoing investigation into relevance of the equilibration times which can clearly run well in excess of 100 days.

13.3.3 Results of the NRVB ^{90}Sr tracer and $Sr(NO_3)_2$ carrier diffusion experiment using NRVB equilibrated water

The results of the ^{90}Sr tracer and $Sr(NO_3)_2$ NRVB diffusion experiment are presented below as figs. 13.7 to 13.9 and as tables 13.6 and 13.7 in appendix 1.

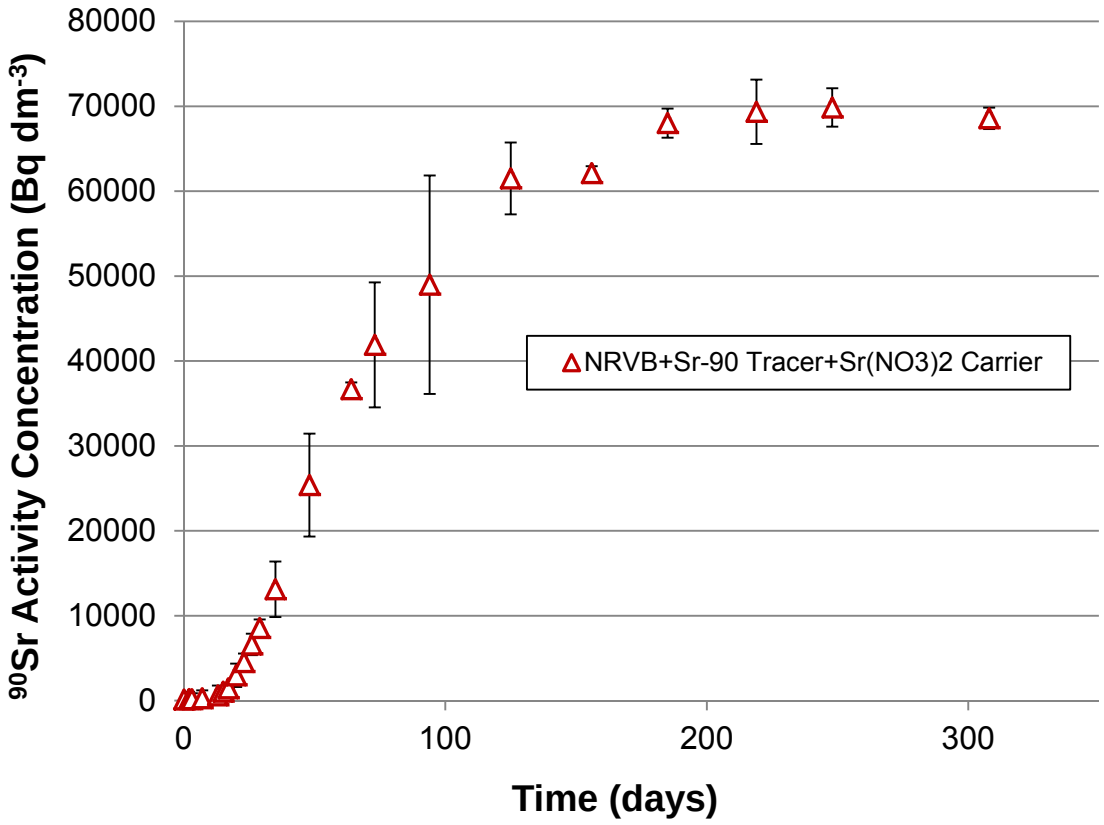

Fig. 13.7 Results of the NRVB ^{90}Sr tracer and $Sr(NO_3)_2$ carrier diffusion experiment using NRVB equilibrated water

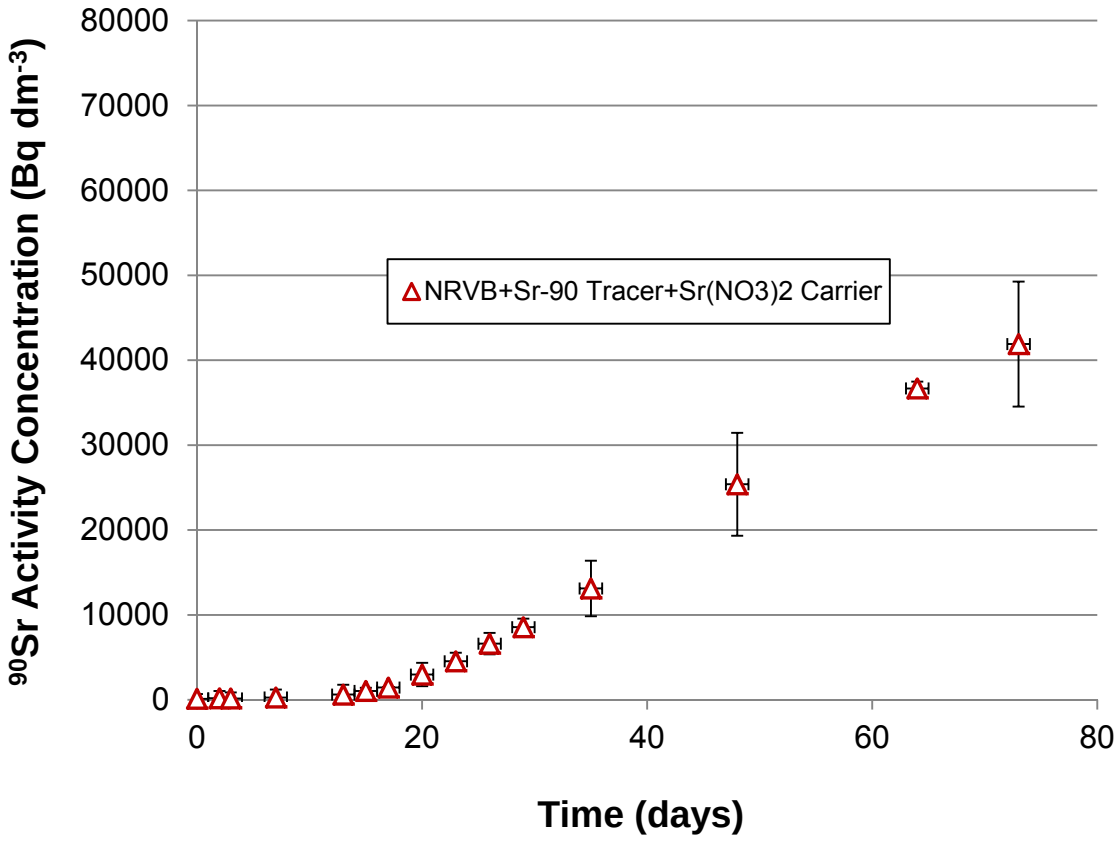

Fig. 13.8 Early data from the NRVB ^{90}Sr tracer and $Sr(NO_3)_2$ carrier diffusion experiment using NRVB equilibrated water

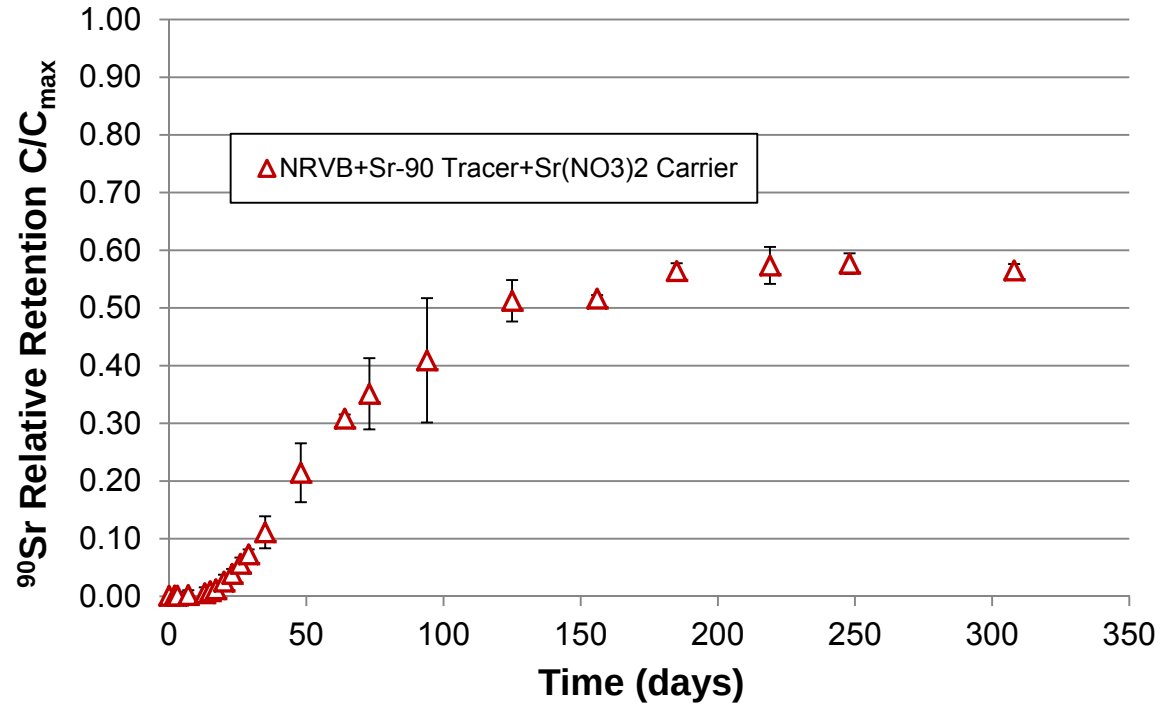

Fig. 13.9 C/C_{max} relative retention plot of the NRVB ^{90}Sr tracer and $Sr(NO_3)_2$ carrier diffusion experiment using NRVB equilibrated water

Commentary

It is important to be aware that double the activity of ^{90}Sr tracer was erroneously added to the carrier experiments although there does not appear to have been any detrimental effect on the results. Breakthrough of ^{90}Sr commenced at approximately 17 days, followed by a linear increase in concentration over the following 66 days, this is clearly shown on fig 13.8 the early data plot. The concentration continued to increase at a slower rate, initially stabilising at ~62000 Bq dm^{-3} after 156 days and then very slowly rising again to stabilise at ~70000 Bq dm^{-3} before achieving a maximum activity concentration of 69858 Bq dm^{-3} at 248 days. The relative retention plot (where initially C_{max} = 6709 d min^{-1}) indicates that ~40% of the tracer was retained on the NRVB cylinder i.e. 60% of the tracer was in solution. The effect of the steadily increasing C_{max} value is still present but not as obvious as on previous plots, due to the shorter experimental duration and the smaller number of samples taken.

13.3.4 Results of the NRVB ^{90}Sr tracer and $Sr(NO_3)_2$ carrier diffusion experiment using CDP solution

The results of the ^{90}Sr tracer and $Sr(NO_3)_2$ NRVB diffusion experiment are presented below as figs. 13.10 to 13.12 and as tables 13.8 and 13.9 in appendix 1.

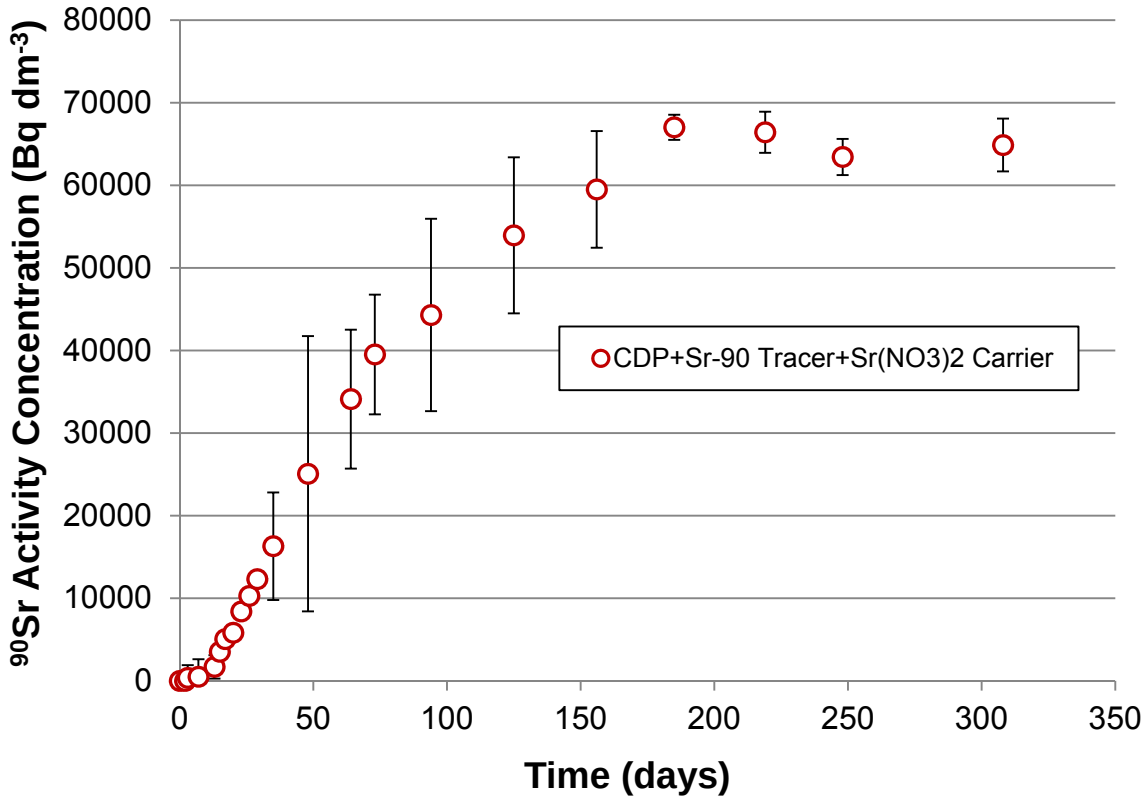

Fig. 13.10 Results of the NRVB ^{90}Sr tracer and and $Sr(NO_3)_2$ carrier diffusion experiment using CDP solution

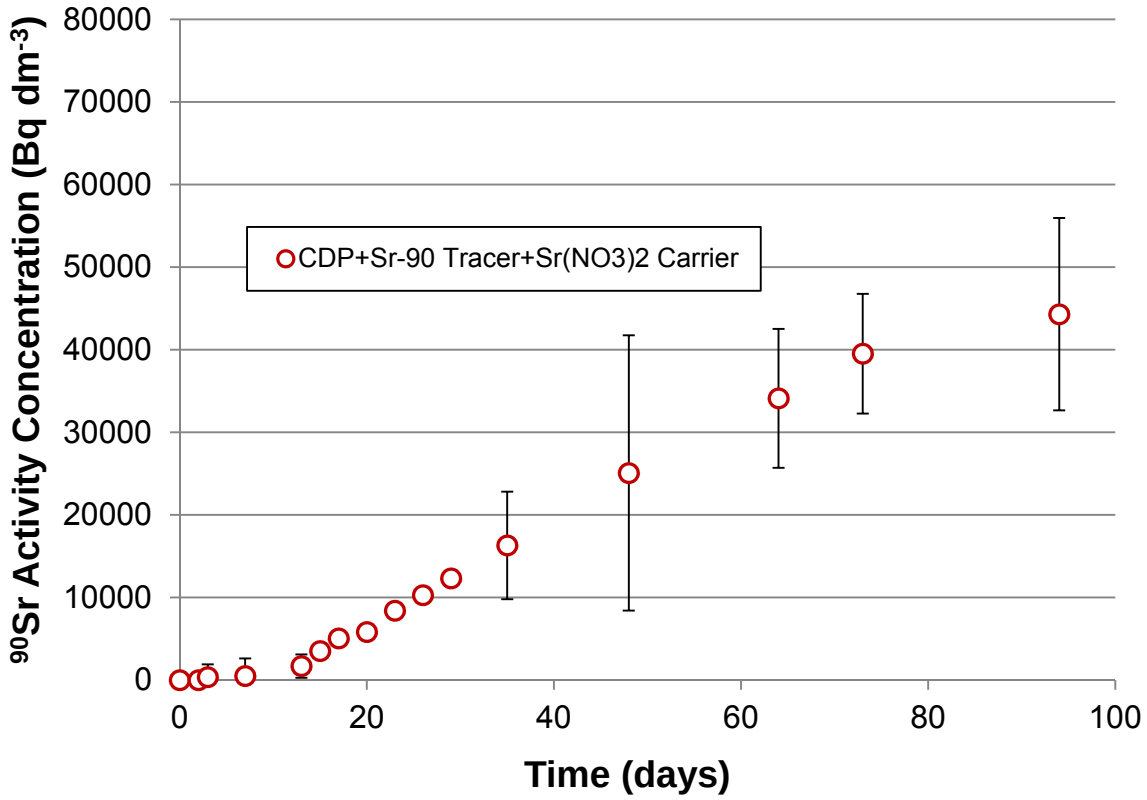

Fig. 13.11 Early data from the NRVB ^{90}Sr tracer and and $Sr(NO_3)_2$ carrier diffusion experiment using CDP solution

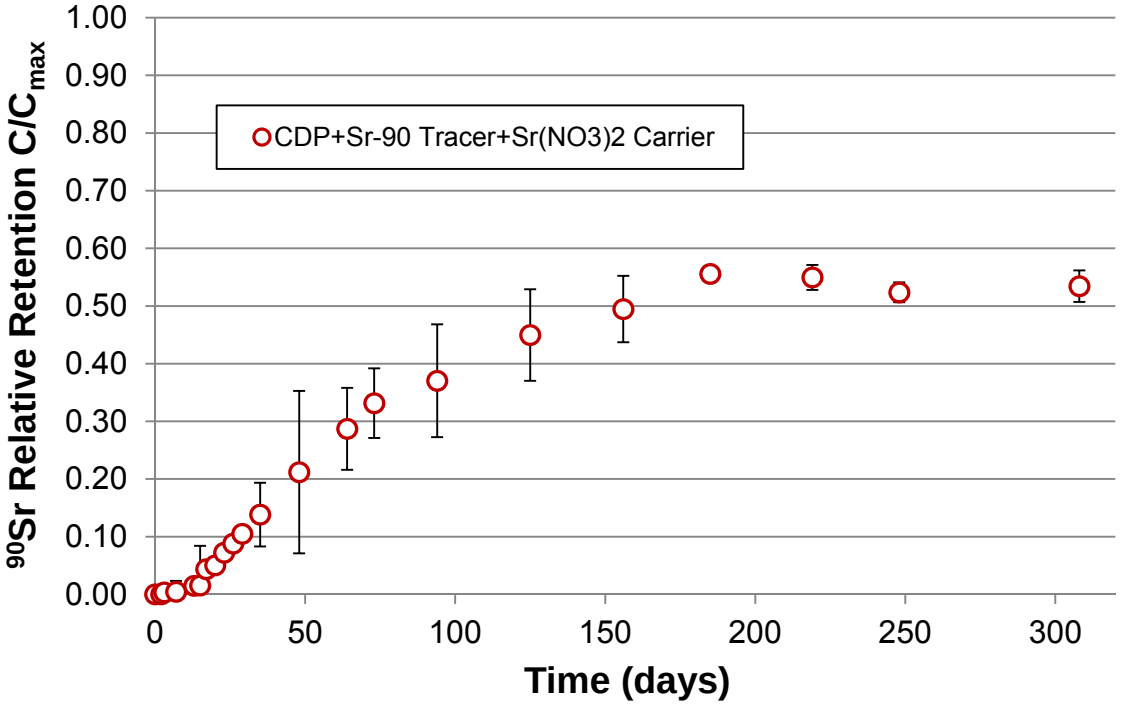

Fig. 13.12 C/C_{max} relative retention plot of the NRVB ^{90}Sr tracer and $Sr(NO_3)_2$ carrier diffusion experiment using CDP solution

Commentary

It is important to be aware that double the activity of ^{90}Sr tracer was erroneously added to the carrier experiments although there does not appear to have been any detrimental effect on the results. In addition, some data points are absent, this can be seen from the tables, the main causes of missing data points were mislabelling of sample vials and spills.

Breakthrough of ^{90}Sr commenced at approximately 13 days, followed by a linear increase in concentration over the following 60 days, this is clearly shown on fig 13.11, the early data plot. The concentration continued to increase at a slower rate, initially stabilising at ~66500 Bq dm^{-3} after around 200 days, achieving a maximum of 67025 Bq dm^{-3} at 185 days. The relative retention plot (where initially C_{max} = 6709 d min^{-1}) indicates that ~45% of the tracer was retained on the NRVB cylinder i.e. ~55% of the tracer was in solution. The flattening effect of the steadily increasing C_{max} value is present but not as obvious as on previous plots, due to the shorter experimental duration and the smaller number of samples taken.

The Sr carrier diffusion results were very similar. The CDP experiment appeared to be a little slower with slightly more retention of Sr but this could be experimental error. The error bars are clearly visible on the Sr carrier plots indicating greater variability between the duplicates compared to other diffusion experiments undertaken in this research. The comparison of the carrier experiments with the other experiments presented in this section can be seen on the composite plots (see section 13.4, figs. 13.21 and 13.22).

13.3.5 Results of the NRVB ^{90}Sr tracer only diffusion experiment using gluconate in NRVB equilibrated water

The results of the ^{90}Sr tracer only diffusion experiment using gluconate in NRVB equilibrated water are presented below as figs. 13.13 to 13.15 and as tables 13.10 and 13.11 in appendix 1.

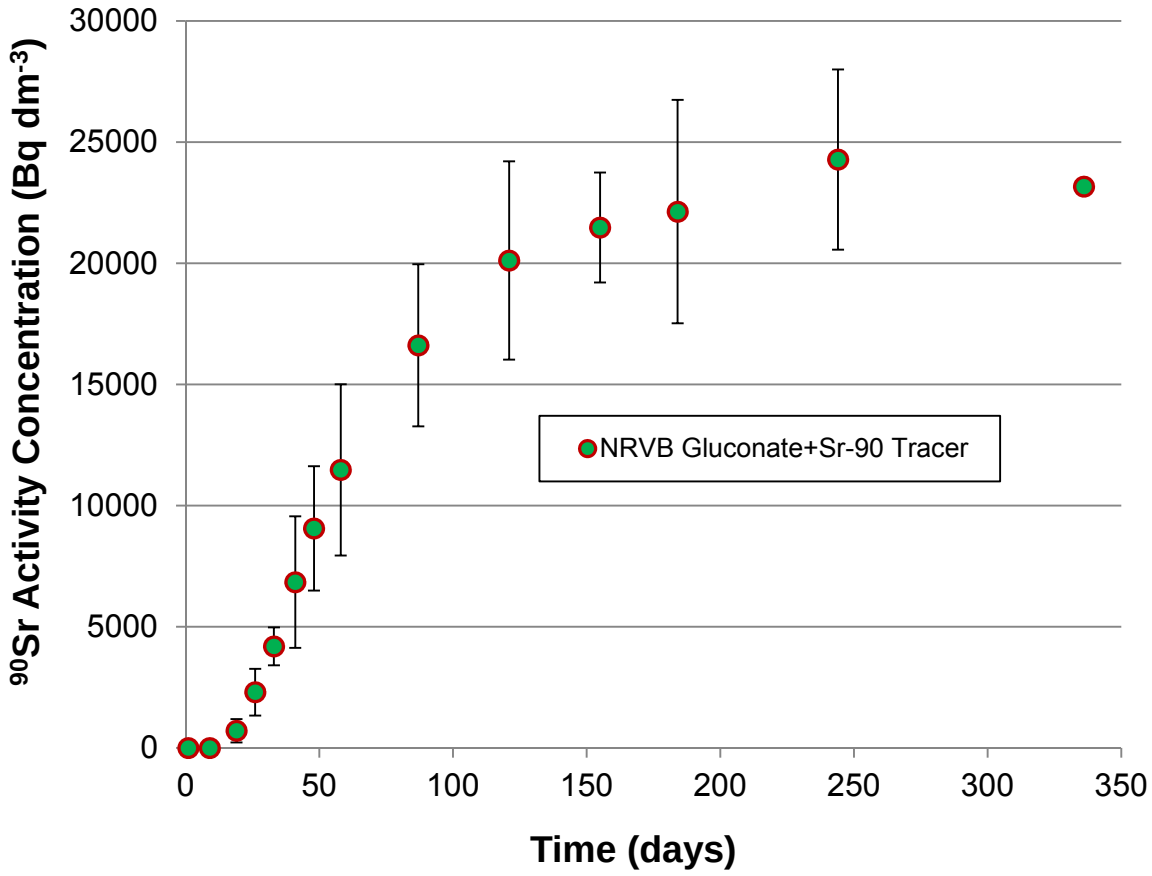

Fig. 13.13 Results of the NRVB ^{90}Sr tracer only diffusion experiment using gluconate in NRVB equilibrated water

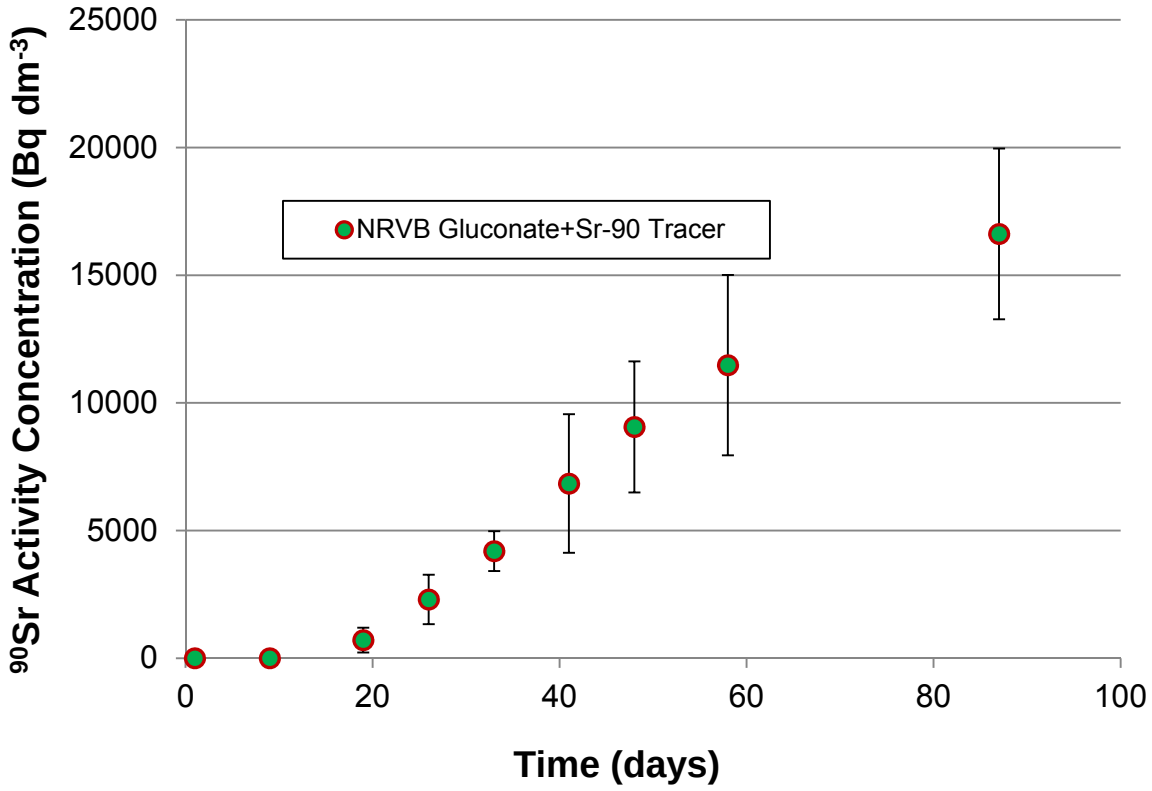

Fig. 13.14 Early data from the NRVB ^{90}Sr tracer only diffusion experiment using gluconate in NRVB equilibrated water

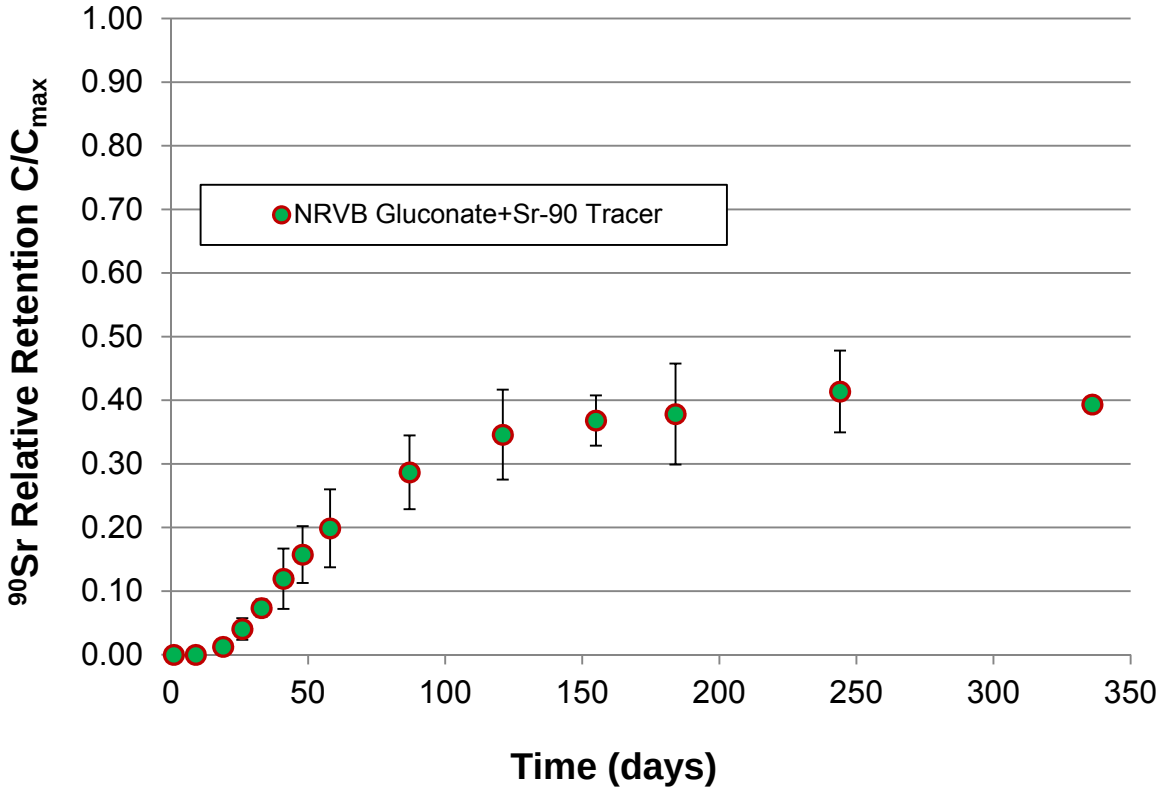

Fig. 13.15 C/C$_{max}$ relative retention plot of the NRVB ^{90}Sr tracer only diffusion experiment using gluconate in NRVB equilibrated water

Commentary

Breakthrough of ^{90}Sr commenced at approximately 19 days, followed by a linear increase in concentration over the following 70 days, this is clearly shown on fig 13.14, the early data plot. The concentration continued to increase at a slower rate, initially stabilising at ~22500 Bq dm^{-3} at 184 days, achieving a maximum of ~24300 Bq dm^{-3} at 244 days. The relative retention plot (where initially C_{max} = 3380 d min^{-1}) indicates that ~60% of the tracer was retained on the NRVB cylinder i.e. ~40% of the tracer was in solution. The flattening effect of the steadily increasing C_{max} value can be seen in the later part of the results. The concentration plot fig. 13.13 exhibits more variability than the somewhat flattened data shown in the relative retention plot, fig. 13.15. Note that the final data point at 336 days is a single value because the duplicate was removed for autoradiography.

The tracer in the gluconate experiment breaks through more quickly than it does in the equivalent CDP experiment. However, the relative retention is very similar at ~60%. The equilibration time for the gluconate solution and NRVB cylinders was over 100 days and for the comparable CDP experiment it was only 30 days. This supported the supposition that the cylinders used in the CDP experiment were still equilibrating when the experiment started i.e. Sr from the CDP solution was migrating into the block and the tracer could not migrate out until the concentration gradient had subsided. The comparison of the carrier experiments with the other experiments presented in this section can be seen on the composite plots (see section 13.4, figs. 13.21 and 13.22).

13.3.6 Results of the NRVB ^{90}Sr tracer only diffusion experiment using high ionic strength NRVB equilibrated water

The results of the ^{90}Sr tracer only diffusion experiment using high ionic strength NRVB equilibrated water are presented below as figs. 13.16 and 13.17 and as tables 13.12 and 13.13 in appendix 1. The early data plot is not presented because the experimental results currently extend to only 115 days.

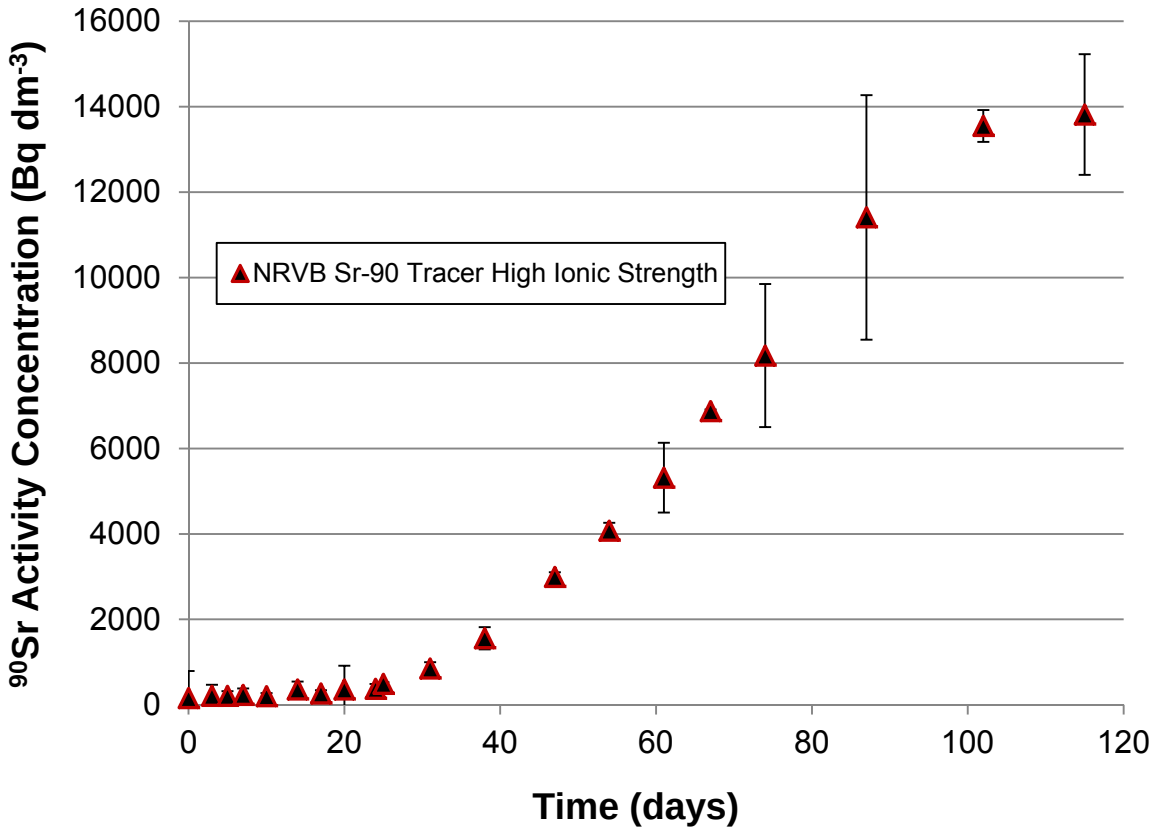

Fig. 13.16 Results of the NRVB ^{90}Sr tracer only diffusion experiment using high ionic strength NRVB equilibrated water

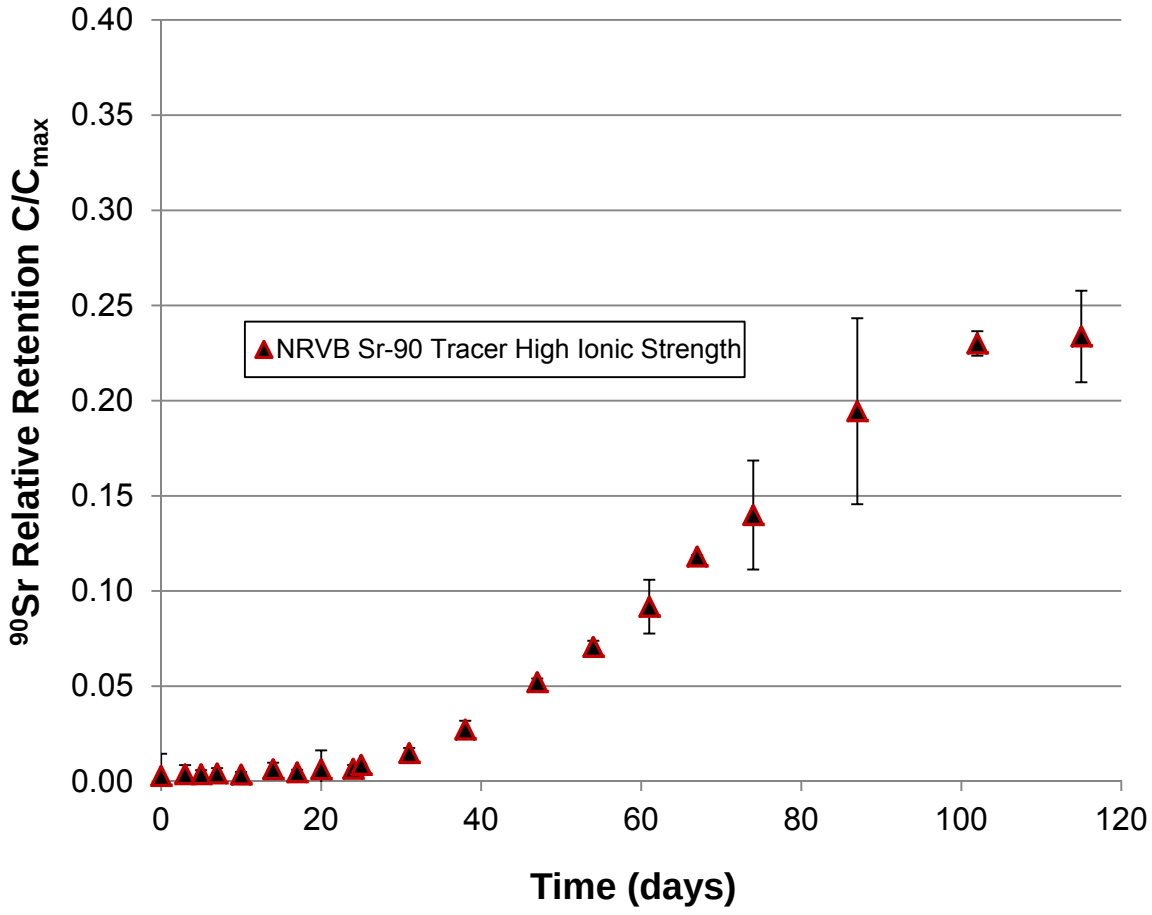

Fig. 13.17 C/C$_{max}$ relative retention plot of the NRVB ^{90}Sr tracer only diffusion experiment using high ionic strength NRVB equilibrated water

Commentary

Breakthrough of ^{90}Sr commenced at approximately 25 days, followed by a linear increase in concentration over the following 62 days, this is clearly shown on fig 13.15. The concentration continued to increase at a slower rate, initially stabilising at ~14000 Bq dm^{-3} after 102 days, achieving a maximum of 13817 Bq dm^{-3} at the latest available data point of 115 days. The relative retention plot (where initially C$_{max}$ = 3279 d min^{-1}) indicates that >75% of the tracer was retained on the NRVB cylinder i.e. <25% of the tracer was in solution.

The tracer in the high ionic strength experiment breaks through more slowly than comparable experiments in the series. The equilibration time for the high ionic strength solution and NRVB cylinders was only 3 days. The results in the phase where concentration is increasing linearly are very similar to the tracer only CDP (see fig. 13.22) indicating an effect on diffusivity. It is not yet possible to state whether the results are beginning to stabilise. Clearly more results need to be

collected before any significant conclusions can be proposed. The comparison of these experiments with the other experiments presented in this section can be seen on the composite plots (see section 13.4, figs. 13.21 and 13.22).

13.3.7 Results of the NRVB ^{90}Sr tracer only diffusion experiment using gradient ionic strength NRVB equilibrated water

The results of the ^{90}Sr tracer only diffusion experiment using gradient ionic strength NRVB equilibrated water are presented below as figs. 13.18 and 13.19 and tables 13.14 and 13.15. The early data plot is not presented because the experimental results currently extend to only 119 days. In addition and for the first time significant and as yet unexplained divergence between the duplicates was observed and consequently they are plotted separately.

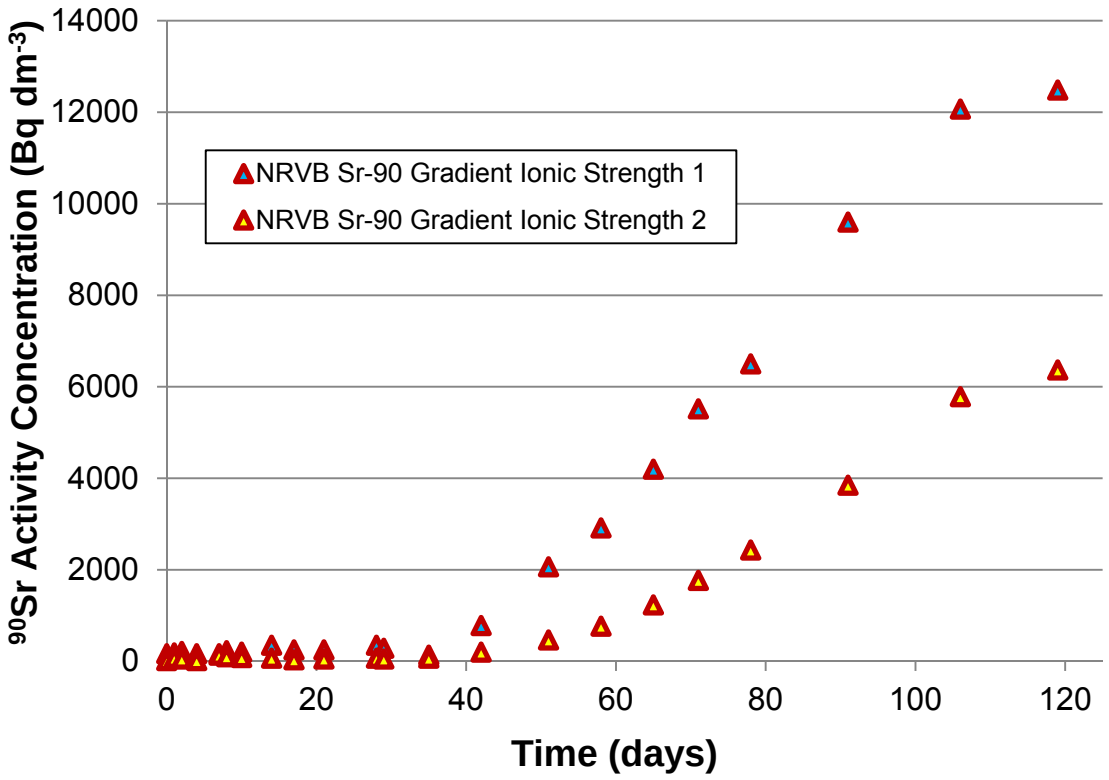

Fig. 13.18 Results of the NRVB ^{90}Sr tracer only diffusion experiment using gradient ionic strength NRVB equilibrated water

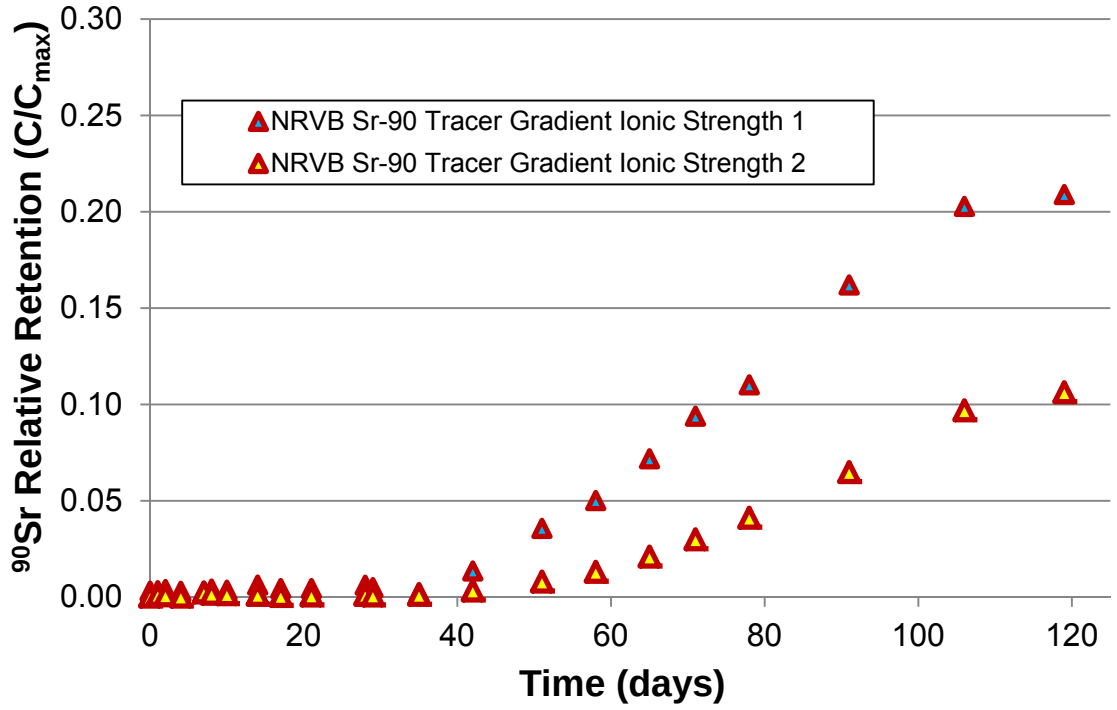

Fig. 13.19 C/C$_{max}$ relative retention plot of the NRVB ^{90}Sr tracer only diffusion experiment using gradient ionic strength NRVB equilibrated water

Commentary

Breakthrough of ^{90}Sr commenced at 42 days for sample 1 and 51 days for sample 2 , followed by a linear increase in concentration over the following ~50 days, this is clearly shown on fig 13.18. The concentrations appeared to be stabilising at ~6000 and 12000 Bq dm^{-3} at the latest available data point of 115 days. The relative retention plot (where initially C_{max} = 3279 d min^{-1}) indicates that the retention on the NRVB is likely to be higher than that observed during the non-gradient high ionic strength experiments. It remains to be seen whether these experiments (gradient and non-gradient) which have the same total amount of NaCl and KCl added will converge over a longer time duration.

It is clear from the longer breakthrough times that the very high ionic strength at the start of these experiments has suppressed diffusivity. These experiments clearly need more data points before any more significant conclusions can be proposed particularly in relation to retention on the NRVB. The comparison of these experiments with the other experiments presented in this section can be seen on the composite plots (see section 13.4, figs. 13.21 and 13.22).

13.3.8 Results of the repeated NRVB ^{90}Sr tracer only diffusion experiment using CDP solution

The results of the repeated ^{90}Sr tracer only diffusion experiment using CDP solution are presented below as figs. 13.20 and 13.21 and as table 13.16 in appendix 1. The experiment was not undertaken in duplicate and an early data plot has not been presented.

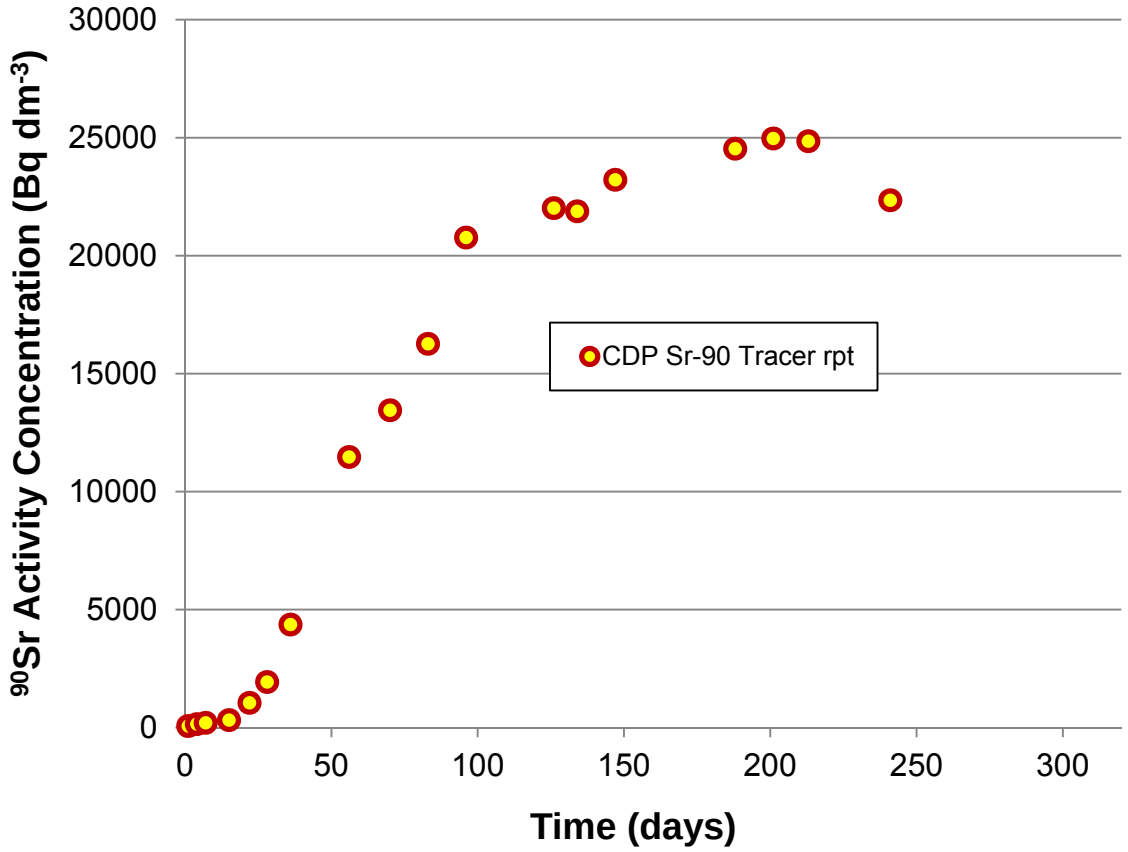

Fig. 13.20 Results of the repeated NRVB ^{90}Sr tracer only diffusion experiment using CDP solution

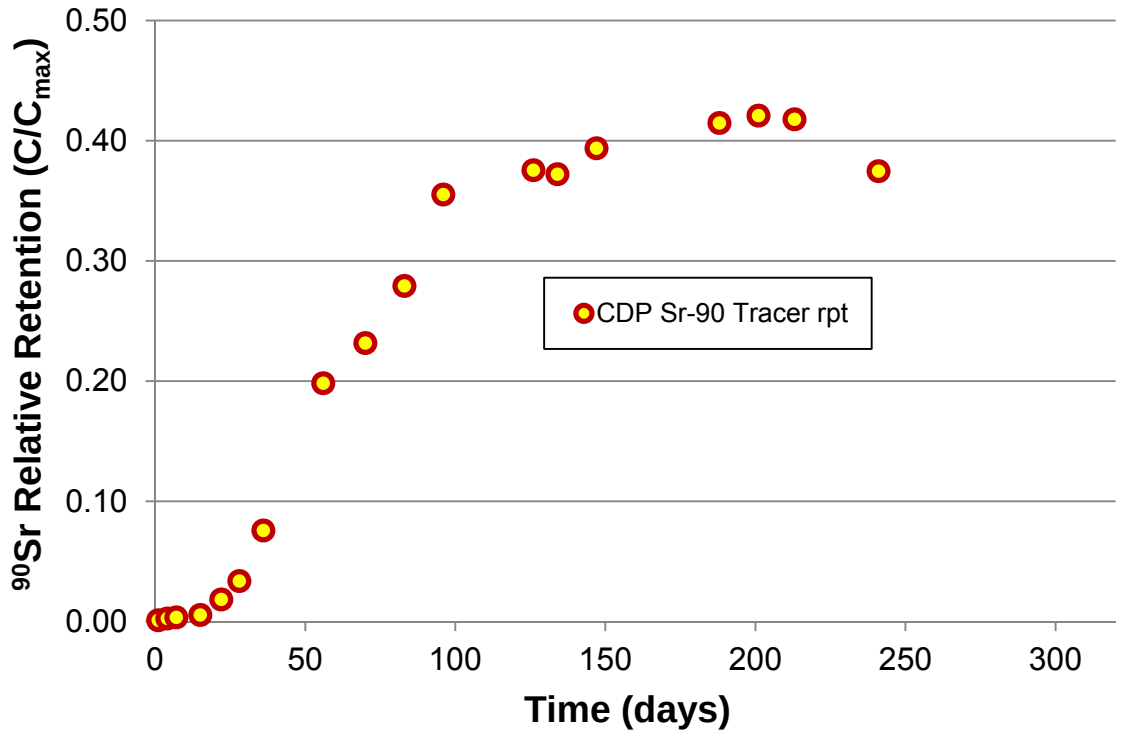

Fig. 13.20 C/C$_{max}$ relative retention plot of the repeated NRVB ^{90}Sr tracer only diffusion experiment using CDP solution

Commentary

Breakthrough of ^{90}Sr commenced at approximately 15 days, followed by an almost linear increase in concentration over the following ~111 days, this is clearly shown on fig 13.19. The concentrations appeared to be stabilising at ~25000 Bq dm^{-3} with the last available data point at 241 days appearing to be anomalously low at 22350 Bq dm^{-3}. The relative retention plot (where initially C$_{max}$ = 3279 d min^{-1}) indicates that the retention of the tracer on the NRVB cylinder is likely to be ~60% similar to the original ^{90}Sr tracer only CDP experiment presented in section 13.3.1.

The main difference between this experiment and the earlier tracer only CDP experiments is the pre-equilibration time in the presence of the CDP solution. The original experiments had a 30 day pre-equilibration and this experiment had a 50 day equilibration. This appeared to shorten the breakthrough time and leave the relative retention unaffected providing more evidence that the original CDP tracer only experiments were still equilibrating when the tracer was added. The comparison of this experiment with the other experiments presented in this section can be seen on the composite plots (see section 13.4, fig. 13.21 and 13.22).

13.4 Composite Plots Comparing the Sr Diffusion Experiments

13.4.1 Discussion of composite plots

The composite plots figs. 13.21 (all data) and 13.22 (early data) may appear complicated at first sight (error bars have been omitted for clarity). However a number of distinct patterns of behaviour are clearly discernible, note that only sample 2 of the divergent gradient ionic strength samples is presented because its separation from the adjacent data on the plot is clearer:

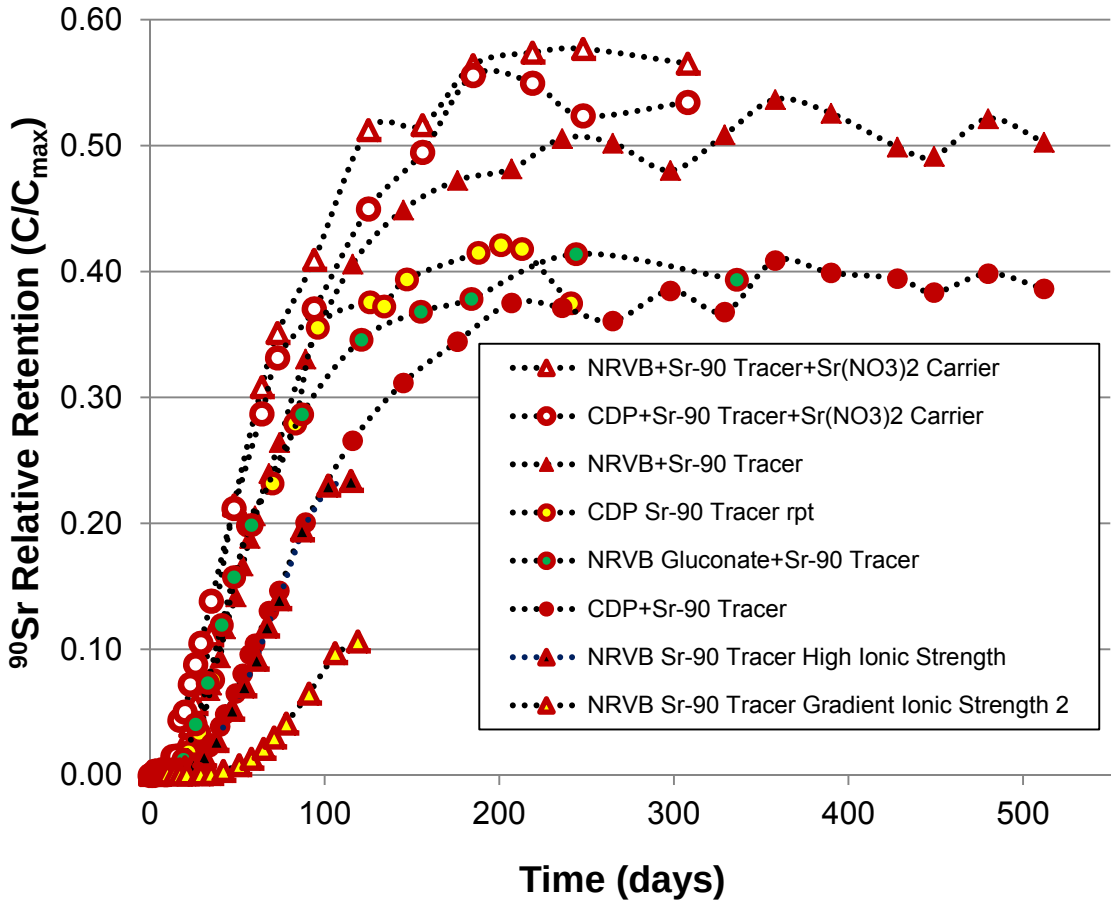

Fig. 13.21 Composite plot of data from the series of Sr diffusion experiments

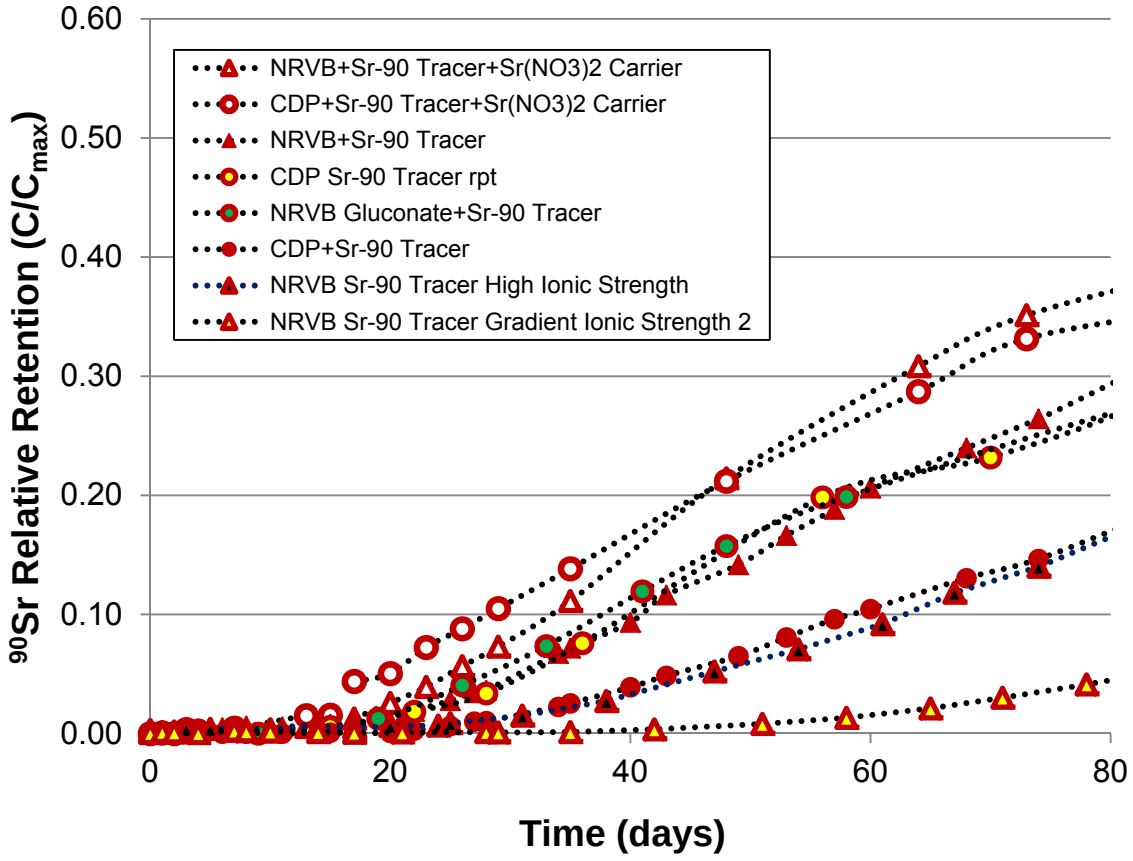

Fig. 13.22 Composite plot of early data from the series of Sr diffusion experiments

Commentary

- The Sr concentration was highest in the carrier experiments and this can be seen to dominate, producing the fastest movement towards stabilisation and highest relative concentrations in solution (lowest relative concentrations retained on the NRVB cylinders). The presence or absence of CDP makes very little difference, similarly the higher ionic strength associated with the CDP solution.
- The ^{90}Sr tracer only with NRVB equilibrated water is very similar to the carrier experiments although marginally slower to stabilise and producing a lower relative concentration of the tracer in solution.
- The tracer only experiments in the presence of organics (CDP with 30 days pre-equilibration, CDP repeat with 50 day pre-equilibration and gluconate with 103 days pre-equilibration) eventually stabilised at very similar relative concentrations in solution, i.e. about 60% retained on the NRVB cylinders.

- The high ionic strength experiments appeared to stabilise at much lower relative concentrations in solution. However it is clear that more results are needed for confirmation).
- The early data shows that the carrier experiments break through most rapidly
- The tracer only experiments with organics and long pre-equilibration times are initially grouped together with the tracer only in the absence of organics.
- The CDP and high ionic strength tracer only experiments are also grouped together initially
- The gradient high ionic strength (sample 2) is much slower than any of the other experiments and has the lowest relative concentration in solution.

The experiments, when considered as a set provide evidence that:

- A high Sr initial concentration dominates other effects, even the presence of CDP solution
- The presence of CDP increases the relative retention of tracer concentrations of ^{90}Sr from 45% to 60%
- Initial breakthrough and subsequent relative concentration increase can be affected by pre-equilibration time, suggesting that “back diffusion” of the higher Sr concentration in the CDP solution into the NRVB cylinder must occur before the ^{90}Sr tracer can begin to migrate.
- The presence of high ionic strength significantly decreases diffusivity and increases relative retention when compared to an increase in the Sr concentration gradient.

Clearly there is a need to undertake the high ionic strength, ^{90}Sr tracer and $Sr(NO_3)_2$ carrier experiments to confirm the dominant mechanism. In addition, the equilibration times for the CDP components and gluconate with NRVB will need to be better defined and understood.

The autoradiographs presented in section 13.6 provide some visual evidence that competing mechanisms may be responsible for the variety of results seen in this series of diffusion experiments. Some of the autoradiographs show spots of activity on the external surface and residual activity in the central core suggesting that precipitation may also need to be considered as this work progresses.

13.5 GoldSim Models for Sr Diffusion Experiments

13.5.1 Additional information relevant to the ^{90}Sr NRVB diffusion modelling

Details of the GoldSim model are fully discussed in section 7. The results from the modelling of the Sr diffusion experiments are presented as figs. 13.23 to 13.32. Initial concentrations are provided in section 12.2. It is important to be aware that for simplicity, activity concentrations were modelled and as a consequence a direct comparison cannot be made in the same manner as possible with the relative retention plots. Partition is referred to as K_d throughout, primarily because this term, rather than R_d is used in GoldSim. The model employs a background activity concentration equivalent to the experimental blanks. This results in the activity concentration points on the plots being approximately 1000 Bq dm^{-3} higher than those shown for the individual experiments earlier in this section. The LOF calculations are built into the model enabling it to determine the combination of parameters that minimise LOF. Data envelopes that encompass all or the majority of the observed data are also included to provide an indication of the variability of the observed data within a range of partition coefficient and diffusivity values. Short commentaries explaining the data envelopes along with K_d, D_e and LOF outputs are also provided.

13.5.2 ^{90}Sr tracer only NRVB equilibrated water diffusion modelling

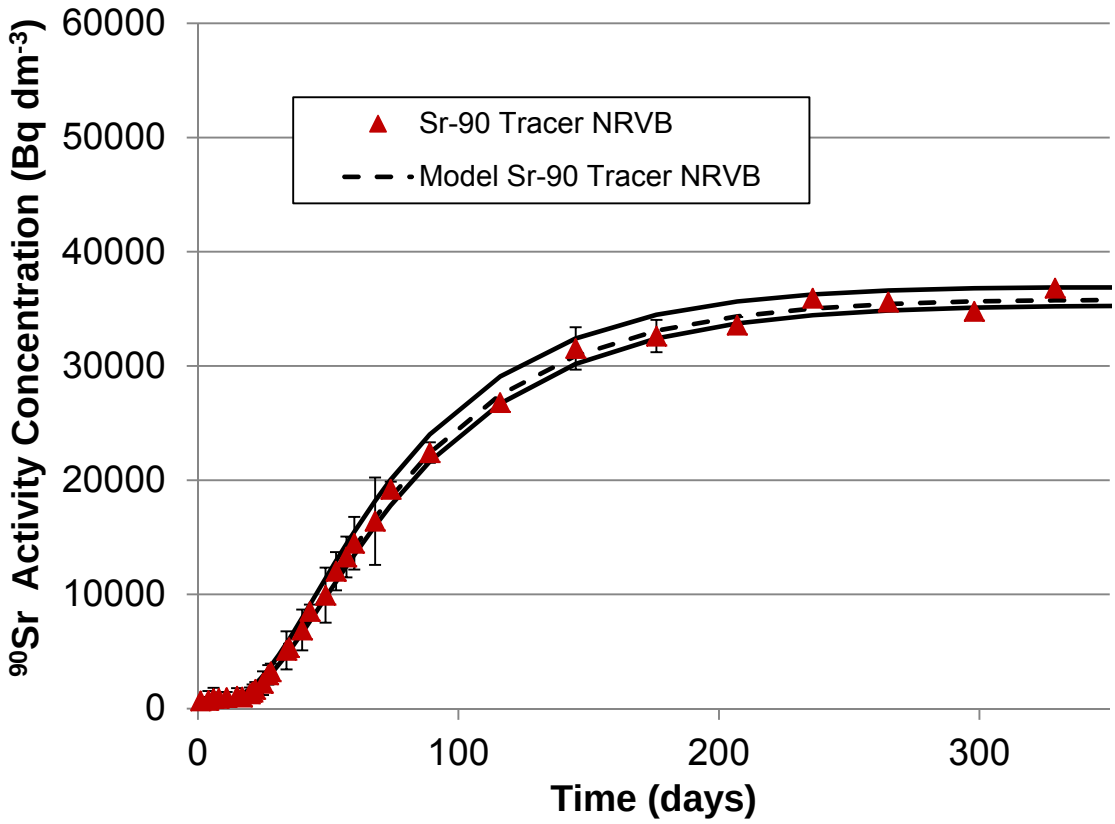

Fig. 13.23 Experimental and modelled NRVB diffusion curves for ^{90}Sr at tracer concentration in NRVB equilibrated water

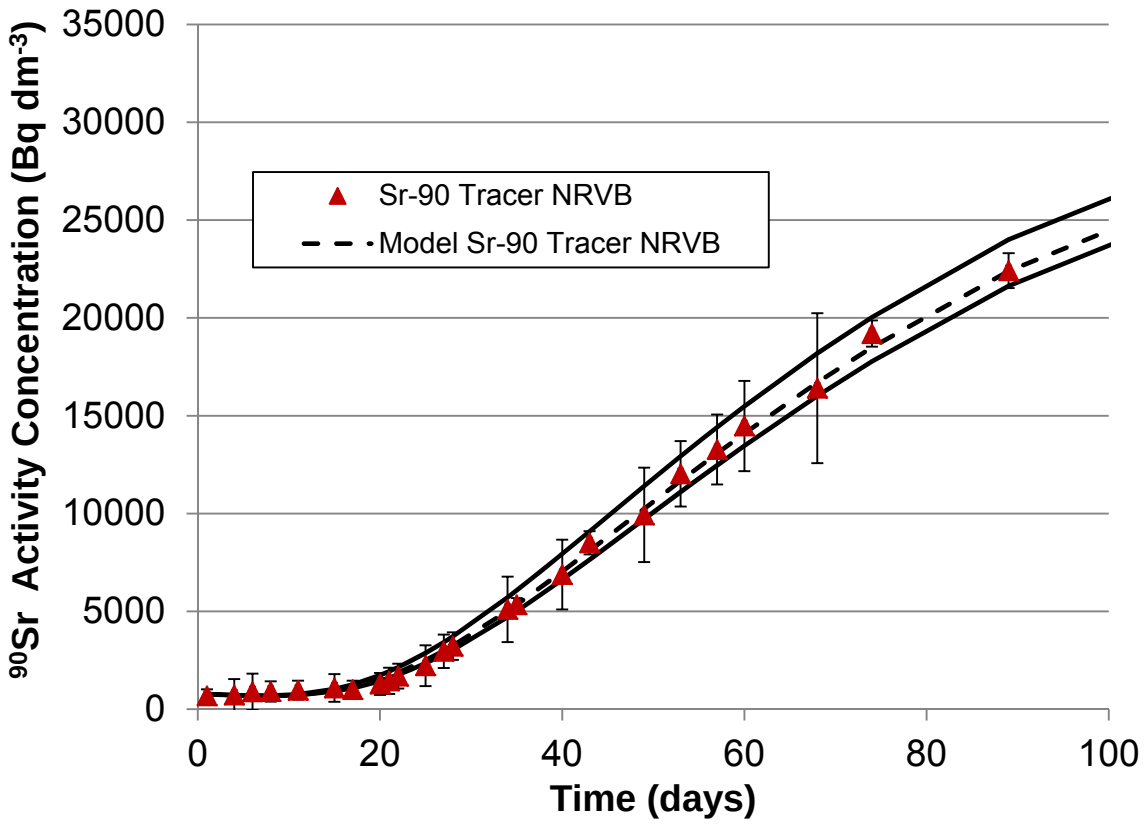

Fig. 13.24 Early data from the experimental and modelled NRVB diffusion curves for ^{90}Sr at tracer concentration in NRVB equilibrated water

Commentary

The best fit D_e and K_d model results for the ^{90}Sr tracer only diffusion with NRVB equilibrated water were 4.4x10^{-11} m^2 s^{-1} and 3.0x10^{-3} m^3 kg^{-1}, respectively (black long hashed line in figs. 13.23 and 13.24). The LOF for the best model result was 3.2%. The majority of the experimental data could be contained in the interval defined by setting D_e in the range 3.5x10^{-11} to 5.4x10^{-11} m^2 s^{-1} and K_d between 2.8x10^{-3} and 3.1x10^{-3} m^3 kg^{-1}, (the solid black lines in fig. 13.23). The early data plot (fig. 13.24) has been provided to illustrate the difficulty of setting a suitable envelope to encompass both parts of the dataset. The results that fall outside the envelope can be clearly seen on the figures. It should be noted that all observed values (except the final somewhat anomalous data point) are included in the LOF results even those outside the envelope.

13.5.3 ^{90}Sr tracer only CDP solution diffusion modelling

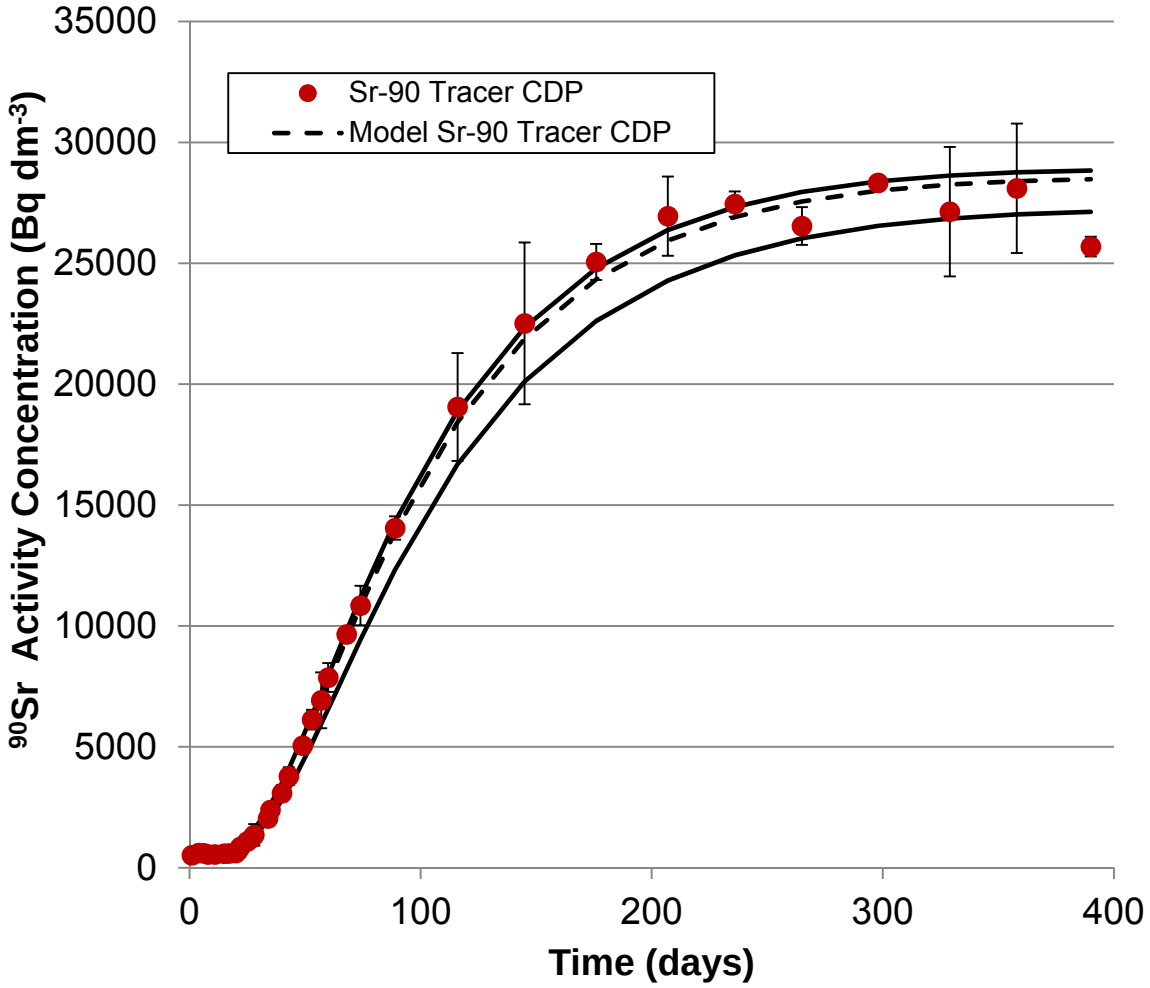

Fig. 13.25 Experimental and modelled NRVB diffusion curves for ^{90}Sr at tracer concentration in CDP solution

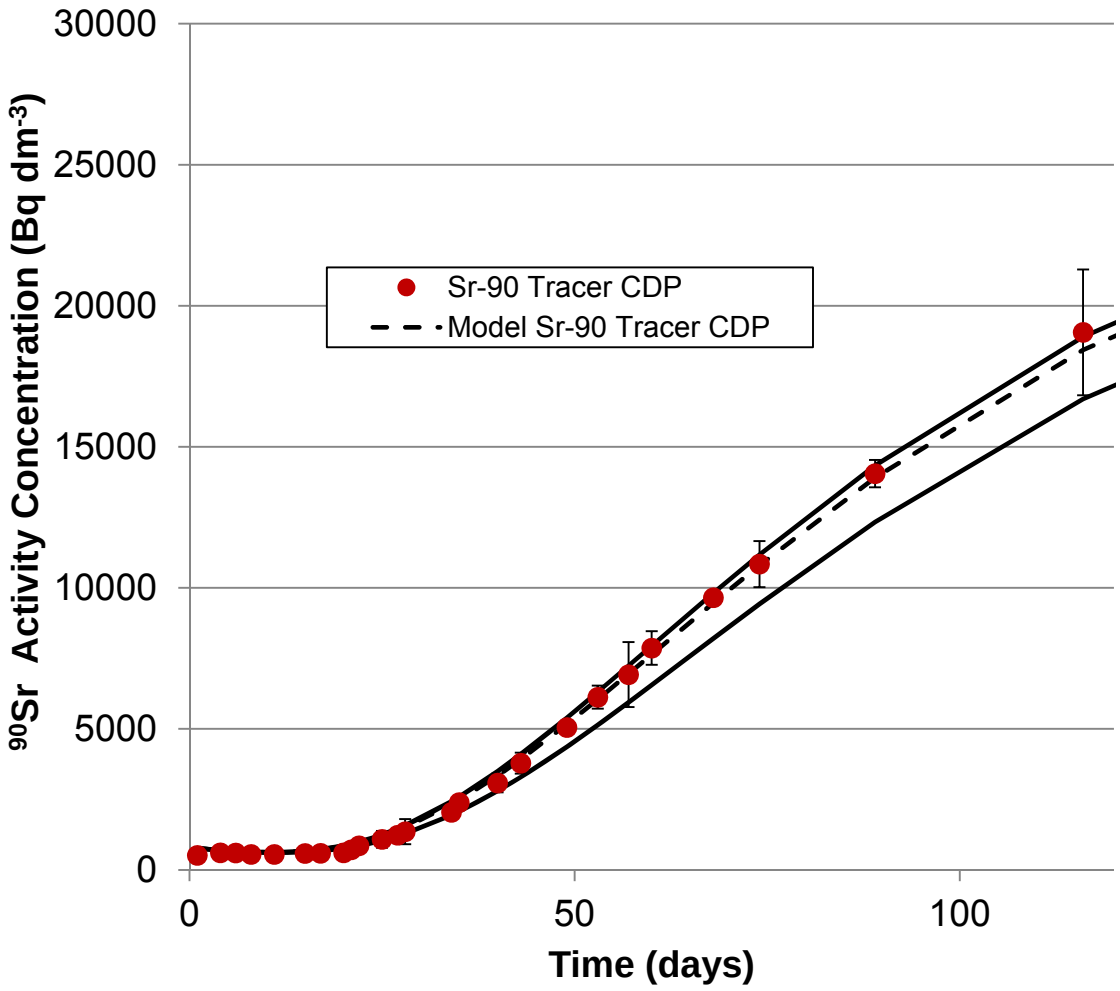

Fig. 13.26 Early data from the experimental and modelled NRVB diffusion curves for ^{90}Sr at tracer concentration in CDP solution

Commentary

The best fit D_e and K_d model results for the ^{90}Sr tracer only diffusion with CDP solution were 4.7x10^{-11} m^2 s^{-1} and 4.7x10^{-3} m^3 kg^{-1}, respectively (black long hashed line in fig. 13.25). The LOF associated with the best model result was 4.3%. The majority of the experimental data could be contained in the interval defined by setting D_e between 3.5x10^{-11} and 5.4x10^{-11} m^2 s^{-1} and K_d between 4.6x10^{-3} and 5.1x10^{-3} m^3 kg^{-1}, (the solid black lines in fig. 13.25 and 13.26). The early data plot (fig. 13.26) has been provided to illustrate the difficulty of setting a suitable envelope to encompass both parts of the dataset. The results that fall outside the envelope can be clearly seen on the figures. It should be noted that all observed values (except the final somewhat anomalous data point) are included in the LOF results even those outside the envelope.

13.5.4 ^{90}Sr tracer and $Sr(NO)_3$ carrier NRVB equilibrated water diffusion modelling

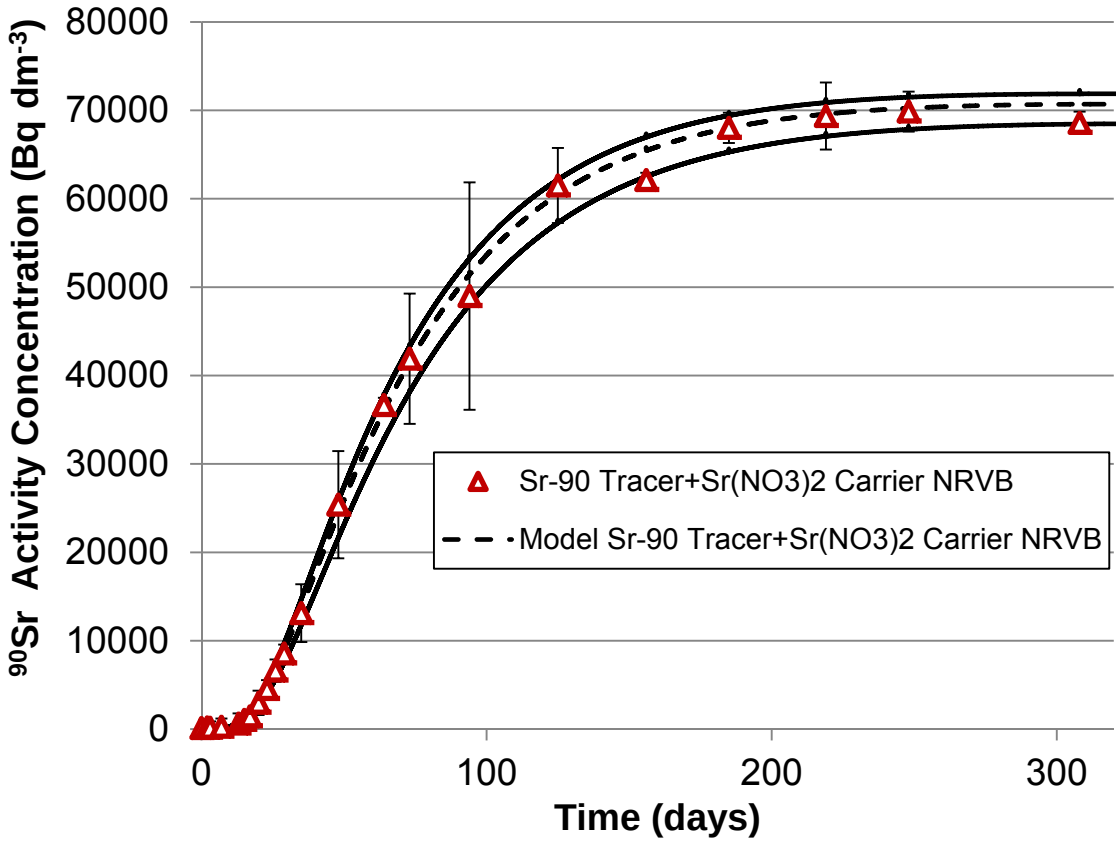

Fig. 13.27 Experimental and modelled NRVB diffusion curves for ^{90}Sr tracer and $Sr(NO_3)_2$ carrier using NRVB equilibrated water

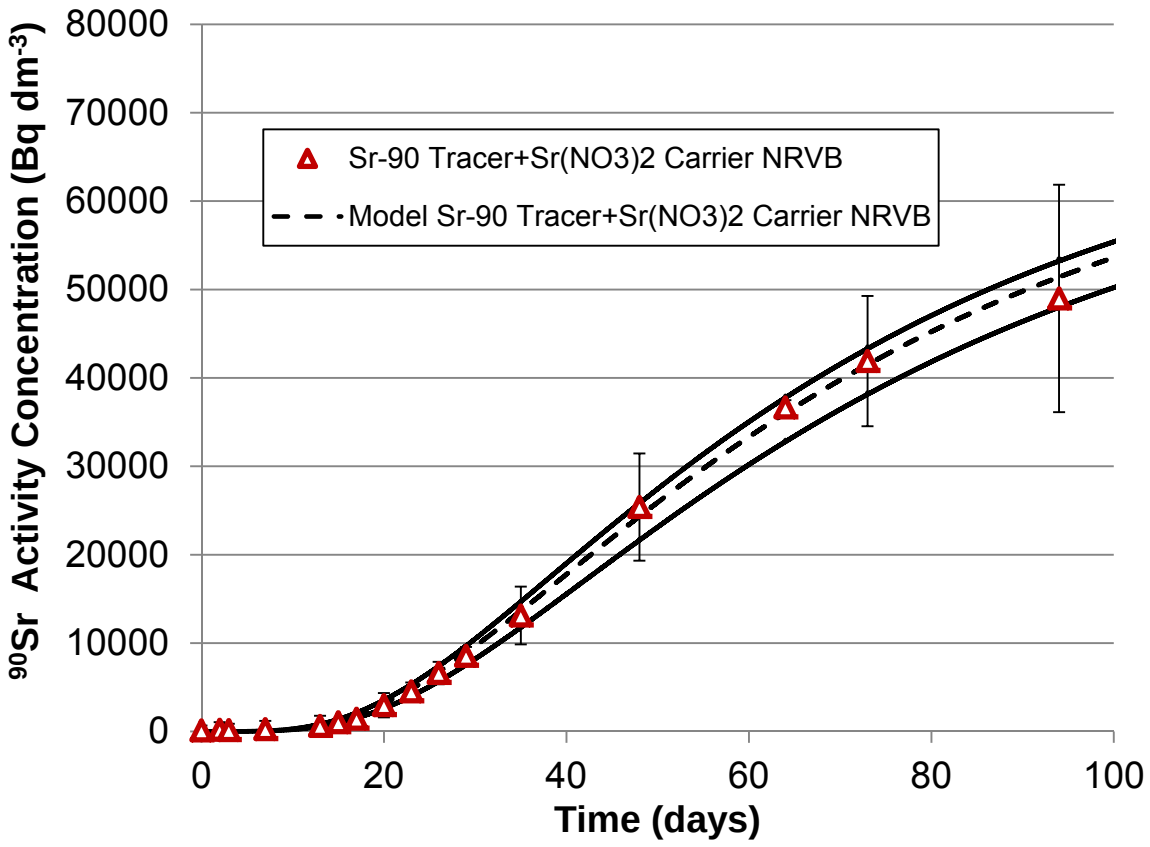

Fig. 13.28 Early data from the experimental and modelled NRVB diffusion curves for ^{90}Sr tracer and $Sr(NO_3)_2$ carrier using NRVB equilibrated water

Commentary

The best fit D_e and K_d model results for the ^{90}Sr tracer and $Sr(NO_3)_2$ diffusion with NRVB equilibrated water were 4.4×10^{-11} m^2 s^{-1} and 2.4×10^{-3} m^3 kg^{-1}, respectively (black long hashed line in fig. 13.25). The LOF associated with the best model result was 3.04%. The majority of the experimental data could be contained in the interval defined by setting D_e between 4.3×10^{-11} and 4.5×10^{-11} m^2 s^{-1} and K_d between values of 2.3×10^{-3} and 2.6×10^{-3} m^3 kg^{-1}, (the solid black lines in fig. 13.25 and 13.26). The early data plot (fig. 13.26) illustrates that data from both parts of the dataset are encompassed in the relatively tight range. The results that fall outside the envelope can be clearly seen on the figures. It should be noted that all observed values are included in the LOF results even those outside the envelope.

13.5.5 ^{90}Sr tracer and $Sr(NO)_3$ carrier CDP solution diffusion modelling

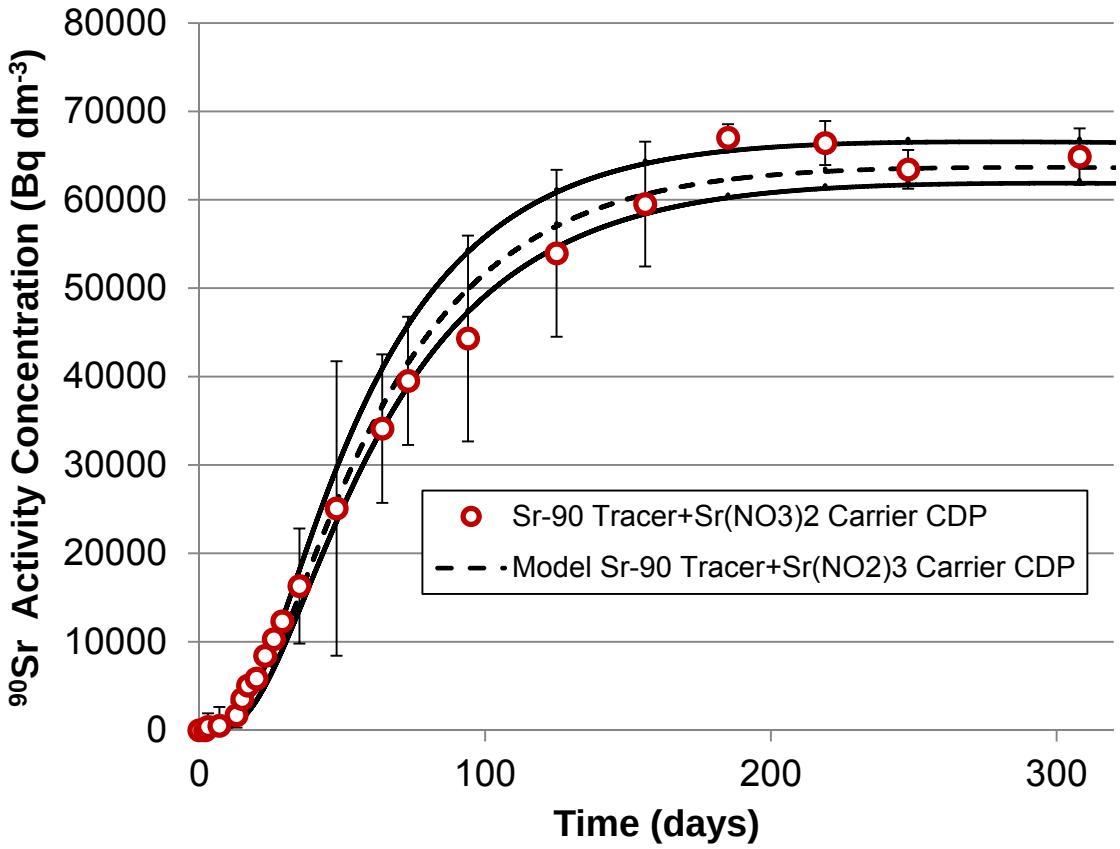

Fig. 13.29 Experimental and modelled NRVB diffusion curves for ^{90}Sr tracer and $Sr(NO_3)_2$ carrier using CDP solution

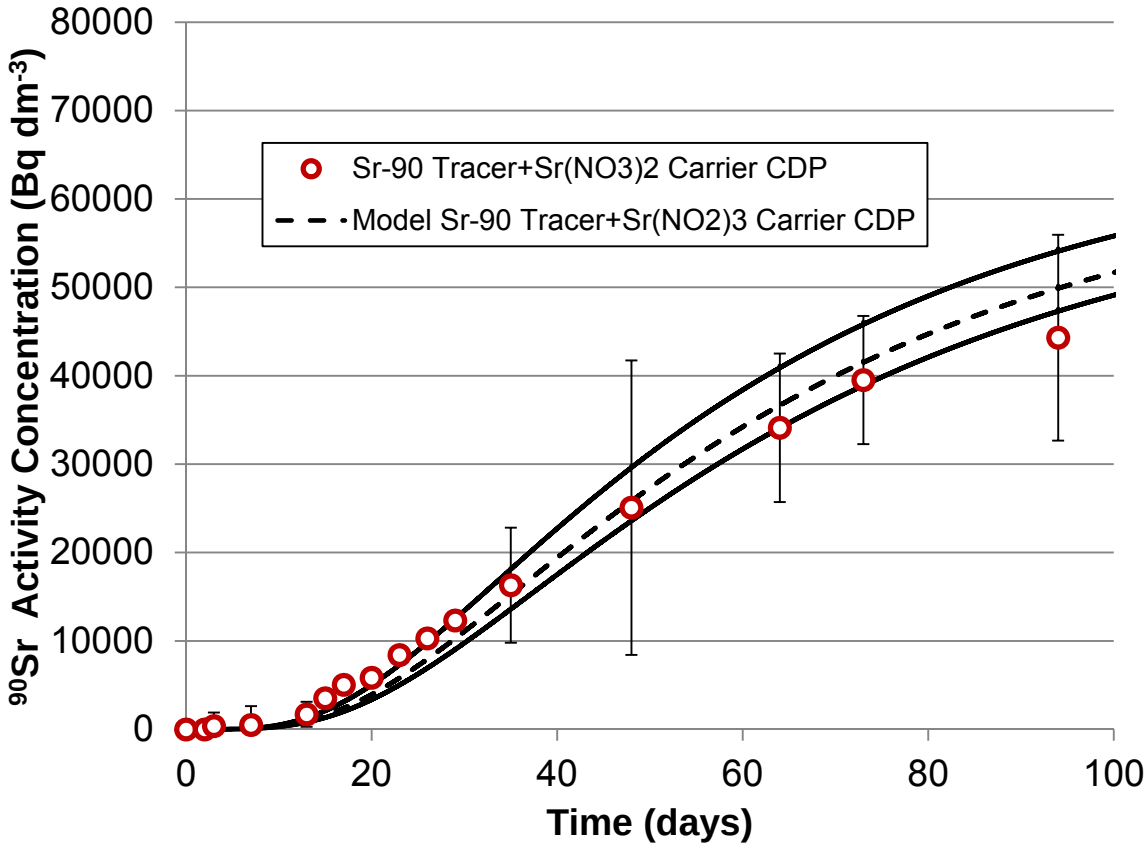

Fig. 13.30 Early data from the experimental and modelled NRVB diffusion curves for ^{90}Sr tracer and $Sr(NO_3)_2$ carrier using NRVB equilibrated water

Commentary

The best fit D_e and K_d model results for the ^{90}Sr tracer and $Sr(NO_3)_2$ diffusion with CDP solution were 5.9×10^{-11} m^2 s^{-1} and 3.1×10^{-3} m^3 kg^{-1}, respectively (black long hashed line in fig. 13.25). The LOF associated with the best model result was 11.0%. The majority of the experimental data could not be easily contained in the type of curves generated by the model. However, an interval defined by setting D_e between 5.6×10^{-11} and 6.1×10^{-11} m^2 s^{-1} and K_d between 2.8×10^{-3} and 3.3×10^{-3} m^3 kg^{-1}, (the solid black lines in figs. 13.27 and 13.28) approximates the data range. The early data plot (fig. 13.26) illustrates the difficulty of encompassing the data range, if a larger diffusivity range is selected the early data points will fall within the envelope but the range for the later data will be very wide and not reflect the actual range observed. The results that fall outside the envelope can be clearly seen on the figures. It should be noted that all observed values are included in the LOF results even those outside the envelope. The differences between the NRVB equilibrated water and CDP solution diffusion profiles is not apparent at first sight but the

modelling and high LOF suggests that CDP is causing an effect. This can also be seen on figs. 13.21 and 13.22 the composite plots; the initial concentration rise is steeper indicating that diffusivity is higher and the final concentration in solution is lower indicating that K_d is higher than in the corresponding NRVB equilibrated water experiment.

13.5.6 ^{90}Sr tracer only gluconate solution diffusion modelling

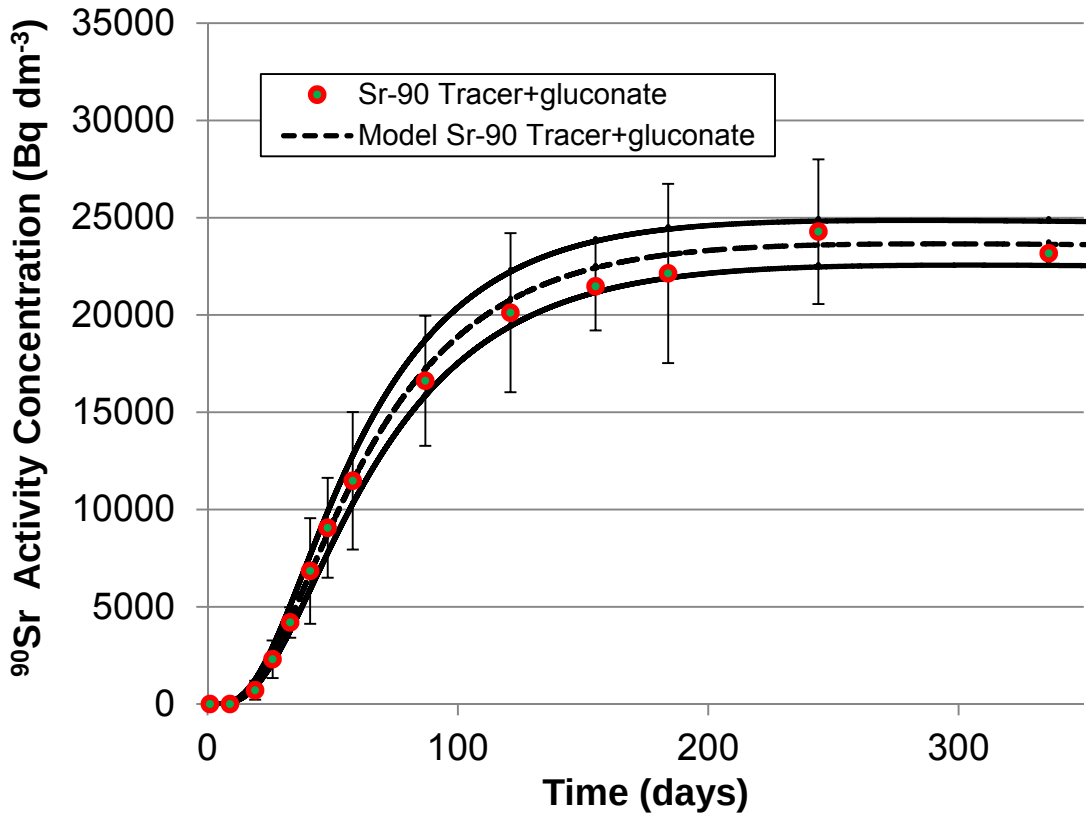

Fig. 13.31 Experimental and modelled NRVB diffusion curves for ^{90}Sr at tracer concentration in gluconate solution

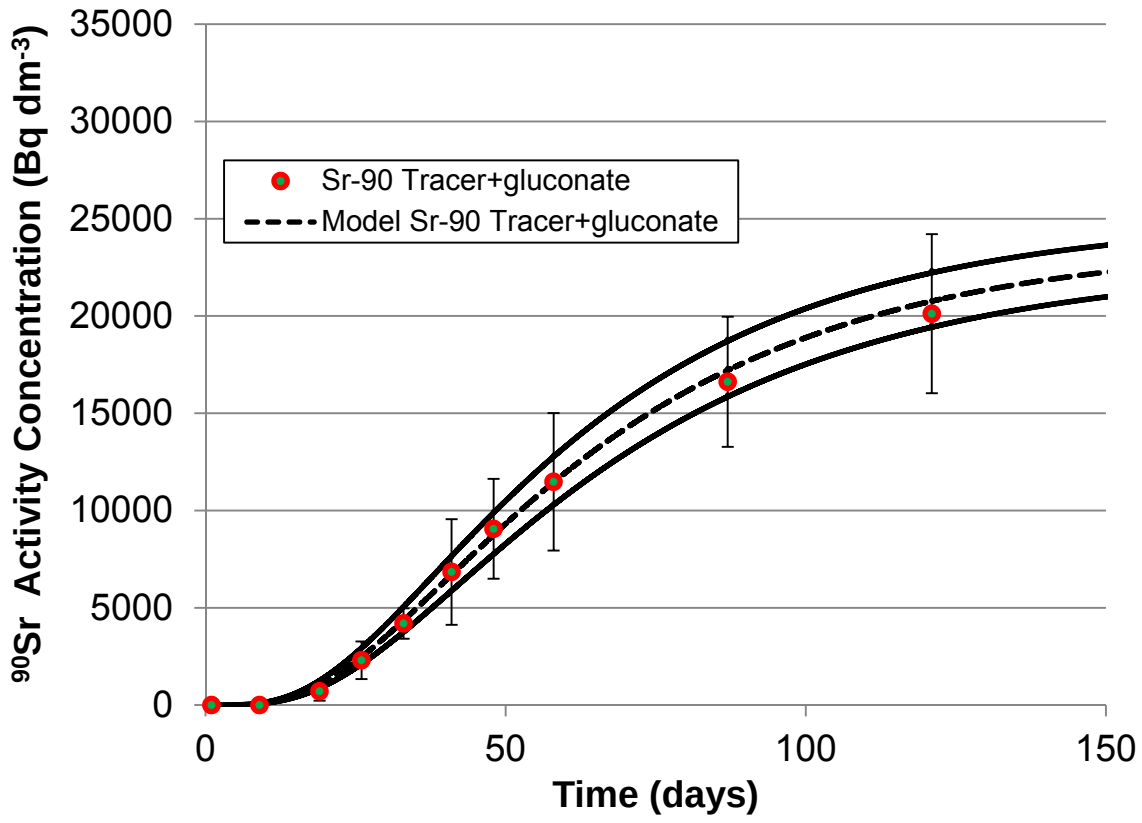

Fig. 13.32 Early data from the experimental and modelled NRVB diffusion curves for ^{90}Sr at tracer concentration in gluconate solution

Commentary

The best fit D_e and K_d model results for the ^{90}Sr tracer only diffusion with gluconate solution were 8.2x10^{-11} m^2 s^{-1} and 5.3x10^{-3} m^3 kg^{-1}, respectively (black dashed line in figs. 13.27 and 13.28). The LOF for the best model result was 5.19%. The majority of the experimental data could be contained in the interval defined by setting D_e between 6.9x10^{-11} and 9.5x10^{-11} m^2 s^{-1} and K_d between values of 5.0x10^{-3} and 5.7x10^{-3} m^3 kg^{-1}, (the solid black lines in fig. 13.31 and 13.32). In this case the early data (fig. 13.32) can be seen to fit the model curve well but the later data are more variable, extending to the upper and lower bounds. All the data points fall within the envelope which is likely a function of the smaller number of samples collected and determined. It should be noted that all observed values are included in the LOF results even those outside the envelope.

13.6 Autoradiographs of the ^{90}Sr Diffusion Experiments

13.6.1 ^{90}Sr tracer only using NRVB equilibrated water

The first NRVB cylinder from a Sr experiment to be autoradiographed was one of the ^{90}Sr tracer only using NRVB equilibrated water duplicates after 207 days had elapsed. The decision to stop one of the duplicate experiments was taken because the concentration in solution appeared to have stabilised and the two samples were behaving very similarly. There was also an interest in whether a concentration gradient could be seen even though a stable concentration was being approached.

The image was produced using a Fuji BAS MP 20 cm x 25cm autoradiography image plate with an exposure duration of 5 days. The plate was developed at BGS, Nottingham and is reproduced below as fig.13.33 in unenhanced and ImageJ enhanced versions.

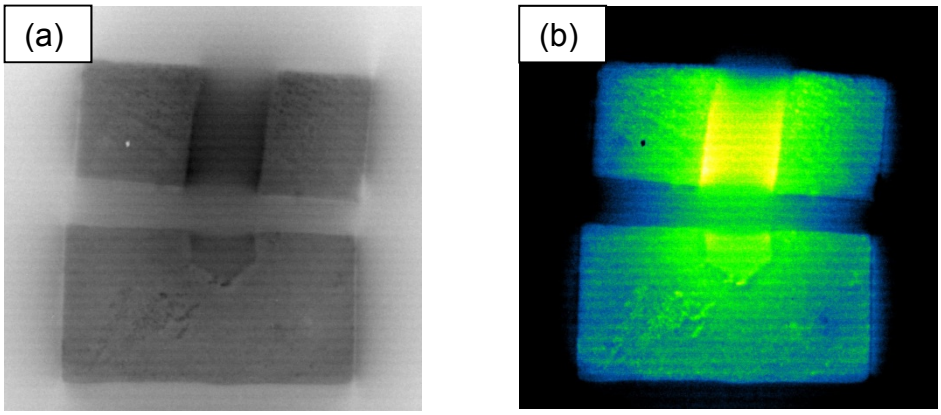

Fig. 13.33 Autoradiograph of NRVB cylinder from^{90}Sr tracer only using NRVB equilibrated water experiment (a) unenhanced and (b) ImageJ enhanced

The 5 day exposure was overly long and the original unenhanced image is intense but ill-defined as a consequence. The enhanced version showed that even after 207 days a concentration gradient was clearly visible from the centre of the cylinder to the edges. There was also a residual amount of the tracer present in the central core. The “spot” to the upper left could not be identified on the cylinder and is assumed to be of no relevance. The “scuff” marks to the lower left may have been caused by the masonary saw when the cylinder was sectioned.

13.6.2 Autoradiographs from the ^{90}Sr tracer, tracer carrier and gluconate experiments

The autoradiographs from the ^{90}Sr diffusion experiments (the exception being the high ionic strength ones which are being allowed to continue) are presented in

unenhanced and ImageJ enhanced versions with short commentaries below. The images were produced using a Fuji BAS MP 20 cm x 25cm autoradiography image plate with an exposure duration of 5 hours. The plate was developed at BGS, Nottingham. Each experiment is represented by a pair of images one of which (the one to the left) has the central core filled with modelling clay to shield radiation coming from any residual tracer that may be present.

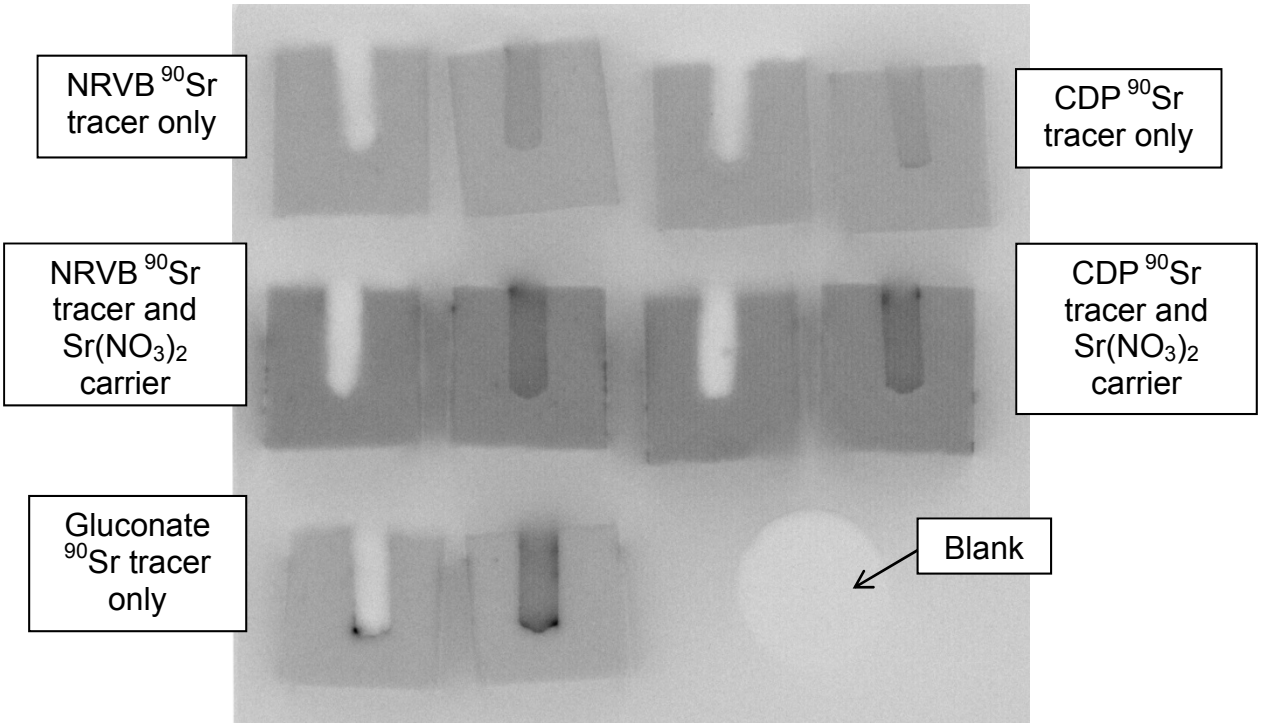

Fig. 13.34 Autoradiographs (unenhanced) from the NRVB/CDP ^{90}Sr tracer, tracer carrier and gluconate experiments

Commentary

The images in the unenhanced version presented in fig. 13.34 above are not particularly informative. However, it is worth noting that the tracer carrier images appeared darker because almost double (1.79 times) the amount of tracer was added. The effect of the modelling clay used as shielding is clear. A few residual high intensity spots can be seen in the central core and on the outer edges of the carrier experiments. The blank (an unused piece of NRVB cylinder) serves to demonstrate the amount of background radiation that the plate is subjected to during the exposure.

The ImageJ enhanced plates are shown in the following figures, they have been separated to allow the intensities of the carrier experiment images to be divided by 1.79 to make them comparable to the tracer only images.

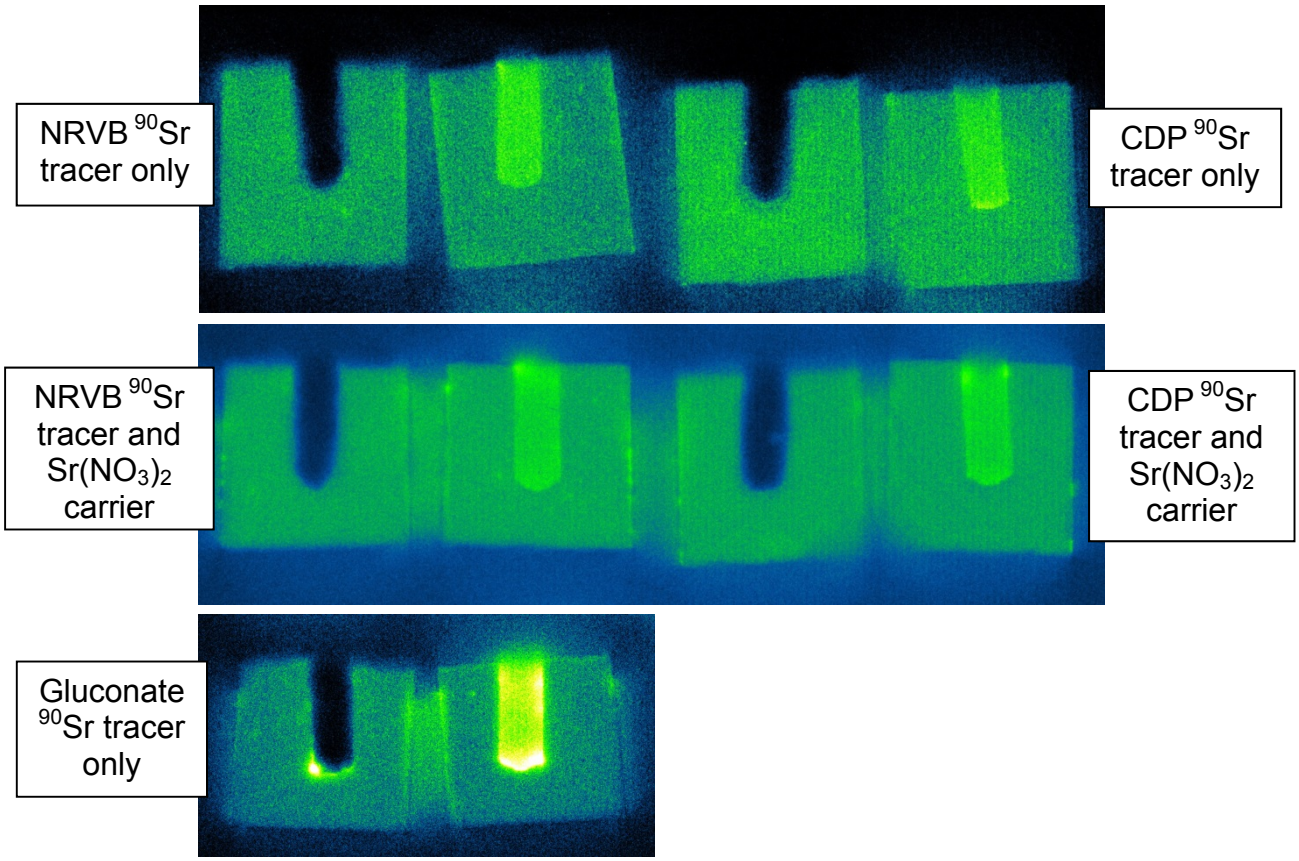

Fig. 13.35 Autoradiographs (ImageJ enhanced) from the NRVB/CDP ^{90}Sr tracer, tracer carrier and gluconate experiments

Commentary

The enhanced autoradiographs in fig.13.35 all exhibited homogeneous distribution of the tracer in the NRVB matrix and a gradient like the one seen in fig.13.33 was not visible. The distribution of tracer in the NRVB matrix for the tracer only experiment was uniform but “grainy”. The cylinder from the CDP tracer experiment was more intense than the one without CDP, reflecting the experimental results. The two carrier experiments were almost identical, both exhibited residual tracer at the central core seal and spots of tracer on external surfaces. The distribution of tracer in the NRVB matrix for the carrier experiments was totally uniform and “smooth”. The increase in intensity associated with the unshielded central cores may have been caused by a larger (curved) area being exposed to irradiate the plate. The cylinder used in the gluconate experiment has more residual tracer in the central core than the others which may be indicative of precipitation but distribution of the tracer that has diffused into the matrix is uniform. The GoldSim modelling suggested that diffusivity and partition were higher than those determined for the tracer and carrier experiments. The autoradiograph casts doubt on the modelling results as it can be

seen that the diffusion is incomplete. The gluconate experiment had run for only 207 days compared to 512 days for the tracer only experiments and 308 days for the carrier experiments. Consequently, the experiment will be continued and further investigated at a later date by sectioning the duplicate for autoradiography.

13.7 ^{90}Sr Tracer Advection Experiments with NRVB Equilibrated Water and CDP solution

13.7.1 Additional information relevant to the ^{90}Sr advection experiments

Three ^{90}Sr tracer only advection experiments have been undertaken; two runs using NRVB equilibrated water, these were undertaken on the same NRVB cylinder and a run using CDP solution undertaken on a separate cylinder.

The experimental procedure, including a 3 day “run in” for the NRVB cylinder was identical to that used in the HTO advection experiments (see section 10.6). The only exception being that the initial injection volume was 50 µL. The injection contained 12346 Bq or 740850 d min^{-1} of ^{90}Sr for each of the NRVB equilibrated water runs and 12409 Bq or 744525 d min^{-1} for the CDP run. All the eluent was collected and analysed for ^{90}Sr and the evaporation of the eluted mass corrected for by comparison with a weighed water blank left in the sample collector for the duration of the experiment. All ^{90}Sr determinations were performed by liquid scintillation counting in the same manner as the diffusion experiments.

The experiments appeared to be quite successful but maintaining a steady driving pressure and flow rate remained issues. Also a malfunction of the sample collector at a critical point in the NRVB equilibrated water runs had an impact on the quality of the data collected.

13.7.2 Run 1 ^{90}Sr tracer advection experiments with NRVB equilibrated water

The results are presented separately below as eluted mass and ^{90}Sr recovery plots on figs. 13.36 and 13.37. A table showing the data is also presented as tables 13.17. A brief commentary on the individual plots is also included. Finally, composite plots showing all three runs for comparative purposes are presented as fig. 13.42 and 13.43.

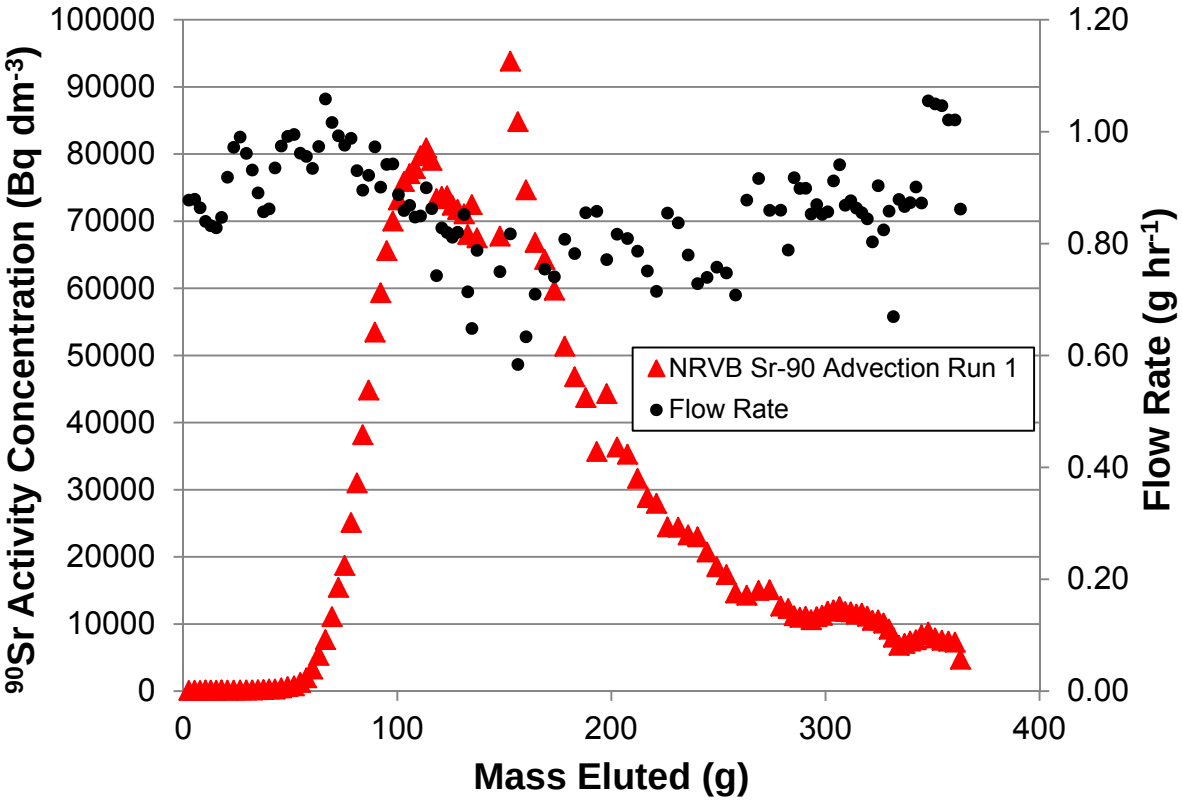

Fig. 13.36 Run 1 results of the ^{90}Sr tracer advection experiments using NRVB equilibrated water

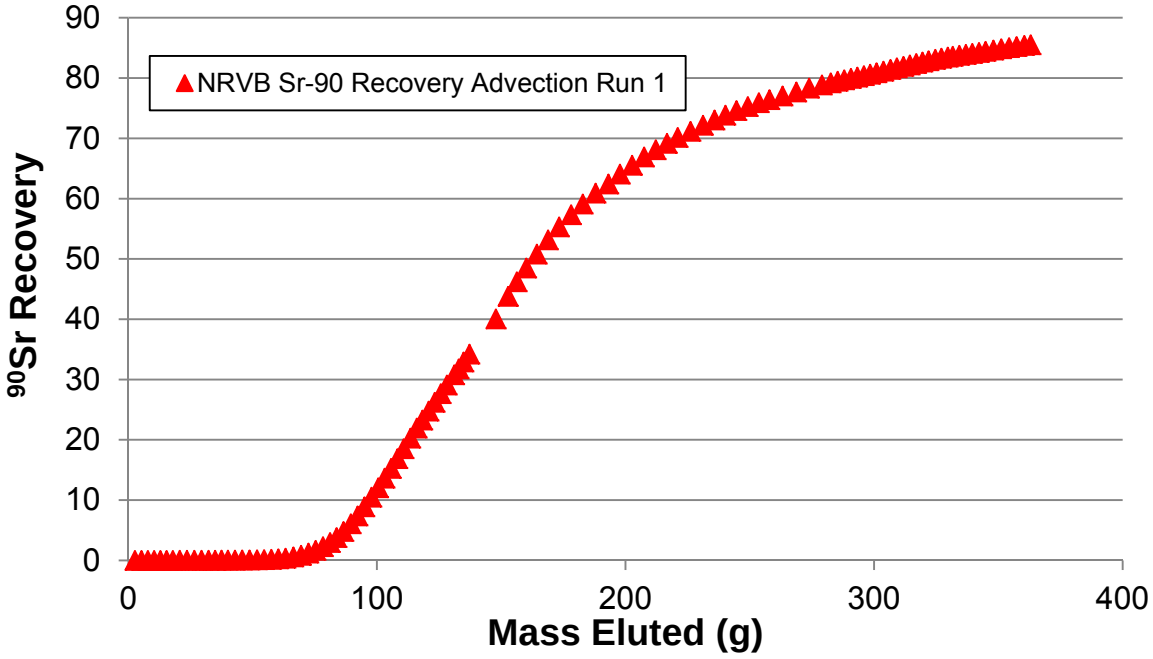

Fig. 13.37 Recovery plot run 1 of the ^{90}Sr tracer advection experiments using NRVB equilibrated water

Commentary

Initial breakthrough of the tracer occurred after approximately 50 g of NRVB equilibrated water had eluted. This was followed by a steep rise in concentration initially maximising at ~80000 Bq dm^{-3}, followed by erratic results caused by a malfunction of the sample collector (the data in this area of the plot contains real, lost and estimated points). The next major feature was a second maximum concentration at ~94000 Bq dm^{-3} followed by a steady fall in concentration and elongated tail slowly returning to concentrations near background. The erratic flow rate was a feature of the experiment and this occurred even though the driving pressure was constant throughout at 21 psi. The tracer recovery plot indicates that over 85% of the ^{90}Sr was recovered.

13.7.3 Run 2 ^{90}Sr tracer advection experiments with NRVB equilibrated water

The results are presented separately below as eluted mass and ^{90}Sr recovery plots on figs. 13.38 – 13.39. The data are also presented as table 13.18. A brief commentary on the individual plots is also included. Finally, composite plots showing all three runs for comparative purposes are presented as fig. 13.42 and 13.43.

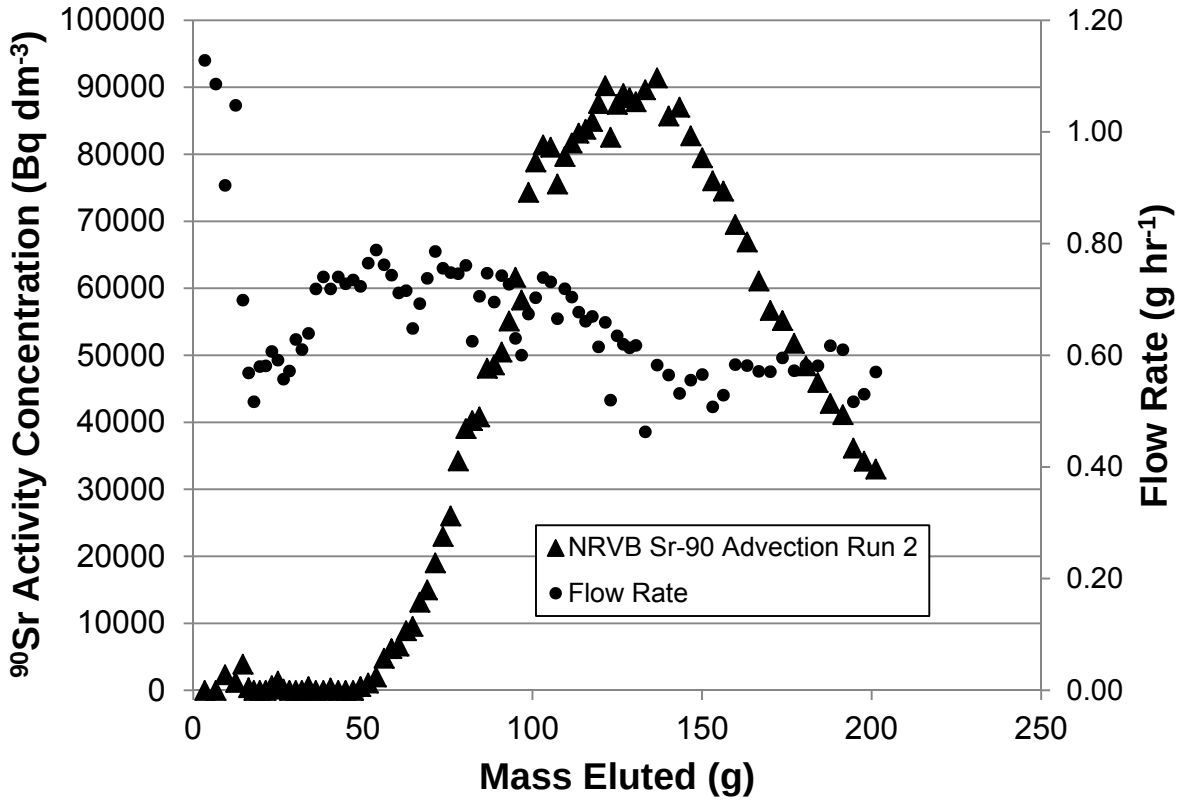

Fig. 13.38 Run 2 results of the ^{90}Sr tracer advection experiments using NRVB equilibrated water

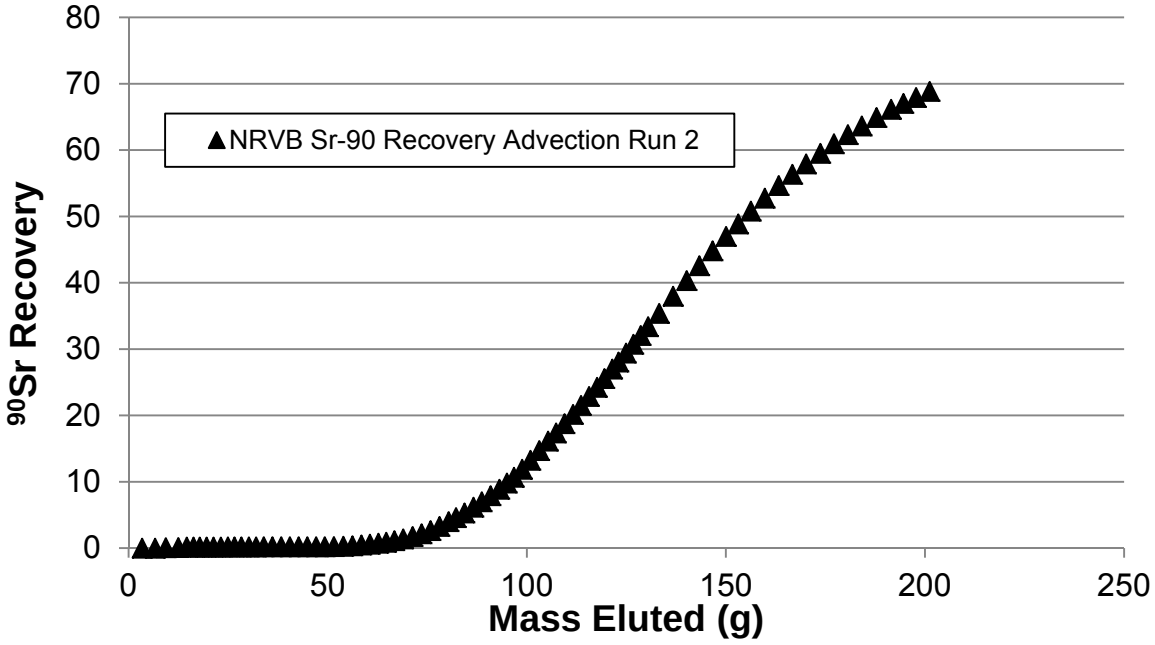

Fig. 13.39 Recovery plot run 2 of the ^{90}Sr tracer advection experiments using NRVB equilibrated water

Commentary

Initial breakthrough of the tracer occurred after approximately 50 g of NRVB equilibrated water had eluted. This was followed by a steep rise in concentration maximising at ~91000 Bq dm^{-3}, followed by a steady fall in concentration and elongated tail slowly returning to concentrations approaching background. There was a minor malfunction of the sample collector at the peak top affecting two of the samples which have been estimated as a consequence. The experiment was stopped before completion to ensure that some tracer was left on the NRVB for autoradiography. The steadily falling flow rate was a feature of the experiment and this occurred even though the driving pressure was constant throughout at 21 psi. The tracer recovery plot indicates that almost 70% of the ^{90}Sr was recovered.

13.7.4 ^{90}Sr tracer advection experiments with CDP solution

The results are presented separately below as eluted mass and ^{90}Sr recovery plots on figs. 13.40 – 13.41. The data are also presented as table 13.19. A brief commentary on the individual plots is also included. Finally, composite plots showing all three runs for comparative purposes are presented as fig. 13.42 and 13.43.

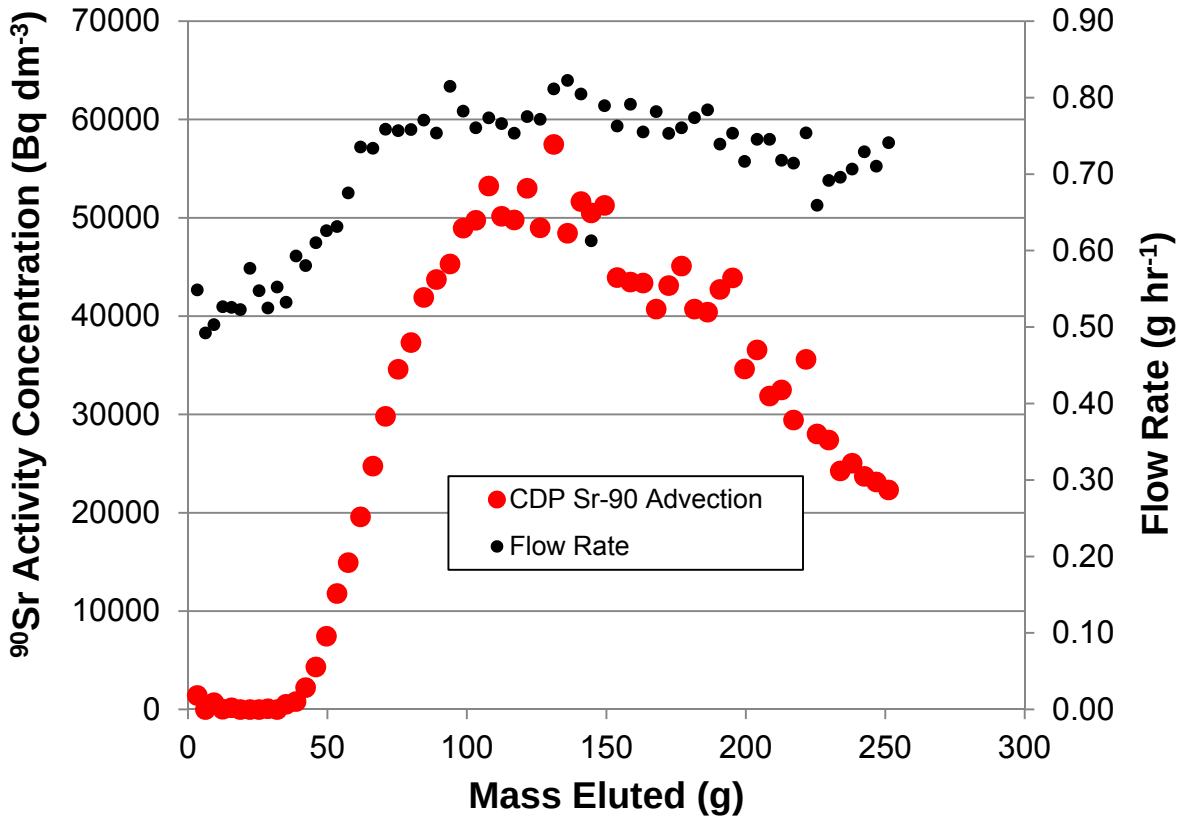

Fig. 13.40 Results of the ^{90}Sr tracer advection experiments using CDP solution

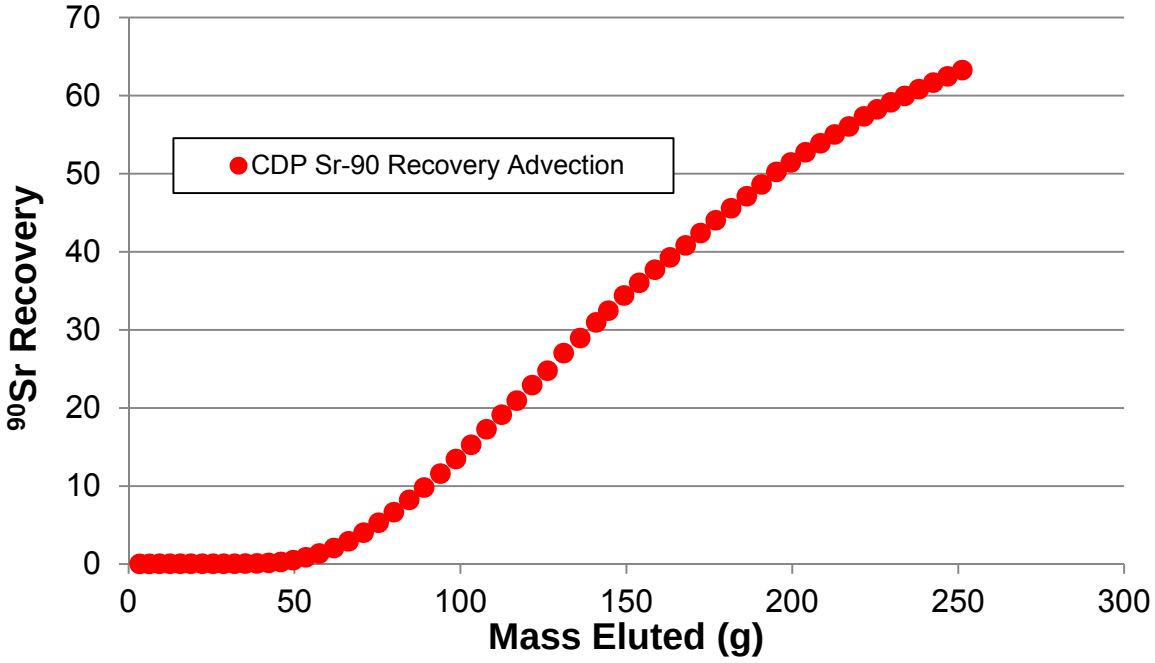

Fig. 13.41 Recovery plot for the ^{90}Sr tracer advection experiments using CDP solution

Commentary

Initial breakthrough of the tracer occurred after approximately 35 g of NRVB equilibrated water had eluted. This was followed by a steep rise in concentration generally peaking at ~50000 Bq dm^{-3} but with excursions as high as 57500 Bq dm^{-3}, followed by a steady fall in concentration and elongated tail slowly returning to concentrations approaching background. The experiment was stopped before completion to ensure that some tracer was left on the NRVB for autoradiography. The initial steady rise in flow rate was a feature of the experiment and this occurred even though the driving pressure was constant throughout at 21 psi. The downslope has three clear spikes that appear to correlate with short term flow rate minima. The tracer recovery plot indicates that almost ~65% of the ^{90}Sr was recovered.

13.7.5 Composite plots comparing the ^{90}Sr tracer advection experiments

The composite plots figs. 13.42 and 13.43 show all the ^{90}Sr tracer data together and whilst initially they may appear complex, a number of important observations can be made.

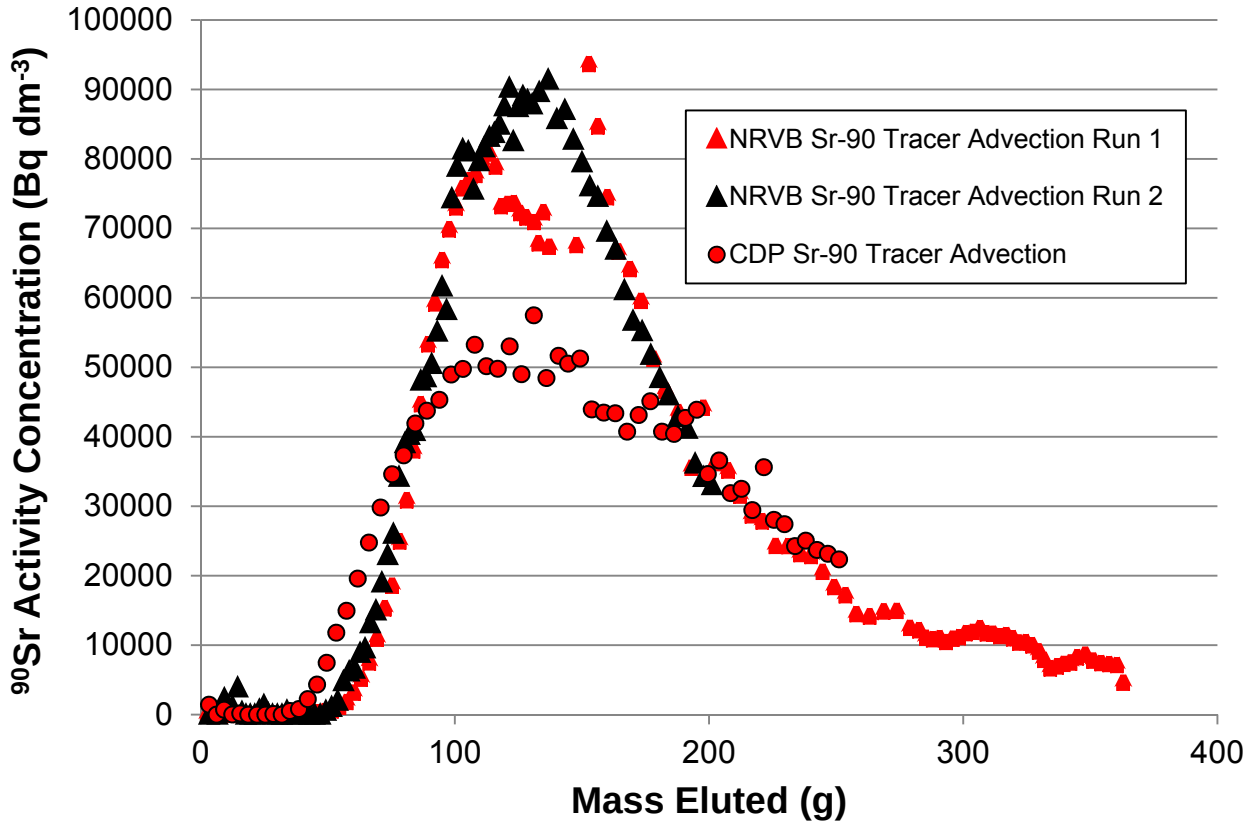

Fig. 13.42 Composite plot comparing the ^{90}Sr tracer advection experiments

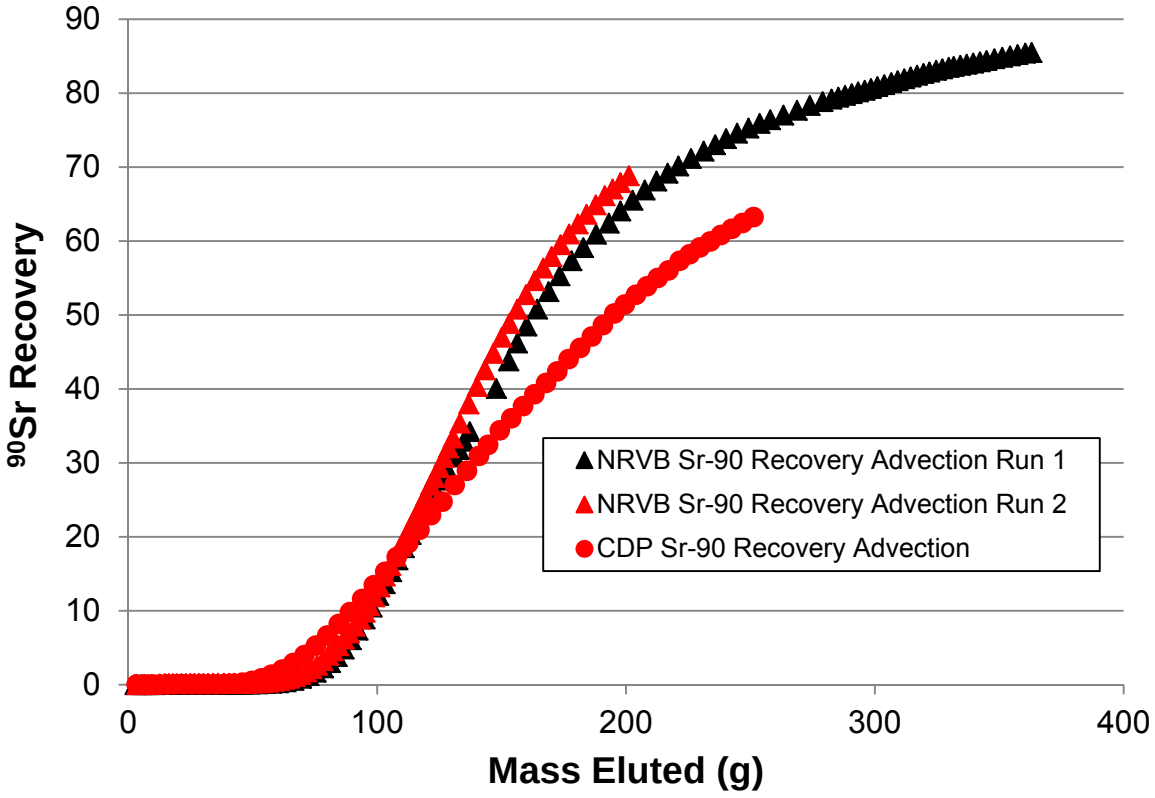

Fig. 13.43 Composite plot comparing recovery of the ^{90}Sr tracer during the advection experiments

Observations from composite plots

- The NRVB equilibrated water runs 1 and 2 show that the experiment is capable of providing reproducible results despite significant changes in flow rate and equipment malfunctions.
- The flat topped peaks and long tails indicate that dispersion is significant for all the experiments but more pronounced in when CDP solution is present.
- More mass appears to have been retained when CDP solution is used (this was also the case for the diffusion experiments).
- The tracer breaks through more quickly when the CDP solution is used, this was not anticipated as increased retention should have produced a delayed breakthrough. It should be noted that the CDP run used a different NRVB cylinder which could have had slightly different, dimensions, hydraulic properties and internal core verticality.
- The composite recovery plot shows that the NRVB advection experiments evolved almost identically and that tracer recovery with CDP solution was noticeably different.

- Final recovery results could not be produced because of the need to leave enough tracer on the cylinders for autoradiography. However the composite recovery plot provided a clear indication that less tracer was recovered when CDP was present.

13.8 Autoradiographs of the ^{90}Sr Advection Experiments

The autoradiographs from the ^{90}Sr tracer advection experiments are presented in unenhanced and ImageJ enhanced versions with short commentaries below. Each experiment is represented by a pair of images one of which (the one to the right) has the central core filled with a polythene plug to shield radiation coming from any residual tracer that may be present. The images were produced using a Fuji BAS MP 20 cm x 25cm autoradiography image plate with an exposure duration of 5 hours. The plate was developed at BGS, Nottingham. The cylinders were widely spaced on the autoradiography plate and were edited to be closer together, explaining the faint straight lines within the background. All images were enhanced at the same time using the same methodology.

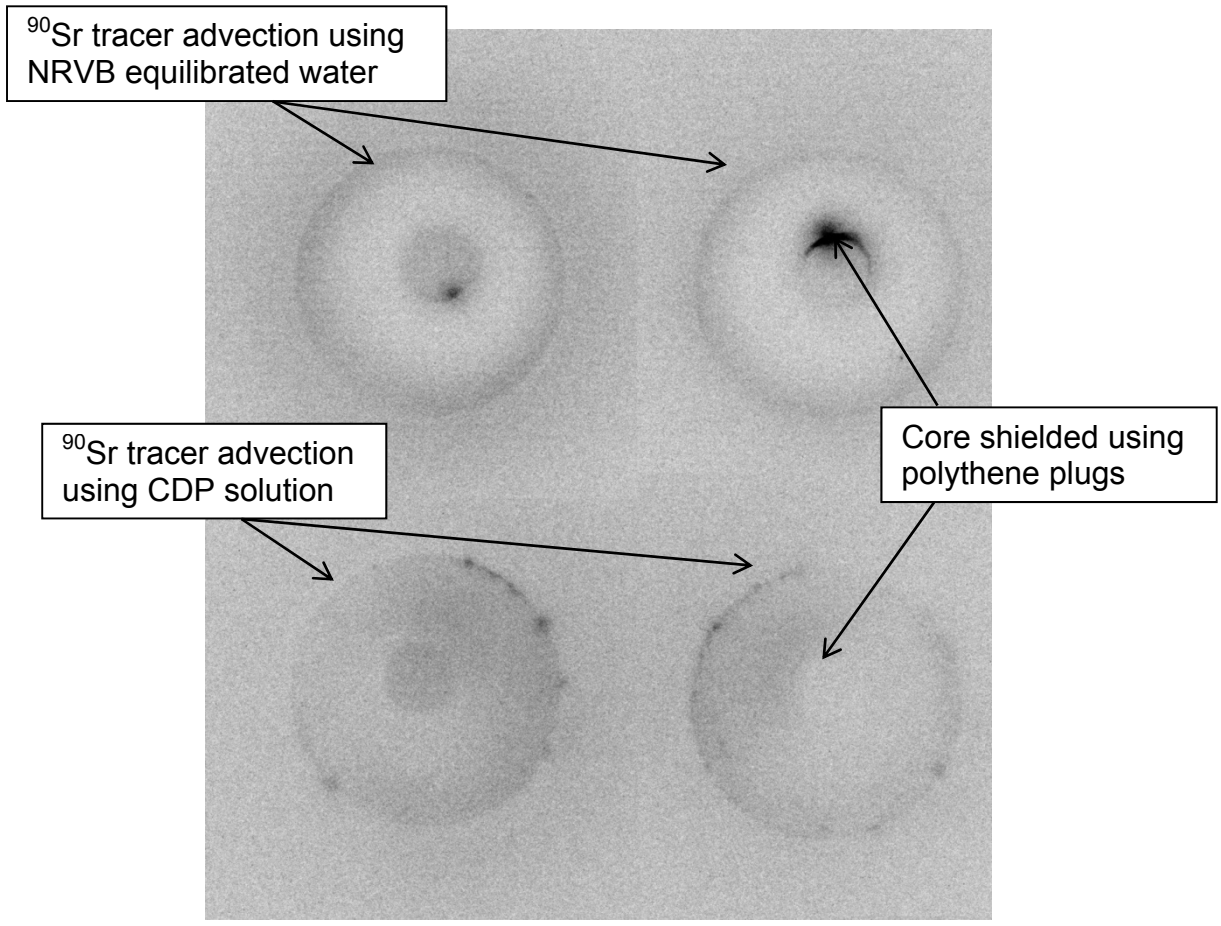

Fig. 13.44 Autoradiographs (unenhanced) from the ^{90}Sr tracer advection experiments

Commentary

The images in the unenhanced version are not particularly informative, even the effect of shielding the central core is not particulary clear. A few residual high intensity spots can be seen in the central core, one of which (the upper right cylinder) is very intense. In addition, spots can be seen on the outer edges of the CDP solution experiments. A blank (an unused piece of NRVB cylinder) was used but was edited out of the final image.

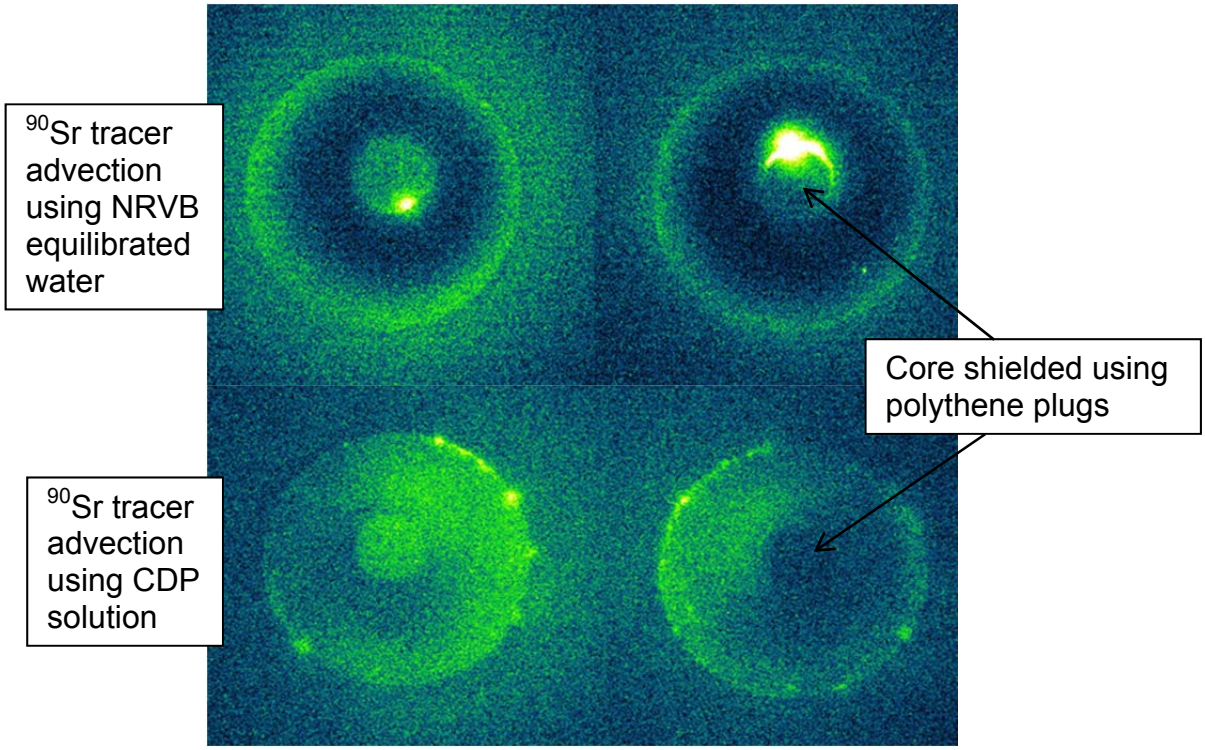

Fig. 13.45 ImageJ enhanced autoradiographs from the ^{90}Sr tracer advection experiments

Commentary

The enhanced images have helped visualise some important features and highlight differences between the two types of advection experiment.

NRVB equilibrated water

- There is a distinct ring of ^{90}Sr tracer activity within the NRVB matrix extending to the outer edge.
- Spots of activity are absent from the outer edge.
- There is a ring of inactivity surrounding the central core.
- The central core has significant residual activity present, this is particularly evident on the upper right image where the intense activity can be clearly seen despite the shielding (Note that this cylinder has had two active runs).
- There is a possibility that the outer ring is Sr and calcite co-precipitation caused by the ingress of atmospheric carbon dioxide similar to that observed in the trial advections.
- The outer ring of activity could also be evidence of the tracer tail being eluted.

- More tracer is present in the NRVB matrix than seen in the NRVB equilibrated water experiment.
- The tracer is more evenly distributed although there are distinct areas where more tracer is present, suggesting preferential flow or an artefact associated with the tracer injection similar to that seen in the iodine CDP advection.
- The experiment was stopped at an earlier stage than the NRVB equilibrated water experiment potentially explaining the presence of more activity.
- There are spots of tracer activity on the outer edge which appear to be contiguous with the areas of possible preferential flow.
- There is residual tracer activity in the central core but none of the very intense spots seen in the central core of the NRVB equilibrated water experiment.
- The ring of activity around the outer edge is present though not as extensive as in the NRVB equilibrated water experiment.
- There is a possibility that the outer ring is Sr and calcite co-precipitation caused by the ingress of atmospheric carbon dioxide similar to that observed in the trial advections.

13.9 GoldSim Models for Sr Advection Experiments

13.9.1 Additional information relevant to the ^{90}Sr NRVB advection modelling

Details of the GoldSim model are fully discussed in section 7. The results from the modelling of the ^{90}Sr tracer advection experiments are presented as fig. 13.46 to 13.48. The advection model is still being developed; the results are presented as GoldSim screenshots as the modelling has been only partially successful. Time is presented on the x axis and not eluted mass because the GoldSim model was found to produce better results against a time base for the HTO advection experiments (see section 10.4). The statistical approach used in the diffusion modelling was not considered appropriate with the advection data because the experimental methodology is still in the trial stage. Partition is referred to as K_d throughout, primarily because this term, rather than R_d is used in GoldSim.

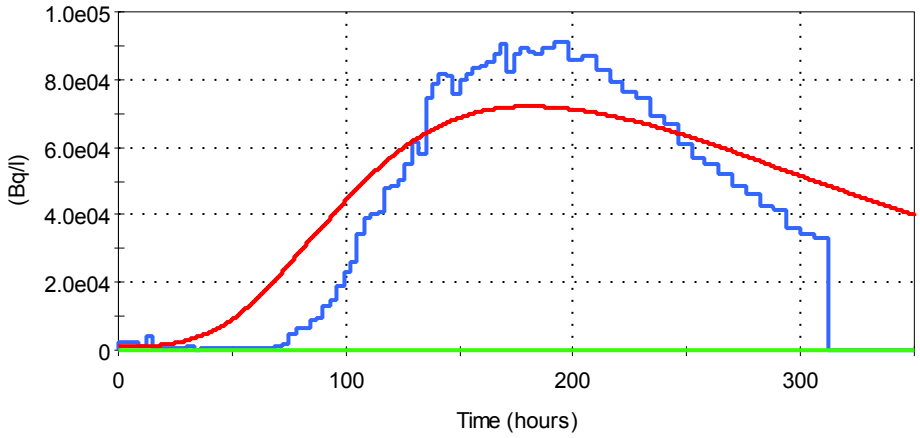

Fig. 13.46 Results and GoldSim model for run 2 of the ^{90}Sr tracer advection experiments using NRVB equilibrated water (—observed —modelled)

Fig 13.46 above was the result of modelling: D_e 4.4x10^{-11} m s^{-2}, K_d 2.7 m^3 kg^{-1} with an initial injection of 13000 Bq ^{90}Sr (slightly higher than the real experiments). All the parameters were very similar to those determined in the diffusion modelling. The GoldSim model has applied the measured experimental flow rate and 10% mechanical dispersion. The result was not a good match; modelled breakthrough is too early, peak concentration too early and low and dispersion too high (the peak is flatter and wider).

However, when the same parameters are modelled against the CDP advection results, a good match for the general shape of the peak is obtained. The result can be seen below in fig. 13.47. The model output has more mass (effectively equal to the area under the curves) present than the real data.

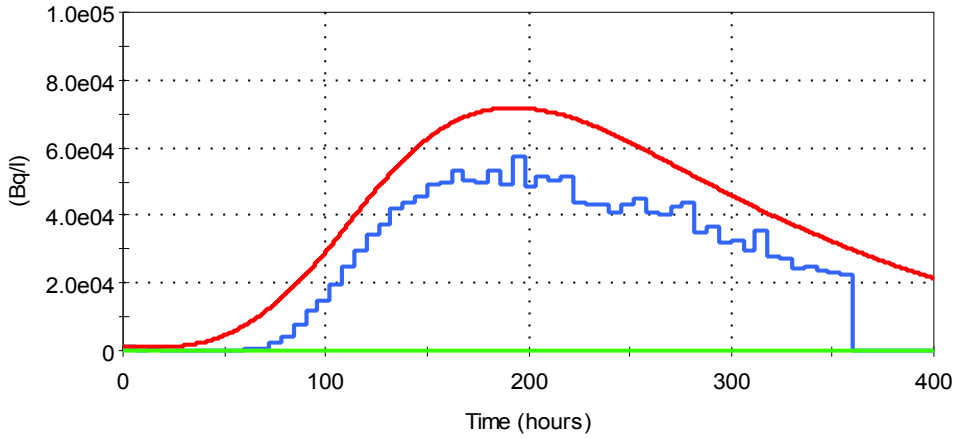

Fig. 13.47 Results and GoldSim model for the ^{90}Sr tracer advection experiment using CDP solution (—observed —modelled)

A third model was tried where the modelled injection was reduced to 10000 Bq (effectively assuming that 3000 Bq are precipitated or irreversibly bound to the NRVB), the results are shown below as fig,13.48. A good match for the CDP advection was obtained. Breakthrough was predicted to be slightly earlier than was observed but in all other respects the result was convincing.

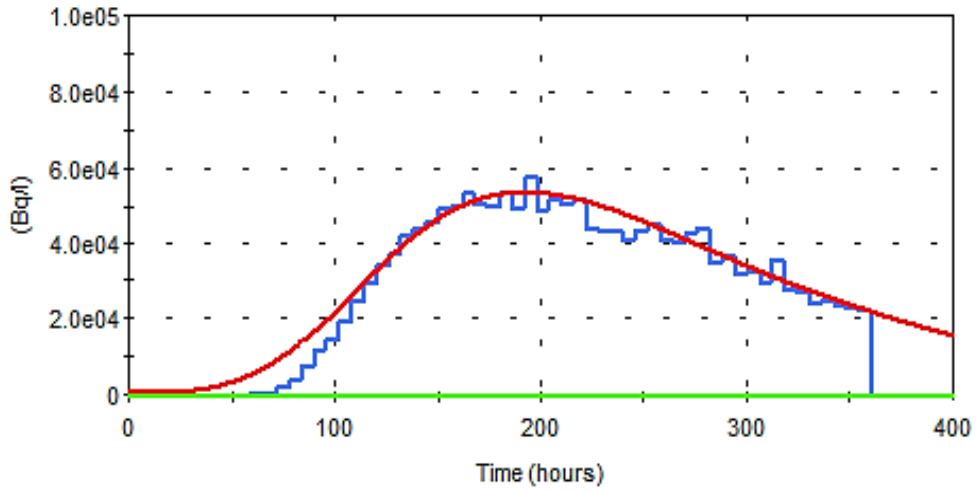

Fig. 13.48 Results and GoldSim model (assume 10000 Bq at start) for the ^{90}Sr tracer advection experiment using CDP solution (—observed —modelled)

It can be seen that the model output did not match the Sr data as well as it did for the HTO experiments. The NRVB advection runs were reproducible and the data was peak shaped suggesting that it should be readily modelled. However the CDP run also suggested that other processes could be occurring involving loss of mass. The most obvious process capable of causing this would be precipitation.

The spike was 13000 Bq but the best fitting model only accounts for 10000 Bq suggesting that 3000 Bq (23% of 13000) remained in the system. The autoradiographs show residual activity in the NRVB but the experiment was curtailed early (only 63% of the spike had been recovered) in order to get them. An additional run over an extended time period is needed to confirm whether this is simply an experiment with a long tail or that a proportion of the tracer is irreversibly bound to the NRVB.

13.10 Discussion of the Suite of ^{90}Sr Diffusion and Advection Results

The radial diffusion technique has been successfully used to observe the migration of Sr through cylinders of the potential backfill NRVB. Notwithstanding the limitations

of the GoldSim model detailed in section 7.5, determinations of D_e and K_d when made, were comparable with literature values (see table 17.1).

Experiments were performed using NRVB equilibrated water and a solution of cellulose degradation products (CDP) produced in the presence of the NRVB components. Additional experiments were undertaken at increased ionic strength and also in the presence of gluconate.

A study undertaken as late as 2002 [167] documented dynamic experiments that were of inadequate duration to make relevant observations and concluded that Sr was strongly bound. In 2003 a study [64] noted that Sr mobility was not affected by the presence of organics.

More recent batch studies have noted that Sr uptake by CSH phases in alkali free solutions can be described in terms of Sr/Ca ion exchange with equal affinity of CSH for Sr and Ca. However, the same study also noted the potential for irreversible incorporation of Sr into the CSH matrix in the presence of artificial cement water where the completion with high concentrations of Na^+ and K^+ ions was also considered.[168] A further study [169] extended the experiments using the radioisotope ^{85}Sr to investigate the uptake of Sr by CSH phases and concluded that the process was reversible. Both studies indicate that sorption models are suitable for predicting Sr interactions with CSH in a GDF environment. The present work suggests that sorption models may be insufficient and that a significant proportion of the Sr could be irreversibly bound to the NRVB solid.

It is important to note that the present experiments have been undertaken on intact samples of NRVB, a high limestone content, backfill material and that alternative sorption and incorporation mechanisms could be occurring.

The diffusion experiments have been affected by the longer than anticipated pre-equilibration time for Sr. Indeed this could be the reason why the gradient is observed on the first autoradiograph (see fig.13.33) even though stable concentrations in the receiving water had been attained i.e. non active Sr could still be migrating within the sample as the ^{90}Sr tracer moves out.

The tracer with carrier experiments in both the presence and absence of CDP were virtually indistinguishable suggesting that the Sr concentration was more significant than the presence of organics. The tracer only experiments did show that the presence of CDP increased uptake.

There is very limited information in the literature relating to the interaction of the organic substances present in CDP with CSH and the consequent effects on Sr mobility. The present series of experiments were not designed to provide an insight into the nature of the interaction. However, the possible mechanisms include precipitation of low solubility organic salts, change in surface Ca to Si ratio (see section 12.10) and formation of tertiary complexes (CSH-Sr-org or CSH-org-Sr).

The gluconate experiment was an attempt to isolate the effect of organics by using a surrogate for CDP that did not increase the ionic strength. The experiment was not entirely successful as it did not have time to run to completion and a significant amount of the ^{90}Sr tracer appeared to have precipitated in the inner core of the NRVB cylinder.

More recently experiments have been commenced to look into the effect of changes in ionic strength, the initial results appear to confirm that there is a decrease in diffusivity associated with increasing ionic strength. The effect is usually attributed to restriction of ion mobility by the electrostatic field created by other ions present in solution (see section 5.0 for theoretical aspects and 11.10 where a similar point is made in relation to the Cs experiments).

The advection experiments that have been completed also show that the presence of CDP slowed the elution of Sr. The associated autoradiographs show evidence of residual Sr in the central core and flows that may not have been as uniform as the elution profiles suggest. However, the method could be seen as a way of providing relevant data very quickly in comparison to the equivalent diffusion experiment.

14.0 Calcium

14.1 Background

The main calcium isotope of interest is ^{41}Ca, it is a component of the UK radioactive waste inventory and is mentioned in the latest estimate at 01/04/2010, [26] and table 14.1 below reproduces the relevant activities.

Isotope	HLW	ILW	LLW	units
^{41}Ca	1.2x10^{-1}	3.6	1.1x10^{-3}	T Bq

Table 14.1 ^{41}Ca in the UK waste inventory at 01/04/2010

The activities in the table above may not appear significant but ^{41}Ca is a long lived isotope (half-life, 103000 years). It arises from the neutron activation of calcium present in the concrete structures of nuclear reactors. It is important to understand the mechanism and rate of migration of radioactive calcium in the geological disposal facility (GDF) environment where the non-active calcium concentration may be very high due to the use of cementitious media in packaging grouts and backfill.[147]

^{41}Ca is a potential hazard to humans as it can replace non-active calcium in the solid tissues of the body preventing effective excretion. After entering the body, most often by ingestion of contaminated food or water, 20 – 30% of the dose may be absorbed and deposited in bones, bone marrow, teeth etc. Its presence in bones can cause bone cancer, cancer of nearby tissues, and leukaemia.

^{41}Ca decays by electron capture to the ground state isotope ^{41}K.

$$^{41}_{20}Ca + {}^{0}_{-1}e \rightarrow {}^{41}_{19}K + \bar{\nu}_e$$

There are no gamma emissions associated with this transition but the subsequent rearrangement of electrons gives rise to x-ray and auger electron emissions.[158]

The weak emissions associated with ^{41}Ca make it unsuitable for use in the diffusion and advection experiments and consequently ^{45}Ca, (half-life, 163 days) has been used as a surrogate. ^{45}Ca decays by beta electron emission with a maximum energy of 0.25 MeV and an average energy of 0.075 MeV, to the ground state isotope ^{45}Sc, according to the equation below.[158]

$$^{45}_{20}Ca \rightarrow {}^{45}_{21}Sc + {}^{0}_{-1}e + \bar{\nu}_e$$

The specific activity of ^{45}Ca is 7.03x10^{14} Bq g^{-1}, it is readily and efficiently detected and determined by liquid scintillation counting.

The Sr experiments provided an indication that experimental timescales for the diffusion experiments would be in the range of months to years. Previous work, suggested that diffusion constrained by isotope exchange with Ca containing gel phases would be the main transport mechanism.[169] Clearly, the short half-live of the isotope becomes an issue as experimental duration increases.

The experiments undertaken were as follows:

- Diffusion with NRVB equilibrated water using ^{45}Ca tracer
- Advection with NRVB equilibrated water and CDP solution using ^{45}Ca tracer only.

Autoradiographs for the diffusion and advection experiments have been produced. The advection experiments were undertaken after the initial results from the diffusion experiments had been seen and the objective was to ascertain whether it was possible to obtain relevant information more quickly.

14.2 ^{45}Ca tracer Diffusion using NRVB equilibrated water

The diffusion experiment used an addition of 9000 Bq ^{45}Ca (produced as the chloride by Perkin Elmer) to duplicate NRVB cylinders. For safety and convenience the addition was not carried out in the nitrogen glove box. The cylinders were submerged in 200 cm^3 of NRVB equilibrated water and sampled weekly for 4 weeks and monthly thereafter. When one year had elapsed and no tracer had been detected in the external solution it was decided that one of the duplicate experiments should be stopped and the cylinder sectioned for autoradiography. The main reason was that over two half-lives had occurred, only 1914 Bq of the original addition remained and it was not known how much activity was required to produce a useable autoradiograph.

14.3 Autoradiographs from the ^{45}Ca NRVB Tracer Diffusion

The two autoradiographs in figs. 14.1 to 14.4 below were produced using a Fuji BAS MP 20 cm x 25cm autoradiography image plate with an exposure duration of 5 days. The plate was developed at BGS, Nottingham. The enhancement and intensity plots were undertaken using ImageJ software. A polythene plug was used to shield radiation from the central core to provide a better visualisation of the migrating isotope. Shielded and unshielded images are presented.

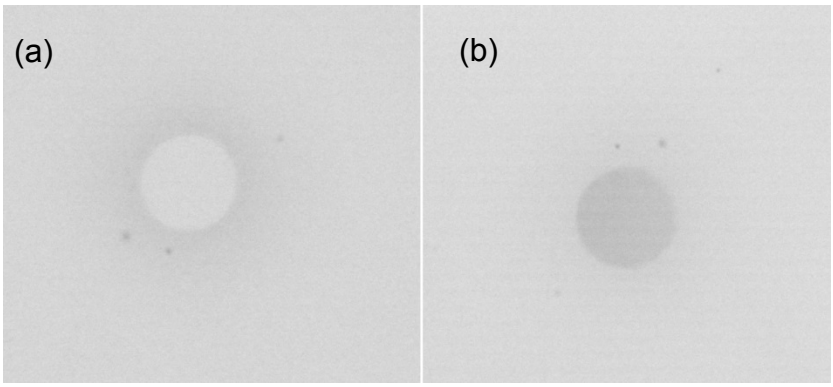

Fig. 14.1 Unenhanced autoradiographs from the ^{45}Ca diffusion experiment using NRVB equilibrated water (a) shielded, (b) unshielded

The unenhanced images are difficult to interpret although the shielding did enable the migrating tracer to be seen. Note: (a) and (b) are the same sample of NRVB which can be seen from the hotspots i.e. rotate (a) to the right and the hotspots will match. Some hotspots matched visible inclusions and voids in the original samples but not all.

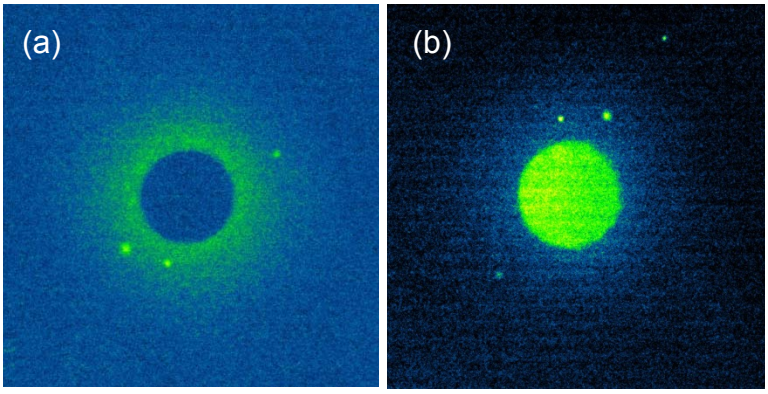

Fig. 14.2 ImageJ enhanced autoradiographs from the ^{45}Ca diffusion experiment using NRVB equilibrated water (a) shielded, (b) unshielded

The enhanced images clearly show that ^{45}Ca has migrated into the NRVB matrix; it is also evident that a significant proportion of the tracer remained in the central core. The migration profile appeared uniform with a similar depth of penetration from the perimeter of the central core. The two images are not directly comparable as they have been adjusted separately and differently to improve the visualisation. The contrast was increased for image (a) to emphasise the activity in the NRVB matrix and decreased for image (b) to reduce the “flare” from the central core. The different treatments are evidenced as a clear difference between the backgrounds.

ImageJ also has a function enabling the relative intensity of the radioactivity to be plotted graphically. Figs. 14.3 and 14.4 show the results of using the function on the autoradiographs. It was originally hoped that it would be possible to attribute the start concentration to the edge of the central core and estimate diffusivity. This was not feasible because a significant proportion of the activity is present, presumably precipitated on the walls of the central core and there is a steep fall in activity to the level observed in the NRVB matrix. This can be seen on fig. 14.4 where the central core is unshielded.

The two images have been subject to a high contrast increase to produce the intensity plots and as a consequence they are not directly comparable. A further consequence is that the hotspot signals have been overwhelmed on the shielded image fig. 14.3.

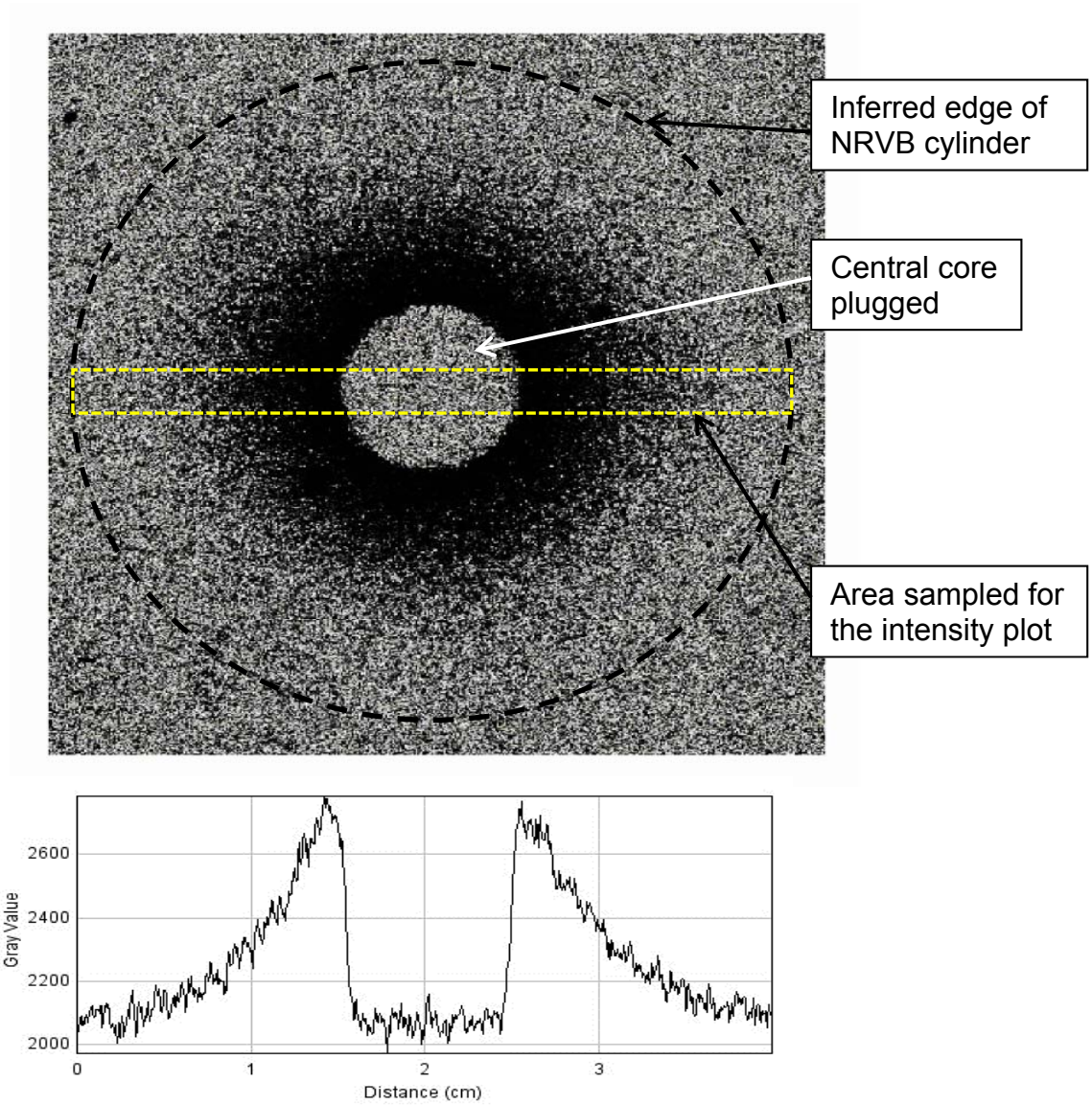

Fig. 14.3 ImageJ enhanced (shielded) autoradiograph and intensity plot from the ^{45}Ca diffusion experiment using NRVB equilibrated water

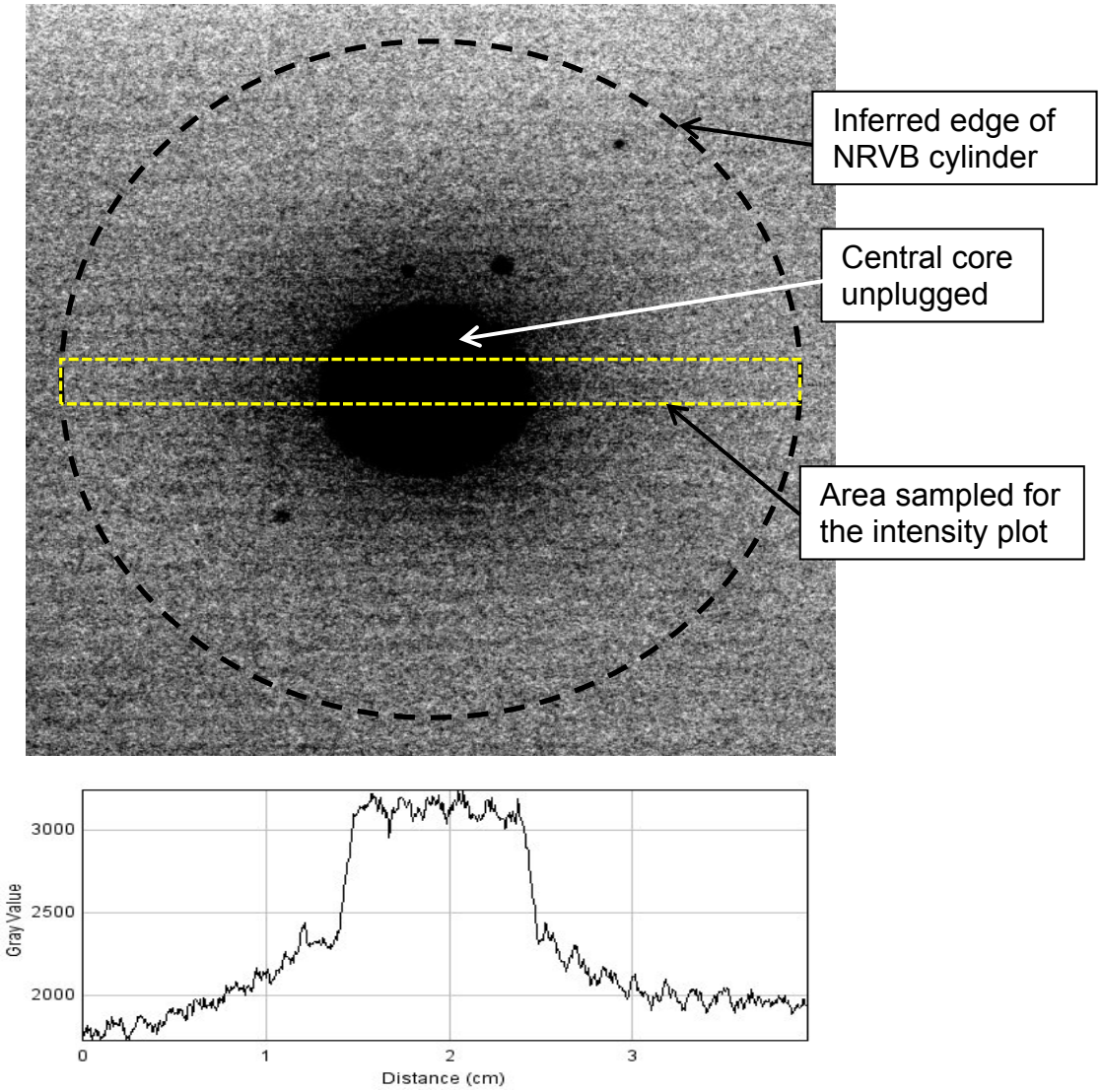

Fig. 14.4 ImageJ enhanced (unshielded) autoradiograph and intensity plot from the ^{45}Ca diffusion experiment using NRVB equilibrated water

The usefulness and flexibility of the autoradiography technique is demonstrated by the images in figs. 14.2 – 14.4. The experiment provided clear evidence that Ca isotopes will migrate through cementitious media even with a very low tracer concentration gradient (the mass of ^{45}Ca added was ~13 pg). Unfortunately it has not been possible to use the data in a quantitative manner to ascertain whether isotope exchange was a factor. This is due to the difficulty of making an estimate the proportion of the ^{45}Ca that has remained in the central core. In addition, the experiment was somewhat compromised by the time taken for it to progress. Indeed the remaining duplicate has not yet (some 2 years after commencement) shown evidence of ^{45}Ca breakthrough. It is now certain that the rate of decay compared to migration rate means that breakthrough will not occur. It is important to note that the Ca isotope of concern for the security of a GDF is ^{41}Ca which has a very long half-life and its migration will not be reduced by radioactive decay in the same way as ^{45}Ca.

14.4 ^{45}Ca Tracer Advection with NRVB Equilibrated Water and CDP Solution

The diffusion experiments were not carried out in the presence of CDP, primarily because there was no requirement from either NDA or the SKIN project. However, the advection experiments undertaken on HTO, Cs, Sr and Ni (see section 15) suggested that it may be possible to acquire some comparative data on the effect of CDP on Ca migration relatively quickly. Consequently both experiments were scheduled and undertaken.

14.4.1 ^{45}Ca tracer advection using NRVB equilibrated water

The experimental procedure, including a 3 day "run in" for the NRVB cylinder was identical to that used in the HTO advection experiments (see section 10). The only exception being that the initial injection volume was 50 µL. The injection contained 6700 Bq or 402000 d min^{-1} of ^{45}Ca. The experiment ran for 49 days after which time radioactive decay meant that 5450 Bq or 327000 d min^{-1} remained in the system. All the eluent was collected and analysed for ^{45}Ca. The evaporation of the eluted mass was corrected for by comparison with a weighed water blank left in the sample collector for the duration of the experiment. All ^{45}Ca determinations were performed by liquid scintillation counting [170] using Goldstar multi-purpose liquid scintillation cocktail and a Packard 2100TR liquid scintillation counter.

The experiment ran without significant problems but there was still some difficulty maintaining a steady driving pressure and flow rate.

The results are presented separately as eluted mass and ^{45}Ca recovery plots on figs. 14.5 and 14.6, the data are presented as table 14.2 in appendix 1. A brief commentary on the individual plots is also included.

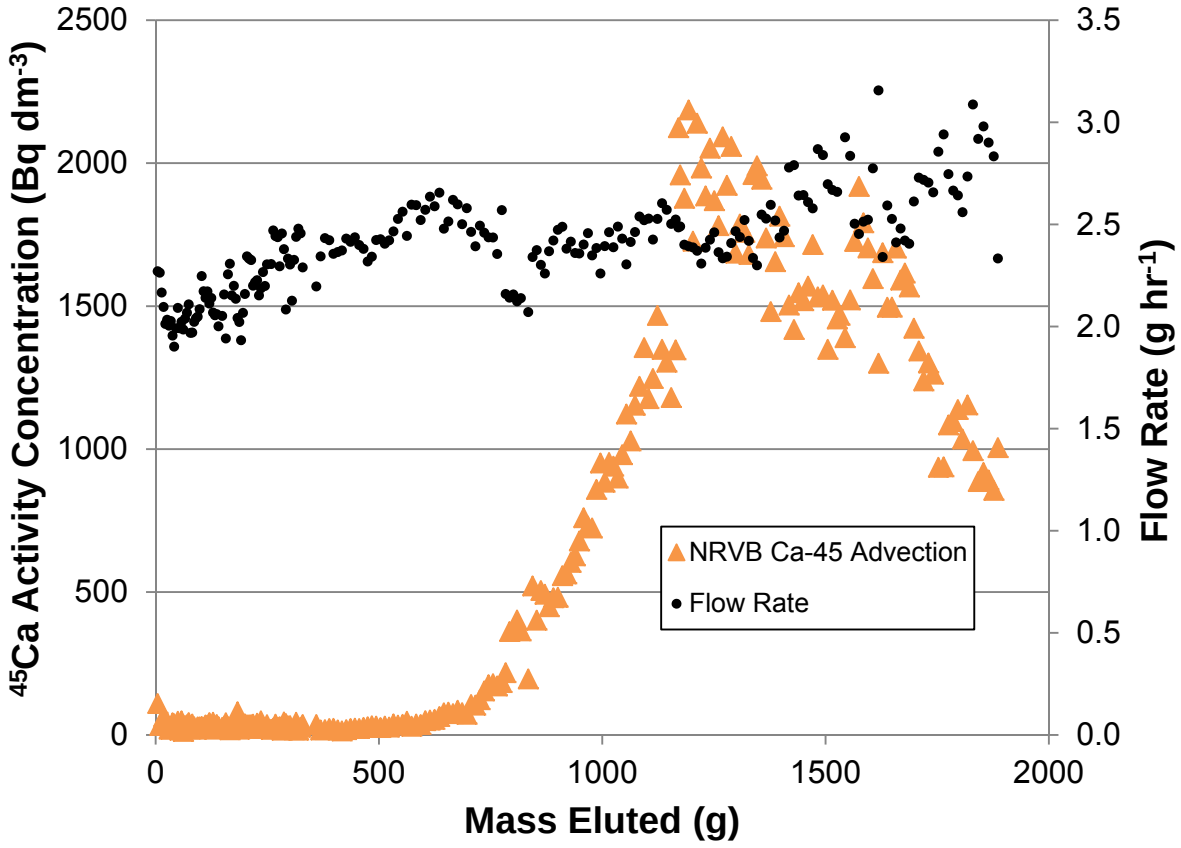

Fig. 14.5 Results of the ^{45}Ca tracer advection experiments using NRVB equilibrated water

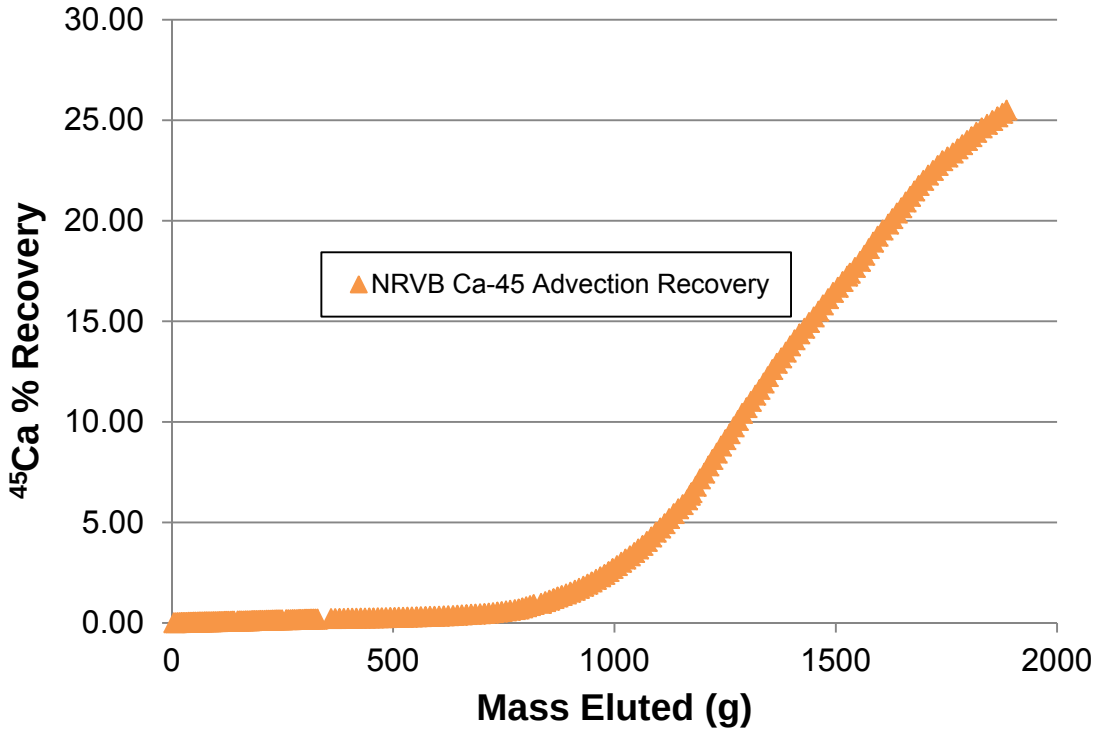

Fig. 14.6 Recovery plot the ^{45}Ca tracer advection experiments using NRVB equilibrated water

Initial breakthrough of the tracer occurred after approximately 500 g of NRVB equilibrated water had eluted. This was followed by a steep rise in concentration initially maximising at ~2200 Bq dm^{-3}, followed by an erratic, general decrease in concentration with second maximum of 1900 Bq dm^{-3} at 1600 g eluted. The eluted volumes prior to breakthrough were over 10 times higher than the equivalent experiment using ^{90}Sr tracer (see section 13.6.1) and over 50 times higher than the equivalent HTO experiment (see section 10.4.1) undertaken in this research. The overall impression is one of steep and steady rise in concentration followed by a much gentler decrease and elongated tail slowly returning to concentrations near background. The experiment was stopped early to leave enough activity in the NRVB to produce an autoradiograph. The recovery plot, which was produced using the lower decayed inventory, estimated at the end of the experiment, shows that more than 70% of the tracer should have remained in the NRVB matrix. The NRVB cylinder was removed from the cell dried and sectioned for autoradiography.

The high and erratic flow rate was a feature of the experiment and this occurred even though the driving pressure was constant throughout at 40-42 psi. The higher flow rate (2 - 3 g hr^{-1}) was used because the diffusion experiments indicated that movement of the tracer through the NRVB would be slower than the other elements under investigation.

14.4.2 ^{45}Ca tracer advection using CDP solution

The experimental procedure, including a 3 day “run in” for the NRVB cylinder was identical to that used in 14.2.1 above. The only exception being that the initial injection volume was 90 µL because 136 days had elapsed since the previous ^{45}Ca tracer advection experiment and the same tracer stock solution was used. Thus the injection contained ~6700 Bq or ~402000 d min^{-1} of ^{45}Ca. The experiment ran until ~1500 g of CDP solution had been eluted. The evaporation of the eluted mass was corrected for by comparison with a weighed water blank left in the sample collector for the duration of the experiment. All the eluent was collected and analysed for ^{45}Ca. No ^{45}Ca tracer was found in any of the samples. The experiment was stopped at approximately 1500 g of CDP solution eluted, which was the point where the maximum concentrations of ^{45}Ca were being eluted during the equivalent NRVB equilibrated water advection. The flow rates recorded throughout the experiment are

presented on fig 14.7. It was not possible to maintain a steady flow rate or driving pressure. The experiment started with a stable flow rate of ~1 g hr^{-1}, but the pressure was increased from 32 to 40 psi increase flow, this worked initially but the flow rate soon started to fall again. The pressure was increased again on two further occasions (at ~550 g and 1100 g) to a final reading of 50 psi, where concern about possible fracturing of the NRVB cylinder prevented further progress. The NRVB cylinder was removed from the cell dried and sectioned for autoradiography.

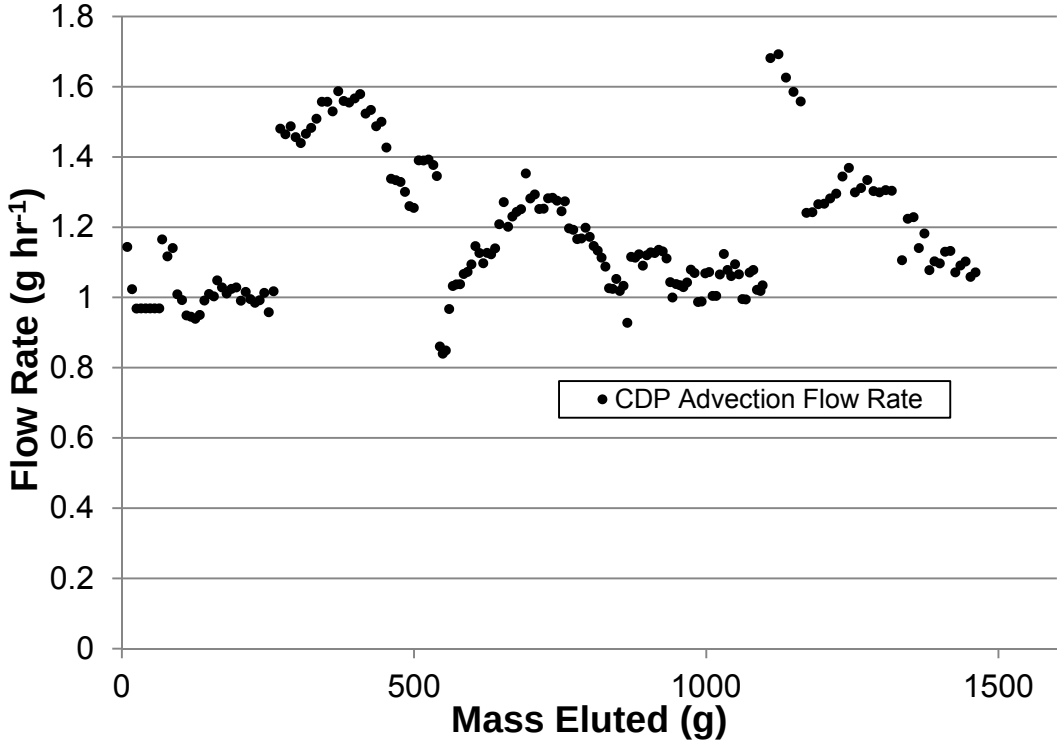

Fig 14.7 Flow rates recorded during the ^{45}Ca tracer advection experiments using CDP solution

14.5 Autoradiographs from the ^{45}Ca NRVB Tracer Advection Experiments

The two autoradiographs in figs. 14.8 to 14.9 below were produced using Fuji BAS MP 20 cm x 25cm autoradiography image plates with an exposure duration of 5 days. The plates were developed at BGS, Nottingham. The enhancements and intensity plots were produced using ImageJ software. Unenhanced images have not been presented. Modelling clay was used to shield radiation from the central core to provide a better visualisation of the migrating isotope. Shielded and unshielded images are presented for the experiment with CDP solution.

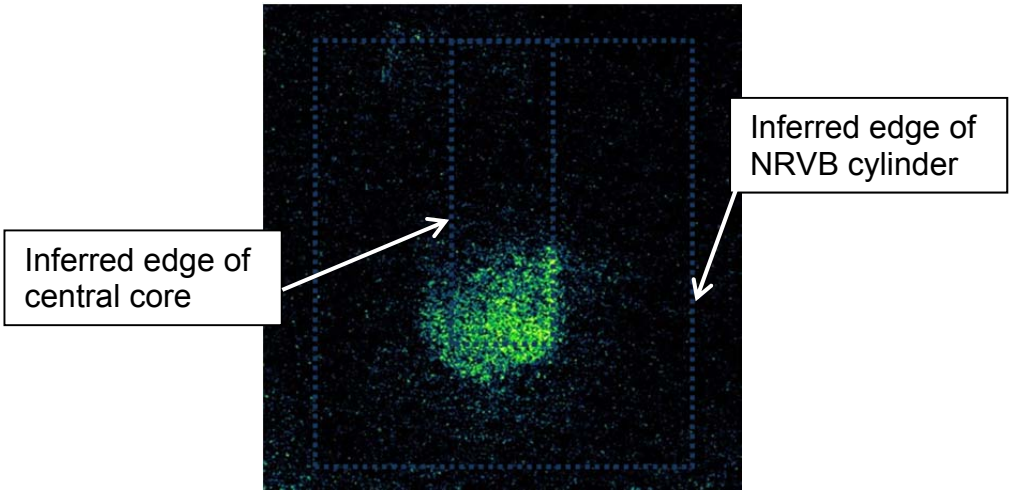

Fig. 14.8 Enhanced autoradiograph from the ^{45}Ca tracer advection experiment using NRVB equilibrated water

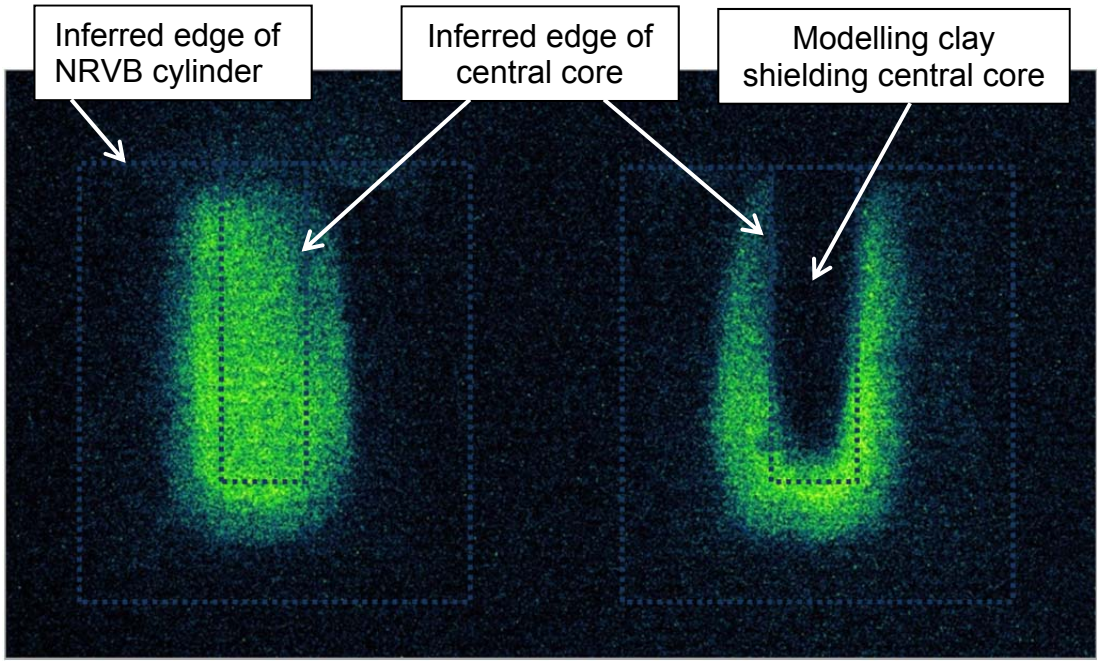

Fig. 14.9 Enhanced autoradiographs with central core (a) unshielded and (b) shielded from the ^{45}Ca tracer advection experiment using CDP solution

Commentary

The enhanced autoradiograph in figs.14.8 shows a residual amount of the tracer in the central core, the experimental data suggested that the residual amount could be as high as 70% of the original inventory injected (after decay correction). It is not clear why there is so little evidence of the tracer in the main body of the NRVB cylinder, or why it “sticks” to the central core and not anywhere else. It can also be implied that this is occurring to all of the Ca present in the advecting solution. A similar phenomenon was observed in the NRVB equilibrated water diffusion

experiments (see section 14.3) where the autoradiograph shows deposition of a significant proportion of the ^{45}Ca addition on the side walls of the central core.

The tracer must have been advected through the cylinder to reach the sample collector and as there is no evidence of leakage around the sides, the images suggest that the inner surface of the central core behaved differently to the main body of the NRVB. In addition the tracer was also only present in the lower part of the central core similar to the finding in the iodine advection experiment (see section 12.9).

The autoradiographs from the CDP solution advection experiment shown in fig. 14.9 are in line with expectations from the experimental results which showed that none of the tracer was eluted from the NRVB cylinder. It is clear from the images that the tracer is moving from the central core and this is more apparent when the central core is shielded with modelling clay. The concentration gradient is visible and there is still a significant signal from the central core where tracer distribution appears to be homogeneous. There is no indication of how much tracer would finally be left in the central core were the experiment to have been extended.

It was noted that the analytical data acquired during “the run in” period showed that sulphate was removed from the eluent. The influent sulphate concentration was $5.14x10^{-3}$ mol dm^{-3} and the effluent concentration was $1.7x10^{-4}$ mol dm^{-3}.(see table 9.2 in section 9.2). The possibility of gypsum ($CaSO_4.2H_2O$) precipitation was examined briefly using the Chess code and user interface JChess.[171] This suggested that gypsum would not form and that portlandite and the sulphate containing mineral, ettringite ($Ca_6Al_2(SO_4)_3(OH)_{12}\cdot 26H_2O$) were likely to precipitate and subsequently redissolve. However, ettringite is known to form in the OPC system as a result of the presence and reaction of calcium sulphate and calcium aluminate. [34] This suggests that the JChess equilibrium model was not suitable. Indeed the JChess model was used originally only as an indicator of possible outcomes and was not pursued further as advective systems are clearly not at equilibrium.

The precipitation of organic salts also remains a possibility. If precipitation in the NRVB was occurring a steady fall in flow rate could be anticipated as porosity was filled with the precipitate. This may have been why it was necessary to keep increasing pressure to maintain the flow rate in the CDP advection experiment. In contrast, a steady rise in flow rate was observed throughout the NRVB equilibrated

water advection experiment suggesting that the organic material in the CDP solution was responsible the precipitation.

These advection experiments have started to provide information on the behaviour and fate of Ca isotopes in Ca rich systems. It is clear that more focussed versions of the experiments are required. In particular the advection experiments with CDP solution need to be run over a much longer duration or to the point where a flow cannot be sustained. This should ensure that sufficient precipitate is present to be able to examine it under the SEM and determine the morphology and composition.

15.0 Nickel

15.1 Background

The main nickel isotopes of interest are ^{59}Ni and ^{63}Ni. They are components of the UK radioactive waste inventory and are mentioned in the latest estimate at 01/04/2010, [26] table 15.1 below reproduces the relevant activities.

Isotope	HLW	ILW	LLW	units
^{59}Ni	3.0	$5.2x10^{3}$	$5.7x10^{-3}$	T Bq
^{63}Ni	$3.4x10^{2}$	$5.6x10^{5}$	$7.9x10^{-1}$	T Bq

Table 15.1 ^{59}Ni and ^{63}Ni in the UK waste inventory at 01/04/2010

The activities in the table above are significant; ^{59}Ni is a long lived isotope (half-life, ~76000 years) and will persist in the inventory into the long term. ^{63}Ni is relatively short lived (half-life, ~100 years) but a large amount is present in the inventory. Were its presence in the environment around a GDF to be detected it would be diagnostic of an early containment failure. [147]

^{59}Ni and ^{63}Ni are present nuclear industry waste as part of the steel and other alloys used in the fuel and plant hardware. ^{63}Ni is initially more prevalent than ^{59}Ni.

When ^{235}U fissions it can split asymmetrically into two large fragments with mass numbers between 90 and 140 these fissions also emit neutrons. The neutrons can cause additional fissions to sustain the chain reaction in the reactor, escape from the reactor, or irradiate nearby materials. Reactor components are constructed from a variety of alloys and steels that contain chromium, manganese, nickel, iron, and cobalt. When the most abundant isotopes of Ni (^{58}Ni and ^{62}Ni) absorb these neutrons the radioisotopes ^{59}Ni and ^{63}Ni are formed along with a range of activation products.[158]

^{59}Ni decays by electron capture to the ground state isotope ^{59}Co.

$$^{59}_{28}Ni + {}^{0}_{-1}e \rightarrow {}^{59}_{27}Co + \bar{\nu}_e$$

There are no gamma emissions associated with this transition but the subsequent rearrangement of electrons gives rise to x-ray and auger electron emissions. There is also a low probability (10^{-8}) positron emission.

$$^{59}_{28}Ni \rightarrow {}^{59}_{27}Co + {}^{0}_{+1}e + \nu_e$$

The weak emissions associated with ^{59}Ni make it unsuitable for use in the diffusion and advection experiments and consequently ^{63}Ni has been used. ^{63}Ni decays by beta electron emission with a maximum energy of 0.67 MeV and an average energy of 0.17 MeV to the ground state isotope ^{63}Cu, according to the equation below.

$$^{63}_{28}Ni \rightarrow {}^{63}_{29}Cu + {}^{0}_{-1}e + \bar{\nu}_e$$

The specific activity of ^{63}Ni is 2.1x10^{12} Bq g^{-1}, it is readily and efficiently detected and determined by liquid scintillation counting.[158]

Ni is known to precipitate at high pH and it was anticipated that experimental timescales for the diffusion experiments would be in the range of months to years.

If it enters the body ^{63}Ni presents a health hazard from the emitted beta particles. The main health concern is the increased likelihood of cancer with the large bowel being the primary target organ.

Ni has some unusual chemical properties including its ability to form square planar complexes in aqueous solutions.[172] It is present in the raw materials for producing grouts and concretes, it is more mobile than Am, U and Th and less mobile than Cs and I in high pH environments where it precipitates as the very low solubility $Ni(OH)_2$ salt.

Ni also exhibits chemical toxicity. The most common effect is an allergic reaction of the skin often caused by the presence of Ni in jewellery. There are recognised occupational issues for Ni workers that include asthma, skin lesions and gastrointestinal disorders. [173]

The experiments undertaken were as follows:

- Diffusion with NRVB equilibrated water using ^{63}Ni tracer and $NiCl_2$ carrier.
- Diffusion with CDP solution with ^{63}Ni tracer and $NiCl_2$ carrier.
- Advection with CDP solution using ^{63}Ni tracer only.

Solubility experiments were also undertaken as part of the chemical containment demonstration project and these indicated that Ni solubility could increase by almost two orders of magnitude in the presence of CDP solution (from $7x10^{-7}$ to $4x10^{-4}$ mol dm^{-3}).[134] As noted previously the elevated temperature used in the manufacture of the CDP solution is likely to be at least in part responsible for the higher concentrations of many species observed including Ni. However, the increase in concentration of Ni was particularly marked implying that mobility could be significantly enhanced in the presence of CDP.

15.2 ^{63}Ni Diffusion Experiments

15.2.1 Additional information for the ^{63}Ni diffusion experiments

The NRVB equilibrated water and CDP solution ^{63}Ni diffusion experiments were set up with a I cm^3 deionised water addition containing 300200 Bq of ^{63}Ni and $NiCl_2.6H_20$ equivalent to $7.3x10^{-4}$ g of Ni (i.e. 1Bq ^{63}Ni counted is equal to $2.4x10^{-9}$ g of non active Ni, assuming the mass of ^{63}Ni added to be insignificant). The NRVB cylinders were topped up with the respective solutions, sealed and submerged in the same manner detailed in previous sections. Deionised water was used to minimise the possibility of precipitation in the tubes used to prepare the addition.

15.2.2 Results for the diffusion of ^{63}Ni tracer with $NiCl_2$ carrier using NRVB equilibrated water

The duplicate experiments have been running for 2 years and no migration of Ni from the blocks into the surrounding solution has been observed.

The decision was taken to stop one of the duplicate experiments at 2 years to investigate and potentially produce an autoradiograph.

When the seal was broken the liquid along with any free solid material inside the central core was collected and counted for ^{63}Ni after acidification with hydrochloric acid to dissolve the solid. Over 80% of the initial addition was present. Unfortunately it was not possible to determine how much was present in the liquid and solid separately. This can be addressed when the second duplicate is opened and analysed.

The cylinder was sectioned using a masonry saw and an autoradiograph produced which is shown below adjacent to a photograph, as fig. 15.1.

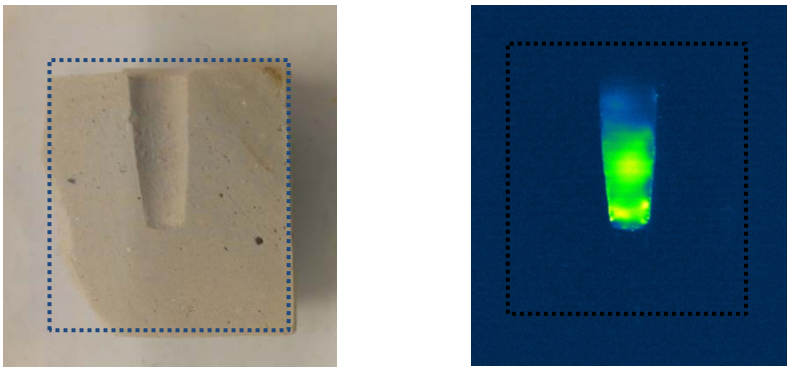

Fig. 15.1 Photograph and autoradiograph of Ni diffusion using NRVB equilibrated water

It is clear from the images in fig. 15.1 that no migration of Ni into the NRVB matrix has occurred during the 2 year period. The edge of the inner core is sharply defined and mirrors the outline seen on the photograph of the same cylinder.

15.2.3 Results for the diffusion of ^{63}Ni tracer with $NiCl_2$ carrier using CDP solution

The results of the ^{63}Ni tracer with $NiCl_2$ carrier are presented below as figs. 15.2 and 15.3; the data is also presented as table 15.2 in appendix 1. The early data plot has not been presented as the early data are clear. The divergence in the duplicate experiments also necessitated presenting both datasets instead of the average with error bars. A brief commentary on the results is also provided.

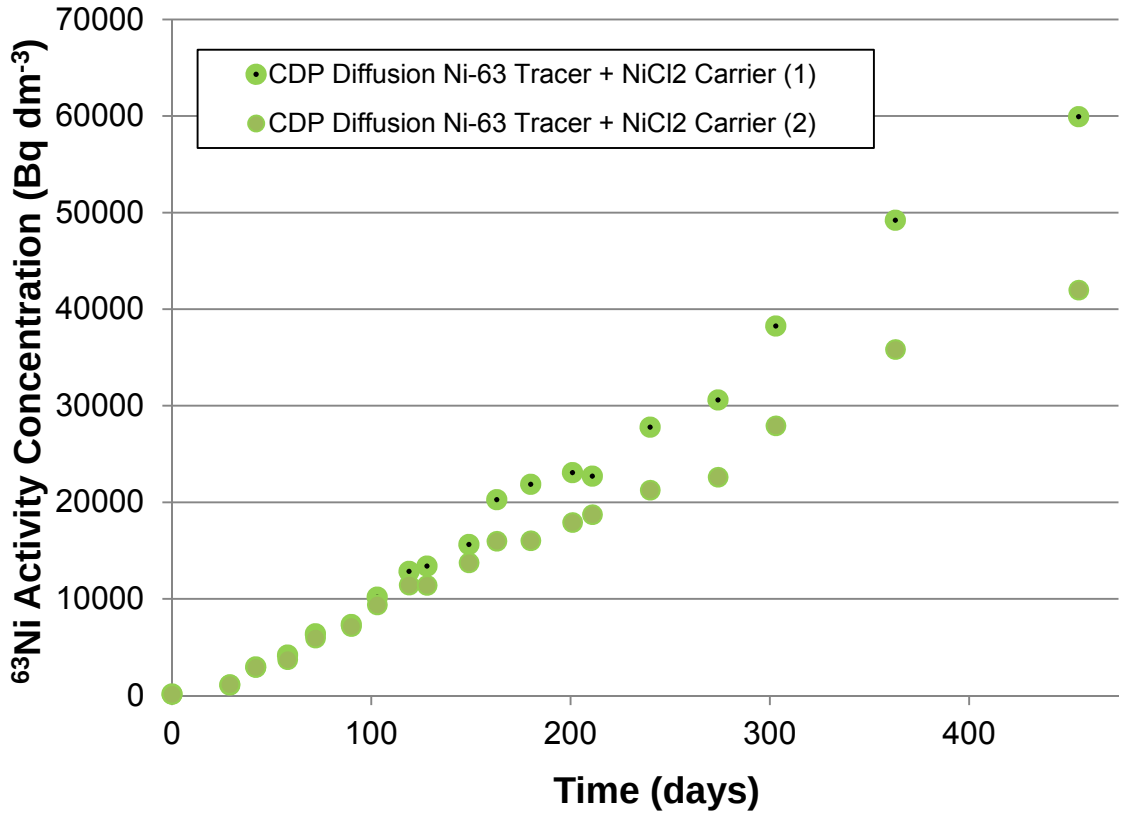

Fig. 15.2 Results for the diffusion of ^{63}Ni tracer with $NiCl_2$ carrier using CDP solution

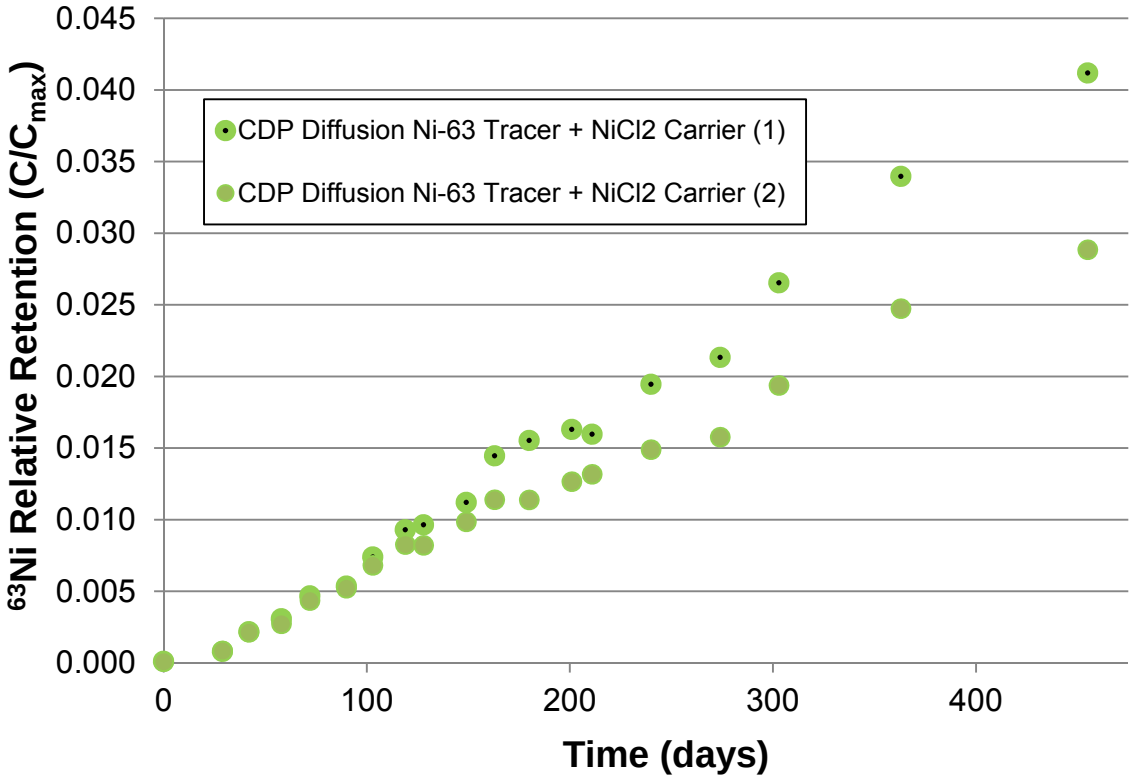

Fig. 15.3 Relative retention plot for the diffusion of ^{63}Ni tracer with $NiCl_2$ carrier using CDP solution

Commentary

Breakthrough of ^{63}Ni commenced at approximately 29 days, followed by a linear increase in concentration continuing to the current position of 455 days, this is clearly shown on fig 15.3. The divergence of the results from the duplicate experiments is marked and has not been observed to the same extent in any off the previous experiments (the gradient ionic strength Sr experiment may be an exception). The relative retention plot (where initially C_{max} = 80060 d min^{-1}) indicates that ~95% of the tracer was retained on the NRVB cylinder i.e. less than 5% of the tracer was in solution. This suggests that the experiment is continuing to develop and consequently neither duplicate has been sacrificed to produce an autoradiograph. The effect of the steadily increasing C_{max} value is present but not obvious.

15.3 Ni in the Mixed Element Diffusion Experiments

15.3.1 Additional information relevant to the mixed element diffusion experiments

The mixed element diffusion experiments were set up to investigate the effect on the diffusion rates of Cs, I, U, Th. Eu and Ni when all were present. The experiments, eleven of each type (NRVB equilibrated water and CDP solution) were the first to be undertaken using the radial approach. Sufficient $CsNO_3$ and KI were added to produce a 10^{-3} mol dm^{-3} solution in the event of complete equilibration. In addition precipitates from a neutralised solution containing $UO_2(NO_3)_2.6H_2O$, $Th(NO_3)_4.4H_2O$, $EuCl_3.6H_2O$ and $NiCl_2.6H_2O$ were mixed with the Cs and I solutions to produce a slurry which was added to the central cores of the NRVB cylinders. The NRVB cylinders used for the CDP experiments were equilibrated in a CDP solution for 30 days prior to commencement. The Ni determinations were performed by ICP-MS.

The Ni data from the eleven replicates of the NRVB equilibrated water and CDP solution diffusion experiments are reproduced below as figs. 15.4 and 15.5.

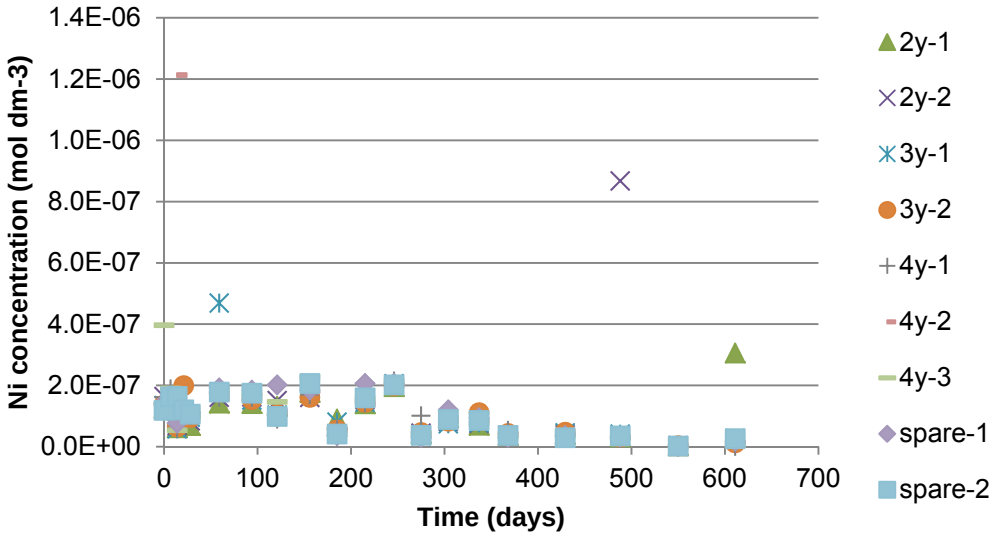

Fig. 15.4 Ni Raw data for the mixed element diffusion experiments in NRVB equilibrated water [134]

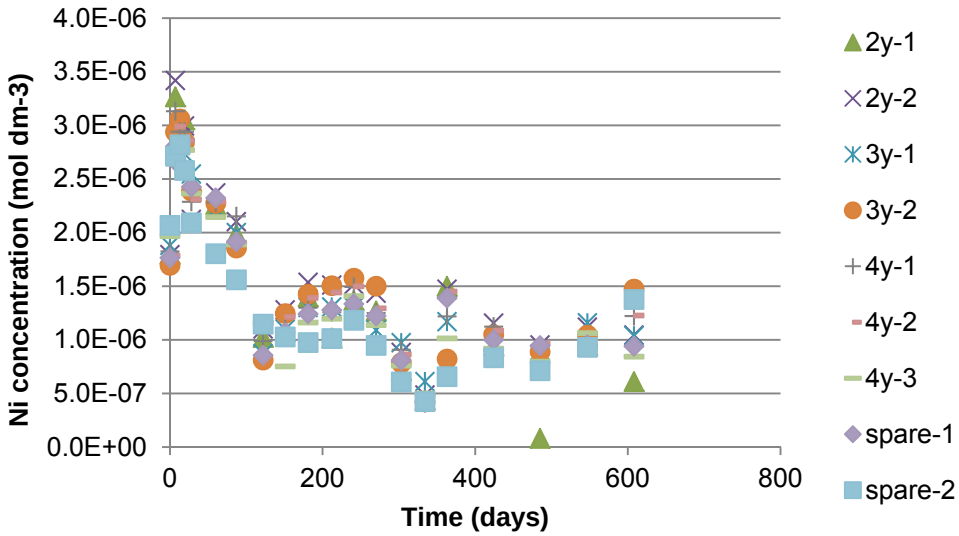

Fig. 15.5 Ni raw data for the mixed element diffusion experiments in CDP solution [134]

Commentary

The behaviour seen in the NRVB equilibrated water mixed element diffusion experiment has been the same as the corresponding single element ^{63}Ni tracer experiment i.e. there is no evidence of migration of Ni through the NRVB cylinder.

However there is a contrast between the single and mixed element experiments in CDP solution. The mixed element Ni results show a clear decrease in concentration with time, suggesting that Ni is migrating back into the NRVB cylinder or potentially

precipitating on the outside surface. The Ni concentration in the multi element CDP diffusion experiment does not approach $4x10^{-4}$ mol dm^{-3} which was seen in the solubility experiments. The pre-equilibration time was only 30 days and so it is possible that the cylinders had not stabilised prior to the start of the experiment. However, the start concentration is in the range seen in CDP solutions at ~$3x10^{-6}$ mol dm^{-3} or ~0.18 ppm, (see table 9.1 for further information). The Ni concentrations reach a low of ~$5.0x10^{-7}$ mol dm^{-3} and then appear to begin rising again. There is no evidence of the steady linear rise in concentration seen in the corresponding single element CDP diffusion experiment.

As mentioned previously it is important to be aware that these experiments were very early attempts at the technique and modifications have been on-going, in particular handling time outside the glove box and dosing of the central cores have been speeded up and subject to more control. The slurry placed in the central core has not been fully characterised but it is a complex mixture of salts that could be affecting precipitation, solubility and subsequent migration.

15.4 ^{63}Ni Tracer Advection with CDP Solution

The single element diffusion experiment that was carried out in the presence of CDP, suggested that it may be possible to acquire data on the effect of CDP on Ni migration relatively quickly from an advection experiment.

15.4.1 ^{63}Ni tracer advection using NRVB equilibrated water

The experimental procedure, including a 3 day “run in” for the NRVB cylinder was identical to that used in the HTO advection experiments (see section 10.4). The only exception being that the initial injection volume was 100 µL. The injection contained 20000 Bq or 1200000 d min^{-1} of ^{63}Ni. All the eluent was collected and analysed for ^{63}Ni. The evaporation of the eluted mass was corrected for by comparison with a weighed water blank left in the sample collector for the duration of the experiment. All ^{63}Ni determinations were performed by liquid scintillation counting using Goldstar multi-purpose liquid scintillation cocktail and a Packard 2100TR liquid scintillation counter

The experiment was successful but maintaining a steady driving pressure and flow rate remained issues.

The results are presented separately as eluted mass and ^{63}Ni recovery plots on figs. 15.6 and 15.7 and the data are presented as table 15.4 in appendix 1. A brief commentary on the individual plots is also included.

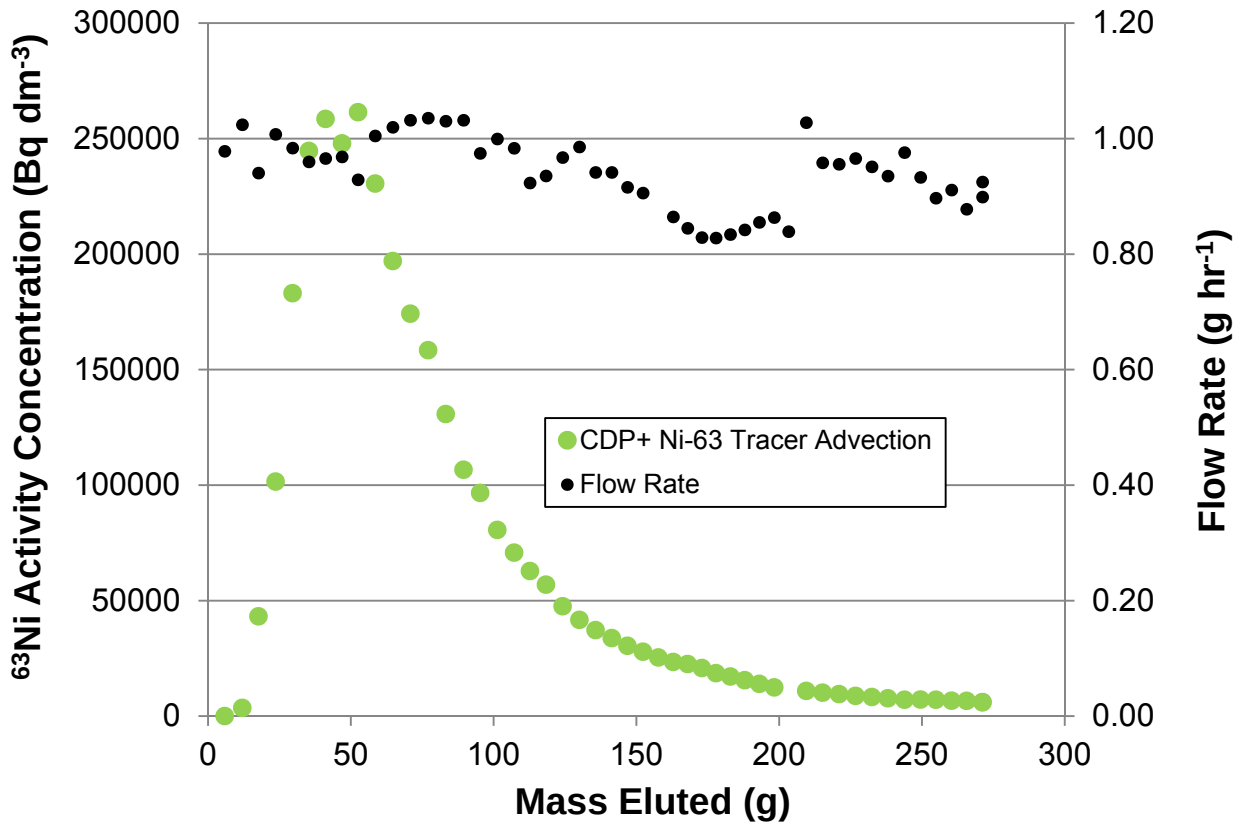

Fig. 15.6 Results of the ^{63}Ni tracer advection experiments using CDP solution

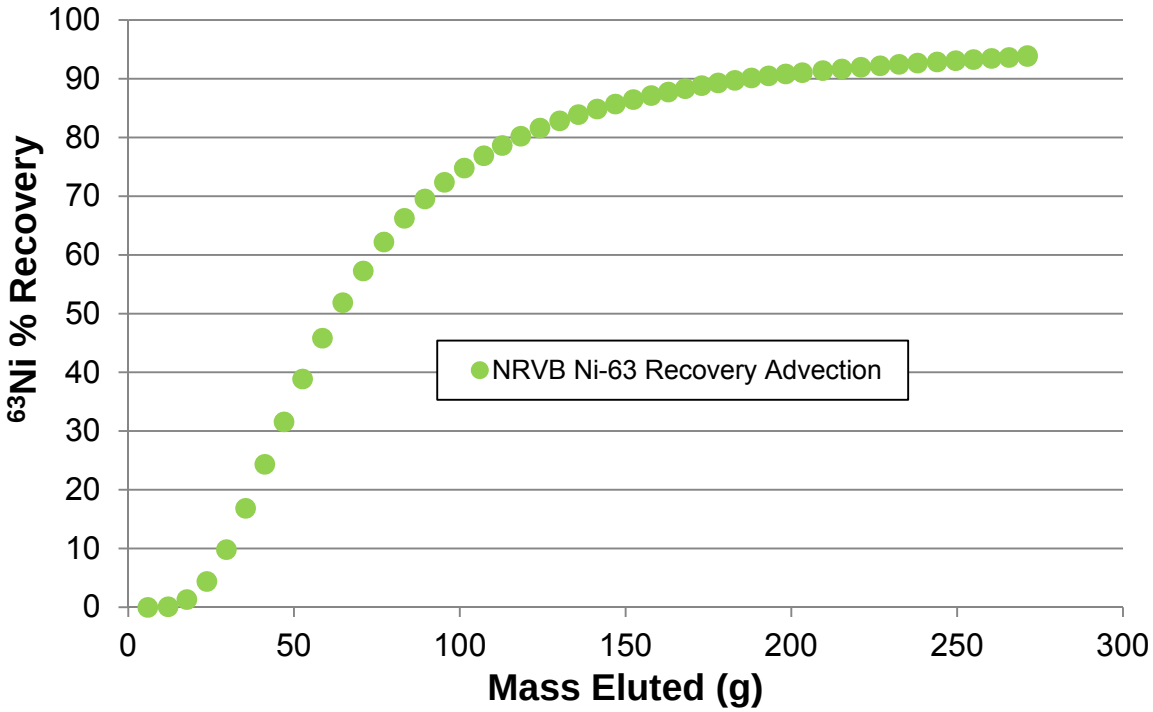

Fig. 15.7 Recovery plot for the ^{63}Ni tracer advection experiments using CDP solution

Commentary

Initial breakthrough of the tracer occurred after approximately 18 g of CDP solution had eluted. This was followed by a steep rise in concentration peaking at ~260000 Bq dm^{-3}, followed by a steady fall in concentration and elongated tail slowly returning to concentrations approaching background. The elution profile is very similar to the one observed for HTO. The steady almost cyclical fall in flow rate throughout was a feature of the experiment and this occurred even though the driving pressure was kept constant at 21 psi. There is a short discontinuity at ~200g eluted that corresponds with a refilling of the eluent reservoir. The tracer recovery plot indicates that almost ~95% of the ^{63}Ni was recovered. The NRVB cylinder was not recovered for autoradiography because the very rapid elution of the tracer caused suspicion that the system had failed in some way. Consequently the system was checked by using a ^{90}Sr tracer injection onto the same NRVB cylinder. The system was found to be functioning correctly.

15.5 Discussion of the Suite of ^{63}Ni Experiments

The ^{63}Ni experiments have demonstrated that the increase in solubility of Ni observed in the presence of CDP translates into an increase in mobility in the diffusion experiments. The effect is very noticeable when compared to the equivalent

experiment in the absence of CDP. This has the potential to affect the security of GDFs accepting cellulose containing waste.

There is a suggestion that the migration of Ni is controlled solely by solubility, this is supported by a previous study [174] and the tracer only (i.e. very low concentration) advection in the presence of CDP which generates results similar to HTO. Other studies [175] [176] note the presence of a Ni-Al layered double hydroxide (LDH) phase which continues to form (provided an Al source is available) consuming $\alpha Ni(OH)_2$ as hydration proceeds. The production of this Ni-Al LDH phase could be a factor in the lack of Ni mobility seen in the diffusion experiments without CDP. Alternatively, it could be interpreted as the CDP hindering the production of the Ni-Al LDH phase and not a simple increase in solubility due to complexation. It should be noted that the concentration of Ni used in the published work is much higher (5000 ppm) than that used in the present work and consequently the comparison may not be appropriate.

The diffusion experiments with CDP solution will need to run to completion (or at least stability) and the autoradiographs produced before any further experiments with a range of Ni concentrations, can be scoped.

16.0 Ongoing Experiments

There are a number of diffusion experiments underway that have yet to show any evidence of migration of the isotope into the external solution. The majority of these experiments have been running over 2 years and consequently can be interpreted as positive results in terms of chemical containment.

The experiments are listed in table 16.1 below:

Element	Cement Matrix	Organic
^{241}Am	NRVB	
^{241}Am	3:1 PFA:OPC	
^{152}Eu	NRVB	
^{152}Eu	NRVB	CDP
^{152}Eu	3:1 PFA:OPC	
U	NRVB	
U	NRVB	CDP
Th	NRVB	
Th	NRVB	CDP
^{90}Sr	3:1 PFA:OPC	
^{45}Ca	3:1 PFA:OPC	

Table 16.1 Ongoing diffusion experiments

A significant proportion of the experiments already described in sections 10 – 15 remain ongoing although many are now only single samples because one of the duplicates has been sacrificed for autoradiography.

In addtion, diffusion experiments with ^{75}Se (half-life 120 days [158]) have also been started. The Se experiments and indeed the ^{45}Ca; 3:1 PFA:OPC ones will not be able to progress into the long term due to the relatively short half-lives.

The PFA containing grout is interesting because it appears to be containing the divalent ions Sr and Ca which were found to be mobile in the NRVB experiments. There is a need to undertake Cs and I diffusion experiments on the PFA grout.

Table 16.1 provides some evidence that the higher valency elements are contained more effectively.

17.0 Conclusions

This research has demonstrated that relatively simple radial diffusion and advection techniques can be used to gather good quaity data relevant to the understanding of the mobility and migration potential of a series of radionuclides.

Radial techniques are unusual in the relevant literature but they have proven to be robust and reproducible in this research. The diffusion results in particular have been very good. The radial geometry allowed the use of a simple 1D GoldSim transport model that successfully produced diffusivities and partition coefficients comparable with literature values (see table 17.1).

Species	Reference		D_e (m^2 s^{-1})	K_d (m^3 kg^{-1})
HTO	This work		0.75×10^{-10}	0.2×10^{-3} (advective flow)
	Tits et al. (2003)		$(2.88 - 3.00)\times10^{-10}$	$(0.808-0.817)\times10^{-3}$
	Bucur et al. (2010)		2.2×10^{-11}; 4.2×10^{-11}	
	Nirex (1994)		$3.7\text{-}4.8\times10^{-10}$	
Cs	This work	No-CDP-tracer	2.0×10^{-10} $(1.3 - 2.8)\times10^{-10}$	2.3×10^{-3} $(2.0 - 3.0)\times10^{-3}$
		No-CDP-carrier	0.9×10^{-10} $(0.7 - 1.2)\times10^{-10}$	0.2×10^{-3} $(0.1 - 0.3)\times10^{-3}$
		CDP-tracer	2.8×10^{-10} $(2.3 - 3.8)\times10^{-10}$	0.7×10^{-3} $(0.3 - 1.0)\times10^{-3}$
		CDP-carrier	1.1×10^{-10} $(0.7 - 1.2)\times10^{-10}$	0.2×10^{-3} $(0 - 0.3)\times10^{-3}$
	Nirex (1994)		1.0×10^{-10}	
	Andersson et al.(1981)		1.7×10^{-14} – 8.1×10^{-14}	
	Atkinson and Nickerson (1984)		1.8×10^{-15} - 6.0×10^{-11}	
	Johnston and Wilmot (1992)		2.6×10^{-13} – 1.1×10^{-12}	
	Sarott et al. (1992)		1.4×10^{-10} - 1.9×10^{-10};	5×10^{-3}; 6×10^{-3}
	Jakob et al. (1999)		11.2×10^{-11} 15.7×10^{-11}	0.61×10^{-3}; 0.84×10^{-3}
	El-Kamash et al. (2002)		5.4×10^{-8} – 4.6×10^{-7}	-
	Plecas (2003)		9.3×10^{-15} – 1×10^{-13}	1.7×10^{-3} – 18.3×10^{-3}
	Bucur et al. (2010)		2.16×10^{-14} 1.8×10^{-12}	4.8×10^{-3} 9.6×10^{-3}
I	This work	No-CDP-carrier	2.5×10^{-10} $(1.8 - 3.3)\times10^{-10}$	3.4×10^{-3} $(3.2 - 3.8)\times10^{-3}$
		CDP-carrier	3.8×10^{-10} $(2.6 - 4.0)\times10^{-10}$	1.7×10^{-3} $(1.6 - 1.9)\times10^{-3}$
	Nirex (1994)		2.6×10^{-10}	
	Andersson et al.(1981)		10^{-14}	
	Atkinson and Nickerson (1984)		1.6×10^{-10}- 2.5×10^{-13}	
	Sarott et al. (1992)		2.2×10^{-11} - 3.0×10^{-11}	
	Jakob et al. (1999)		$(2.22 \pm 0.06)\times10^{-11}$	1×10^{-3}
Sr	This work	No-CDP-tracer	4.4×10^{-11} $(3.5 - 5.4)\times10^{-10}$	3.0×10^{-3} $(2.8 - 3.1)\times10^{-3}$
		No-CDP-carrier	4.7×10^{-10} $(3.5 - 5.4)\times10^{-10}$	2.4×10^{-3} $(2.3 - 2.6)\times10^{-3}$
		CDP-tracer	4.4×10^{-10} $(4.3 - 4.5)\times10^{-10}$	4.7×10^{-3} $(4.6 - 5.1)\times10^{-3}$
		CDP-carrier	5.9×10^{-10} $(5.6 - 6.1)\times10^{-10}$	3.1×10^{-3} $(2.8 - 3.3)\times10^{-3}$
	Wieland et al (2008)			$0.08\text{-}0.12\times10^{-3}$
	Savage and Stenhouse (2002)			$1.0\text{-}5.0\times10^{-3}$
	El-Kamash et al. (2006)		0.54×10^{-10}	

Table 17.1 Effective Diffusivity (D_e) and partition ratios (K_d) derived from the models in comparison with literature values

The table shows that the range of diffusivity values reported for cementitious media is significant and extends over eight orders of magnitude. The majority of the diffusivity values in the table are for OPC or hardened cement pastes which exhibit

lower diffusivity than the highly porous NRVB. However, there is good agreement with the values published by Nirex when developing this backfill material. The literature values also illustrate the lack of consistency in the reporting of diffusivity e.g. including or excluding tortuosity or capacity factors (this lack of consistency is itself the subject of technical discussion [177]).

The relevant K_d values are subject to much lower variation both in the literature and the results produced in the course of this work.

These dynamic experiments were aimed at demonstrating the effectiveness of chemical containment and arriving at a detailed understanding of the mechanisms by which CDP affects migration was not part of this work.

It has been possible to observe a wide range of behaviour from the highly mobile monovalent ions (Cs, I), through the lower mobility divalent ions (Sr, Ca, Ni) to the apparent immobilisation of the trivalent Eu, Am, tetravalent Th and hexavalent U.

The diffusion experiments involving the higher valency elements are being maintained and regular observations and determinations of the mineral phases present and morphological changes occurring have been scheduled over the next few years.

Differences in behaviour dependent on concentration have also been observed with the tracer only experiments behaving differently to those with tracer and non active carrier. Radionuclide uptake is also different i.e. K_d varies with concentration; this can be seen clearly in the Cs and Sr diffusion experiments (and I, although the relevant experiment could not be completed) where higher K_d values have been indicated by the models i.e proportionately more of the radionuclide is retained at very low concentration. This suggests NRVB has a small but finite capacity to retain some radionuclides irreversibly.

The combination of diffusivity and partition can be discerned; in particular it is possible to see that diffusivities of the monovalent ions (Cs and I) are similar or higher than that of HTO and that partition is the main contributor to mobility. This result contrasts with the Nirex literature values where HTO exhibits the highest diffusivity. It is also appears that the presence of CDP affects diffusivity and partition at tracer concentrations but only diffusivity at carrier concentrations. It is important to

note that these diffusivity and partition variations occur within one order of magnitude.

The Sr suite of experiments was the most extensive and investigated the competing effects of concentration, CDP and ionic strength. The ^{90}Sr tracer only experiments showed significantly increased uptake of the tracer in the presence of CDP. The Sr carrier experiments demonstrated that concentration will dominate other effects including the presence of CDP and the increased ionic strength associated with the CDP solution. More recent results indicate that increasing ionic strength significantly will dramatically slow the migration of Sr at tracer concentration. This implies that increasing ionic strength can be used to limit diffusivity of Sr which could have consequences for GDF location i.e a hypersaline, high pH environment reduces the migration potential of Sr. There is also some evidence that the gluconate surrogate increases uptake by precipitation and that whilst a tertiary complex (NRVB-Sr-CDP or NRVB- CDP-Sr) is still a possibility it may be more productive to study the NRVB/CDP and NRVB/gluconate systems in more detail.

The ^{45}Ca experiments present an insight into its behaviour in a Ca saturated environment. The diffusion results showed that Ca is mobile in the NRVB system in the absence of a significant concentration gradient. However, a significant proportion of the ^{45}Ca tracer did not not move, appearing to precipitate on the surface of the internal core. The advection experiments produced results and autoradiography supporting the suggestion that precipitation/dissolution is important when CDP are present. JChess was used as a scoping tool and the modelling results indicated that precipitation of portlandite and ettringite was possible but the changing conditions of these dynamic experiments could not be modelled with the programme. Clearly the work on Ca is incomplete and additional experiments need to be undertaken to understand what processes occur when CDP is present (see section 18.0).

In contrast to Ca and Sr the migration of Ni, the third divalent ion to be studied was found to be much faster in the presence of CDP. Indeed, migration had not commenced after two years of the diffusion experiments without CDP. Batch data acquired in a related part of this work indicated an increase in solubility between one and two orders of magnitude was possible. This increase in solubility was found to correspond to increased mobility of Ni suggesting solubility control. This suggestion

was further supported by the advection experiment with CDP where a tracer quantity of ^{63}Ni (i.e well below any solubility limit) was found to be as mobile as HTO. The solubility increase found in the batch experiments occurred in the absence of the NRVB solid and consequently interaction of the CDP and solid in contrast to Sr and Ca, can be discounted as a reason for the increased mobility. Clearly the work on Ni is incomplete and additional experiments at a variety of concentrations need to be undertaken to confirm the details of the solubility control (see section 18.0).

The data generated by the radial method are reproducible and it is hoped that they can be used to provide a more representative basis for performance assessment as the UK GDF programme is developed.

The diffusion technique was demonstrated to be suitable for low strength porous grouts and backfills, producing data in a cost effective manner with no significant management requirements. The method is flexible and could be scaled up (or down) and potentially trialled for other cementitious construction materials. The method is unlikely to be suitable for structural concrete or concretes with large particle size aggregate due to very low diffusivity and difficulty obtaining a representative sample for laboratory scale work.

The advection technique also appeared to be suitable for low strength porous grouts and backfills although the results were not always reproducible. The technique and equipment are still being developed with minor modifications to the injection system and sample collection currently underway. The problems with flow rate and pressure control can almost certainly be addressed by using pumps with constant flow or constant pressure capabilities. It should be appreciated that the flow rates used in the advection experiments were extremely high in relation to what might be experienced by the backfill in the real GDF scenario. Consequently there could be other phenomena which have not yet been considered (e.g mass removal by dissolution and washing out of fines causing an increase of porosity) affecting the way the experiments proceed over time.

Autoradiography proved to be an effective technique for visualising the fate of the radionuclides used in the experiments. It was possible to see when diffusion had been homogeneous and where diffusion gradients were present. Residual activity could clearly be identified in the central cores along with the presence of hotspots in the NRVB matrix and on the outer surface of the cylinders.

The experiments were undertaken on intact samples of the actual materials at the associated high pH values and directly relevant concentrations so the effects seen must be anticipated, to be present for the full scale GDF scenario.

There are areas where better control would have improved the outcome, these include:

Less variability in the solutions used, the CDP solution in particular has significant variabilty between batches, this is also true of the NRVB equilibrated water. Synthetic solutions were considered but it was decided to proceed in a realistic manner with realistic variability to observe the full range of results.

The effect of counter ions has not been considered and these may be important as significant amounts of chloride and nitrate can be present in the isotope solutions when purchased. Effects due to these counter ions were not considered as the concentrations could not be accurately measured in the presence of the radioisotopes.

18.0 Future Work

This research has collected and processed information relevant to the potential for escape and subsequent migration of selected radionuclides from a GDF. It is clear that the research could be expanded to cover a wider range of elements and it is also clear that the diffusion and advection methods that have been developed can provide results quickly for monovalent and divalent ions.

Despite the significant amount of data gathered in the course of this research significant gaps remain. The data that have been gathered also have shortcomings that could be addressed in the future. In particular it should be possible to augment the methods with spectroscopic techniques and electron microscopy to understand the transport process at a more fundamental level.

A number of ideas with the potential to provide meaningful results can be suggested to progress the research, these include:

Fill in the gaps in the current series; in particular the HTO CDP diffusion experiments, the Ca diffusion experiments with CDP solution and the work at varied Ni concentrations needed to confirm that migration in NRVB is solubility controlled.

The diffusion experiment can be modified to eliminate the downward diffusion that was not accounted for in the modelling. The solution would be to drill the central core all the way through the sample and seal both ends. This was not done for the current programme of experiments because during development, the seals were viewed as a weakness and using two for each experiment would double the chance of failure. This hollow cylinder geometry would also make the need to construct a 3D GoldSim model less important.

The Cs advection experiment in the presence of CDP needs to be undertaken as it would provide information about the CDP interaction with NRVB and its effect on the migration of monovalent ions.

Maintain the current long term experiments for further investigation.

To make the simulations more realistic more processes need to be included in the advection models, in particular precipitation and consequent source depletion.

The use of reactive transport models should be explored to simulate thermodynamics and chemical processes.

Full characterisation of the CDP solution and determination of the influence of component(s) of significance, other than ISA, on radionuclide mobility. This would be particularly interesting for the Ni experiments where a radical change in migration behaviour was observed in the presence of the CDP solution.

Investigation of the long term changes in the CDP solution due to exposure to cementitious materials and high pH.

The interaction of the CDP solution with NRVB has been shown to be complex. In particular, the sorption/precipitation of ISA needs to be investigated further by running the advection experiments for longer durations (months to years) and establishing whether precipitation will eventually prevent flow.

The isotope pair $^{82}Sr/^{82}Rb$ (^{82}Rb is a short half-life; 1.27 minutes, positron emitter) could be utilised to visualise the Sr migration if access to suitable PET scanner facilities can be arranged.

Reversibility remains an issue, it could be further investigated by sequential removal of the receiving water and replacement with equilibrated water free from the radionuclide of interest.

The experiments should be repeated, where possible, at sufficently high concentration with non radioactivactive isotopes to facilitate surface characterisation and identification of mineral phases using SEM/EDX and spectroscopic techniques.

The diffusion and advection techniques could be used to assess the effect of other organic materials likely to be used in cementitious media associated with radioactive waste disposal. In particular, NDA is known to be concerned about the effect of super plasticisers, having recently commissioned studies at Loughborough University.

The majority of the work has been undertaken on NRVB (with a few experiments on a PFA packaging grout) and should be widened to include a range of cementitious construction materials including bentonite cements, BFS formulations and shotcrete.

Scaled up experiments should be attempted to ascertain if the same phenomena are observed.

All the experiments have been undertaken in carbon dioxide free conditions and it would be prudent to assess the effect of carbon dioxide better reflecting the potential siting of a GDF in carbonate rich groundwater.

It is possible to artificially age cements [178] [179] by forcing complete carbonation using high pressure carbon dioxide innundation or exposure to supercritical carbon dioxide. Using fully carbonated cementitious media in diffusion and advection experiments could provide insights into performance at timescales exceeding 1000 years.

3D X ray tomography should be used to record the physical nature of the samples at defined time intervals to ascertain what effect, if any, the testing is having on the integrity of the cements.

The techniques could be easily modified to allow interfaces to be studied by casting concentric rings of the media of interest e.g. mimicking the shotcrete to backfill interface likely to be present at the outer edge of the GDF excavation.

The ^{45}Ca experiments could be extended to more conventional cementitious construction materials to track Ca movement under saturated conditions.

19.0 References

1. UK Government White Paper by Defra, BERR and the devolved administrations for Wales and Northern Ireland: *Managing radioactive waste safely: A framework for implementing geological disposal* June 2008.

2. Inspectors Report. Cumbria County Council Appeal by United Kingdom NIREX, APP1H09001M9412470 19. March 1997.

3. Francis, A J, Cather, R, and Crossland, I G, *Development of the Nirex Reference Vault Backfill; report on current status in 1994*, Nirex Science Report S/97/014, UK Nirex Ltd., Harwell, UK, 1997.

4. Colin Knipe's statement accessed at http://www.jpb.co.uk/nirexinquiry/nirex.htm August 2013.

5. House of Lords Committee: *Management of Nuclear Waste, 3rd Report*, Session 1998-1999 (HL Paper 41),

6. Personal opinion based on 25 years working in a technical capacity in the nuclear sector.

7. DEFRA, *Managing Radioactive Waste Safely; Proposals for developing a policy for managing solid radioactive waste in the UK.* 2001

8. DTI White Paper: *Managing the Nuclear Legacy - A strategy for action.* July 2002.

9. Nirex Technical Note: *Site selection and investigations for a deep geological repository, preliminary technical planning in support of the stepwise process*. July 2003.

10. House of Lords Science and Technology Committee - *Second Report, Radioactive Waste Management: a further update.* Accessed August 2013 http://www.publications.parliament.uk/pa/ld200910/ldselect/ldsctech/95/9502.htm.

11. CoRWM "*Long List of Options*" November 2004 accessed at http://www.nda.gov.uk/aboutus/geological-disposal/history.cfm on 21 July 2011.

12. CoRWM, *Managing our Radioactive Waste Safely: CoRWM's Recommendations to Government*, 700, July 2006.

13. Rawles K, *Compensation in radioactive waste management: Ethical issues in the treatment of host communities.* Nirex paper May 2002**.**

14 CoRWM: *Position paper on public and stakeholder engagement.* 2850 Draft 12 February 2011.

15. Geological disposal options: *CoRWM's government advice* July 2006, accessed July 2013 at https://www.gov.uk/government/publications/geological-disposal-options-corwms-government-advice.

16. Current CoRWM membership and management structure can be accessed at https://www.gov.uk/government/organisations/committee-on-radioactive-waste-management/about/our-governance.

17. NDA established April 2005 under the provisions of The Energy Act 2004, Accessed July 2013 at http://www.legislation.gov.uk/ukpga/2004/20/contents.

18. CoRWM, *Review of managing radioactive waste safely: A framework for implementing geological disposal.* (7386, June 2008).

19. W. F. Falck, K F Nilsson. "Geological Disposal of Radioactive Waste: Moving Towards Implementation". Joint Research Centre of the European Commission JRC 45385 October 2009.

20. NDA, *Radioactive Waste Management Directorate Proposed Research and Development Strategy*. 2008

21. Cumbria County Council. *Minutes of a Meeting of the Cabinet held on Wednesday, 30 January 2013 at 10.00 am at The Courts, Carlisle*. Accessed at http://councilportal.cumbria.gov.uk/ieListDocuments.aspx?CId=123&MId=6834&Ver=4 July 2013.

22. Hicks T W, Baldwin T D, Hooker P J, Richardson P J, Chapman N A, McKinley I G, and Neall F B: *Concepts for the Geological Disposal of Intermediate-level Radioactive Waste*, April 2008.

23. Chapman N A, McKinley I G, Hill M D, *The geological disposal of nuclear waste*, (J. Wiley, 1987) ISBN: 0471912492.

24. Savage D: *The Scientific and regulatory basis for the geological disposal of radioactive waste*, (J Wiley 1995) ISBN-10: 047196090X.

25. UK DEFRA, *Guidance on the scope of and exemptions from the radioactive substances legislation in the UK*. Guidance Document September 2011, Version 1.0.

26. *The 2010 UK Radioactive Waste Inventory; Report prepared for the Department of Energy & Climate Change (DECC) and the Nuclear Decommissioning Authority (NDA)* by Pöyry Energy Limited, February 2011 (URN 10D/987 NDA/ST/STY(11) 006).

27. Glaus, M.A., van Loon, L.R., Achatz, S., Chodura, A., Fischer, K., 1999. *Degradation of cellulosic materials under the alkaline conditions of a cementitious repository for low and intermediate level radioactive waste Part I: Identification of degradation products.* Anal. Chim. Acta. 398, 111–122.

28. Chambers, A.V., Williams, S.J. *Parameter value selection for performance assessments: The impact of cellulosic degradation on repository performance*. Serco Assurance Report SA/ENV-0595 2006.

29. Pointeau, I., Coreau, N., Reiller, P.E. *Uptake of anionic radionuclides onto degraded cement pastes and competing effect of organic ligands*. Radiochim.Acta.96, 367-374 2008.

30. Warwick, P., Evans, N., Heath, C. *Effect of experimental method on the solubility of thorium in the presence of cellulose degradation products*. NDA Report LBORO CMNDA2 2012.

31. William M Miller: *Geological disposal of radioactive wastes and natural analogues* (Elsevier 2000) ISBN: 0444542523.

32. NDA News article, February 2011; *Multi-barrier approach is the key to safe disposal of radioactive waste*. Accessed at http://www.nda.gov.uk/news/multi-barrier-approach-key-to-safety.cfm on July 15 2011.

33. Nirex Report No: N/034 *Why a cementitious repository*? June 2001

34. Taylor H F W: *Cement Chemistry* (Thomas Telford 1997, first published 1990).

35. Lea F M, Hewlett P C: *Chemistry of cement and concrete* (Arnold 1998).

36. Taylor H F W; *The chemistry of cement, volume 2*, (Academic Press 1964).

37. Malhotra P, V M Mehta K: *Pozzolanic and cementitious materials*. (Spon Press 1996) ISBN- 2884492119.

38. Magistri, Matteo and Padovani, Davide; *"Chromate Reducing Agents", International Cement Review*, October, 2005 pages 49-56.

39. Spence R D; *Chemistry and microstructure of solidified wasteforms* (Lewis1993) ISBN-10: 0873717481.

40. Nielsen EP, Herfort D, Geiker MR. *Phase equilibria of hydrated portland cement.* Cement and Concrete Research Volume 35, January 2005, pages 109-115.

41. Wesselsky A, Jensen OM. *Synthesis of pure portland cement phases*. Cement and Concrete Research Volume 39, November 2009, pages 973-980.

42. Sun J, Simons S J R; *Experimental investigation of the carbonation of NRVB*. Centre for CO2 Technology, Department of Chemical Engineering, University College London (undated), accessed at http://archivos.labcontrol.cl/wcce8/offline/techsched/manuscripts%5Cqouprm.pdf on 3 August 2011.

43. Freeze R A, Cherry J A; *Groundwater* (Prentice-Hall 1979).

44. Abdullah M. Alshamsi and Hassan D. A. Imran; *Development of a permeability apparatus for concrete and mortar*. Cement and Concrete Research Volume 32, Issue 6, June 2002, Pages 923-929.

45. Personal communication with S Williams of NDA, March 2011 and reference to Nexia Solutions memorandum regarding grout sample preparation from J Borthwick dated August 2007

46. McCarter W J, Crossland I, and Chrisp T M: *Hydration and drying of Nirex Reference Vault Backfill* August 2003.

47. Crank J; *The mathematics of diffusion* (Clarendon Press 1979).

48. 114. L. R. van Loon, J. M. Soler, W. Muller, M. H. Bradbury. *Anisotropic Diffusion in Layered Argillaceous Rocks:* A Case Study with Opalinus Clay Environ. Sci. Technol. 2004, 38, 5721-5728.

49. van Brakel, J., Heertjes, P. M. (1974): *Analysis of diffusion in macroporous media in terms of a porosity, a tortuosity and a constrictivity factor.* Int. J. Heat Mass Transfer, 17: 1093–1103

50. Pulkkanen, V.M., Nordman, H., 2010. Modelling of near-field radionuclide transport phenomena ina KBS-3V type of repository from nuclear waste with Goldsim code – and verification against previous methods. Posiva working report 2010-14.

51. Andersson, K.,Torstenfelt, B., Allard, B., 1981. *Diffusion of cesium in concrete*. Mater. Res. Soc. Symp. Proc. 3, 235-242.

52. Andersson K, Torstenfelt B. Allard B: *Sorption and diffusion studies of Cs and I in concrete* Department of Nuclear Chemistry Chalmers University of Technology Göteborg, Sweden January 1983.

53. Massoudieh, A., Ju, D., Young, T. M., Ginn, T. R., 2008. *Approximation of a radial diffusion model with a multiple-rate model for hetero-disperse particle mixtures.* J. Contam. Hydrol. 97, 55-66.

54. Felipe-Sotelo, M., Hinchliff, J., Drury, D., Evans, N., Williams, S., Read, D., *Radial diffusion of radiocaesium and radioiodide through cementitious backfill,* JPCE 2285 (2014).

55. Understanding Variation in Partition Coefficient, K_d, Values, 1999, Volume I, K_d Model, Measurement Methods, and Application of Chemical Reaction Codes, USEPA 402-R-99-004A.

56. Savage D, Stenhouse M: SKI Report 02 53 SRF 1 Vault Database April 2002 www.stralsakerhetsmyndigheten.se%2fGlobal%2fPublikationer%2fSKI_import%2f040303%2f97c461bb623c92855d73209a530f1ee5%2f02_53.pdf last accessed on 2 Feb 2014.

57. M. Felipe-Sotelo, J. Hinchliff, N. Evans, P. Warwick and D. Read. *Sorption of radionuclides to a cementitious backfill material under near-field conditions*. Mineral Mag, December 2012, v. 76, p. 2865-287

58. Baker S.,Oliver P. and McCrohon R.*(2002) Near-field batch sorption studies* – 1992 to 1998. AEA Technology Report AEAT/ERRA-0345

59. G. M. N. Baston1, M. M. Cowper1 and T. A. Marshall. *Sorption properties of aged cements*. Mineral Mag, December 2012, v. 76, p. 2865-2871.

60. Chatterji, S., 1994. *Transportation of ions through cement based materials. Part 1: Fundamental equations and basic measurement techniques*. Cem. Concr. Res. 24, 907-912.

61. Chatterji, S., 1995. *On the applicability of Fick's second law to chloride ion migration through Portland cement concrete*. Cem. Concr. Res. 25, 299-303.

62. Chatterji, S., 1999. *Evidence of variable diffusivity of ions in saturated cementitious materials*. Cem. Concr. Res. 29, 595-598.

63. Albinsson, Y., Andersson, K., Börjesson, S., Allard, B., 1996. *Diffusion of radionuclides in concrete and concrete-bentonite systems.* J. Contam. Hydrol. 21, 189-200.

64. Bath A, Deissmann G, Jefferis, S; *Radioactive contamination of concrete: uptake and release of radionuclides.* Proceedings of ICEM 2003 (ICEM03 4814).

65. Atkinson, A., Nickerson, A.K., 1984. *The diffusion of ions through water-saturated cement*. J. Mater. Sci. 19, 3068-3078.

66. Johnston, H.M., Wilmot, D.J., 1992. *Sorption and diffusion studies in cementitious grouts. Waste Manage.* 12, 289-297.

67. Sarott, F.A., Bradbury, M.H., Pandolfo, P., Spieler, P., 1992. *Diffusion and adsorption studies on hardened cement paste and the effect of carbonation on diffusion rates*. Cem. Concr. Res. 22, 439-444.

68. Jakob, A., Sarott, F.A., Spieler, P., 1999. *Diffusion and sorption on hardened cement pastes – experiments and modelling results.* PSI-Bericht, Nr. 99-05.

69. Chida, T., Sugiyama, D., 2009. *Diffusion behaviour of organic carbon and iodine in low-heat Portland cement containing fly ash.* Mater. Res. Soc. Symp. Proc., 1124, 379-384.

70. Bucur, C., Olteanu, M., Cristache, C., Palevescu, M., 2010. *Radionuclide transport through matrices.* Rev. Chim. 61, 458-461.

71. Mattigod, S.V., Whyat, G.A., Serne, R.J., Martin, P.F., Schwab, K.B., Wood, M.I., 2001. *Diffusion and leaching of selected radionuclides (Iodine-129, Technetium-99, and Uranium) through category 3 waste encasement concrete and soil fill material.* PNNL-13639 for the U.S. Department of Energy (DE-AC06-76RL01830).

72. El-Kamash, A.M., El-Dakroury, A.M., Aly, H.F., 2002. *Leaching kinetics of ^{137}Cs and ^{60}Co radionuclides fixed in cements and cement-based materials*. Cem. Concr. Res. 32, 1797-1803.

73. Plecas, I., 2003. *Immobilisation of ^{137}Cs and ^{60}Co in concrete matrix.* Ann. Nucl. Energy. 30, 1899-1903.

74. Papadokostaki, K.G., Savidou, A., 2009. *Study of leaching of caesium ions incorporated in ordinary Portland cement*. J. Hazard. Mater. 171, 1024-1031.

75. Sinha, P.K., Shanmugamani, A.G., Renganathan, K., Muthia, R., 2009. *Fixation of radioactive chemical sludge in a matrix containing cement and additives* Ann. Nucl. Energy. 36, 620-525.

76. Ojovan, M.I., Varlackova, G.A., Golubeva, Z.I., Burlaka, O.N., 2011. *Long-term field and laboratory leaching tests of cemented radioactive wastes*. J. Hazard. Mater. 187, 296-302.

77. Tits, J., Jakob, A., Wieland, E., Spiler, P., 2003. *Diffusion of tritiated water and $^{22}Na^{+}$ through non-degraded hardened cement pastes*. J. Contam. Hydrol. 61, 45-62.

78. Jakob A, *Diffusion of tritiated water (HTO) and $^{22}Na^{+}$-ions through non-degraded hardened cement pastes – II. Modelling results.* PSI-Bericht Nr. 02-21 December 2002.

79. Mibus J, Sachs S, Pfingsten W, Nebelung C, Bernhard G, *Migration of uranium(IV)/(VI) in the presence of humic acids in quartz sand: A laboratory column study.* Journal of Contaminant Hydrology 89 (2007).

80. Pala´gyi S, Tamberg K S, Vodickova H; *Transport and sorption of Sr-85 and I-125 in crushed crystalline rocks under dynamic flow conditions.* Journal of Radioanalytical Nuclear Chemistry 2010 page 283.

81. Hölttä P, Poteri A, Siitari-Kauppi M, Huittinen N; *Retardation of mobile radionuclides in granitic rock fractures by matrix diffusion* University of Helsinki, Laboratory of Radiochemistry June 2008.

82. García-Gutiérrez M, Cormenzana J L, Missana T, Mingarro M, Alonso U, Samper J, Yang Q, Yi S, *Diffusion experiments in Callovo-Oxfordian clay from the Meuse/Haute-Marne URL, France. Experimental setup and data analyses* CIEMAT, Departamento de Medio Ambiente, Av. Complutense 22, 28040 Madrid, Spain.

83. Read D, Ross D, Sims RJ. *The migration of uranium through Clashach Sandstone: the role of low molecular weight organics in enhancing radionuclide transport.* Journal of Contamaminant Hydrology 1998 12/15;35(1-3): pages 235-248.

84. Berry J.A., Bond K.A., Brownsword M., Ferguson D.R., Green A., Littleboy A.K. 1990. *Radionuclide sorption on generic rock types*. Nirex Report NSS/R182.

85. Baker A.J., Jackson C.P., Jefferies N.L., Lineham T.R. 2002. *The role of rock-matrix diffusion in retarding the migration of radionuclides from a radioactive waste repository.* Nirex Report N/051.

86. Jefferies N.L. & Swanton S.W. 2003. *An overview of research on diffusion in the geosphere undertaken within the Nirex Safety Assessment Research Programme.* Serco Assurance Report SA/ENV-0447.

87. Quintessa Report (L. Knight, J. Black S. Watson) QRS-1421A-R3 *Measurement of rock properties relevant to radionuclide migration* NDA-RWMD Geosphere Characterisation Project: Data Acquisition Report: April 2008.

88. Tits J, Wieland R, Bradbury M H; *The effect of isosaccharinic acid and gluconic acid on the retention of Eu(III), Am(III) and Th(IV) by calcite.* Applied Geochemistry 20 November 2005 Volume 20, Issue 11 pages 2082-2096.

89. Hurdus, M.H., Pilkington, N.J., 2000. *The solubility and sorption of 2-C-(hydroxymethyl)-3-deoxy-D-pentonic acid in the presence of Nirex Reference Vault Backfill and its degradation under alkaline conditions*. Nirex report, AEAT/ERRA-0153.

90. Holgersson, S., Albinsson, Y., Allard, B., Borén, H., Pavasars, I., Engkvist, I., 1998. *Effects of gluco-isosaccharinate on Cs, Ni, Pm and Th sorption onto, and diffusion into cement.* Radiochim. Acta. 82, 893-398.

91. Savage D, Soler JM, Yamaguchi K, Walker C, Honda A, Inagaki M, et al. *A comparative study of the modelling of cement hydration and cement-rock laboratory experiments.* Applied Geochemistry 26 July 2011 pages 1138–1152.

92. Massazza F. Pozzolanic cements. *Cement and Concrete Composites* 1993; 15(4): pages 185-214.

93. Nielsen EP, Herfort D, Geiker MR. *Phase equilibria of hydrated Portland cement*. Cement and Concrete Research Volume 40, Number 4, 2005 pages 405-417.

94. Lawrence CE. *International review of the composition of cement pastes, mortars, concretes and aggregates likely to be used in water retaining structures.* London : HMSO; 1994.

95. Pankow J F, Cherry J A; *Dense chlorinated solvents and other DNAPLs in groundwater* (Waterloo Press 1996).

96. Altenhein-Haese C, Bischoff H, Fu L, Mao J, Marx G. Adsorption of actinides on cement compounds. Journal of Alloys and Compounds Volumes 213-214 October 1994, pages 554-556.

97. Markovaara-Koivisto, M., Read, D., Lindberg, A., Siitari-Kauppi, M., Togneri, L., 2009. *Geology of the Sievi, Kuru and Askola sites. Uranium mineralogy at Askola.* Research Report TKK-GT-A-4, Helsinki University of Tecnology.

98. J. Hill, J. H. Sharp. *The hydration products of Portland cement in the presence of tin(II) chloride*. Cement and Concrete Research Volume 33, Issue 1, January 2003, Pages 121–124.

99. K.K. Sagoe-Crentsil, F.P. Glasser, V.T. Yilmaz. *Corrosion inhibitors for mild steel; stannous tin, Sn(II) in ordinary portland cement.* Cement and Concrete Research Volume 33, Volume 24, Issue 2, 1994, Pages 313–318.

100. Leslie A. Jardine, Charles R. Cornman, Vijay Gupta, Byong-Wa Chun. *Cement composition having chromium reducer.* US Patent number 7232483.June 2007.

101. Roto P, Sainio H, Reunala T, Laippala P. *Addition of ferrous sulfate to cement and risk of chromium dermatitis among construction workers.* Contact Dermatitis. 1996 Jan;34(1):43-50.

102. 29. McCarter W J, Crossland I, and Chrisp T M: *Hydration and drying of Nirex Reference Vault Backfill.* August 2003.

103. Nirex Report No: N/034 Why a cementitious repository? June 2001.

104. Personal communication with S Williams of NDA, March 2011 and reference to Nexia Solutions memorandum regarding grout sample preparation from J. Borthwick dated August 2007.

105. Rice G, Miles N, and Farris S: *Approaches to control the quality of cementitious PFA grouts for nuclear waste encapsulation,* Powder Technology 174, Issues 1-2, 16 May 2007, Pages 56-59.

106. NDA Report SA/ENV-0805, M C Cowper, C P Jackson and D A Partington, Serco Assurance, Implications of Using Smaller Cores to Prepare Rock Beakers for In-diffusion Tests.

107. Millington R J, Quirk J P: *The permeability of porous solids. Departments of Agronomy and agricultural chemistry*, University of Adelaide 1960.

108. Domenico, P.A., and F.W. Schwartz. 1998. *Physical and Chemical Hydrogeology, 2nd ed.*, 506. New York: John Wiley &Sons.

109. L.F. Konikow *The Secret to Successful Solute-Transport Modeling* Groundwater 49, no. 2: 144–159.

110. Poster presentation: *Advective Transport Experiments Through Crushed Cementitious Backfill Under Near Field Conditions.* M. Felipe-Sotelo, J. Hinchliff, P. Warwick, N. D. M. Evans. 11th Environmental Radiochemical Analysis- 15-17 September 2010- Chester, UK.

111. C. M. Filomena, J. Hornung, and H. Stollhofen. Assessing accuracy of gas-driven permeability measurements: a comparative study of diverse Hassler-cell and probe permeameter devices. Solid Earth Discuss., 5, 1163–1190, 2013.

112. P.Warwick, M. Felipe-Sotelo: Deep geological disposal of intermediate and low level waste in UK: Experiments to demonstrate chemical containment. Proc 11th International symposium on radiochemical analysis, Chester, UK RSC 2011

113. Rowe P W, Barden L; A new consolidation cell. Géotechnique, Vol. 16, No. 2, 1966, pages 116-124.

114. Berner UR. Evolution of pore water chemistry during degradation of cement in a radioactive waste repository environment. Cementitious materials in radioactive waste management 12, Issues 2-3, 1992, pages 201-219.

115. Edvardsen, C. *Water permeability and autogenous healing of cracks in concrete* ACI Materials Journal Volume 96, Issue 4, July 1999, Pages 448-454.

116. Y. Yang, M. D. Lepech, E. Yang, V. C. Li. *Autogenous healing of engineered cementitious composites under wet–dry cycles.* Cement and Concrete Research 39 (2009) 382–390.

117. GoldSim Technology Group LLC, 2011. *The GoldSim Monte Carlo Simulation Software.* Issaquah, Washington.

118. E.A., Environment Agency for England and Wales, July 2002. *Performance Assessment Codes for Radioactive Waste Repositories.* R&D Technical Report P3-069/TR.

119. Personal conversation with Mr D Drury of Golder Associates UK (Ltd) March 2013 after consulting the GoldSim team in Seattle.

120. GoldSim User Guide Vols 1 - 2, GoldSim Technology Group LLC Version 11.1 May 2014

121. GoldSim Contaminant Transport Module, GoldSim Technology Group LLC, Version 6.4 May 2014

122. E. Henley, J. Seader, D. Roper, *Separation Process Principles*, Third Edition 2011, John Wiley & Sons, ISBN 978-0-470-64611-3.

123. K. A. Atkinson, *An Introduction to Numerical Analysis* Second edition 1989, New York: John Wiley & Sons, ISBN 978-0-471-50023-0

124. Gelhar, FW, Welty, C and Rehfeldt, KR. July 1992. *A critical review of data on field-scale dispersion in aquifers.* Water Resources Research, 28, No.7, pp1955-1974.

125. Takahashi K, *Progress in science and technology on photostimulable BaFX : Eu2+ (X = Cl, Br, I) and imaging plates.* Journal of Luminescence 100(1-4): 307-315 2002

126. Rufer, D and Preusser, F. *Potential of autoradiography to detect spatially resolved radiation patterns in the context of trapped charge dating*. Institute of Geological Sciences, University of Bern, Baltzerstrasse 1+3, 3012 Bern, Switzerland

127. Salis M. *On the photo-stimulated luminescence of BaFBr : Eu+2 phosphors*. Journal of Luminescence 2003104(1-2): 17-25.

128. Rasband, W.S. *ImageJ*, U. S. National Institutes of Health, Bethesda, Maryland, USA, http://imagej.nih.gov/ij/, 1997-2012.

129. Z. Liu, L. Wyffels, C. Barber, L. Wan, H. Xu, M. M. Hui, L. R. Furenlid, and J. M. Woolfenden *Characterization of ^{99m}Tc-labeled cytokine ligands for inflammation imaging via TNF and IL-1 pathways.* Nucl Med Biol. October 2012; 39(7): 905–915.

130. S. Suksi, M. Siitari-Kauppi, E. Kamarainen and A.Lindberg. *The Effect of Groundwater - Rock interactions on the migration of redox sensitive radionuclides.* Mat. Res. Soc. Syrup. Proc. Vol. 127.1989.

131. S. Muuronen, E. Kamarainen, T. Jaakkola, S. Pinnioja and A. Lindberg. *Sorption and diffusion of radionuclides in rock matrix and natural fracture surfaces studied by autoradiography*. Mat. Res. Soc. Syrup. Proc. Vol. 50. 1985.

132. A.J.Young. *The Stability of Cement Superplasticiser and its Effect on Radionuclide Behaviour* Unpublished PhD Loughborough University 2012.

133. A. Young, P. Warwick, A. E Milowdowski, D. Read, *Behaviour of radionuclides in the presence of superplasticiser,* Advances in Cement Research, 2013, 25(1), 32-43.

134. Dr M. Felipe-Sotelo, Mr. J. Hinchliff, Prof. D. Read, *Chemical Containment Demonstration Experiments,* Quarterly Report Jan-Mar 2013. Loughborough University (available on request).

135. Chambers, A.V., Williams, S.J., 2006. *Parameter value selection for performance assessments: The impact of cellulosic degradation on repository performance*. Serco Assurance Report SA/ENV-0595.

136. Chambers, A.V., Green, A., Harris, A.W., Heath, T.G., Hunter, F.M.I., Manning, M.C., Williams, S.J., 2006. *The Diffusion of Radionuclides through Waste Encapsulation Grouts.* Mater. Res. Soc. Symp. Proc. 932, 705-712.

137. Jarvis K E, Gray A L, Houk R S: *Handbook of inductively coupled plasma mass spectrometry* (Blackie 1992).

138. Hill S J; *Inductively Coupled Plasma Spectrometry and Its Applications* (J Wiley 2008).

139. Methods, columns, reagents etc. available at http://www.dionex.com/en-us/products/columns/lp-81265.html accessed July 2013.

140. Details available at http://www.geinstruments.com/products-and-services/toc-analyzers-and-sensors/innovox-laboratory accessed July 2013.

141. C. R. Heath. *Interactions of radionuclides with cellulose degradation products*. Unpublished PhD thesis, Loughborough University (2008).

142. Glaus, M.A., van Loon, L.R., 2008. *Degradation of cellulose under alkaline conditions: New insights from a 12 years degradation study.* Env. Sci. Technol. 42, 2906–2911.

143. Idemitsu, K., Kuwata, K.I., Furuta, H., Inagaki, Y., Arima, T., 1997. *Diffusion paths of cesium in water-saturated mortar.* Nucl. Technol, 118, 233-241.

144. Abdel Rahman, R.O., Zaki, A.A, El-Kamash, A.M., 2007. *Modeling the long-term leaching behaviour of ^{137}Cs, ^{60}Co and $^{152,154}Eu$ radionuclides from cement-clay matrices.* J. Hazard. Mater. 145, 372-380.

145. Volchek, K., Miah, M.Y., Kuang, W., DeMaleki, Z., Tezel, F.H., 2011. *Adsorption of cesium on cement mortar from aqueous solutions.* J. Hazard. Mater. 194, 331-337.

146. Bamforth, P.B., Baston, G.M.N., Beryy, J.A., Glasser, F.P., Heath, T.G., Jackson, C.P., Savage, D., Swanton, S.W., 2012. *Cement material for use as backfill, sealing and structural materials in geological disposal concepts. A review of the current status*. Serco report for NDA serco-005125-001.

147. D. Delacroix, J. P. Guerre, P. Leblanc, C. Hickman *Radionuclide and radiation protection data handbook* 2002. Radiation protection dosimetry Vol. 98 No 1, 2002. ISBN 1 870965 87 6.

148. Weaver, C L, Harward, E D, Peterson, H T. *Tritium in the environment from nuclear powerplants.* Public health reports 84 (4): 363-371; 1969.

149. Weaver, C L; Harward, E D. *Surveillance of nuclear power reactors.* Public health reports 82 (10): 899-912; 1967.

150. Personal communication with Mr T Uppington Business Lines Director. URS Corporation Ltd November 2012.

151. Dyer A: *Liquid scintillation counting practice* (Heyden 1980).

152. Ross H, Noakes J E, Spaulding J; *Liquid scintillation counting and organic scintillators* (Lewis 1991).

153 C. Shackelford, P. Redmond, *Solute breakthrough curves for processed kaolin at low flow rates* J. Geotech. Engrg. 1995.121:17-32.

154. A.H. Price. *Vapour pressure of tritiated water.* January 1958, Nature vol 181 page 262.

155. R. Rosson, P. D. Fledderman, S. Klima, and B. Kahn *2000.Correcting tritium concentrations in water vapor monitored with silica gel. Health Phys.,78–83.*

156. M. Herranz, N.Alegrian, R.Idoeta, F.Legarda. *Sampling tritiated water vapor from the atmosphere by an active system using silica gel.* Radiation Physics and Chemistry 80 (2011) 1172–1177.

157. Lovera, O., Galle, C., Le Bescop, P., 2001. *Towards an intrinsic relationship between diffusion coefficients and microscopic features of cements?* Mat. Res. Soc. Symp. Proc. 663, 81-88.

158. Laboratoire National Henri Bequerel, *Recommended Data* accessed July 2012 at http://www.nucleide.org/DDEP_WG/DDEPdata.htm.

159. Argonne National Laboratory Fact Sheets 2005 accessed on 21 July 2012 at http://www.doeal.gov/SWEIS/OtherDocuments/499%20cesium.pdf.

160. 47. Siegbahn K; *Alpha, beta and gamma-ray spectroscopy* (North-Holland Publishing Company 1965).

161. Ochs, M., Pointeau, I., Giffaut, E., 2006. *Caesium sorption by hydrated cement as a function of degradation state: Experiments and modelling.* Waste Manage. 26, 725-732.

162. Argonne National Laboratory Fact Sheets 2005 accessed July 2012 at http://www.evs.anl.gov/pub/doc/Iodine.pdf.

163. I. Kiss, P. Groz, A. Revesz and T. Sipos. *Production of ^{125}I from pile irradiated xenon difluoride.* J. inorg, nucl. Chem., 1969, Vol. 31, pp. 1225 to 1227.

164. S.B. Hassal. United States Patent 6056929 *Method and apparatus for production of radioactive iodine* 1997.

165. Pointeau, I., Coreau, N., Reiller, P.E., 2008. *Uptake of anionic radionuclides onto degraded cement pastes and competing effect of organic ligands.* Radiochim. Acta. 96, 367-374.

166. Argonne National Laboratory Fact Sheets 2005 accessed July 2012 http://doeal.gov/SWEIS/OtherDocuments/500 strontium.pdf

167. Zs. Szántó, É. Svingor, M. Molnár, L. Palcsu, I. Futó, Z. Szucs. Diffusion of ^{3}H, ^{99}Tc, ^{125}I, ^{36}Cl and ^{85}Sr in granite, concrete and bentonite

168. J. Tits, E. Wieland, C.J. Müller, C. Landesman, M.H. Bradbury. *Strontium binding by calcium silicate hydrates.* Journal of Colloid and Interface Science 300 (2006) 78–87

169. E. Wieland , J Tits , D Kunz and R Dahn. *Strontium uptake by cementitious Materials.* Environ. Sci. Technol. 2008, 42, 403–409.

170. 43. Carr T E F and Parsons B J: *A method for the assay of calcium-45 by liquid scintillation counting.* The International Journal of Applied Radiation and Isotopes Volume 13, Issue 2 February 1962.

171. J. van der Lee and L. De Windt (2002). *CHESS Tutorial and Cookbook. Updated for version 3.0. Users Manual* Nr. LHM/RD/02/13,´Ecole des Mines de Paris, Fontainebleau, France.

172. J.C. Pleskowicz, E.J. Billo. *Mechanisms of ligand replacement in square planar nickel(II) complexes. II. Reaction of cyanide with nickel(II) complexes of two methyl-substituted ethylenediamine ligands.*

173. UK HPA. Public Health England *Nickel toxicological overview,* accessed at http://www.hpa.org.uk/webc/HPAwebFile/HPAweb_C/1236757324101 July 2013.

174. Wieland, E., Tits, J., Ulrich, A., Bradbury, M.H. *Experimental evidence for solubility limitation of the aqueous Ni(II) concentration and isotopic exchange of ^{63}Ni in cementitious systems.* Radiochimica Acta Volume 94, Issue 1, 2006, Pages 29-36.

175. M. Vespa, R. Dahn, D. Grolimund, M. Harfouche, E. Wieland, A. M. Scheidegger, *Speciation of heavy metals in cement-stabilized waste forms: A micro-spectroscopic study*. Journal of Geochemical Exploration 88 (2006) 77–80.

176. M. Vespa, R. Dahn, D. Grolimund, E. Wieland, A. M. Scheidegger *Spectroscopic Investigation of Ni Speciation in Hardened Cement Paste* Environ. Sci. Technol. 2006, 40, 2275-2282

177. Shackelford, C. Moore, S. *Fickian diffusion of radionuclides for engineered containment barriers: Diffusion coefficients, Porosities, and complicating issues.* Engineering Geology Volume 152, 18 January 2013, Pages 133-147.

178. L. Fernández-Carrascoa, J. Rius, Carles Miravitlles. *Supercritical carbonation of calcium aluminate cement*. Cement and Concrete Research Volume 38, Issues 8–9, August 2008, Pages 1033–1037.

179. Carlos A. García-González, Nadia el Grouh, Ana Hidalgo, Julio Fraile, Ana M. López-Periago, Carmen Andrade, Concepción Domingo,*New insights on the use of supercritical carbon dioxide for the accelerated carbonation of cement pastes*. The Journal of Supercritical Fluids Volume 43, Issue 3, January 2008, Pages 500–509.

APPENDIX 1

Data Tables

List of Data Tables

Time	Sample 1	Sample 1	Sample 2	Sample 2	Average	90% conf	Retention	90% conf
days	d min^{-1} cm^{-3}	Bq dm^{-3}	d min^{-1} cm^{-3}	Bq dm^{-3}	Bq dm^{-3}	+/-		+/-
0	25	417	24	400	408	36	0.03	0.002
0.1	22	367	22	367	367	0	0.02	0.000
0.9	26	433	27	450	442	36	0.03	0.002
1.1	26	433	24	400	417	76	0.03	0.004
1.9	60	1000	53	883	942	259	0.06	0.015
2.1	158	2633	72	1200	1917	3199	0.13	0.189
2.9	152	2533	125	2083	2308	1004	0.16	0.059
3.2	162	2700	139	2317	2508	857	0.17	0.051
3.9	211	3517	218	3633	3575	259	0.24	0.015
4.1	221	3683	224	3733	3708	112	0.25	0.007
7	363	6050	353	5883	5967	370	0.4	0.022
8	433	7217	397	6617	6917	1339	0.47	0.079
9	487	8117	551	9183	8650	2378	0.59	0.141
10	522	8700	585	9750	9225	2342	0.63	0.139
11	567	9450	628	10467	9958	2267	0.68	0.134
12	664	11067	654	10900	10983	370	0.74	0.022
15	647	10783	678	11300	11042	1151	0.75	0.068
17	714	11900	721	12017	11958	259	0.81	0.015
18	726	12100	759	12650	12375	1227	0.84	0.073
21	772	12867	792	13200	13033	745	0.88	0.044
24	762	12700	797	13283	12992	1303	0.88	0.077
30	774	12900	739	12317	12608	1303	0.86	0.077
36	759	12650	791	13183	12917	1191	0.88	0.071
49	724	12067	801	13350	12708	2865	0.86	0.170
65	736	12267	783	13050	12658	1749	0.86	0.104
95	764	12733	752	12533	12633	446	0.86	0.026
125	806	13433	806	13433	13433	0	0.91	0.000
156	815	13583	843	14050	13817	1040	0.94	0.062
187	937	15622	965	16089	15856	1040	1.08	0.062
217	879	14644	892	14867	14756	495	1	0.029
248	873	14550	925	15417	14983	1932	1.02	0.114
308	909	15150	952	15867	15508	1597	1.05	0.095
Total (d min^{-1})	16696		17092					

Table 10.1 Results of the NRVB HTO diffusion experiment using NRVB equilibrated water

Mass eluted (g)	Cumulative mass eluted (g)	Flow rate (g hr^{-1})	Time (hr)	d min^{-1} g^{-1}	Total (d min^{-1})	Bq dm^{-3}	Cumulative counts	% recovery
3.7227	3.7227	1.2409	3	127	474	2122	474	0.45
3.5982	7.3210	1.1994	6	122	439	2032	913	0.86
3.5755	10.8964	1.1918	9	136	488	2273	1400	1.32
3.3184	14.2149	1.1061	12	291	967	4855	2367	2.24
3.3782	17.5931	1.1261	15	817	2761	13622	5128	4.84
3.2675	20.8606	1.0892	18	1559	5093	25977	10221	9.65
3.2606	24.1212	1.0869	21	2137	6967	35614	17188	16.23
3.4833	27.6045	1.1611	24	2623	9139	43725	26327	24.86
3.5743	31.1788	1.1914	27	2829	10113	47156	36440	34.41
3.2156	34.3944	1.0719	30	2708	8709	45141	45149	42.63
3.2127	37.6071	1.0709	33	2583	8297	43044	53446	50.47
3.1182	40.7254	1.0394	36	2323	7244	38720	60690	57.31
3.0432	43.7685	1.0144	39	2127	6472	35444	67162	63.42
2.9590	46.7275	0.9863	42	1945	5755	32414	72917	68.85
2.7579	49.4854	0.9193	45	1699	4686	28316	77602	73.28
3.0932	52.5786	1.0311	48	1403	4340	23384	81942	77.38
2.7542	55.3328	0.9181	51	1289	3550	21484	85493	80.73
2.8250	58.1578	0.9417	54	1169	3302	19481	88795	83.85
2.1288	60.2867	0.7096	57	980	2087	16338	90882	85.82
2.7885	63.0751	0.9295	60	836	2330	13927	93212	88.02
2.6901	65.7653	0.8967	63	766	2061	12766	95272	89.96
2.6531	68.4183	0.8844	66	713	1891	11878	97163	91.75
2.7692	71.1875	0.9231	69	657	1818	10944	98981	93.47
3.2236	74.4111	1.0745	72	578	1863	9633	100845	95.23
3.5003	77.9115	1.1668	75	521	1823	8680	102668	96.95
3.4259	81.3374	1.1420	78	520	1782	8669	104450	98.63
3.3580	84.6953	1.1193	81	449	1509	7490	105959	100.06
3.2128	87.9081	1.0709	84	421	1353	7021	107312	101.33
3.1533	91.0614	1.0511	87	393	1239	6548	108551	102.50
2.5956	93.6570	0.8652	90	262	681	4373	109232	103.15
2.7182	96.3753	0.9061	93	225	612	3750	109844	103.72
5.1500	101.5252	1.7167	96	213	1099	3557	110943	104.76
2.3501	103.8753	0.7834	99	241	566	4015	111509	105.30
2.2860	106.1613	0.7620	102	249	570	4154	112078	105.83
1.7547	107.9159	0.5849	105	236	414	3930	112492	106.22
1.9677	109.8836	0.6559	108	179	352	2985	112845	106.56
1.9603	111.8440	0.6534	111	186	364	3093	113208	106.90
2.1754	114.0194	0.7251	114	173	376	2878	113584	107.26

Table 10.2 Results of the HTO NRVB advection experiment using NRVB equilibrated water

Mass eluted (g)	Cumulative mass eluted (g)	Flow rate (g hr^{-1})	Time (hr)	d min^{-1} g^{-1}	Total d min^{-1}	Bq dm^{-3}	Cumulative counts	% Recovery
2.6553	2.6553	0.89	3	12	33	205	33	0.03
2.6380	5.2933	0.88	6	12	31	197	64	0.05
2.6366	7.9299	0.88	9	18	49	307	112	0.09
2.5638	10.4937	0.85	12	136	348	2262	460	0.37
2.5114	13.0051	0.84	15	1201	3015	20009	3475	2.76
2.4442	15.4493	0.81	18	2867	7008	47784	10483	8.32
2.4173	17.8665	0.81	21	4199	10151	69988	20634	16.38
2.3596	20.2261	0.79	24	4216	9949	70272	30582	24.27
2.3743	22.6004	0.79	27	4127	9798	68781	40381	32.05
2.3034	24.9038	0.77	30	3779	8704	62978	49085	38.96
2.2841	27.1879	0.76	33	3343	7636	55722	56721	45.02
1.9847	29.1727		36		5332		62053	49.25
2.2573	31.4300	0.75	39	2681	6053	44690	68106	54.05
2.2389	33.6688	0.75	42		6230		74336	59.00
2.2586	35.9274	0.75	45	2405	5431	40079	79767	63.31
2.2627	38.1901	0.75	48	2138	4837	35627	84604	67.15
2.1927	40.3828	0.73	51	1801	3950	30023	88554	70.28
2.1119	42.4947	0.70	54	1640	3464	27337	92018	73.03
2.1387	44.6334	0.71	57	1513	3236	25221	95254	75.60
2.0970	46.7304	0.70	60	1408	2953	23466	98206	77.94
2.0431	48.7735	0.68	63	1285	2626	21419	100832	80.03
2.0013	50.7748	0.67	66	1211	2423	20181	103255	81.95
1.9303	52.7051	0.64	69	1130	2181	18829	105436	83.68
1.8889	54.5940	0.63	72	1040	1965	17335	107401	85.24
1.6489	56.2429	0.55	75	957	1577	15942	108978	86.49
1.9235	58.1663	0.64	78	970	1866	16169	110844	87.97
1.8424	60.0087	0.61	81	788	1451	13128	112295	89.12
1.8869	61.8956	0.63	84	732	1381	12200	113676	90.22
1.8834	63.7790	0.63	87	670	1262	11170	114939	91.22
1.8492	65.6282	0.62	90	600	1110	10008	116049	92.10
1.7869	67.4151	0.60	93	573	1024	9555	117073	92.92
2.2411	69.6562	0.75	96	469	1051	7818	118125	93.75
2.0861	71.7423	0.70	99	465	971	7756	119096	94.52
3.6646	75.4069	0.61	105	380	1391	6326	120487	95.62
3.2407	78.6476	0.54	111	439	1421	7310	121908	96.75
3.3551	82.0027	0.56	117	342	1146	5695	123054	97.66
3.5018	85.5045	0.58	123	270	947	4507	124001	98.41
3.6319	89.1364	0.61	129	252	917	4206	124918	99.14
3.5506	92.6871	0.59	135	225	799	3750	125717	99.78
3.6710	96.3581	0.61	141	204	749	3400	126466	100.37
3.6770	100.0350	0.61	147	184	676	3063	127141	100.91
3.7245	103.7595	0.62	153	165	615	2750	127756	101.39
3.5300	107.2895	0.59	159	146	514	2425	128270	101.80
3.5045	110.7941	0.58	165	132	464	2208	128734	102.17
2.7216	113.5157		171	151	411	2516	129145	102.50

Table 10.3 Results of the HTO NRVB advection experiment using CDP solution

Time	Sample 1	Minus blank	Counts Removed	C_{max}	C/C_{max}	Sample 2	Minus Blank	Counts Removed	C_{max}	C/C_{max}	Mean C/C_{max}	90% conf
Days	d min^{-1} cm^{-3}	d min^{-1} cm^{-3}	d min^{-1} cm^{-3}	d min^{-1} cm^{-3}		d min^{-1} cm^{-3}	d min^{-1} cm^{-3}	d min^{-1} cm^{-3}	d min^{-1} cm^{-3}			+/-
0	86	23	23	2589	0.009	71	8	8	2589	0.003	0.006	0.013
0.5	83	20	43	2600	0.008	65	2	10	2589	0.001	0.004	0.015
1	77	14	57	2612	0.005	64	1	11	2600	0.000	0.003	0.011
1.5	97	34	91	2623	0.013	68	5	16	2612	0.002	0.007	0.025
2	155	92	183	2635	0.035	78	15	31	2624	0.006	0.020	0.065
3	255	192	375	2646	0.073	197	134	165	2635	0.051	0.062	0.048
4	329	266	641	2657	0.100	222	159	324	2646	0.060	0.080	0.089
5	428	365	1006	2667	0.137	365	302	626	2657	0.114	0.125	0.052
6	532	469	1475	2678	0.175	607	544	1170	2667	0.204	0.190	0.064
7	619	556	2031	2688	0.207	597	534	1704	2677	0.199	0.203	0.016
8	693	630	2661	2697	0.234	693	630	2334	2686	0.235	0.234	0.002
9	807	744	3405	2706	0.275	802	739	3073	2695	0.274	0.275	0.002
10	824	761	4166	2715	0.280	876	813	3886	2704	0.301	0.290	0.045
13	1059	996	5162	2724	0.366	1057	994	4880	2712	0.367	0.366	0.002
14	1081	1018	6180	2732	0.373	1125	1062	5942	2720	0.390	0.382	0.040
15	1193	1130	7310	2739	0.413	1178	1115	7057	2728	0.409	0.411	0.009
16	1223	1160	8470	2747	0.422	1157	1094	8151	2735	0.400	0.411	0.050
22	1360	1297	9767	2754	0.471	1375	1312	9463	2742	0.478	0.475	0.017
23	1405	1342	11109	2761	0.486	1383	1320	10783	2749	0.480	0.483	0.013
28	1380	1317	12426	2768	0.476	1546	1483	12266	2755	0.538	0.507	0.139
31	1508	1445	13871	2774	0.521	1565	1502	13768	2761	0.544	0.532	0.052
37	1557	1494	15365	2781	0.537	1553	1490	15258	2768	0.538	0.538	0.002
38	1605	1542	16907	2787	0.553	1606	1543	16801	2774	0.556	0.555	0.007
41	1614	1551	18458	2793	0.555	1673	1610	18411	2779	0.579	0.567	0.054
44	1703	1640	20098	2799	0.586	1633	1570	19981	2785	0.564	0.575	0.050
45	1637	1574	21672	2805	0.561	1642	1579	21560	2791	0.566	0.563	0.010
48	1608	1545	23217	2811	0.550	1689	1626	23186	2797	0.581	0.565	0.071
50	1862	1799	25016	2816	0.639	1759	1696	24882	2803	0.605	0.622	0.075
56	1625	1562	26578	2823	0.553	1777	1714	26596	2808	0.610	0.582	0.127
62	1659	1596	28174	2829	0.564	1749	1686	28282	2814	0.599	0.582	0.078
69	1732	1669	29843	2835	0.589	1769	1706	29988	2820	0.605	0.597	0.036
77	1770	1707	31550	2841	0.601	1780	1717	31705	2825	0.608	0.604	0.015
83	1728	1665	33215	2847	0.585	1805	1742	33447	2831	0.615	0.600	0.068
104	1738	1675	34890	2853	0.587	1886	1823	35270	2836	0.643	0.615	0.124
133	1852	1789	36679	2859	0.626	1792	1729	36999	2842	0.608	0.617	0.039
164	1799	1736	38415	2865	0.606	1822	1759	38758	2848	0.618	0.612	0.026
195	1734	1671	40086	2871	0.582	1880	1817	40575	2853	0.637	0.609	0.122
224	1715	1652	41738	2878	0.574	1778	1715	42290	2859	0.600	0.587	0.058
253	1686	1623	43361	2884	0.563	1775	1712	44002	2865	0.598	0.580	0.078
286	1780	1717	45078	2891	0.594	1852	1789	45791	2871	0.623	0.609	0.065
316	1659	1596	46674	2898	0.551	1653	1590	47381	2878	0.552	0.552	0.004
344	1730	1667	48341	2904	0.574	1660	1597	48978	2885	0.554	0.564	0.046
378	1731	1668	50009	2911	0.573	1658	1595	50573	2892	0.552	0.562	0.048

407	1737	1674	51683	2918	0.574	1724	1661	52234	2899	0.573	0.573	0.002
437	1608	1545	53228	2926	0.528	1635	1572	53806	2906	0.541	0.534	0.029
499						1929	1866	55672	2912	0.641	0.641	
528						1918	1855	57527	2918	0.636	0.636	
560						1834	1771	59298	2924	0.606	0.606	
591						1841	1778	61076	2931	0.607	0.607	

Table 11.2 Results of the NRVB ^{137}Cs tracer only diffusion experiment using NRVB equilibrated water

Time	Sample 1	Sample 2	Mean	90% conf
Days	Bq dm^{-3}	Bq dm^{-3}	Bq dm^{-3}	+/-
0	383	133	258	558
0.5	333	33	183	669
1	233	17	125	482
1.5	567	83	325	1080
2	1533	250	892	2865
3	3200	2233	2717	2155
4	4433	2650	3542	3980
5	6083	5033	5558	2342
6	7817	9067	8442	2789
7	9267	8900	9083	817
8	10500	10500	10500	0
9	12400	12317	12358	187
10	12683	13550	13117	1932
13	16600	16567	16583	76
14	16967	17700	17333	1637
15	18833	18583	18708	558
16	19333	18233	18783	2454
22	21617	21867	21742	558
23	22367	22000	22183	817
28	21950	24717	23333	6171
31	24083	25033	24558	2119
37	24900	24833	24867	147
38	25700	25717	25708	36
41	25850	26833	26342	2195
44	27333	26167	26750	2601
45	26233	26317	26275	187
48	25750	27100	26425	3012
50	29983	28267	29125	3828
56	26033	28567	27300	5653
62	26600	28100	27350	3346
69	27817	28433	28125	1374
77	28450	28617	28533	370
83	27750	29033	28392	2865
104	27917	30383	29150	5501
133	29817	28817	29317	2231
164	28933	29317	29125	857
195	27850	30283	29067	5430
224	27533	28583	28058	2342
253	27050	28533	27792	3311
286	28617	29817	29217	2677
316	26600	26500	26550	223
344	27783	26617	27200	2601
378	27800	26583	27192	2713
407	27900	27683	27792	482
437	25750	26200	25975	1004
499		31100	31100	
528		30917	30917	

Table 11.3 Results of the NRVB ^{137}Cs tracer only diffusion experiment using NRVB equilibrated water expressed as activity concentrations

Time	Sample 1	Minus blank	Counts Remove	C_{max}	C/C_{max}	Sample 2	Minus Blank	Counts Remove	C_{max}	C/C_{max}	Mean C/C_{max}	90% conf.
Days	d min^{-1} cm^{-3}	d min^{-1} cm^{-3}	d min^{-1} cm^{-3}	d min^{-1} cm^{-3}		d min^{-1} cm^{-3}	d min^{-1} cm^{-3}	d min^{-1} cm^{-3}	d min^{-1} cm^{-3}			+/-
0.5	78	0	0	2568	0.00	78	0	0	2568	0.00	0.00	0.000
1	78	0	0	2568	0.00	103	25	25	2568	0.01	0.00	0.022
1.5	80	17	17	2580	0.01	106	43	68	2580	0.02	0.01	0.022
2	168	105	122	2591	0.04	244	181	249	2591	0.07	0.06	0.065
2.5	319	256	378	2603	0.10	448	385	634	2602	0.15	0.12	0.111
3	515	452	830	2613	0.17	747	684	1318	2612	0.26	0.22	0.198
3.5	984	921	1751	2623	0.35	1172	1109	2427	2621	0.42	0.39	0.161
4	1240	1177	2928	2631	0.45	1376	1313	3740	2628	0.50	0.47	0.117
4.5	1339	1276	4204	2638	0.48	1544	1481	5221	2634	0.56	0.52	0.175
5	1458	1395	5599	2644	0.53	1706	1643	6864	2639	0.62	0.58	0.212
7	1716	1653	7252	2650	0.62	1819	1756	8620	2644	0.66	0.64	0.090
8	1827	1764	9016	2654	0.66	1993	1930	10550	2648	0.73	0.70	0.143
9	2006	1943	10959	2659	0.73	2074	2011	12561	2651	0.76	0.74	0.062
10	1969	1906	12865	2662	0.72	2247	2184	14745	2654	0.82	0.77	0.238
11	1920	1857	14722	2666	0.70	2345	2282	17027	2657	0.86	0.78	0.362
12	2037	1974	16696	2669	0.74	2294	2231	19258	2658	0.84	0.79	0.223
15	2119	2056	18752	2673	0.77	2394	2331	21589	2661	0.88	0.82	0.238
17	2211	2148	20900	2663	0.81	2350	2287	26324	2663	0.86	0.83	0.116
18	2302	2239	23139	2665	0.84	2243	2180	28504	2665	0.82	0.83	0.049
37	2370	2307	25446	2667	0.86	2326	2263	30767	2667	0.85	0.86	0.037
66	2364	2301	27747	2669	0.86	2403	2340	33107	2669	0.88	0.87	0.033
96	2233	2170	29917	2671	0.81	2121	2058	35165	2671	0.77	0.79	0.094
127	2442	2379	32296	2673	0.89	2402	2339	37504	2674	0.87	0.88	0.034
158	2454	2391	34687	2675	0.89	2472	2409	39913	2676	0.90	0.90	0.014
187	2529	2466	37153	2676	0.92	2605	2542	42455	2677	0.95	0.94	0.063
209	2542	2479	39632	2677	0.93	2313	2250	44705	2678	0.84	0.88	0.192
240	2480	2417	42049	2678	0.90	2436	2373	47078	2680	0.89	0.89	0.038
300	2423	2360	44409	2680	0.88	2498	2435	49513	2681	0.91	0.89	0.062

Table 11.4 Results of the NRVB ^{137}Cs tracer only diffusion experiment using CDP solution

Time	Sample 1	Sample 2	Mean	90% conf
Days	Bq dm^{-3}	Bq dm^{-3}	Bq dm^{-3}	+/-
0.5	0	0	0	0
1	0	417	208	928
1.5	283	717	500	968
2	1750	3017	2383	2824
2.5	4267	6417	5342	4796
3	7533	11400	9467	8625
3.5	15350	18483	16917	6992
4	19617	21883	20750	5055
4.5	21267	24683	22975	7621
5	23250	27383	25317	9223
7	27550	29267	28408	3828
8	29400	32167	30783	6171
9	32383	33517	32950	2530
10	31767	36400	34083	10338
11	30950	38033	34492	15804
12	32900	37183	35042	9557
15	34267	38850	36558	10227
17	35800	38117	36958	5167
18	37317	36333	36825	2195
37	38450	37717	38083	1637
66	38350	39000	38675	1450
96	36167	34300	35233	4163
127	39650	38983	39317	1486
158	39850	40150	40000	669
187	41100	42367	41733	2824
209	41317	37500	39408	8513
240	40283	39550	39917	1637
300	39333	40583	39958	2789

Table 11.5 Results of the NRVB ^{137}Cs tracer only diffusion experiment using CDP solution expressed as activity concentrations

Time	Sample 1	Minus blank	Counts Remove	C_{max}	C/C_{max}	Sample 2	Minus Blank	Counts Removed	C_{max}	C/C_{max}	Mean C/C_{max}	90% conf
Days	d min^{-1} cm^{-3}	d min^{-1} cm^{-3}	d min^{-1} cm^{-3}	d min^{-1} cm^{-3}		d min^{-1} cm^{-3}	d min^{-1} cm^{-3}	d min^{-1} cm^{-3}	d min^{-1} cm^{-3}			+/-
0	107	44	44	3038.3	0.01	67	4	4	3038	0.00	0.008	0.032
0.5	101	38	82	3051.7	0.01	72	9	13	3052	0.00	0.008	0.021
1	136	73	155	3065.3	0.02	63	0	13	3066	0.00	0.012	0.053
1.5	127	64	219	3078.8	0.02	80	17	30	3079	0.01	0.013	0.034
2	138	75	294	3092.5	0.02	109	46	76	3093	0.01	0.02	0.021
2.5	161	98	392	3106.3	0.03	122	59	135	3107	0.02	0.025	0.028
3	260	197	589	3120.1	0.06	227	164	299	3121	0.05	0.058	0.024
3.5	319	256	845	3133.6	0.08	280	217	516	3135	0.07	0.075	0.028
4	432	369	1214	3146.9	0.12	400	337	853	3148	0.11	0.112	0.023
4.5	502	439	1653	3159.8	0.14	473	410	1263	3161	0.13	0.134	0.021
6	981	918	2571	3172.5	0.29	870	807	2070	3174	0.25	0.272	0.078
7	976	913	3484	3183.1	0.29	1247	1184	3254	3185	0.37	0.329	0.189
8	1559	1496	4980	3193.8	0.47	2064	2001	5255	3195	0.63	0.547	0.352
9	1728	1665	6645	3201.9	0.52	1841	1778	7033	3201	0.56	0.538	0.079
10	2054	1991	8636	3209.2	0.62	2094	2031	9064	3207	0.63	0.627	0.029
11	2319	2256	10892	3215	0.70	2233	2170	11234	3213	0.68	0.689	0.059
14	2384	2321	13213	3219.6	0.72	2543	2480	13714	3218	0.77	0.746	0.111
16	2577	2514	15727	3224	0.78	2606	2543	16257	3222	0.79	0.785	0.021
18	2634	2571	18298	3227.4	0.80	2906	2843	19100	3225	0.88	0.839	0.189
21	2847	2784	21082	3230.6	0.86	2809	2746	21846	3227	0.85	0.856	0.024
36	3071	3008	24090	3232.8	0.93	2693	2630	24476	3229	0.81	0.872	0.259
65	2730	2667	26757	3233.9	0.82	3066	3003	27479	3232	0.93	0.877	0.233
95	2665	2602	29359	3236.7	0.80	2799	2736	30215	3233	0.85	0.825	0.095
126	3258	3195	32554	3239.9	0.99	3204	3141	33356	3236	0.97	0.978	0.035
157	3251	3188	35742	3240.1	0.98	3115	3052	36408	3236	0.94	0.964	0.091
186	3213	3150	38892	3240.4	0.97	3222	3159	39567	3237	0.98	0.974	0.008
218	3110	3047	41939	3240.8	0.94	3212	3149	42716	3237	0.97	0.956	0.073
249	3216	3153	45092	3241.8	0.97	3106	3043	45759	3238	0.94	0.956	0.073
309	3187	3124	48216	3242.3	0.96	3070	3007	48766	3239	0.93	0.946	0.078

Table 11.6 Results of the NRVB ^{137}Cs tracer; $CsNO_3$ carrier diffusion experiment using NRVB equilibrated water

Time	Sample 1	Sample 2	Mean	90% conf
Days	Bq dm^{-3}	Bq dm^{-3}	Bq dm^{-3}	+/-
0	733	67	400	1486
0.5	633	150	392	1080
1	1217	0	608	2713
1.5	1067	283	675	1749
2	1250	767	1008	1080
2.5	1633	983	1308	1450
3	3283	2733	3008	1227
3.5	4267	3617	3942	1450
4	6150	5617	5883	1191
4.5	7317	6833	7075	1080
6	15300	13450	14375	4127
7	15217	19733	17475	10075
8	24933	33350	29142	18775
9	27750	29633	28692	4203
10	33183	33850	33517	1486
11	37600	36167	36883	3199
14	38683	41333	40008	5912
16	41900	42383	42142	1080
18	42850	47383	45117	10115
21	46400	45767	46083	1414
36	50133	43833	46983	14055
65	44450	50050	47250	12493
95	43367	45600	44483	4984
126	53250	52350	52800	2008
157	53133	50867	52000	5055
186	52500	52650	52575	335
218	50783	52483	51633	3793
249	52550	50717	51633	4092
309	52067	50117	51092	4350

Table 11.7 Results of the NRVB ^{137}Cs tracer; $CsNO_3$ carrier diffusion experiment using NRVB equilibrated water

Time	Sample 1	Minus blank	Counts Removed	C_{max}	C/C_{max}	Sample 2	Minus Blank	Counts Removed	C_{max}	C/C_{max}	Mean C/C_{max}	90% conf
Days	d min^{-1} cm^{-3}	d min^{-1} cm^{-3}	d min^{-1} cm^{-3}	d min^{-1} cm^{-3}		d min^{-1} cm^{-3}	d min^{-1} cm^{-3}	d min^{-1} cm^{-3}	d min^{-1} cm^{-3}			+/-
0	101	38	38	3024.8	0.01	83	20	20	3025	0.01	0.01	0.013
0.5	136	73	111	3038.1	0.02	98	35	55	3038	0.01	0.018	0.028
1	146	83	194	3051.4	0.03	108	45	100	3052	0.01	0.021	0.028
1.5	150	87	281	3064.8	0.03	167	104	204	3065	0.03	0.031	0.012
2	228	165	446	3078.3	0.05	205	142	346	3079	0.05	0.05	0.017
2.5	254	191	637	3091.5	0.06	249	186	532	3092	0.06	0.061	0.004
3	424	361	998	3104.7	0.12	437	374	906	3105	0.12	0.118	0.009
3.5	438	375	1373	3117.3	0.12	477	414	1320	3118	0.13	0.127	0.028
4	586	523	1896	3130	0.17	728	665	1985	3130	0.21	0.19	0.101
4.5	763	700	2596	3142	0.22	1143	1080	3065	3142	0.34	0.283	0.270
6	1162	1099	3695	3153.4	0.35	1553	1490	4555	3151	0.47	0.411	0.277
7	1516	1453	5148	3163	0.46	1909	1846	6401	3159	0.58	0.522	0.279
8	1593	1530	6678	3171	0.48	2007	1944	8345	3165	0.61	0.548	0.294
9	1870	1807	8485	3178.8	0.57	2296	2233	10578	3171	0.70	0.636	0.303
10	2088	2025	10510	3185.3	0.64	2531	2468	13046	3175	0.78	0.706	0.316
11	2414	2351	12861	3190.8	0.74	2607	2544	15590	3179	0.80	0.769	0.142
14	2596	2533	15394	3194.8	0.79	2782	2719	18309	3182	0.85	0.824	0.138
16	2930	2867	18261	3198	0.90	2812	2749	21058	3184	0.86	0.88	0.074
18	2825	2762	21023	3199.6	0.86	2957	2894	23952	3186	0.91	0.886	0.101
21	3029	2966	23989	3201.7	0.93	2853	2790	26742	3187	0.88	0.901	0.114
36	2959	2896	26885	3202.9	0.90	3008	2945	29687	3189	0.92	0.914	0.043
65	2993	2930	29815	3204.4	0.91	2761	2698	32385	3191	0.85	0.88	0.154
95	3175	3112	32927	3205.7	0.97	3027	2964	35349	3193	0.93	0.95	0.095
126	3241	3178	36105	3206.2	0.99	2580	2517	37866	3194	0.79	0.89	0.453
157	3215	3152	39257	3206.3	0.98	3065	3002	40868	3198	0.94	0.961	0.099
186	3328	3265	42522	3206.6	1.02	3165	3102	43970	3199	0.97	0.994	0.108
218	3151	3088	45610	3206.3	0.96	3095	3032	47002	3199	0.95	0.955	0.034
249	3051	2988	48598	3206.9	0.93	3154	3091	50093	3200	0.97	0.949	0.076
309	3041	2978	51576	3208	0.93	3086	3023	53116	3200	0.94	0.936	0.037

Table 11.8 Results of the NRVB ^{137}Cs tracer; $CsNO_3$ carrier diffusion experiment using CDP solution

Time	Sample1	Sample 2	Mean	90% conf
Days	Bq dm^{-3}	Bq dm^{-3}	Bq dm^{-3}	
0	633	333	483	669
0.5	1217	583	900	1414
1	1383	750	1067	1414
1.5	1450	1733	1592	634
2	2750	2367	2558	857
2.5	3183	3100	3142	187
3	6017	6233	6125	482
3.5	6250	6900	6575	1450
4	8717	11083	9900	5278
4.5	11667	18000	14833	14131
6	18317	24833	21575	14537
7	24217	30767	27492	14613
8	25500	32400	28950	15393
9	30117	37217	33667	15840
10	33750	41133	37442	16473
11	39183	42400	40792	7175
14	42217	45317	43767	6916
16	47783	45817	46800	4386
18	46033	48233	47133	4908
21	49433	46500	47967	6546
36	48267	49083	48675	1820
65	48833	44967	46900	8625
95	51867	49400	50633	5501
126	52967	41950	47458	24576
157	52533	50033	51283	5577
186	54417	51700	53058	6059
218	51467	50533	51000	2084
249	49800	51517	50658	3828
309	49633	50383	50008	1673

Table 11.9 Results of the NRVB ^{137}Cs tracer; $CsNO_3$ carrier diffusion experiment using CDP solution

Sample	1y-1	1y-2	2y-1	2y-2	3y-1	3y-2	4y-1	4y-2	4y-3	Spare 1	Spare 2	Average
Days	10^{-3} mol dm^{-3}	10^{-3} mol dm^{-3}	10^{-3} mol dm^{-3}	10^{-3} mol dm^{-3}	10^{-3} mol dm^{-3}	10^{-3} mol dm^{-3}	10^{-3} mol dm^{-3}	10^{-3} mol dm^{-3}	10^{-3} mol dm^{-3}	10^{-3} mol dm^{-3}	10^{-3} mol dm^{-3}	10^{-3} mol dm^{-3}
0	0.00	0.01	0.01	0.00	0.00	0.00	0.01	0.01	0.01	0.01	0.01	0.01
7	0.07	0.04	0.06	0.07	0.08	0.05	0.08	0.00	0.01	0.10	0.06	0.06
14	0.18	0.13	0.22	0.19	0.24	0.17	0.20	0.17	0.17	0.24	0.23	0.19
21	0.25	0.16	0.32	0.27	0.31	0.24	0.25	0.24	0.28	0.31	0.25	0.26
28	0.33	0.24	0.47	0.37	0.45	0.33	0.34	0.34	0.41	0.39	0.46	0.38
59	0.33	0.25	0.47	0.40	0.51	0.39	0.40	0.34	0.45	0.46	0.40	0.40
94	0.40	0.28	0.48	0.36	0.14	0.33	0.43	0.34	0.40	0.38	0.40	0.36
121	0.40	0.25	0.62	0.54	0.40	0.50	0.42	0.07	0.59	0.49	0.51	0.43
156	0.39	0.26	0.50	0.44	0.17	0.36	0.55	0.37	0.44	0.58	0.41	0.41
185	0.35	0.24	0.47		0.46	0.36	0.35	0.31	0.44	0.41	0.37	0.38
215	0.57	0.31	0.60	0.47	0.66	0.16	0.17	0.50	0.53	0.59	0.64	0.47
246	0.39	0.33	0.70	0.41	0.66	0.56	0.31	0.49	0.52	0.57	0.37	0.48
275	0.38	0.22	0.46	0.31	0.51	0.26	0.30	0.34	0.35	0.39	0.30	0.35
304	0.36	0.21	0.41	0.33	0.40	0.30	0.32	0.33	0.38	0.41	0.34	0.35
337	0.31	0.23	0.50	0.31	0.35	0.43	0.36	0.35	0.40	0.43	0.35	0.37
368	0.38	0.25	0.47	0.35	0.49	0.35	0.36	0.34	0.42	0.43	0.42	0.39
488			0.90	0.86	0.84	0.66	0.48	0.43	0.73	0.84	0.68	0.71
550			0.60	0.69	1.00	0.40	0.42	0.57	0.36	0.69	0.57	0.59

Table 11.10 Cs Results for the mixed element diffusion experiments in NRVB equilibrated water

Sample	1y-1	1y-2	2y-1	2y-2	3y-1	3y-2	4y-1	4y-2	4y-3	Spare 1	Spare 2	Average
Days	10^{-3} mol dm^{-3}	10^{-3} mol dm^{-3}	10^{-3} mol dm^{-3}	10^{-3} mol dm^{-3}	10^{-3} mol dm^{-3}	10^{-3} mol dm^{-3}	10^{-3} mol dm^{-3}	10^{-3} mol dm^{-3}	10^{-3} mol dm^{-3}	10^{-3} mol dm^{-3}	10^{-3} mol dm^{-3}	10^{-3} mol dm^{-3}
0	0.00	0.00	0.00	0.00	0.00	0.00	0.00	0.00	0.00	0.00	0.00	0.00
7	0.32	0.23	0.27	0.28	0.34	0.29	0.32	0.27	0.31	0.27	0.25	0.29
13	0.45	0.30	0.34	0.41	0.47	0.43	0.54	0.42	0.42	0.36	0.35	0.41
19	0.44	0.24	0.36	0.42	0.53	0.49	0.58	0.45	0.50	0.41	0.38	0.44
28	0.50	0.32	0.33	0.40	0.52	0.40	0.55	0.42	0.51	0.43	0.43	0.44
60	0.49	0.32	0.35	0.41	0.52	0.40	0.59	0.46	0.50	0.44	0.43	0.45
87	0.73	0.41	0.48	0.68	0.63	0.91	0.80	0.41	0.91	0.69	0.50	0.65
122	0.48	0.40	0.44	0.46	0.57	0.49	0.62	0.46	0.53	0.46	0.45	0.49
151	0.43	0.39	0.41	0.46	0.47	0.43	0.59	0.47	0.47	0.45	0.40	0.45
181	0.35	0.24	0.47	0.00	0.46	0.36	0.35	0.31	0.44	0.41	0.37	0.38
212	0.61	0.47	0.35	0.33	0.54	0.49	0.70	0.59	0.71	0.32	0.62	0.52
241	0.40	0.29	0.35	0.36	0.36	0.46	0.53	0.40	0.44	0.37	0.44	0.40
270	0.42	0.27	0.32	0.38	0.42	0.38	0.50	0.39	0.41	0.41	0.38	0.39
303	0.53	0.32	0.36	0.43	0.43	0.44	0.50	0.39	0.41	0.52	0.49	0.44
334	0.48	0.34	0.36	0.40	0.50	0.46	0.58	0.45	0.48	0.43	0.41	0.44
424			0.53	0.56	0.83	0.65	0.63	0.76	0.82	0.85	0.00	0.70
485			0.58	0.75	0.84	0.82	0.75	1.05	0.00	0.70	0.73	0.78

Table 11.11 Cs Results for the mixed element NRVB diffusion experiments in CDP solution

Mass eluted (g)	Cumulative mass eluted (g)	Flow rate (g hr^{-1})	Time (hr)	d min^{-1} g^{-1}	Total d min^{-1}	Bq dm^{-3}	Cumulative counts min^{-1}	% recovery
3.6031	3.6031	1.80	2	24	87	1450	87	0.00
3.4189	7.0220	1.71	4	21	73	1217	160	0.00
3.5667	10.5886	1.78	6	24	84	1400	244	0.00
3.5600	14.1486	1.78	8	42	150	2500	394	0.00
3.6011	17.7497	1.80	10	85	307	5117	701	0.00
3.3494	21.0992	1.67	12	224	749	12483	1450	0.01
2.9809	24.0801	1.49	14	471	1403	23383	2853	0.02
2.7390	26.8191	1.37	16	769	2106	35100	4959	0.03
2.6690	29.4881	1.33	18	1051	2804	46733	7763	0.04
2.6501	32.1382	1.33	20	1280	3391	56517	11154	0.06
2.4701	34.6083	1.24	22	1674	4136	68933	15290	0.09
2.5819	37.1901	1.29	24	1700	4389	73150	19679	0.11
2.3736	39.5637	1.19	26	1834	4353	72550	24032	0.14
2.5193	42.0830	1.26	28	1863	4693	78217	28725	0.16
2.5284	44.6115	1.26	30	1832	4633	77217	33358	0.19
2.2606	46.8721	1.13	32	1857	4197	69950	37555	0.21
2.4939	49.3660	1.25	34	1718	4285	71417	41840	0.24
2.4793	51.8453	1.24	36	1687	4183	69717	46023	0.26
2.4673	54.3126	1.23	38	1603	3955	65917	49978	0.29
2.3167	56.6293	1.16	40	1525	3534	58900	53512	0.31
2.4499	59.0791	1.22	42	1483	3632	60533	57144	0.33
2.2643	61.3434	1.13	44	1356	3071	51183	60215	0.34
2.4229	63.7663	1.21	46	1188	2879	47983	63094	0.36
2.4650	66.2314	1.23	48	1153	2843	47383	65937	0.38
2.4551	68.6865	1.23	50	1074	2638	43967	68575	0.39
2.5035	71.1900	1.25	52	977	2445	40750	71020	0.41
2.4928	73.6828	1.25	54	965	2405	40083	73425	0.42
2.4873	76.1701	1.24	56	912	2269	37817	75694	0.43
2.4905	78.6606	1.25	58	835	2079	34650	77773	0.45
2.2205	80.8810	1.11	60	770	1709	28483	79482	0.46
2.4616	83.3426	1.23	62	682	1679	27983	81161	0.46
2.4440	85.7866	1.22	64	643	1571	26183	82732	0.47
2.4503	88.2370	1.23	66	589	1444	24067	84176	0.48
2.4432	90.6802	1.22	68	572	1397	23283	85573	0.49
2.4875	93.1677	1.24	70	560	1394	23233	86967	0.50
2.1631	95.3308	1.08	72	516	1117	18617	88084	0.50
2.4669	97.7978	1.23	74	454	1119	18650	89203	0.51
2.3386	100.1364	1.17	76	528	1234	20567	90437	0.52
2.4770	102.6134	1.24	78	508	1259	20983	91696	0.52
2.4491	105.0625	1.22	80	456	1117	18617	92813	0.53
2.4956	107.5580	1.25	82	418	1043	17383	93856	0.54
2.4727	110.0307	1.24	84	339	838	13967	94694	0.54
2.4546	112.4853	1.23	86	281	690	11500	95384	0.55
2.4715	114.9568	1.24	88	287	710	11833	96094	0.55
2.4891	117.4459	1.24	90	271	675	11250	96769	0.55
2.4793	119.9253	1.24	92	269	667	11117	97436	0.56
2.5357	122.4610	1.27	94	249	631	10517	98067	0.56
2.1145	124.5755	1.06	96	276	583	9717	98650	0.56
1.7030	126.2785	0.85	98	313	533	8883	99183	0.57
1.7483	128.0268	0.87	100	298	521	8683	99704	0.57

1.7564	129.7832	0.88	102	278	489	8150	100193	0.57
1.6938	131.4770	0.85	104	270	457	7617	100650	0.58
1.7027	133.1796	0.85	106	250	426	7100	101076	0.58
1.7123	134.8919	0.86	108	244	417	6950	101493	0.58
1.6475	136.5394	0.82	110	238	392	6533	101885	0.58
1.6544	138.1939	0.83	112	233	385	6417	102270	0.59
1.6610	139.8549	0.83	114	215	357	5950	102627	0.59
1.6656	141.5205	0.83	116	215	358	5967	102985	0.59
1.7316	143.2521	0.87	118	198	342	5700	103327	0.59
1.2078	144.4600	0.60	120	223	269	4483	103596	0.59
1.4336	145.8936	0.72	122	148	212	3533	103808	0.59
1.9249	147.8185	0.96	124	142	274	4567	104082	0.60
1.8986	149.7171	0.95	126	153	290	4833	104372	0.60
1.7948	151.5119	0.90	128	162	290	4833	104662	0.60
1.7272	153.2391	0.86	130	158	273	4550	104935	0.60
1.6966	154.9356	0.85	132	157	267	4450	105202	0.60
1.6637	156.5993	0.83	134	157	262	4367	105464	0.60
1.6690	158.2683	0.83	136	152	253	4217	105717	0.61
1.5959	159.8643	0.80	138	145	232	3867	105949	0.61
1.6386	161.5029	0.82	140	143	234	3900	106183	0.61
1.6414	163.1443	0.82	142	135	221	3683	106404	0.61

Table 11.12 Results of the ^{137}Cs tracer advection using NRVB equilibrated water

Time	Sample 1	Minus blank	Counts Removed	C_{max}	C/C_{max}	Sample 2	Minus Blank	Counts Removed	C_{max}	C/C_{max}	Mean C/C_{max}	90% conf
Days	d min^{-1} cm^{-3}	d min^{-1} cm^{-3}	d min^{-1} cm^{-3}	d min^{-1} cm^{-3}		d min^{-1} cm^{-3}	d min^{-1} cm^{-3}	d min^{-1} cm^{-3}	d min^{-1} cm^{-3}			+/-
0	17	2	2	665	0.00	24	9	9	662	0.01	0.01	0.024
3	18	3	5	668	0.00	23	8	17	665	0.01	0.01	0.017
4	30	15	20	671	0.02	34	19	36	668	0.03	0.03	0.014
5	50	35	55	674	0.05	49	34	70	671	0.05	0.05	0.003
6	76	61	116	676	0.09	71	56	126	673	0.08	0.09	0.016
7	108	93	209	679	0.14	94	79	205	676	0.12	0.13	0.045
10	164	149	358	682	0.22	146	131	336	679	0.19	0.21	0.057
11	197	182	540	684	0.27	189	174	510	682	0.26	0.26	0.024
12	203	188	728	687	0.27	199	184	694	684	0.27	0.27	0.011
13	228	213	941	689	0.31	215	200	894	686	0.29	0.30	0.040
14	228	213	1154	691	0.31	226	211	1105	689	0.31	0.31	0.004
17	269	254	1408	694	0.37	288	273	1378	691	0.40	0.38	0.064
19	296	281	1689	696	0.40	297	282	1660	693	0.41	0.41	0.007
25	323	308	1997	698	0.44	366	351	2011	695	0.51	0.47	0.142
31	378	363	2360	699	0.52	367	352	2363	696	0.51	0.51	0.030
38	380	365	2725	701	0.52	366	351	2714	698	0.50	0.51	0.040
46	380	365	3090	703	0.52	384	369	3083	700	0.53	0.52	0.017
52	379	364	3454	704	0.52	403	388	3471	701	0.55	0.53	0.081
73	364	349	3803	706	0.49	389	374	3845	703	0.53	0.51	0.084
102	386	371	4174	708	0.52	396	381	4226	705	0.54	0.53	0.037
133	376	361	4535	709	0.51	364	349	4575	706	0.49	0.50	0.033

Table 12.2 Results of the NRVB ^{125}I tracer; KI carrier diffusion experiment using NRVB equilibrated water

Time	Sample 1	Sample 2	Mean	90% conf
Days	Bq dm^{-3}	Bq dm^{-3}	Bq dm^{-3}	+/-
0	33	150	92	260
3	50	133	92	186
4	250	317	283	149
5	583	567	575	37
6	1017	933	975	186
7	1550	1317	1433	521
10	2483	2183	2333	669
11	3033	2900	2967	297
12	3133	3067	3100	149
13	3550	3333	3442	483
14	3550	3517	3533	74
17	4233	4550	4392	706
19	4683	4700	4692	37
25	5133	5850	5492	1599
31	6050	5867	5958	409
38	6083	5850	5967	521
46	6083	6150	6117	149
52	6067	6467	6267	892
73	5817	6233	6025	930
102	6183	6350	6267	372
133	6017	5817	5917	446

Table 12.3 Results of the NRVB ^{125}I tracer; KI carrier diffusion experiment using NRVB equilibrated water expressed as Bq dm^{-3}

Time	Sample 1	Minus blank	Counts Remove	C_{max}	C/C_{max}	Sample 2	Minus Blank	Counts Remove	C_{max}	C/C_{max}	Mean C/C_{max}	90% conf
Days	d min^{-1} cm^{-3}	d min^{-1} cm^{-3}	d min^{-1} cm^{-3}	d min^{-1} cm^{-3}		d min^{-1} cm^{-3}	d min^{-1} cm^{-3}	d min^{-1} cm^{-3}	d min^{-1} cm^{-3}			+/-
0	19	1	1	1248	0.00	16	0	0	1248	0.00	0.00	0.002
0.5	19	1	2	1254	0.00	18	0	0	1254	0.00	0.00	0.002
1	22	4	6	1260	0.00	16	0	0	1260	0.00	0.00	0.007
2	80	62	68	1265	0.05	63	45	45	1265	0.04	0.04	0.030
3	189	171	239	1271	0.13	165	147	192	1271	0.12	0.13	0.042
4	293	275	514	1276	0.22	262	244	436	1276	0.19	0.20	0.054
5	417	399	913	1281	0.31	399	381	817	1281	0.30	0.30	0.032
7	562	544	1457	1285	0.42	557	539	1356	1285	0.42	0.42	0.009
8	622	604	2061	1288	0.47	595	577	1933	1289	0.45	0.46	0.047
9	666	648	2709	1291	0.50	637	619	2552	1292	0.48	0.49	0.051
10	719	701	3410	1294	0.54	692	674	3226	1295	0.52	0.53	0.047
13	741	723	4133	1297	0.56	738	720	3946	1298	0.55	0.56	0.006
14	829	811	4944	1300	0.62	798	780	4726	1301	0.60	0.61	0.054
15	850	832	5776	1302	0.64	823	805	5531	1303	0.62	0.63	0.047
16	869	851	6627	1304	0.65	886	868	6399	1306	0.66	0.66	0.028
19	918	900	7527	1307	0.69	898	880	7279	1308	0.67	0.68	0.035
20	919	901	8428	1309	0.69	870	852	8131	1310	0.65	0.67	0.085
21	954	936	9364	1311	0.71	919	901	9032	1312	0.69	0.70	0.061
22	932	914	10278	1312	0.70	910	892	9924	1314	0.68	0.69	0.039
38	908	890	11168	1314	0.68	892	874	10798	1316	0.66	0.67	0.029
67	886	868	12036	1317	0.66	932	914	11712	1318	0.69	0.68	0.076

Table 12.4 Results of the NRVB ^{125}I tracer; KI carrier diffusion experiment using CDP solution

Time	Sample 1	Sample 2	Mean	90% conf
Days	Bq dm^{-3}	Bq dm^{-3}	Bq dm^{-3}	+/-
0	17	0	8	37
0.5	17	0	8	37
1	67	0	33	149
2	1033	750	892	632
3	2850	2450	2650	892
4	4583	4067	4325	1153
5	6650	6350	6500	669
7	9067	8983	9025	186
8	10067	9617	9842	1004
9	10800	10317	10558	1078
10	11683	11233	11458	1004
13	12050	12000	12025	112
14	13517	13000	13258	1153
15	13867	13417	13642	1004
16	14183	14467	14325	632
19	15000	14667	14833	744
20	15017	14200	14608	1822
21	15600	15017	15308	1301
22	15233	14867	15050	818
38	14833	14567	14700	595
67	14467	15233	14850	1710

Table 12.5 Results of the NRVB ^{125}I tracer; KI carrier diffusion experiment using CDP solution

Sample	1y-1	1y-2	2y-1	2y-2	3y-1	3y-2	4y-1	4y-2	4y-3	Spare 1	Spare 2	Mean
Days	10^{-3} mol dm^{-3}	10^{-3} mol dm^{-3}	10^{-3} mol dm^{-3}	10^{-3} mol dm^{-3}	10^{-3} mol dm^{-3}	10^{-3} mol dm^{-3}	10^{-3} mol dm^{-3}	10^{-3} mol dm^{-3}	10^{-3} mol dm^{-3}	10^{-3} mol dm^{-3}	10^{-3} mol dm^{-3}	10^{-3} mol dm^{-3}
0	0.00	0.00	0.00	0.00	0.00	0.00	0.00	0.00	0.00	0.00	0.00	0.00
7	0.00	0.00	0.00	0.02	0.02	0.00	0.01	0.00	0.00	0.03	0.00	0.01
14	0.08	0.03	0.08	0.09	0.09	0.07	0.10	0.08	0.12	0.10	0.09	0.08
21	0.14	0.03	0.14	0.14	0.18	0.14	0.16	0.17	0.22	0.17	0.12	0.15
28	0.19	0.11	0.31	0.18	0.22	0.18	0.20	0.18	0.24	0.22	0.18	0.20
59	0.23	0.14	0.24	0.24	0.27	0.22	0.21	0.23	0.26	0.25	0.22	0.23
94	0.26	0.14	0.26	0.24	0.28	0.22	0.25	0.24	0.28	0.26	0.23	0.24
121	0.25	0.15	0.26	0.25	0.28	0.22	0.25	0.25	0.28	0.25	0.21	0.24
156	0.22	0.13	0.23	0.22	0.25	0.21	0.23	0.21	0.25	0.23	0.20	0.22
185	0.21	0.14	0.25		0.27	0.21	0.23	0.22	0.27	0.23	0.21	0.22
215	0.26	0.11	0.33	0.21	0.27	0.16	0.20	0.22	0.26	0.24	0.15	0.22
246		0.11	0.20	0.22	0.22	0.17	0.25	0.26	0.37	0.12	0.19	0.21
275	0.24	0.12	0.22	0.23	0.26	0.19	0.21	0.23	0.25	0.23	0.21	0.22
304	0.23	0.13	0.24	0.22		0.21	0.23	0.22	0.30	0.23	0.20	0.22
337	0.19	0.11	0.21	0.22	0.20	0.24	0.22	0.19	0.22	0.23	0.20	0.20
368	0.21	0.13	0.24	0.22	0.25	0.16	0.22	0.25	0.26	0.23	0.18	0.21

Table 12.6 I Results for the mixed element diffusion experiments in NRVB equilibrated water

Sample	1y-1	1y-2	2y-1	2y-2	3y-1	3y-2	4y-1	4y-2	4y-3	Spare 1	Spare 2	Mean
Days	10^{-3} mol dm^{-3}	10^{-3} mol dm^{-3}	10^{-3} mol dm^{-3}	10^{-3} mol dm^{-3}	10^{-3} mol dm^{-3}	10^{-3} mol dm^{-3}	10^{-3} mol dm^{-3}	10^{-3} mol dm^{-3}	10^{-3} mol dm^{-3}	10^{-3} mol dm^{-3}	10^{-3} mol dm^{-3}	10^{-3} mol dm^{-3}
0	0.00	0.00	0.00	0.00	0.00	0.00	0.00	0.00	0.00	0.00	0.00	0.00
7	0.15	0.10	0.13	0.15	0.20	0.12	0.11	0.12	0.13	0.13	0.09	0.13
14	0.26	0.17	0.25	0.25	0.32	0.23	0.23	0.21	0.22	0.23	0.19	0.23
21	0.28	0.21	0.27	0.30	0.38	0.28	0.27	0.28	0.28	0.28	0.23	0.28
28	0.30	0.24	0.27	0.31	0.39	0.31	0.32	0.30	0.31	0.33	0.31	0.31
59	0.32	0.25	0.30	0.34	0.41	0.32	0.32	0.30	0.32	0.33	0.27	0.32
94	0.33	0.21	0.31	0.35	0.40	0.32	0.34	0.34	0.32	0.33	0.28	0.32
121	0.30	0.29	0.29	0.32	0.40	0.30	0.33	0.28	0.30	0.31	0.26	0.31
151	0.30	0.23	0.28	0.31	0.39	0.30	0.32	0.30	0.29	0.30	0.26	0.30
181	0.22	0.22	0.28	0.31	0.38	0.29	0.32		0.25	0.30	0.25	0.28
212	0.30	0.17	0.27	0.41	0.31	0.41	0.35	0.31	0.33	0.32	0.30	0.32
241	0.29	0.28	0.30	0.36	0.28	0.27	0.30		0.30	0.28	0.24	0.29
270	0.33	0.24	0.28	0.30	0.39	0.16	0.31	0.29	0.28	0.27	0.25	0.28
303	0.27	0.25	0.26	0.31	0.30	0.37	0.32	0.28	0.30	0.32	0.25	0.29
334	0.33	0.21	0.27	0.29	0.34	0.27	0.29	0.28	0.28	0.29	0.23	0.28

Table 12.7 I Results for the mixed element diffusion experiments in CDP solution

Time	Sample 1	Minus blank	Counts Removed	C_{max}	C/C_{max}	Sample 2	Minus Blank	Counts Removed	C_{max}	C/C_{max}	Mean C/C_{max}	90% conf
Days	d min^{-1} cm^{-3}	d min^{-1} cm^{-3}	d min^{-1} cm^{-3}	d min^{-1} cm^{-3}		d min^{-1} cm^{-3}	d min^{-1} cm^{-3}	d min^{-1} cm^{-3}	d min^{-1} cm^{-3}			+/-
0	19	1	1	1369	0.00	18	0	0	1369	0.00	0.00	0.002
1	16	0	1	1375	0.00	19	1	1	1378	0.00	0.00	0.002
2	21	3	4	1382	0.00	18	0	1	1385	0.00	0.00	0.004
3	16	0	4	1388	0.00	17	0	1	1391	0.00	0.00	0.000
4	17	0	4	1394	0.00	17	0	1	1397	0.00	0.00	0.000
5	17	0	4	1400	0.00	20	2	3	1404	0.00	0.00	0.003
6	19	1	5	1407	0.00	17	0	3	1410	0.00	0.00	0.002
7	23	5	10	1413	0.00	18	0	3	1416	0.00	0.00	0.008
8	19	1	11	1420	0.00	16	0	3	1423	0.00	0.00	0.001
9	23	5	16	1426	0.00	23	5	8	1430	0.00	0.00	0.000
10	18	0	16	1433	0.00	21	3	11	1436	0.00	0.00	0.005
13	19	1	17	1440	0.00	18	0	11	1443	0.00	0.00	0.002
14	20	2	19	1447	0.00	17	0	11	1450	0.00	0.00	0.003
15	21	3	22	1453	0.00	25	7	18	1457	0.00	0.00	0.006
16	21	3	25	1460	0.00	20	2	21	1464	0.00	0.00	0.001
22	29	11	37	1467	0.01	28	10	31	1471	0.01	0.01	0.002
23	28	10	47	1474	0.01	32	14	45	1478	0.01	0.01	0.005
28	37	19	66	1481	0.01	41	23	68	1485	0.02	0.01	0.006
31	48	30	97	1489	0.02	49	31	98	1492	0.02	0.02	0.000
35	53	35	132	1496	0.02	62	44	142	1499	0.03	0.03	0.013
36	54	36	168	1503	0.02	60	42	184	1506	0.03	0.03	0.008
37	54	36	204	1510	0.02	60	42	227	1513	0.03	0.03	0.009
38	55	37	241	1517	0.02	68	50	276	1521	0.03	0.03	0.019
41	72	54	295	1525	0.04	75	57	333	1528	0.04	0.04	0.004
43	69	51	347	1532	0.03	77	59	392	1535	0.04	0.04	0.011
44	72	54	400	1539	0.03	77	59	451	1543	0.04	0.04	0.007
45	73	55	455	1547	0.04	88	70	521	1550	0.05	0.04	0.022
48	90	72	527	1555	0.05	80	62	583	1558	0.04	0.04	0.015
50	91	73	600	1562	0.05	92	74	657	1565	0.05	0.05	0.002

Table 12.8 Results of the NRVB ^{125}I tracer only experiment using NRVB equilibrated water

Time	Sample 1	Sample 2	Mean	90% conf
Days	Bq dm^{-3}	Bq dm^{-3}	Bq dm^{-3}	+/-
0	20	0	10	45
1	0	20	10	45
2	43	0	22	97
3	0	0	0	0
4	0	0	0	0
5	0	30	15	67
6	20	0	10	45
7	87	0	43	193
8	10	0	5	22
9	83	83	83	0
10	0	57	28	126
13	17	0	8	37
14	33	0	17	74
15	57	117	87	134
16	53	40	47	30
22	190	163	177	59
23	173	233	203	134
28	320	383	352	141
31	503	510	507	15
35	587	737	662	335
36	603	697	650	208
37	607	707	657	223
38	610	830	720	491
41	907	950	928	97
43	853	980	917	283
44	897	980	938	186
45	910	1163	1037	565
48	1203	1037	1120	372
50	1210	1230	1220	45

Table 12.9 Results of the NRVB ^{125}I tracer only diffusion experiment using NRVB equilibrated water expressed as concentration

Mass eluted (g)	Cumulative mass eluted (g)	Flow rate (g hr^{-1})	Time (hr)	d min^{-1} g^{-1}	Total d min^{-1}	Cumulative d min^{-1}	Bq dm^{-3}	% recovery
1.2187	1.2187	0.61	2	31	25	31	517	0.03
1.2205	2.4392	0.61	4	30	25	61	500	0.06
1.1719	3.6111	0.59	6	30	26	91	500	0.09
1.1688	4.7799	0.58	8	31	27	122	517	0.12
1.1042	5.8841	0.55	10	31	28	153	517	0.16
1.1701	7.0542	0.59	12	34	29	187	567	0.19
1.2123	8.2666	0.61	14	32	26	219	533	0.22
1.1340	9.4005	0.57	16	30	26	249	500	0.25
1.1361	10.5366	0.57	18	30	26	279	500	0.28
1.0662	11.6028	0.53	20	29	27	308	483	0.31
1.1525	13.9297	0.58	24	36	31	369	600	0.38
0.6110	14.5406	0.61	26	8	13	377	133	0.38
1.1828	15.7234	0.59	28	32	27	409	533	0.42
1.2761	16.9995	0.64	30	32	25	441	533	0.45
1.2872	18.2866	0.64	32	28	22	469	467	0.48
1.2021	19.4887	0.60	34	27	22	496	450	0.50
1.1917	20.6804	0.60	36	29	24	525	483	0.53
1.2102	21.8906	0.61	38	27	22	552	450	0.56
1.2121	23.1027	0.61	40	27	22	579	450	0.59
1.2081	24.3108	0.60	42	22	18	601	367	0.61
1.1513	25.4621	0.58	44	24	21	625	400	0.64
1.1943	26.6564	0.60	46	24	20	649	400	0.66
1.2683	27.9247	0.63	48	27	21	676	450	0.69
1.2269	29.1516	0.61	50	29	24	705	483	0.72
1.2683	30.4199	0.63	52	23	18	728	383	0.74
1.2291	31.6491	0.61	54	20	16	748	333	0.76
1.2284	32.8774	0.61	56	25	20	773	417	0.79
1.2285	34.1059	0.61	58	25	20	798	417	0.81
1.2331	35.3390	0.62	60	32	26	830	533	0.84
1.2311	36.5701	0.62	62	30	24	860	500	0.88
1.2338	37.8039	0.62	64	37	30	897	617	0.91
1.1868	38.9907	0.59	66	33	28	930	550	0.95
1.1831	40.1739	0.59	68	43	36	973	717	0.99
1.0751	41.2490	0.54	70	33	31	1006	550	1.02
1.2292	42.4782	0.61	72	48	39	1054	800	1.07
1.2225	43.7006	0.61	74	54	44	1108	900	1.13
1.2188	44.9194	0.61	76	57	47	1165	950	1.19
1.2205	46.1399	0.61	78	65	53	1230	1083	1.25
1.2207	47.3606	0.61	80	64	52	1294	1067	1.32
1.1072	48.4678	0.55	82	57	51	1351	950	1.37
1.1729	49.6408	0.59	84	67	57	1418	1117	1.44
1.1370	50.7778	0.57	86	61	54	1479	1017	1.51
1.1376	51.9154	0.57	88	71	62	1550	1183	1.58
1.1449	53.0603	0.57	90	76	66	1626	1267	1.65
1.0953	54.1556	0.55	92	76	69	1702	1267	1.73
1.1709	55.3265	0.59	94	87	74	1789	1450	1.82
1.1033	56.4298	0.55	96	83	75	1872	1383	1.91
2.4766	58.9065	0.62	100	157	63	2029	2617	2.06
2.3714	61.2779	0.59	104	184	78	2213	3067	2.25
2.3633	63.6412	0.59	108	196	83	2409	3267	2.45
2.3584	65.9996	0.59	112	218	92	2627	3633	2.67
2.3154	68.3150	0.58	116	214	92	2841	3567	2.89
2.2931	70.6081	0.57	120	221	96	3062	3683	3.12
2.3543	72.9624	0.59	124	239	102	3301	3983	3.36
2.3177	75.2802	0.58	128	248	107	3549	4133	3.61
2.3819	77.6620	0.60	132	270	113	3819	4500	3.89
2.4314	80.0934	0.61	136	283	116	4102	4717	4.17
2.2751	82.3685	0.57	140	294	129	4396	4900	4.47
2.3638	84.7324	0.59	144	306	129	4702	5100	4.78
2.3284	87.0608	0.58	148	312	134	5014	5200	5.10
2.1954	89.2562	0.55	152	309	141	5323	5150	5.42
2.2963	91.5525	0.57	156	331	144	5654	5517	5.75
2.3075	93.8600	0.58	160	312	135	5966	5200	6.07
2.1465	96.0065	0.54	164	314	146	6280	5233	6.39
2.3228	98.3293	0.58	168	334	144	6614	5567	6.73
2.3729	100.7022	0.59	172	353	149	6967	5883	7.09
2.3101	103.0123	0.58	176	365	158	7332	6083	7.46

Table 12.10 Results of the ^{125}I tracer advection using CDP solution

Time	Sample 1	Minus blank	Counts Removed	C_{max}	C/C_{max}	Sample 2	Minus Blank	Counts Remove	C_{max}	C/C_{max}	Mean C/C_{max}	90% conf
Days	d min^{-1} cm^{-3}	d min^{-1} cm^{-3}	d min^{-1} cm^{-3}	d min^{-1} cm^{-3}		d min^{-1} cm^{-3}	d min^{-1} cm^{-3}	d min^{-1} cm^{-3}	d min^{-1} cm^{-3}			+/-
1	48	9	9	3736	0.00	30	0	0	3736	0.00	0.00	0.005
4	65	26	35	3752	0.01	43	4	4	3752	0.00	0.00	0.013
6	70	31	66	3769	0.01	45	6	10	3769	0.00	0.00	0.015
8	70	31	97	3786	0.01	56	17	27	3786	0.00	0.01	0.008
11	67	28	125	3803	0.01	54	15	42	3803	0.00	0.01	0.008
15	78	39	164	3820	0.01	59	20	62	3821	0.01	0.01	0.011
17	75	36	200	3838	0.01	63	24	86	3838	0.01	0.01	0.007
20	86	47	247	3855	0.01	71	32	118	3856	0.01	0.01	0.009
21	92	53	300	3873	0.01	74	35	153	3873	0.01	0.01	0.010
22	120	81	381	3891	0.02	103	64	217	3891	0.02	0.02	0.010
25	161	122	503	3908	0.03	133	94	311	3909	0.02	0.03	0.016
27	185	146	649	3926	0.04	162	123	434	3927	0.03	0.03	0.013
28	192	153	802	3944	0.04	173	134	568	3945	0.03	0.04	0.011
34	328	289	1091	3962	0.07	283	244	812	3963	0.06	0.07	0.025
35	320	281	1372	3979	0.07	329	290	1102	3981	0.07	0.07	0.005
40	436	397	1769	3997	0.10	388	349	1451	3998	0.09	0.09	0.027
43	498	459	2228	4014	0.11	514	475	1926	4016	0.12	0.12	0.009
49	643	604	2832	4032	0.15	578	539	2465	4033	0.13	0.14	0.036
53	735	696	3528	4048	0.17	690	651	3116	4050	0.16	0.17	0.025
57	828	789	4317	4065	0.19	780	741	3857	4067	0.18	0.19	0.027
60	911	872	5189	4081	0.21	849	810	4667	4083	0.20	0.21	0.034
68	1073	1034	6223	4096	0.25	970	931	5598	4099	0.23	0.24	0.056
74	1135	1096	7319	4112	0.27	1117	1078	6676	4115	0.26	0.26	0.010
89	1416	1377	8696	4127	0.33	1392	1353	8029	4130	0.33	0.33	0.014
116	1723	1684	10380	4140	0.41	1718	1679	9708	4144	0.41	0.41	0.003
145	1879	1840	12220	4153	0.44	1929	1890	11598	4156	0.45	0.45	0.026
176	1988	1949	14169	4164	0.47	2026	1987	13585	4168	0.48	0.47	0.020
207	2060	2021	16190	4176	0.48	2041	2002	15587	4179	0.48	0.48	0.011
236	2156	2117	18307	4187	0.51						0.51	
265	2146	2107	20414	4197	0.50						0.50	
298	2060	2021	22435	4208	0.48						0.48	
329	2185	2146	24581	4219	0.51						0.51	
358	2309	2270	26851	4230	0.54						0.54	
390	2268	2229	29080	4240	0.53						0.53	
428	2160	2121	31201	4251	0.50						0.50	
449	2134	2095	33296	4262	0.49						0.49	
480	2267	2228	35524	4274	0.52						0.52	
512	2193	2154	37678	4285	0.50						0.50	

Table 13.2 Results of the NRVB ^{90}Sr tracer only diffusion experiment using NRVB equilibrated water

Time	Sample 1	Sample 2	Mean	90% conf
Days	Bq dm^{-3}	Bq dm^{-3}	Bq dm^{-3}	+/-
1	150	0	75	335
4	433	67	250	818
6	517	100	308	930
8	517	283	400	521
11	467	250	358	483
15	650	333	492	706
17	600	400	500	446
20	783	533	658	558
21	883	583	733	669
22	1350	1067	1208	632
25	2033	1567	1800	1041
27	2433	2050	2242	855
28	2550	2233	2392	706
34	4817	4067	4442	1673
35	4683	4833	4758	335
40	6617	5817	6217	1785
43	7650	7917	7783	595
49	10067	8983	9525	2417
53	11600	10850	11225	1673
57	13150	12350	12750	1785
60	14533	13500	14017	2305
68	17233	15517	16375	3830
74	18267	17967	18117	669
89	22950	22550	22750	892
116	28067	27983	28025	186
145	30667	31500	31083	1859
176	32483	33117	32800	1413
207	33683	33367	33525	706
236	35283		35283	
265	35117		35117	
298	33683		33683	
329	35767		35767	
358	37833		37833	
390	37150		37150	
428	35350		35350	
449	34917		34917	
480	37133		37133	
512	35900		35900	

Table 13.3 Results of the NRVB ^{90}Sr tracer only diffusion experiment using NRVB equilibrated water expressed as activity concentration

Time	Sample 1	Minus blank	Counts Removed	C_{max}	C/C_{max}	Sample 2	Minus Blank	Counts Removed	C_{max}	C/C_{max}	Mean C/C_{max}	90% conf
Days	d min^{-1} cm^{-3}	d min^{-1} cm^{-3}	d min^{-1} cm^{-3}	d min^{-1} cm^{-3}		d min^{-1} cm^{-3}	d min^{-1} cm^{-3}	d min^{-1} cm^{-3}	d min^{-1} cm^{-3}			+/-
1	32	0	9	3736	0.00	27	0	0	3736	0.00	0.00	0.000
4	35	0	9	3752	0.00	36	0	0	3752	0.00	0.00	0.000
6	38	0	9	3769	0.00	39	0	0	3769	0.00	0.00	0.000
8	35	0	9	3786	0.00	31	0	0	3786	0.00	0.00	0.000
11	35	0	9	3803	0.00	34	0	0	3804	0.00	0.00	0.000
15	45	6	15	3821	0.00	33	0	0	3821	0.00	0.00	0.004
17	39	0	15	3838	0.00	37	0	0	3838	0.00	0.00	0.000
20	44	5	20	3856	0.00	39	0	0	3856	0.00	0.00	0.003
21	46	7	27	3874	0.00	44	5	5	3874	0.00	0.00	0.001
22	51	12	39	3892	0.00	46	7	12	3892	0.00	0.00	0.003
25	60	21	60	3910	0.01	68	29	41	3910	0.01	0.01	0.005
27	76	37	97	3928	0.01	81	42	83	3928	0.01	0.01	0.003
28	74	35	132	3947	0.01	86	47	130	3947	0.01	0.01	0.007
34	126	87	219	3965	0.02	130	91	221	3965	0.02	0.02	0.002
35	139	100	319	3984	0.03	141	102	323	3984	0.03	0.03	0.001
40	190	151	470	4002	0.04	199	160	483	4002	0.04	0.04	0.005
43	239	200	670	4021	0.05	229	190	673	4021	0.05	0.05	0.006
49	300	261	931	4039	0.06	303	264	937	4039	0.07	0.06	0.002
53	361	322	1253	4057	0.08	372	333	1270	4057	0.08	0.08	0.006
57	446	407	1660	4076	0.10	415	376	1646	4076	0.09	0.10	0.017
60	475	436	2096	4094	0.11	459	420	2066	4094	0.10	0.10	0.009
68	578	539	2635	4112	0.13	573	534	2600	4112	0.13	0.13	0.003
74	655	616	3251	4129	0.15	633	594	3194	4130	0.14	0.15	0.012
89	865	826	4077	4147	0.20	878	839	4033	4147	0.20	0.20	0.007
116	1175	1136	5213	4163	0.27	1115	1076	5109	4164	0.26	0.27	0.032
145	1386	1347	6560	4179	0.32	1296	1257	6366	4179	0.30	0.31	0.048
176	1493	1454	8014	4193	0.35	1473	1434	7800	4194	0.34	0.34	0.011
207	1639	1600	9614	4207	0.38	1595	1556	9356	4208	0.37	0.38	0.024
236	1613	1574	11188	4220	0.37	1599	1560	10916	4222	0.37	0.37	0.008
265	1577	1538	12726	4234	0.36	1556	1517	12433	4235	0.36	0.36	0.011
298	1676	1637	14363	4248	0.39	1670	1631	14064	4249	0.38	0.38	0.003
329	1643	1604	15967	4261	0.38	1571	1532	15596	4263	0.36	0.37	0.038
358	1823	1784	17751	4275	0.42	1751	1712	17308	4277	0.40	0.41	0.038
390	1745	1706	19457	4288	0.40	1756	1717	19025	4290	0.40	0.40	0.005
428	1751	1712	21169	4302	0.40	1721	1682	20707	4304	0.39	0.39	0.016
449	1665	1626	22795	4315	0.38	1723	1684	22391	4318	0.39	0.38	0.029
480	1736	1697	24492	4330	0.39	1792	1753	24144	4332	0.40	0.40	0.028
512	1715	1676	26168	4344	0.39	1720	1681	25825	4346	0.39	0.39	0.002

Table 13.4 Results of the NRVB ^{90}Sr tracer only diffusion experiment using CDP solution

Time	Sample 1	Sample 2	Mean	90% conf
Days	Bq dm^{-3}	Bq dm^{-3}	Bq dm^{-3}	+/-
1	0	0	0	0
4	0	0	0	0
6	0	0	0	0
8	0	0	0	0
11	0	0	0	0
15	100	0	50	223
17	0	0	0	0
20	83	0	42	186
21	117	83	100	74
22	200	117	158	186
25	350	483	417	297
27	617	700	658	186
28	583	783	683	446
34	1450	1517	1483	149
35	1667	1700	1683	74
40	2517	2667	2592	335
43	3333	3167	3250	372
49	4350	4400	4375	112
53	5367	5550	5458	409
57	6783	6267	6525	1153
60	7267	7000	7133	595
68	8983	8900	8942	186
74	10267	9900	10083	818
89	13767	13983	13875	483
116	18933	17933	18433	2231
145	22450	20950	21700	3346
176	24233	23900	24067	744
207	26667	25933	26300	1636
236	26233	26000	26117	521
265	25633	25283	25458	781
298	27283	27183	27233	223
329	26733	25533	26133	2677
358	29733	28533	29133	2677
390	28433	28617	28525	409
428	28533	28033	28283	1115
449	27100	28067	27583	2157
480	28283	29217	28750	2082
512	27933	28017	27975	186

Table 13.5 Results of the NRVB ^{90}Sr tracer only diffusion experiment using CDP solution expressed as activity concentration

Time	Sample 1	Minus blank	Counts Remove	C_{max}	C/C_{max}	Sample 2	Minus Blank	Counts Removed	C_{max}	C/C_{max}	Mean C/C_{max}	90% conf
Days	d min^{-1} cm^{-3}	d min^{-1} cm^{-3}	d min^{-1} cm^{-3}	d min^{-1} cm^{-3}		d min^{-1} cm^{-3}	d min^{-1} cm^{-3}	d min^{-1} cm^{-3}	d min^{-1} cm^{-3}			+/-
0	47	15	15	6707	0.00	25	0	0	6707	0.00	0.00	0.005
2	55	23	38	6737	0.00	30	0	0	6737	0.00	0.00	0.008
3	51	19	57	6767	0.00	32	0	0	6767	0.00	0.00	0.006
7	61	29	86	6798	0.00	36	4	4	6798	0.00	0.00	0.008
13	85	53	139	6828	0.01	54	22	26	6829	0.00	0.01	0.010
15	90	58	197	6859	0.01	100	68	94	6860	0.01	0.01	0.003
16			197	6890				94	6891			0.000
17	119	87	284	6922	0.01			94	6923		0.01	0.000
20	192	160	444	6954	0.02	229	197	291	6955	0.03	0.03	0.012
23	291	259	703	6985	0.04	318	286	577	6986	0.04	0.04	0.009
26	412	380	1083	7017	0.05	446	414	991	7018	0.06	0.06	0.011
29	532	500	1583	7048	0.07	559	527	1518	7049	0.07	0.07	0.009
35	775	743	2326	7079	0.10	863	831	2349	7079	0.12	0.11	0.028
48	1474	1442	3768	7109	0.20	1637	1605	3954	7109	0.23	0.21	0.051
64	2221	2189	5957	7136	0.31	2243	2211	6165	7135	0.31	0.31	0.007
73	2447	2415	8372	7160	0.34	2645	2613	8778	7159	0.37	0.35	0.062
94	2798	2766	11138	7182	0.39	3144	3112	11890	7181	0.43	0.41	0.108
125	3665	3633	14771	7204	0.50	3779	3747	15637	7200	0.52	0.51	0.036
156	3770	3738	18509	7221	0.52	3748	3716	19353	7217	0.51	0.52	0.006
185	4136	4104	22613	7238	0.57	4090	4058	23411	7234	0.56	0.56	0.013
219	4142	4110	26723	7253	0.57	4244	4212	27623	7250	0.58	0.57	0.032
248	4254	4222	30945	7269	0.58	4193	4161	31784	7265	0.57	0.58	0.018
308	4130	4098	35043	7284	0.56	4164	4132	35916	7280	0.57	0.57	0.011

Table 13.6 Results of the NRVB ^{90}Sr tracer and $Sr(NO_3)_2$ carrier diffusion experiment using NRVB equilibrated water

Time	Sample 1	Sample 2	Mean	90% conf
Days	Bq dm^{-3}	Bq dm^{-3}	Bq dm^{-3}	+/-
0	250	0	125	558
2	383	0	192	855
3	317	0	158	706
7	483	67	275	930
13	883	367	625	1153
15	967	1133	1050	372
16				0
17	1450		1450	0
20	2667	3283	2975	1376
23	4317	4767	4542	1004
26	6333	6900	6617	1264
29	8333	8783	8558	1004
35	12383	13850	13117	3272
48	24033	26750	25392	6061
64	36483	36850	36667	818
73	40250	43550	41900	7362
94	46100	51867	48983	12865
125	60550	62450	61500	4239
156	62300	61933	62117	818
185	68400	67633	68017	1710
219	68500	70200	69350	3793
248	70367	69350	69858	2268
308	68300	68867	68583	1264

Table 13.7 Results of the NRVB ^{90}Sr tracer and $Sr(NO_3)_2$ carrier diffusion experiment using NRVB equilibrated water expressed as activity concentration

Time	Sample 1	Minus blank	Counts Remove	C_{max}	C/C_{max}	Sample 2	Minus Blank	Counts Removed	C_{max}	C/C_{max}	Mean C/C_{max}	90% conf
Days	d min^{-1} cm^{-3}	d min^{-1} cm^{-3}	d min^{-1} cm^{-3}	d min^{-1} cm^{-3}		d min^{-1} cm^{-3}	d min^{-1} cm^{-3}	d min^{-1} cm^{-3}	d min^{-1} cm^{-3}			+/-
0	30	0	15	6707	0.00	78	0	0	6707	0.00	0.00	0.000
2	32	0	15	6737	0.00	77	0	0	6737	0.00	0.00	0.000
3	34	2	17	6767	0.00	75	43	43	6767	0.01	0.00	0.014
7	34	2	19	6798	0.00	91	59	102	6798	0.01	0.00	0.019
13	115	83	102	6829	0.01	153	121	223	6828	0.02	0.01	0.012
15			102	6859	0.00	243	211	434	6859	0.03	0.02	0.069
16			102	6891		249		434	6889			0.000
17	338	306	408	6923	0.04	332	300	734	6921	0.04	0.04	0.002
20	372	340	748	6953	0.05	392	360	1094	6952	0.05	0.05	0.006
23	537	505	1253	6984	0.07			1094	6982		0.07	0.000
26	657	625	1878	7014	0.09	642	610	1704	7015	0.09	0.09	0.005
29	784	752	2630	7044	0.11	758	726	2430	7045	0.10	0.10	0.008
35	1098	1066	3696	7074	0.15	923	891	3321	7075	0.13	0.14	0.055
48	1761	1729	5425	7103	0.24	1313	1281	4602	7104	0.18	0.21	0.141
64	2192	2160	7585	7128	0.30	1966	1934	6536	7132	0.27	0.29	0.071
73	2306	2274	9859	7152	0.32	2501	2469	9005	7157	0.34	0.33	0.060
94	2847	2815	12674	7175	0.39	2534	2502	11507	7179	0.35	0.37	0.098
125	3396	3364	16038	7196	0.47	3142	3110	14617	7202	0.43	0.45	0.079
156	3508	3476	19514	7215	0.48	3698	3666	18283	7222	0.51	0.49	0.058
185	4033	4001	23515	7233	0.55	4074	4042	22325	7239	0.56	0.56	0.012
219	4051	4019	27534	7249	0.55	3984	3952	26277	7255	0.54	0.55	0.022
248	3809	3777	31311	7265	0.52	3868	3836	30113	7271	0.53	0.52	0.017
308	3968	3936	35247	7282	0.54	3882	3850	33963	7288	0.53	0.53	0.027

Table 13.8 Results of the NRVB ^{90}Sr tracer and $Sr(NO_3)_2$ carrier diffusion experiment using CDP solution

Time	Sample 1	Sample 2	Mean	90% conf
Days	Bq dm^{-3}	Bq dm^{-3}	Bq dm^{-3}	+/-
0	0	0	0	0
2	0	0	0	0
3	33	717	375	1524
7	33	983	508	2119
13	1383	2017	1700	1413
15		3517	3517	0
16				0
17	5100	5000	5050	223
20	5667	6000	5833	744
23	8417		8417	0
26	10417	10167	10292	558
29	12533	12100	12317	967
35	17767	14850	16308	6507
48	28817	21350	25083	16658
64	36000	32233	34117	8403
73	37900	41150	39525	7250
94	46917	41700	44308	11638
125	56067	51833	53950	9444
156	57933	61100	59517	7065
185	66683	67367	67025	1524
219	66983	65867	66425	2491
248	62950	63933	63442	2194
308	65600	64167	64883	3198

Table 13.9 Results of the NRVB ^{90}Sr tracer and $Sr(NO_3)_2$ carrier diffusion experiment using CDP solution expressed as activity concentration

Time	Sample 1	Minus blank	Counts Removed	C_{max}	C/C_{max}	Sample 2	Minus Blank	Counts Removed	C_{max}	C/C_{max}	Mean C/C_{max}	90% conf
Days	d min^{-1} cm^{-3}	d min^{-1} cm^{-3}	d min^{-1} cm^{-3}	d min^{-1} cm^{-3}		d min^{-1} cm^{-3}	d min^{-1} cm^{-3}	d min^{-1} cm^{-3}	d min^{-1} cm^{-3}			+/-
1	27	0	15	3363	0.00	24	0	0	3363	0.00	0.00	0.00
9	27	0	15	3378	0.00	32	0	0	3378	0.00	0.00	0.00
19	81	49	64	3393	0.01	68	36	36	3393	0.01	0.01	0.009
26	183	151	215	3408	0.04	157	125	161	3408	0.04	0.04	0.017
33	294	262	477	3423	0.08	273	241	402	3423	0.07	0.07	0.014
41	479	447	924	3438	0.13	406	374	776	3438	0.11	0.12	0.047
48	610	578	1502	3451	0.17	541	509	1285	3452	0.15	0.16	0.045
58	768	736	2238	3465	0.21	673	641	1926	3466	0.18	0.20	0.061
87	1074	1042	3280	3477	0.30	984	952	2878	3479	0.27	0.29	0.058
121	1294	1262	4542	3488	0.36	1184	1152	4030	3490	0.33	0.35	0.071
155	1351	1319	5861	3499	0.38	1290	1258	5288	3501	0.36	0.37	0.039
184	1422	1390	7251	3509	0.40	1298	1266	6554	3512	0.36	0.38	0.079
244	1539	1507	8758	3519	0.43	1439	1407	7961	3522	0.40	0.41	0.064
336			8758	3529		1422	1390	9351	3532	0.39	0.39	

Table 13.10 Results of the NRVB ^{90}Sr tracer only diffusion experiment using gluconate in NRVB equilibrated water

Time	Sample 1	Sample 2	Mean	90% conf
Days	Bq dm^{-3}	Bq dm^{-3}	Bq dm^{-3}	+/-
1	0	0	0	0
9	0	0	0	0
19	817	600	708	483
26	2517	2083	2300	967
33	4367	4017	4192	781
41	7450	6233	6842	2714
48	9633	8483	9058	2566
58	12267	10683	11475	3532
87	17367	15867	16617	3346
121	21033	19200	20117	4090
155	21983	20967	21475	2268
184	23167	21100	22133	4611
244	25117	23450	24283	3718
336		23167	23167	

Table 13.11 Results of the NRVB ^{90}Sr tracer only diffusion experiment using gluconate in NRVB equilibrated water expressed as activity concentration

Time	Sample 1	Minus blank	Counts Removed	C_{max}	C/C_{max}	Sample 2	Minus Blank	Counts Removed	C_{max}	C/C_{max}	Mean C/C_{max}	90%
Days	d min^{-1} cm^{-3}	d min^{-1} cm^{-3}	d min^{-1} cm^{-3}	d min^{-1} cm^{-3}		d min^{-1} cm^{-3}	d min^{-1} cm^{-3}	d min^{-1} cm^{-3}	d min^{-1} cm^{-3}			+/-
0	50	18	15	3261	0.01	33	1	0	3261	0.00	0.00	0.012
3	48	16	31	3276	0.00	41	9	9	3276	0.00	0.00	0.005
5	46	14	45	3291	0.00	43	11	20	3291	0.00	0.00	0.002
7	48	16	61	3306	0.00	44	12	32	3306	0.00	0.00	0.003
10	45	13	74	3321	0.00	43	11	43	3321	0.00	0.00	0.001
14	56	24	98	3336	0.01	51	19	62	3336	0.01	0.01	0.003
17	47	15	113	3351	0.00	49	17	79	3351	0.01	0.00	0.001
20	46	14	127	3366	0.00	61	29	108	3366	0.01	0.01	0.010
24	53	21	148	3382	0.01	56	24	132	3382	0.01	0.01	0.002
25	62	30	178	3397	0.01	61	29	161	3397	0.01	0.01	0.001
31	81	49	227	3413	0.01	85	53	214	3413	0.02	0.01	0.003
38	129	97	324	3429	0.03	122	90	304	3429	0.03	0.03	0.005
47	210	178	502	3445	0.05	213	181	485	3445	0.05	0.05	0.002
54	279	247	749	3460	0.07	274	242	727	3460	0.07	0.07	0.003
61	362	330	1079	3475	0.09	340	308	1035	3475	0.09	0.09	0.014
67	445	413	1492	3490	0.12	444	412	1447	3491	0.12	0.12	0.001
74	545	513	2005	3505	0.15	500	468	1915	3505	0.13	0.14	0.029
87	755	723	2728	3520	0.21	678	646	2561	3520	0.18	0.19	0.049
102	850	818	3546	3533	0.23	840	808	3369	3534	0.23	0.23	0.006
115	880	848	4394	3546	0.24	842	810	4179	3547	0.23	0.23	0.024

Table 13.12 Results of the NRVB ^{90}Sr tracer only diffusion experiment using high ionic strength NRVB equilibrated water

Time	Sample 1	Sample 2	Mean	90% conf
Days	Bq dm^{-3}	Bq dm^{-3}	Bq dm^{-3}	+/-
0	300	17	158	632
3	267	150	208	260
5	233	183	208	112
7	267	200	233	149
10	217	183	200	74
14	400	317	358	186
17	250	283	267	74
20	233	483	358	558
24	350	400	375	112
25	500	483	492	37
31	817	883	850	149
38	1617	1500	1558	260
47	2967	3017	2992	112
54	4117	4033	4075	186
61	5500	5133	5317	818
67	6883	6867	6875	37
74	8550	7800	8175	1673
87	12050	10767	11408	2863
102	13633	13467	13550	372
115	14133	13500	13817	1413

Table 13.13 Results of the NRVB ^{90}Sr tracer only diffusion experiment using high ionic strength NRVB equilibrated water expressed as activity concentration

Time	Sample 1	Minus blank	Counts Removed	C_{max}	C/C_{max}	Sample 2	Minus Blank	Counts Removed	C_{max}	C/C_{max}	Mean C/C_{max}
Days	d min^{-1} cm^{-3}	d min^{-1} cm^{-3}	d min^{-1} cm^{-3}	d min^{-1} cm^{-3}		d min^{-1} cm^{-3}	d min^{-1} cm^{-3}	d min^{-1} cm^{-3}	d min^{-1} cm^{-3}		
0	42	10	15	3261	0.00	33	1	0	3261	0.00	0.00
1	43	11	26	3276	0.00	36	4	4	3276	0.00	0.00
2	45	13	39	3291	0.00	35	3	7	3291	0.00	0.00
4	42	10	49	3306	0.00	33	1	8	3306	0.00	0.00
7	42	10	59	3321	0.00	40	8	16	3321	0.00	0.00
8	46	14	73	3336	0.00	38	6	22	3336	0.00	0.00
10	44	12	85	3351	0.00	37	5	27	3351	0.00	0.00
14	53	21	106	3366	0.01	36	4	31	3367	0.00	0.00
17	47	15	121	3382	0.00	34	2	33	3382	0.00	0.00
21	47	15	136	3397	0.00	35	3	36	3398	0.00	0.00
28	53	21	157	3413	0.01	36	4	40	3414	0.00	0.00
29	49	17	174	3429	0.00	35	3	43	3430	0.00	0.00
35	40	8	182	3445	0.00	36	4	47	3446	0.00	0.00
42	79	47	229	3462	0.01	44	12	59	3462	0.00	0.01
51	156	124	353	3478	0.04	60	28	87	3479	0.01	0.02
58	207	175	528	3494	0.05	78	46	133	3495	0.01	0.03
65	284	252	780	3510	0.07	106	74	207	3512	0.02	0.05
71	363	331	1111	3526	0.09	138	106	313	3528	0.03	0.06
78	422	390	1501	3541	0.11	178	146	459	3545	0.04	0.08
91	608	576	2077	3556	0.16	263	231	690	3562	0.06	0.11
106	756	724	2801	3571	0.20	379	347	1037	3578	0.10	0.15
119	781	749	3550	3585	0.21	414	382	1419	3594	0.11	0.16

Table 13.14 Results of the NRVB ^{90}Sr tracer only diffusion experiment using gradient ionic strength NRVB equilibrated water

Time	Sample 1	Sample 2	Mean
Days	Bq dm^{-3}	Bq dm^{-3}	Bq dm^{-3}
0	167	17	92
1	183	67	125
2	217	50	133
4	167	17	92
7	167	133	150
8	233	100	167
10	200	83	142
14	350	67	208
17	250	33	142
21	250	50	150
28	350	67	208
29	283	50	167
35	133	67	100
42	783	200	492
51	2067	467	1267
58	2917	767	1842
65	4200	1233	2717
71	5517	1767	3642
78	6500	2433	4467
91	9600	3850	6725
106	12067	5783	8925
119	12483	6367	9425

Table 13.15 Results of the NRVB ^{90}Sr tracer only diffusion experiment using gradient ionic strength NRVB equilibrated water expressed as concentration

Time	Sample 1	Minus Blank	Counts Removed	C_{max}	C/C_{max}	Activity concentration
Days	d min^{-1} cm^{-} $_{3}$	d min^{-1} cm^{-3}	d min^{-1} cm^{-3}	d min^{-1} cm^{-3}		Bq dm^{-3}
1	36	4	4	3363	0.00	67
4	41	9	13	3378	0.00	150
7	44	12	25	3393	0.00	200
15	51	19	44	3408	0.01	317
22	95	63	107	3424	0.02	1050
28	148	116	223	3439	0.03	1933
36	294	262	485	3454	0.08	4367
56	720	688	1173	3469	0.20	11467
70	839	807	1980	3482	0.23	13450
83	1008	976	2956	3495	0.28	16267
96	1278	1246	4202	3506	0.36	20767
126	1353	1321	5523	3517	0.38	22017
134	1345	1313	6836	3527	0.37	21883
147	1425	1393	8229	3538	0.39	23217
188	1504	1472	9701	3548	0.41	24533
201	1530	1498	11199	3558	0.42	24967
213	1523	1491	12690	3568	0.42	24850
241	1373	1341	14031	3578	0.37	22350

Table 13.16 Results of the repeated NRVB ^{90}Sr tracer only diffusion experiment using CDP solution

Mass eluted (g)	Cumulative mass eluted (g)	Flow rate (g hr^{-1})	Time (hr)	d min^{-1} g^{-1}	Total d min^{-1}	Bq dm^{-3}	Cumulative d min^{-1}	% recovery
2.6335	2.6335	0.8778	3.0	8	20	127	20	0.00
2.6375	5.2710	0.8792	6.0	9	23	145	43	0.01
2.5923	7.8633	0.8641	9.0	8	20	129	63	0.01
2.5193	10.3826	0.8398	12.0	11	28	185	91	0.01
2.4959	12.8785	0.8320	15.0	10	25	167	116	0.02
2.4849	15.3634	0.8283	18.0	8	21	141	137	0.02
2.5411	17.9045	0.8470	21.0	12	31	203	168	0.02
2.7561	20.6606	0.9187	24.0	10	28	169	196	0.03
2.9170	23.5776	0.9723	27.0	10	28	160	224	0.03
2.9719	26.5495	0.9906	30.0	11	33	185	257	0.03
2.8845	29.4340	0.9615	33.0	11	31	179	288	0.04
2.7953	32.2293	0.9318	36.0	11	32	191	320	0.04
2.6723	34.9016	0.8908	39.0	14	38	237	358	0.05
2.5712	37.4728	0.8571	42.0	16	41	266	399	0.05
2.5868	40.0596	0.8623	45.0	19	50	322	449	0.06
2.8059	42.8655	0.9353	48.0	20	56	333	505	0.07
2.9235	45.7890	0.9745	51.0	29	86	490	591	0.08
2.9749	48.7639	0.9916	54.0	41	122	684	713	0.10
2.9856	51.7495	0.9952	57.0	49	145	809	858	0.12
2.8854	54.6349	0.9618	60.0	79	227	1311	1085	0.15
2.8682	57.5031	0.9561	63.0	120	344	1999	1429	0.19
2.8034	60.3065	0.9345	66.0	199	559	3323	1988	0.27
2.9209	63.2274	0.9736	69.0	320	934	5329	2922	0.39
3.1760	66.4034	1.0587	72.0	462	1466	7693	4388	0.59
3.0497	69.4531	1.0166	75.0	667	2033	11110	6421	0.87
2.9784	72.4315	0.9928	78.0	929	2766	15478	9187	1.24
2.9283	75.3598	0.9761	81.0	1124	3290	18725	12477	1.68
2.9649	78.3247	0.9883	84.0	1507	4468	25116	16945	2.29
2.7913	81.1160	0.9304	87.0	1861	5196	31025	22141	2.99
2.6870	83.8030	0.8957	90.0	2293	6161	38215	28302	3.82
2.7668	86.5698	0.9223	93.0	2692	7449	44872	35751	4.83
2.9195	89.4893	0.9732	96.0	3209	9370	53491	45121	6.09
2.7031	92.1924	0.9010	99.0	3562	9628	59364	54749	7.39
2.8251	95.0175	0.9417	102.0	3938	11124	65625	65873	8.89
2.8275	97.8450	0.9425	105.0	4202	11882	70038	77755	10.50
2.6632	100.5082	0.8877	108.0	4391	11694	73184	89449	12.07
2.5776	103.0858	0.8592	111.0	4556	11743	75929	101192	13.66
2.6052	105.6910	0.8684	114.0	4626	12051	77096	113243	15.29
2.5423	108.2333	0.8474	117.0	4672	11877	77861	125120	16.89
2.5483	110.7816	0.8494	120.0	4785	12194	79751	137314	18.53
2.6996	113.4813	0.8999	123.0	4855	13108	80925	150422	20.30
2.5878	116.0690	0.8626	126.0	4744	12277	79070	162699	21.96
2.2282	118.2973	0.7427	129.0	4403	9810	73376	172509	23.29
2.4843	120.7816	0.8281	132.0	4422	10986	73703	183495	24.77

2.4606	123.2421	0.8202	135.0	4429	10897	73811	194392	26.24
2.4342	125.6764	0.8114	138.0	4343	10572	72385	204964	27.67
2.4610	128.1373	0.8203	141.0	4304	10593	71740	215557	29.10
2.9822	131.1195	0.8521	144.5	4266	12721	71095	228278	30.81
1.7848	132.9043	0.7139	147.0	4082	7286	68038	235564	31.80
1.9456	134.8499	0.6485	150.0	4350	8463	72498	244027	32.94
2.3643	137.2142	0.7881	153.0	4052	9580	67531	253607	34.23
10.6500	147.8642	0.7500	171.0	4067	43314	67784	296921	40.08
4.9043	152.7686	0.8174	177.0	5630	27613	93839	324534	43.81
3.5044	156.2729	0.5841	183.0	5091	17840	84847	342374	46.21
3.8011	160.0740	0.6335	189.0	4480	17030	74672	359404	48.51
4.2588	164.3328	0.7098	195.0	4010	17080	66842	376484	50.82
4.5270	168.8598	0.7545	201.0	3859	17469	64315	393953	53.18
4.4446	173.3044	0.7408	207.0	3584	15929	59732	409882	55.33
4.8461	178.1505	0.8077	213.0	3083	14942	51388	424824	57.34
4.6943	182.8448	0.7824	219.0	2810	13190	46830	438014	59.12
5.1324	187.9772	0.8554	225.0	2624	13468	43735	451482	60.94
5.1463	193.1235	0.8577	231.0	2143	11027	35712	462509	62.43
4.6281	197.7515	0.7713	237.0	2661	12313	44342	474822	64.09
4.9010	202.6525	0.8168	243.0	2182	10695	36370	485517	65.54
4.8554	207.5080	0.8092	249.0	2119	10287	35311	495804	66.92
4.7203	212.2282	0.7867	255.0	1902	8976	31693	504780	68.14
4.5071	216.7353	0.7512	261.0	1731	7803	28855	512583	69.19
4.2897	221.0250	0.7150	267.0	1679	7202	27982	519785	70.16
5.1282	226.1532	0.8547	273.0	1468	7530	24473	527315	71.18
5.0239	231.1771	0.8373	279.0	1467	7368	24443	534683	72.17
4.6778	235.8549	0.7796	285.0	1397	6537	23291	541220	73.05
4.3712	240.2261	0.7285	291.0	1380	6034	23007	547254	73.87
4.4383	244.6644	0.7397	297.0	1244	5521	20732	552775	74.61
4.5477	249.2121	0.7580	303.0	1112	5058	18537	557833	75.30
4.4871	253.6992	0.7478	309.0	1042	4676	17368	562509	75.93
4.2498	257.9490	0.7083	315.0	879	3734	14644	566243	76.43
5.2673	263.2163	0.8779	321.0	858	4517	14292	570760	77.04
5.4985	268.7148	0.9164	327.0	901	4954	15016	575714	77.71
5.1576	273.8724	0.8596	333.0	907	4676	15110	580390	78.34
5.1591	279.0315	0.8599	339.0	760	3923	12673	584313	78.87
3.5488	282.5804	0.7886	343.5	740	2625	12328	586938	79.22
2.7536	285.3340	0.9179	346.5	674	1857	11240	588795	79.48
2.6960	288.0299	0.8987	349.5	661	1783	11023	590578	79.72
2.6971	290.7270	0.8990	352.5	670	1807	11166	592385	79.96
2.5586	293.2856	0.8529	355.5	639	1634	10644	594019	80.18
2.6099	295.8955	0.8700	358.5	666	1738	11099	595757	80.42
2.5577	298.4531	0.8526	361.5	679	1737	11319	597494	80.65
2.5709	301.0241	0.8570	364.5	715	1837	11909	599331	80.90
2.7368	303.7609	0.9123	367.5	726	1987	12100	601318	81.17
2.8233	306.5843	0.9411	370.5	757	2136	12609	603454	81.45
2.6061	309.1904	0.8687	373.5	713	1858	11882	605312	81.71

2.6303	311.8207	0.8768	376.5	709	1866	11824	607178	81.96
2.5910	314.4117	0.8637	379.5	689	1785	11482	608963	82.20
2.5655	316.9772	0.8552	382.5	697	1789	11622	610752	82.44
2.5332	319.5104	0.8444	385.5	670	1698	11172	612450	82.67
2.4093	321.9197	0.8031	388.5	633	1525	10549	613975	82.87
2.7110	324.6306	0.9037	391.5	637	1728	10624	615703	83.11
2.4744	327.1050	0.8248	394.5	609	1507	10151	617210	83.31
2.5742	329.6791	0.8581	397.5	555	1429	9252	618639	83.50
2.0088	331.6880	0.6696	400.5	483	971	8056	619610	83.64
2.6367	334.3247	0.8789	403.5	410	1081	6833	620691	83.78
2.5990	336.9237	0.8663	406.5	427	1111	7124	621802	83.93
2.6199	339.5437	0.8733	409.5	448	1175	7475	622977	84.09
2.7039	342.2476	0.9013	412.5	460	1244	7668	624221	84.26
2.6183	344.8659	0.8728	415.5	505	1322	8415	625543	84.44
3.1655	348.0314	1.0552	418.5	528	1672	8803	627215	84.66
3.1494	351.1807	1.0498	421.5	477	1501	7943	628716	84.86
3.1403	354.3211	1.0468	424.5	456	1431	7595	630147	85.06
3.0633	357.3844	1.0211	427.5	448	1371	7459	631518	85.24
3.0638	360.4481	1.0213	430.5	439	1346	7322	632864	85.42
2.5857	363.0338	0.8619	433.5	286	740	4770	633604	85.52

Table 13.17 Run 1 results of the ^{90}Sr tracer advection experiments using NRVB equilibrated water

Mass eluted (g)	Cumulative mass eluted (g)	Flow rate (g hr^{-1})	Time (hr)	d min^{-1} g^{-1}	Total d min^{-1}	Bq dm^{-3}	Cumulative d min^{-1}	% recovery
3.3852	3.3852	1.1284	3	0	0	0	0	0.00
3.2578	6.6430	1.0859	6	0	0	0	0	0.00
2.7137	9.3567	0.9046	9	141	382	2345	382	0.05
3.1438	12.5005	1.0479	12	72	226	1197	608	0.08
2.0974	14.5979	0.6991	15	234	491	3900	1098	0.15
1.7056	16.3035	0.5685	18	23	40	391	1138	0.15
1.5507	17.8542	0.5169	21	0	0	0	1138	0.15
1.7404	19.5946	0.5801	24	0	0	0	1138	0.15
1.7433	21.3379	0.5811	27	0	0	0	1138	0.15
1.8211	23.1590	0.6070	30	42	76	700	1215	0.16
1.7744	24.9334	0.5915	33	83	147	1379	1362	0.18
1.6719	26.6053	0.5573	36	11	19	189	1381	0.19
1.7165	28.3218	0.5722	39	0	0	0	1381	0.19
1.8852	30.2070	0.6284	42	0	0	0	1381	0.19
1.8316	32.0386	0.6105	45	0	0	0	1381	0.19
1.9186	33.9572	0.6395	48	34	64	560	1445	0.20
2.1572	36.1144	0.7191	51	0	0	0	1445	0.20
2.2219	38.3363	0.7406	54	0	0	0	1445	0.20
2.1569	40.4932	0.7190	57	21	46	358	1491	0.20
2.2218	42.7150	0.7406	60	0	0	0	1491	0.20
2.1847	44.8997	0.7282	63	0	0	0	1491	0.20
2.2053	47.1050	0.7351	66	0	0	0	1491	0.20
2.1707	49.2757	0.7236	69	33	72	554	1564	0.21
2.2960	51.5717	0.7653	72	66	152	1102	1715	0.23
2.3659	53.9376	0.7886	75	120	285	2006	2000	0.27
2.2873	56.2250	0.7624	78	288	658	4798	2659	0.36
2.2308	58.4557	0.7436	81	373	832	6219	3491	0.47
2.1360	60.5917	0.7120	84	397	848	6615	4339	0.59
2.1475	62.7392	0.7158	87	534	1147	8898	5485	0.74
1.9448	64.6840	0.6483	90	572	1113	9539	6598	0.89
2.0779	66.7619	0.6926	93	790	1641	13161	8239	1.11
2.2137	68.9756	0.7379	96	900	1993	15003	10232	1.38
2.3580	71.3337	0.7860	99	1142	2693	19031	12924	1.74
2.2680	73.6017	0.7560	102	1378	3125	22967	16050	2.17
2.2452	75.8468	0.7484	105	1562	3506	26028	19556	2.64
2.2388	78.0857	0.7463	108	2055	4600	34243	24156	3.26
2.2839	80.3696	0.7613	111	2345	5355	39077	29511	3.98
1.8763	82.2458	0.6254	114	2417	4534	40275	34045	4.60
2.1179	84.3637	0.7060	117	2449	5186	40810	39231	5.30
2.2412	86.6049	0.7471	120	2884	6465	48073	45695	6.17
2.0865	88.6914	0.6955	123	2914	6081	48575	51776	6.99
2.2286	90.9200	0.7429	126	3029	6751	50485	58527	7.90
2.1820	93.1020	0.7273	129	3307	7217	55122	65744	8.87
1.8911	94.9931	0.6304	132	3698	6993	61631	72737	9.82
1.8016	96.7947	0.6005	135	3495	6297	58252	79033	10.67

2.0224	98.8171	0.6741	138	4459	9018	74319	88052	11.89
2.1096	100.9268	0.7032	141	4732	9983	78872	98035	13.23
2.2184	103.1451	0.7395	144	4884	10834	81399	108870	14.70
2.1952	105.3403	0.7317	147	4864	10677	81065	119547	16.14
1.9969	107.3373	0.6656	150	4533	9053	75557	128600	17.36
2.1581	109.4954	0.7194	153	4780	10315	79665	138915	18.75
2.1134	111.6088	0.7045	156	4900	10356	81672	149272	20.15
2.0326	113.6414	0.6775	159	4990	10143	83168	159414	21.52
1.9836	115.6249	0.6612	162	5024	9966	83734	169380	22.86
2.0096	117.6346	0.6699	165	5095	10239	84914	179619	24.24
1.8459	119.4804	0.6153	168	5255	9699	87576	189318	25.55
1.9775	121.4580	0.6592	171	5414	10707	90238	200025	27.00
1.5594	123.0174	0.5198	174	4952	7723	82540	207748	28.04
1.9052	124.9226	0.6351	177	5248	9998	87460	217745	29.39
1.8597	126.7823	0.6199	180	5343	9937	89057	227682	30.73
1.8411	128.6233	0.6137	183	5306	9769	88440	237452	32.05
1.8537	130.4771	0.6179	186	5271	9770	87845	247222	33.37
2.7794	133.2565	0.4632	192	5378	14947	89631	262169	35.39
3.4965	136.7530	0.5828	198	5485	19178	91416	281348	37.98
3.3884	140.1414	0.5647	204	5143	17427	85720	298775	40.33
3.1912	143.3325	0.5319	210	5223	16666	87044	315441	42.58
3.3341	146.6667	0.5557	216	4965	16555	82753	331996	44.81
3.3937	150.0603	0.5656	222	4770	16187	79496	348183	47.00
3.0474	153.1078	0.5079	228	4562	13904	76041	362087	48.87
3.1729	156.2807	0.5288	234	4471	14187	74520	376273	50.79
3.5004	159.7810	0.5834	240	4171	14600	69518	390874	52.76
3.4908	163.2719	0.5818	246	4015	14017	66921	404890	54.65
3.4288	166.7006	0.5715	252	3666	12570	61101	417460	56.35
3.4252	170.1259	0.5709	258	3402	11654	56707	429114	57.92
3.5737	173.6996	0.5956	264	3312	11836	55201	440951	59.52
3.4349	177.1345	0.5725	270	3108	10674	51792	451625	60.96
3.4933	180.6278	0.5822	276	2906	10152	48437	461777	62.33
3.4892	184.1170	0.5815	282	2757	9621	45954	471398	63.63
3.7045	187.8214	0.6174	288	2569	9517	42818	480915	64.91
3.6602	191.4817	0.6100	294	2468	9034	41137	489949	66.13
3.1018	194.5834	0.5170	300	2169	6728	36154	496677	67.04
3.1822	197.7657	0.5304	306	2052	6530	34203	503208	67.92
3.4226	201.1883	0.5704	312	1982	6784	33036	509992	68.84

Table 13.18 Run 2 results of the ^{90}Sr tracer advection experiments using NRVB equilibrated water

Mass eluted (g)	Cumulative mass eluted (g)	Flow rate (g hr^{-1})	Time (hr)	d min^{-1} g^{-1}	Total d min^{-1}	Bq dm^{-3}	Cumulative d min^{-1}	% recovery
3.2923	3.2923	0.5487	6	86	282	1427	282	0.04
2.9545	6.2468	0.4924	12	0	0	0	282	0.04
3.0194	9.2662	0.5032	18	42	128	704	410	0.06
3.1602	12.4264	0.5267	24	1	4	23	414	0.06
3.1550	15.5814	0.5258	30	10	32	171	446	0.06
3.1377	18.7191	0.5230	36	0	0	0	446	0.06
3.4622	22.1814	0.5770	42	0	0	0	446	0.06
3.2854	25.4667	0.5476	48	0	0	0	446	0.06
3.1497	28.6164	0.5250	54	5	16	83	462	0.06
3.3145	31.9310	0.5524	60	0	0	0	462	0.06
3.1952	35.1261	0.5325	66	32	102	533	564	0.08
3.5587	38.6848	0.5931	72	48	171	803	735	0.10
3.4825	42.1674	0.5804	78	133	464	2222	1200	0.16
3.6632	45.8305	0.6105	84	259	949	4320	2149	0.29
3.7572	49.5877	0.6262	90	447	1680	7452	3829	0.51
3.7890	53.3768	0.6315	96	708	2682	11799	6511	0.87
4.0537	57.4304	0.6756	102	897	3635	14946	10147	1.36
4.4130	61.8435	0.7355	108	1175	5187	19589	15333	2.06
4.4030	66.2465	0.7338	114	1486	6541	24758	21874	2.94
4.5532	70.7997	0.7589	120	1789	8146	29818	30020	4.03
4.5417	75.3414	0.7570	126	2077	9431	34608	39451	5.30
4.5499	79.8913	0.7583	132	2240	10191	37329	49642	6.67
4.6240	84.5153	0.7707	138	2514	11626	41903	61267	8.23
4.5228	89.0381	0.7538	144	2624	11869	43739	73137	9.82
4.8892	93.9273	0.8149	150	2719	13295	45321	86432	11.61
4.6949	98.6222	0.7825	156	2937	13790	48952	100221	13.46
4.5637	103.1859	0.7606	162	2986	13626	49763	113847	15.29
4.6418	107.8277	0.7736	168	3195	14829	53244	128676	17.28
4.5968	112.4245	0.7661	174	3010	13834	50159	142511	19.14
4.5213	116.9458	0.7536	180	2987	13506	49788	156017	20.96
4.6524	121.5982	0.7754	186	3181	14800	53018	170817	22.94
4.6310	126.2292	0.7718	192	2940	13614	48997	184431	24.77
4.8695	131.0987	0.8116	198	3449	16793	57475	201224	27.03
4.9356	136.0343	0.8226	204	2907	14346	48443	215569	28.95
4.8290	140.8633	0.8048	210	3100	14968	51659	230537	30.96
3.6781	144.5414	0.6130	216	3031	11147	50512	241684	32.46
4.7372	149.2786	0.7895	222	3076	14571	51266	256256	34.42
4.5784	153.8570	0.7631	228	2635	12066	43923	268321	36.04
4.7483	158.6053	0.7914	234	2608	12385	43471	280706	37.70
4.5318	163.1372	0.7553	240	2603	11796	43382	292502	39.29
4.6909	167.8280	0.7818	246	2443	11461	40720	303963	40.83
4.5202	172.3482	0.7534	252	2587	11695	43123	315658	42.40
4.5638	176.9120	0.7606	258	2706	12349	45099	328008	44.06
4.6433	181.5553	0.7739	264	2443	11345	40722	339353	45.58

4.7042	186.2595	0.7840	270	2425	11407	40415	350760	47.11
4.4364	190.6959	0.7394	276	2563	11372	42721	362132	48.64
4.5214	195.2173	0.7536	282	2634	11907	43893	374039	50.24
4.3000	199.5173	0.7167	288	2078	8936	34634	382975	51.44
4.4736	203.9909	0.7456	294	2194	9817	36573	392792	52.76
4.4739	208.4647	0.7456	300	1913	8560	31888	401351	53.91
4.3088	212.7735	0.7181	306	1950	8402	32501	409754	55.04
4.2864	217.0599	0.7144	312	1766	7570	29434	417324	56.05
4.5242	221.5841	0.7540	318	2137	9668	35617	426992	57.35
3.9564	225.5405	0.6594	324	1681	6652	28023	433644	58.24
4.1509	229.6914	0.6918	330	1644	6826	27407	440470	59.16
4.1762	233.8676	0.6960	336	1456	6079	24261	446549	59.98
4.2403	238.1079	0.7067	342	1503	6371	25043	452921	60.83
4.3764	242.4843	0.7294	348	1423	6225	23709	459146	61.67
4.2626	246.7469	0.7104	354	1388	5918	23138	465064	62.46
4.4469	251.1938	0.7411	360	1340	5959	22332	471022	63.26

Table 13.19 Results of the ^{90}Sr tracer advection experiments using CDP solution

Mass eluted (g)	Cumulative mass eluted (g)	Flow rate (g hr^{-1})	Time (hr)	d min^{-1} g^{-1}	Total d min^{-1}	Bq dm^{-3}	Cumulative d min^{-1}	% recovery
9.7095	503.2505	2.43	226	2	15	26	932	0.27
9.6233	512.8738	2.41	230	2	18	31	950	0.28
9.6903	522.5641	2.42	234	2	16	28	966	0.28
9.8657	532.4297	2.47	238	2	23	39	989	0.29
10.1090	542.5387	2.53	242	2	21	35	1010	0.30
10.2503	552.7890	2.56	246	2	23	37	1033	0.30
9.7780	562.5670	2.44	250	3	28	48	1061	0.31
10.3875	572.9545	2.60	254	2	19	30	1080	0.32
10.3773	583.3318	2.59	258	2	24	39	1104	0.32
10.0882	593.4201	2.52	262	2	22	36	1126	0.33
10.2875	603.7076	2.57	266	3	31	50	1157	0.34
10.5451	614.2527	2.64	270	3	33	52	1190	0.35
10.3575	624.6102	2.59	274	3	34	55	1224	0.36
10.6238	635.2341	2.66	278	4	41	64	1265	0.37
9.9180	645.1521	2.48	282	5	46	77	1311	0.38
10.0581	655.2102	2.51	286	5	48	80	1359	0.40
10.4827	665.6930	2.62	290	4	47	75	1406	0.41
10.3936	676.0865	2.60	294	5	54	87	1460	0.43
10.0060	686.0925	2.50	298	5	47	78	1507	0.44
10.3182	696.4107	2.58	302	4	45	73	1552	0.45
9.8541	706.2647	2.46	306	6	63	107	1615	0.47
9.5743	715.8390	2.39	310	6	60	104	1675	0.49
9.9765	725.8155	2.49	314	7	74	124	1749	0.51
9.8389	735.6544	2.46	318	9	91	154	1840	0.54
9.7475	745.4018	2.44	322	11	103	176	1943	0.57
9.7457	755.1475	2.44	326	11	105	180	2048	0.60
9.4233	764.5708	2.36	330	10	97	172	2145	0.63
10.2808	774.8516	2.57	334	11	113	183	2258	0.66
8.6376	783.4893	2.16	338	13	113	218	2371	0.69
8.5652	792.0545	2.14	342	22	186	362	2557	0.75
8.6287	800.6832	2.16	346	22	193	373	2750	0.80
8.4943	809.1775	2.12	350	24	205	402	2955	0.86
8.5584	817.7359	2.14	354	22	187	364	3142	0.92
16.5689	834.3048	2.07	362	12	195	196	3337	0.98
9.3617	843.6666	2.34	366	31	293	522	3630	1.06
9.4972	853.1638	2.37	370	24	229	402	3859	1.13
9.2083	862.3721	2.30	374	30	279	505	4138	1.21
9.0390	871.4112	2.26	378	30	267	492	4405	1.29
9.4747	880.8859	2.37	382	27	255	449	4660	1.36
9.6847	890.5706	2.42	386	29	279	480	4939	1.44
9.8961	900.4668	2.47	390	29	286	482	5225	1.53
9.9553	910.4220	2.49	394	33	333	557	5558	1.62
9.5261	919.9481	2.38	398	34	322	563	5880	1.72
9.6647	929.6128	2.42	402	36	350	604	6230	1.82
9.4397	939.0524	2.36	406	38	355	627	6585	1.92
9.4330	948.4854	2.36	410	41	384	678	6969	2.04
9.6064	958.0917	2.40	414	46	438	760	7407	2.17
9.8302	967.9219	2.46	418	44	431	731	7838	2.29
9.3934	977.3153	2.35	422	43	408	724	8246	2.41
9.5396	986.8549	2.38	426	52	492	859	8738	2.55
9.0399	995.8947	2.26	430	57	516	951	9254	2.70
9.5766	1005.4713	2.39	434	53	508	884	9762	2.85

9.8472	1015.3185	2.46	438	57	563	953	10325	3.02
9.5553	1024.8738	2.39	442	56	539	940	10864	3.18
9.9575	1034.8313	2.49	446	54	537	899	11401	3.33
9.7217	1044.5530	2.43	450	59	572	981	11973	3.50
9.2181	1053.7711	2.30	454	67	621	1123	12594	3.68
9.6560	1063.4271	2.41	458	62	596	1029	13190	3.86
9.8526	1073.2797	2.46	462	69	682	1154	13872	4.05
10.1563	1083.4360	2.54	466	73	743	1219	14615	4.27
10.0849	1093.5208	2.52	470	81	820	1355	15435	4.51
10.1155	1103.6363	2.53	474	71	714	1176	16149	4.72
9.7040	1113.3404	2.43	478	75	726	1247	16875	4.93
10.1089	1123.4493	2.53	482	88	890	1467	17765	5.19
10.4170	1133.8662	2.60	486	81	843	1349	18608	5.44
10.2884	1144.1546	2.57	490	78	805	1304	19413	5.67
10.0120	1154.1666	2.50	494	71	709	1180	20122	5.88
10.0948	1164.2614	2.52	498	81	816	1347	20938	6.12
6.2146	1170.4760	2.49	500.5	127	792	2124	21730	6.35
3.7350	1174.2110	2.49	502	118	439	1959	22169	6.48
9.6044	1183.8154	2.40	506	113	1082	1878	23251	6.80
9.5738	1193.3891	2.39	510	131	1256	2187	24507	7.16
9.5512	1202.9403	2.39	514	104	990	1728	25497	7.45
9.4860	1212.4263	2.37	518	128	1218	2140	26715	7.81
9.2354	1221.6618	2.31	522	119	1099	1983	27814	8.13
9.5445	1231.2063	2.39	526	113	1080	1886	28894	8.45
9.7024	1240.9087	2.43	530	123	1195	2053	30089	8.80
9.8452	1250.7539	2.46	534	112	1104	1869	31193	9.12
9.4566	1260.2105	2.36	538	107	1011	1782	32204	9.41
9.3362	1269.5467	2.33	542	126	1172	2092	33376	9.76
9.3696	1278.9163	2.34	546	115	1081	1923	34457	10.07
9.6340	1288.5503	2.41	550	124	1190	2059	35647	10.42
9.8679	1298.4182	2.47	554	101	998	1686	36645	10.71
9.7543	1308.1726	2.44	558	107	1046	1787	37691	11.02
10.0860	1318.2585	2.52	562	105	1064	1758	38755	11.33
9.6787	1327.9372	2.42	566	101	976	1681	39731	11.61
9.3443	1337.2815	2.34	570	118	1099	1960	40830	11.93
9.2001	1346.4816	2.30	574	119	1099	1991	41929	12.26
10.1938	1356.6754	2.55	578	117	1189	1944	43118	12.60
10.1139	1366.7894	2.53	582	104	1055	1739	44173	12.91
10.3853	1377.1746	2.60	586	89	923	1481	45096	13.18
10.0769	1387.2515	2.52	590	99	1001	1656	46097	13.47
9.7458	1396.9973	2.44	594	109	1061	1814	47158	13.78
9.8770	1406.8743	2.47	598	105	1033	1743	48191	14.09
11.1150	1417.9893	2.78	602	90	1003	1504	49194	14.38
11.1614	1429.1507	2.79	606	85	950	1419	50144	14.66
10.5675	1439.7182	2.64	610	93	981	1547	51125	14.94
10.5770	1450.2952	2.64	614	91	964	1519	52089	15.23
10.4368	1460.7320	2.61	618	94	983	1570	53072	15.51
10.3164	1471.0484	2.58	622	103	1062	1716	54134	15.82
11.4744	1482.5228	2.87	626	92	1055	1532	55189	16.13
11.3591	1493.8819	2.84	630	92	1049	1539	56238	16.44
10.7882	1504.6701	2.70	634	81	873	1349	57111	16.69
10.6752	1515.3452	2.67	638	91	974	1521	58085	16.98
10.6382	1525.9835	2.66	642	87	929	1455	59014	17.25
5.8000	1531.7835		646	88	511	1468	59525	17.40
11.7068	1543.4903	2.93	650	83	976	1390	60501	17.68

11.3438	1554.8340	2.84	654	91	1036	1522	61537	17.99
10.0139	1564.8479	2.50	658	104	1037	1726	62574	18.29
9.8144	1574.6623	2.45	662	115	1130	1919	63704	18.62
10.0544	1584.7167	2.51	666	108	1081	1792	64785	18.94
10.0936	1594.8103	2.52	670	102	1032	1704	65817	19.24
11.0994	1605.9097	2.77	674	96	1063	1596	66880	19.55
12.6258	1618.5355	3.16	678	78	985	1300	67865	19.84
9.3641	1627.8996	2.34	682	101	948	1687	68813	20.11
10.3731	1638.2727	2.59	686	90	931	1496	69744	20.39
10.1094	1648.3821	2.53	690	90	908	1497	70652	20.65
9.6485	1658.0307	2.41	694	102	986	1703	71638	20.94
9.9193	1667.9500	2.48	698	95	947	1591	72585	21.22
9.6856	1677.6356	2.42	702	97	939	1616	73524	21.49
9.6235	1687.2592	2.41	706	94	905	1567	74429	21.76
10.4504	1697.7095	2.61	710	85	892	1423	75321	22.02
10.9176	1708.6271	2.73	714	81	880	1343	76201	22.27
10.8729	1719.5000	2.72	718	74	808	1239	77009	22.51
10.8216	1730.3216	2.71	722	78	845	1301	77854	22.76
10.6283	1740.9498	2.66	726	76	805	1262	78659	22.99
11.4257	1752.3755	2.86	730	56	642	936	79301	23.18
11.7652	1764.1407	2.94	734	56	662	938	79963	23.37
10.9852	1775.1260	2.75	738	65	715	1085	80678	23.58
10.6633	1785.7893	2.67	742	66	701	1096	81379	23.79
10.5701	1796.3594	2.64	746	68	722	1138	82101	24.00
10.2406	1806.6000	2.56	750	62	636	1035	82737	24.18
10.9406	1817.5407	2.74	754	69	758	1155	83495	24.41
12.3506	1829.8912	3.09	758	60	737	995	84232	24.62
11.6754	1841.5666	2.92	762	53	621	886	84853	24.80
11.9212	1853.4878	2.98	766	55	657	919	85510	25.00
11.6050	1865.0928	2.90	770	54	621	892	86131	25.18
11.3354	1876.4281	2.83	774	51	582	856	86713	25.35
9.3346	1885.7627	2.33	778	60	563	1005	87276	25.51

Table 14.2 Results of the ^{45}Ca tracer advection experiments using NRVB equilibrated water

Time	Sample 1	Minus blank	Counts Removed	C_{max}	C/C_{max}	Sample 2	Minus Blank	Counts Removed	C_{max}	C/C_{max}	Mean C/C_{max}
Days	d min^{-1} cm^{-3}	d min^{-1} cm^{-3}	d min^{-1} cm^{-3}	d min^{-1} cm^{-3}		d min^{-1} cm^{-3}	d min^{-1} cm^{-3}	d min^{-1} cm^{-3}	d min^{-1} cm^{-3}		
0	51	9	9	80373	0.000	49	7	7	80373	0.000	0.000
29	107	65	74	80733	0.001	110	68	75	80733	0.001	0.001
42	219	177	251	81097	0.002	216	174	249	81097	0.002	0.002
58	293	251	502	81463	0.003	265	223	472	81463	0.003	0.003
72	425	383	885	81832	0.005	399	357	829	81832	0.004	0.005
90	483	441	1326	82204	0.005	471	429	1258	82204	0.005	0.005
103	653	611	1937	82579	0.007	605	563	1821	82579	0.007	0.007
119	813	771	2708	82957	0.009	728	686	2507	82957	0.008	0.009
128	846	804	3512	83337	0.010	726	684	3191	83338	0.008	0.009
149	980	938	4450	83721	0.011	867	825	4016	83723	0.010	0.011
163	1258	1216	5666	84108	0.014	1001	959	4975	84110	0.011	0.013
180	1354	1312	6978	84497	0.016	1004	962	5937	84500	0.011	0.013
201	1426	1384	8362	84889	0.016	1117	1075	7012	84894	0.013	0.014
211	1404	1362	9724	85285	0.016	1166	1124	8136	85292	0.013	0.015
240	1709	1667	11391	85685	0.019	1318	1276	9412	85692	0.015	0.017
274	1878	1836	13227	86087	0.021	1399	1357	10769	86096	0.016	0.019
303	2337	2295	15522	86492	0.027	1718	1676	12445	86504	0.019	0.023
363	2994	2952	18474	86899	0.034	2192	2150	14595	86914	0.025	0.029
455	3638	3596	22070	87306	0.041	2561	2519	17114	87325	0.029	0.035

Table 15.2 Results for the diffusion of ^{63}Ni tracer with $NiCl_2$ carrier using CDP solution

	Sample 1	Sample 2	Mean	SD
Days	Bq dm^{-3}	Bq dm^{-3}	Bq dm^{-3}	
0	150	117	133	17
29	1083	1133	1108	25
42	2950	2900	2925	25
58	4183	3717	3950	233
72	6383	5950	6167	217
90	7350	7150	7250	100
103	10183	9383	9783	400
119	12850	11433	12142	708
128	13400	11400	12400	1000
149	15633	13750	14692	942
163	20267	15983	18125	2142
180	21867	16033	18950	2917
201	23067	17917	20492	2575
211	22700	18733	20717	1983
240	27783	21267	24525	3258
274	30600	22617	26608	3992
303	38250	27933	33092	5158
363	49200	35833	42517	6683
455	59933	41983	50958	8975

Table 15.3 Results for the diffusion of ^{63}Ni tracer with $NiCl_2$ carrier using CDP solution expressed as activity concentration

Mass eluted (g)	Cumulative mass eluted (g)	Flow rate (g hr^{-1})	Time (hr)	d min^{-1} g^{-1}	Total d min^{-1}	Bq dm^{-3}	Cumulative d min^{-1}	% recovery
5.8689	5.8689	0.9782	6	28	5	80	28	0.00
6.1449	12.0138	1.0242	6	1331	217	3610	1359	0.11
5.6434	17.6572	0.9406	6	14627	2592	43198	15986	1.33
6.0455	23.7028	1.0076	6	36850	6095	101590	52836	4.41
5.9034	29.6062	0.9839	6	64849	10985	183084	117685	9.82
5.7596	35.3658	0.9599	6	84563	14682	244700	202248	16.87
5.7942	41.1600	0.9657	6	89885	15513	258549	292133	24.37
5.8107	46.9707	0.9685	6	86444	14877	247943	378577	31.58
5.5740	52.5447	0.9290	6	87449	15689	261480	466026	38.88
6.0284	58.5732	1.0047	6	83393	13833	230555	549419	45.83
6.1191	64.6923	1.0198	6	72344	11823	197045	621763	51.87
6.1912	70.8835	1.0319	6	64731	10455	174255	686494	57.27
6.2140	77.0975	1.0357	6	59084	9508	158471	745578	62.20
6.1816	83.2791	1.0303	6	48526	7850	130834	794104	66.25
6.1923	89.4714	1.0320	6	39636	6401	106681	833740	69.55
5.8473	95.3187	0.9746	6	33907	5799	96645	867647	72.38
5.9979	101.3166	0.9996	6	29031	4840	80670	896678	74.80
5.9012	107.2178	0.9835	6	25076	4249	70822	921754	76.89
5.5395	112.7572	0.9232	6	20885	3770	62837	942639	78.64
5.6131	118.3704	0.9355	6	19170	3415	56920	961809	80.24
5.8049	124.1752	0.9675	6	16577	2856	47595	978386	81.62
5.9147	130.0899	0.9858	6	14800	2502	41704	993186	82.85
5.6495	135.7394	0.9416	6	12627	2235	37251	1005813	83.91
5.6497	141.3891	0.9416	6	11462	2029	33813	1017275	84.86
5.4946	146.8837	0.9158	6	10041	1827	30457	1027316	85.70
5.4363	152.3200	0.9061	6	9097	1673	27890	1036413	86.46
5.3870	157.7069	1.3467	4	8226	1527	25450	1044639	87.15
5.1884	162.8953	0.8647	6	7319	1411	23511	1051958	87.76
5.0696	167.9649	0.8449	6	6875	1356	22602	1058833	88.33
4.9735	172.9384	0.8289	6	6227	1252	20867	1065060	88.85
4.9675	177.9059	0.8279	6	5558	1119	18648	1070618	89.31
5.0049	182.9108	0.8342	6	5160	1031	17183	1075778	89.74
5.0523	187.9631	0.8421	6	4720	934	15570	1080498	90.14
5.1308	193.0939	0.8551	6	4312	840	14007	1084810	90.50
5.1807	198.2746	0.8635	6	3884	750	12495	1088694	90.82
5.0343	203.3089	0.8391	6	2754	547	9117	1091448	91.05
6.1676	209.4765	1.0279	6	4050			1095498	91.39
5.7494	215.2259	0.9582	6	3521	612	10207	1099019	91.68
5.7340	220.9599	0.9557	6	3296	575	9580	1102315	91.96
5.7945	226.7544	0.9658	6	3055	527	8787	1105370	92.21
5.7089	232.4633	0.9515	6	2850	499	8320	1108220	92.45
5.6113	238.0746	0.9352	6	2613	466	7761	1110833	92.67
5.8555	243.9301	0.9759	6	2517	430	7164	1113350	92.88
5.5983	249.5284	0.9331	6	2418	432	7199	1115768	93.08
5.3823	254.9107	0.8971	6	2310	429	7153	1118078	93.27
5.4668	260.3775	0.9111	6	2213	405	6747	1120291	93.46
5.2671	265.6446	0.8779	6	2097	398	6636	1122388	93.63
5.5503	271.1949	0.9251	6	2015	363	6051	1124403	93.80

Table 15.4 Results of the ^{63}Ni tracer advection experiments using NRVB CDP solution

APPENDIX 2

Detailed Information for Mass Balances and Discretisation

A. Mass Balance and K_d Calculation Checks

The model should automatically conserve mass and account for the reduction in liquid and tracer mass removed due to sampling.

A manual check (mass balance) that the correct curves were being generated for a given NRVB mass, K_d, tracer mass and receiving water mass was undertaken to validate the model.

The data used were from the ^{137}Cs NRVB tracer only experiment. The best fit K_d value was 2.3 $m^3 kg^{-1}$ (see graph below).

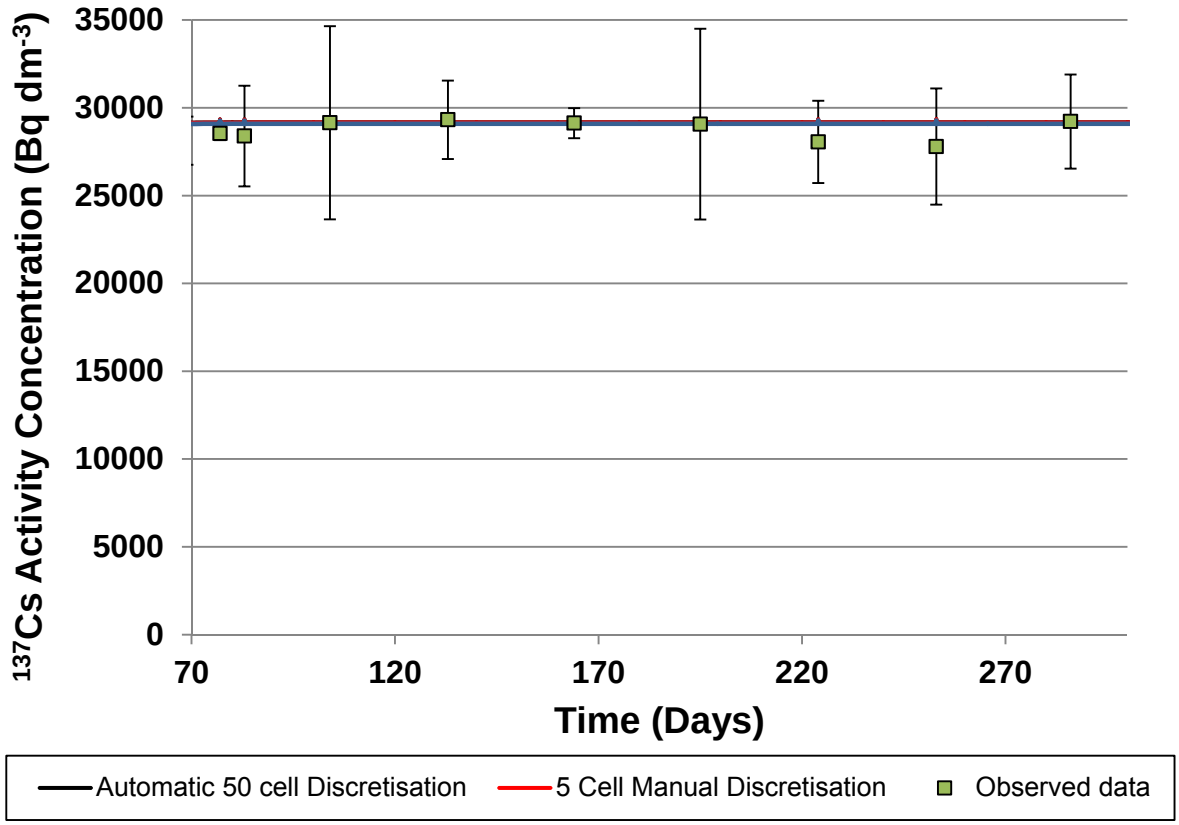

Later data from the ^{137}Cs NRVB tracer only experiment

Do the relevant masses and volumes at the times of the observations produce a K_d of 2.3 $m^3 kg^{-1}$?

Taking point at time T_{104} the information needed is:

Mass of NRVB = (volume of cylinder – volume of central hole).dry bulk density ((43.π.400)-(30.π.25)).1.095 = 56.6 g.

Height of both cylinders was 43 mm, the value originally used in the modelling; bulk dry density is the literature value.

Volume of receiving water and water in porosity at T_{104} = Initial vol. – sample vol.
225 - 34 = 191 cm^3

T_{104} is sample number 34 therefore 34 cm^3 have been removed during sampling, starting mass was 225 cm^3.

^{137}Cs tracer remaining at T_{104} = Initial inventory - tracer removed during sampling
9979 – 585 = 9394 Bq
Information calculated from section 11.2 and table 11.2 respectively, average values from the two experiments have been used.

Then to determine K_d using:

$$K_d = \frac{V_w(C_0 - C_{104})}{M_{nrvb}\, C_{104}}$$

C_0 = 9394 (1000/191) = 49183 Bq dm^3
C_{104} = 29150 Bq dm^3 (taken from table 11.3)
Substituting into the equation gives:

$$K_d = \frac{191(49183 - 29150)}{56.6 \cdot 29150}$$

$$K_d = 2.32 \text{ m}^3 \text{ kg}^{-1}$$

The point is on the model line and 2.3 is the expected result.

Using the same procedure at T_{253} the result is:

$$K_d = \frac{186(49737 - 29092)}{56.6 \cdot 29092}$$

$$K_d = 2.33 \text{ m}^3 \text{ kg}^{-1}$$

The observed data point at the same time is given by:

$$K_d = \frac{186(49737 - 27792)}{56.6 \cdot 27792}$$

$$K_d = 2.59 \text{ m}^3 \text{ kg}^{-1}$$

The observed point is below the model line so a K_d higher than 2.3 is expected.

The checks confirm that the model calculates K_d correctly and is compensating for the removal of water and tracer due to sampling. It also means that the initial modelling stage of fixing K_d from the later, flat part of the graph is appropriate.

B. Details of Changing the Degree of Discretisation

GoldSim has a mesh generator capable of automatically increasing the number of elements (in this case mixing cells).

The original 5 cell model was set up manually so a parallel 5 cell model was created using the mesh generator as a cross check. Both models produced identical outputs.

A 50 cell model was produced using the mesh generator. The effective diffusivity and partition coefficient previously used to fit the CDP ^{137}Cs tracer only experiment (2.8×10^{-10} m^2 s^{-1} and 0.7 m^3 kg^{-1}) were inputted to produce the model curve. The outputs for the 5 and 50 cell model together with the (5 cell) curves for 2.5 and 3.0×10^{-10} m^2 s^{-1} and the relevant experimental data points are shown below.

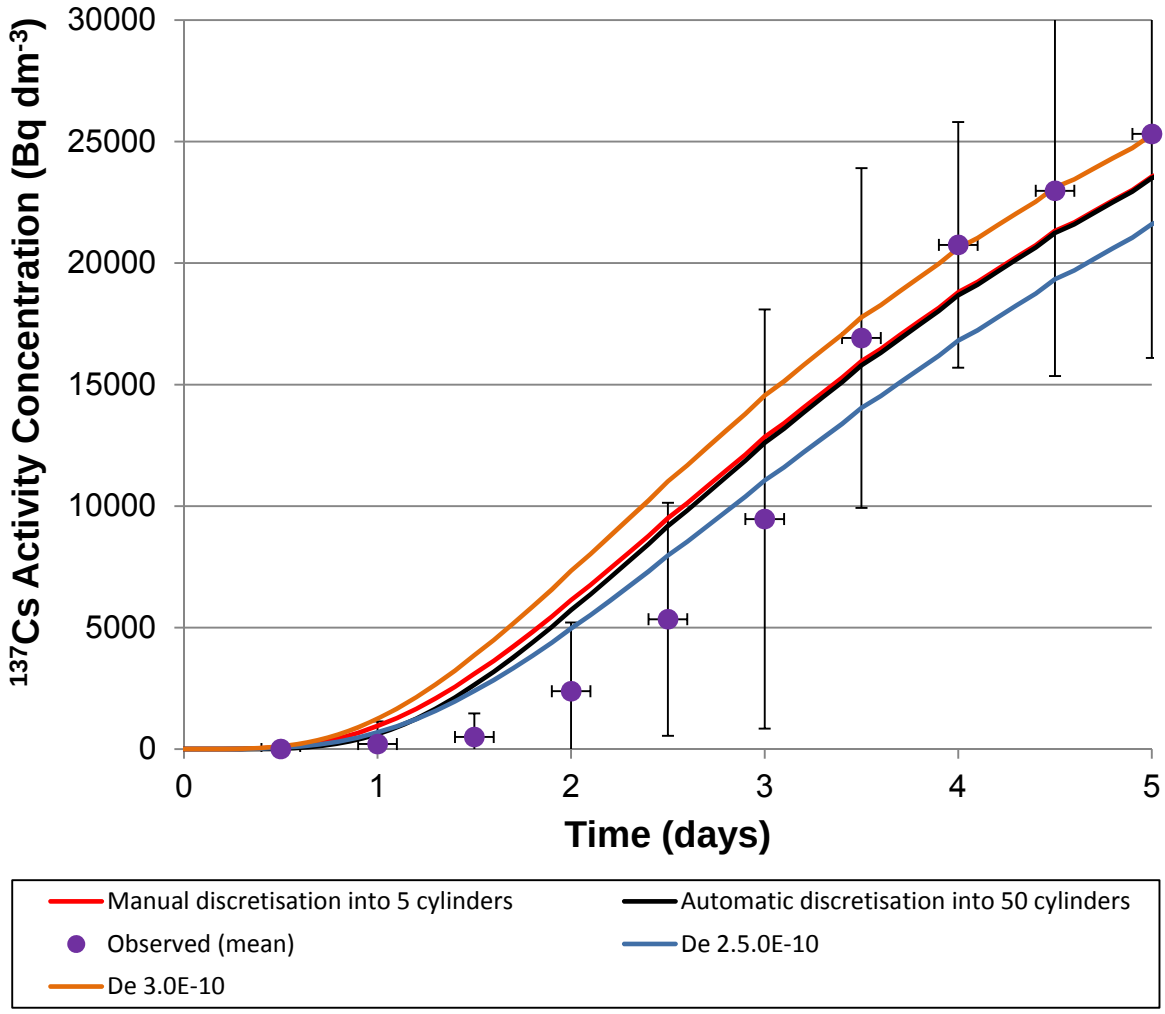

Comparison of 5 and 50 cell discretisations at D_e 2.8x10^{-10} m^2 s^{-1} and K_d 0.7 dm^3 kg^{-1} with observed CDP ^{137}Cs tracer only data over first 5 days, with model curves for D_e 2.5x10^{-10} and 3.0x10^{-10} m^2 s^{-1}

The 20 day plot below is provided to show more of the data in relation to the modelled curves

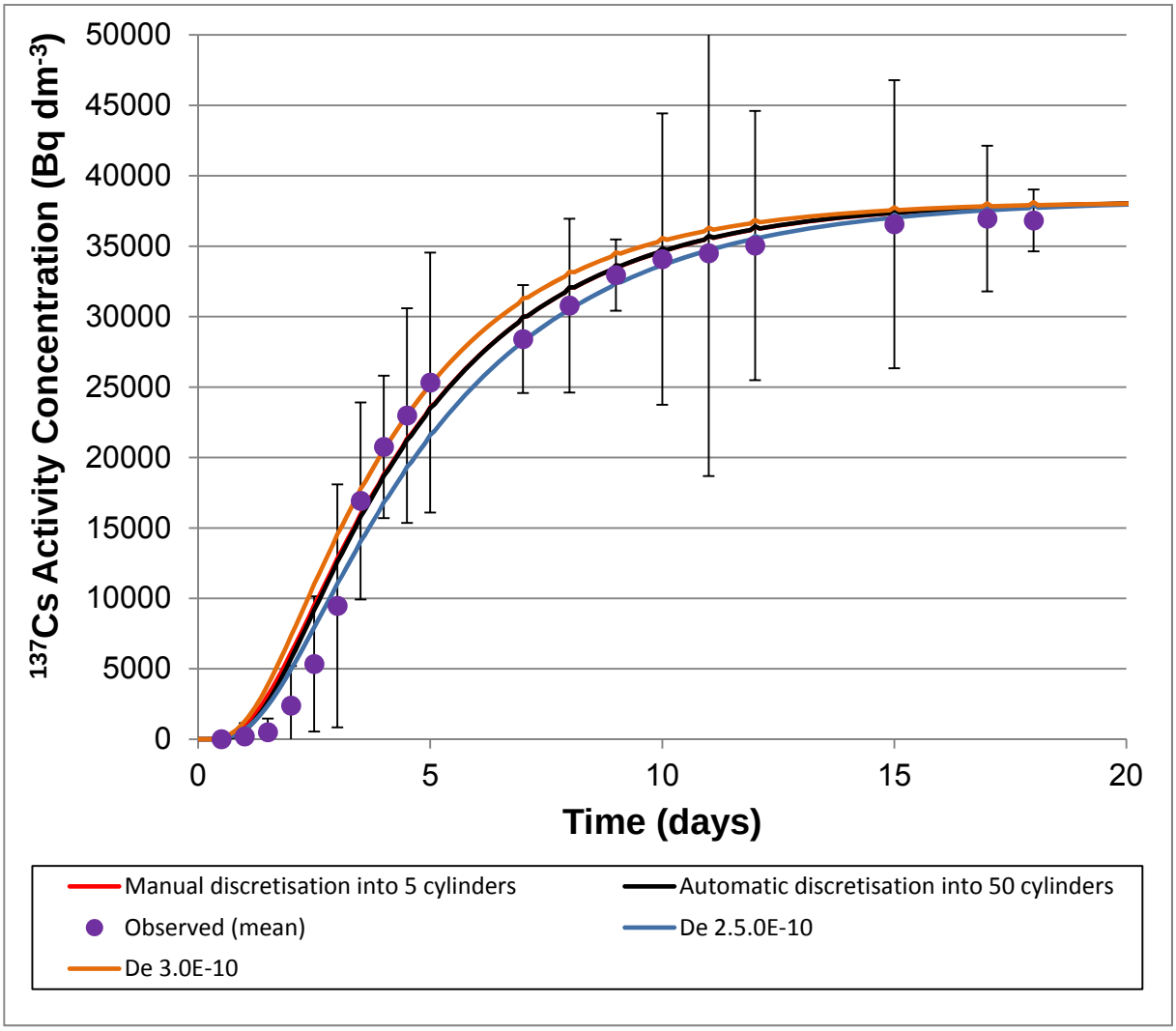

Comparison of 5 and 50 cell discretisations at D_e 2.8x10^{-10} m^2 s^{-1} and K_d 0.7 m^3 kg^{-1} with CDP ^{137}Cs tracer only data observed data over first 20 days, with model curves for D_e 2.5x10^{-10} and 3.0x10^{-10} m^2 s^{-1}

The curves from the 5 and 50 cell model are very similar. The difference between the two curves persists over the initial 4-5 days after which no further differences are observed.

The best fit for the entire dataset remains 2.8×10^{-10} $m^2 s^{-1}$ for diffusivity and 0.7 $dm^3 kg^{-1}$ for K_d

The LOF values for the first 5 days are 17.8% for the 5 cell model 16.7% for the 50 cell model.

The LOF values for the entire data set are 6.0% for the 5 cell model and 6.2% for the 50 cell model.

The 50 cell model is a slightly poorer fit to the early data but indistinguishable over the entire data set.

The uncertainty in the observed values far outweighs any difference between the two degrees of discretisation.

Due to the difference between the different degrees of discretisation being small the procedure was repeated with the data from the ^{137}Cs NRVB tracer only experiments. The input values were 2.0x10^{-10} m^{2}s^{-1} for D_e and 2.3 dm^3 kg^{-1} for K_d.

The results are shown below.

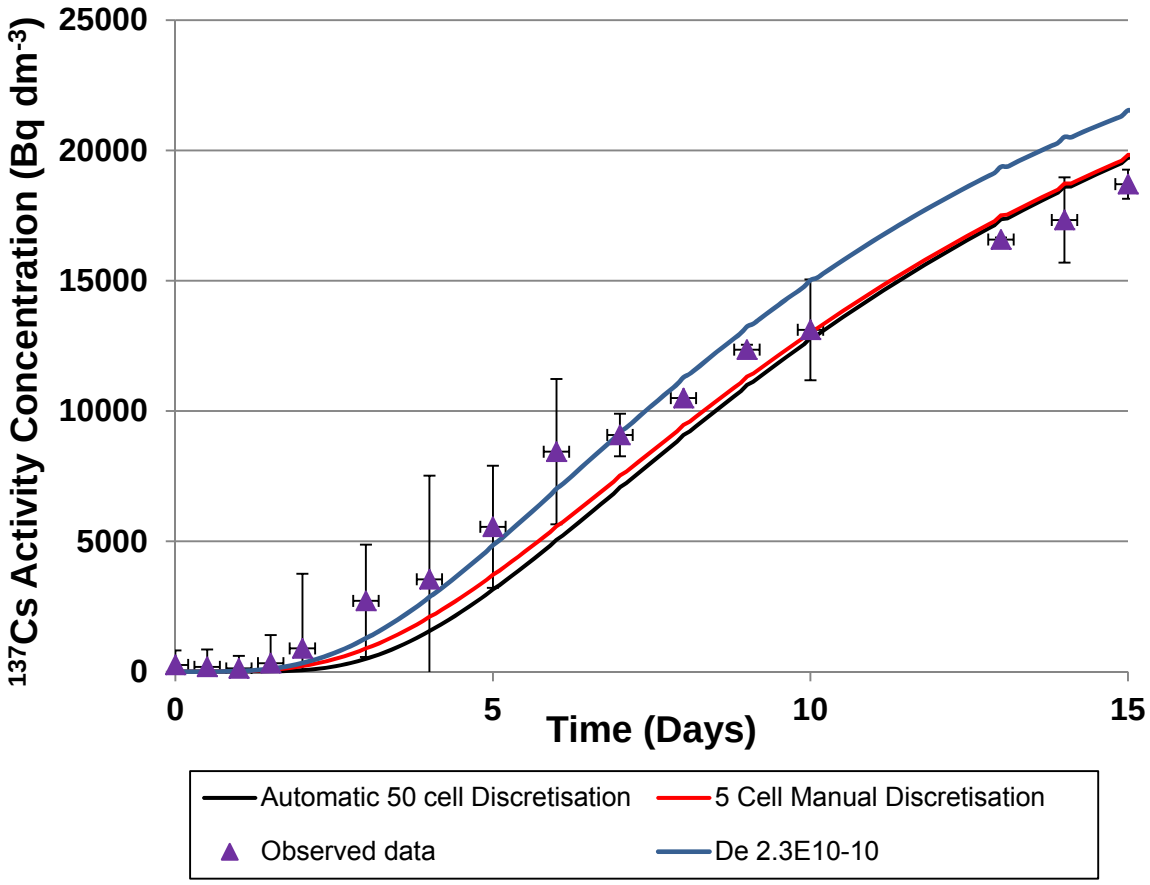

Comparison of 5 and 50 cell discretisations at D_e 2.0x10^{-10} m^2 s^{-1} and K_d 2.3 dm^3 kg^{-1} with observed data^{137}Cs tracer only data over first 15 days, with model curve for D_e 2.3x10^{-10} m^2 s^{-1}

The 30 day plot below is provided to show more of the data in relation to the modelled curves.

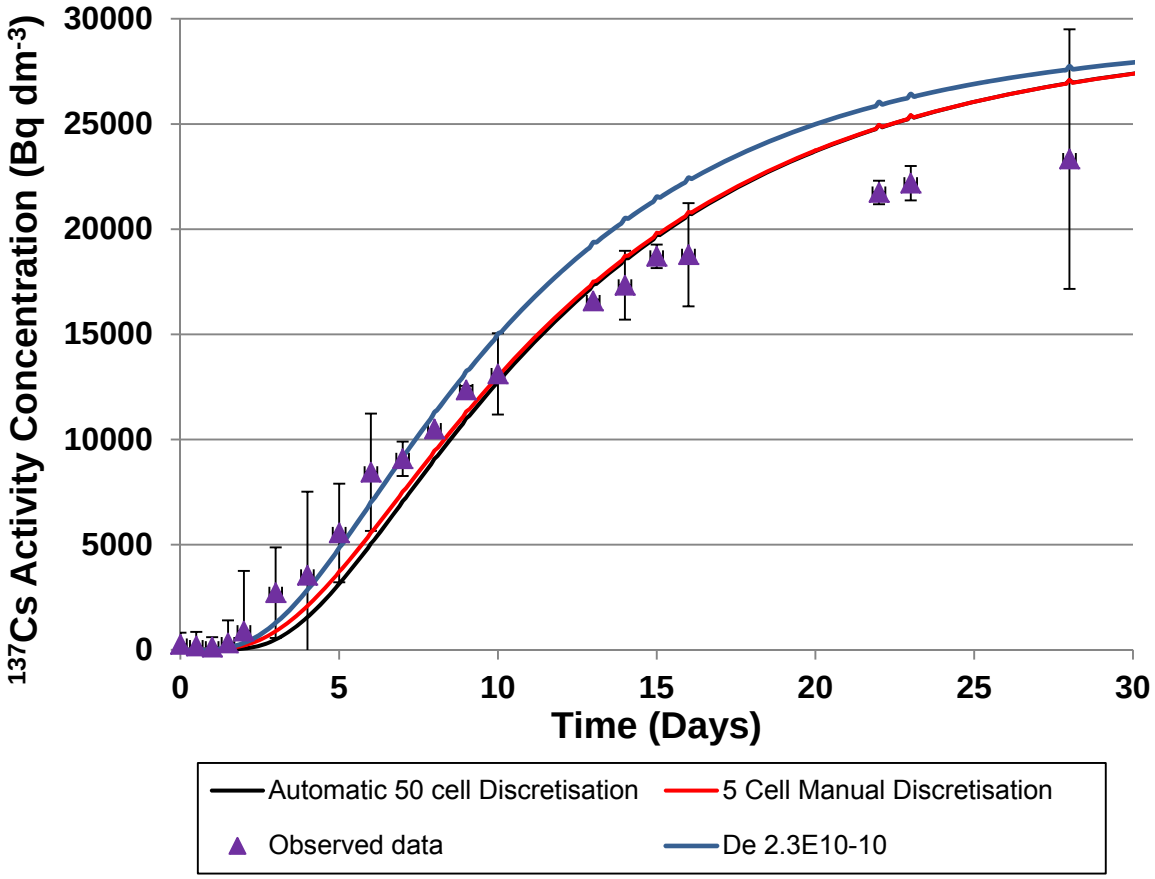

Comparison of 5 and 50 cell discretisations at D_e 2.0x10^{-10} m^2 s^{-1} and K_d 2.3 dm^3 kg^{-1} with observed ^{137}Cs tracer only data over first 30 days, with model curve for D_e 2.3x10^{-10} m^2 s^{-1}

The curves from the 5 and 50 cell model are again very similar but the difference between the two curves persists over the initial ~15 days.

The best fit for the entire dataset remains 2.0x10^{-10} m^{2}s^{-1} for diffusivity and 2.3 dm^3 kg^{-1} for K_d

The LOF values for the first 15 days are 14.2% for the 5 cell model and 16.8% for the 50 cell model.

The LOF values for the entire data set are 8.5% for the 5 cell model and 8.7% for the 50 cell model.

Again the 50 cell model is a slightly poorer fit to the early data but indistinguishable over the entire data set.

The next nearest fit was the model curve for diffusivity 2.3x10^{-10} m^2 s^{-1} which had LOF values of 15.0% over the first 15 days and 9.6% over the entire dataset. The inclusion of the curve on the plots above illustrates the difficulty of fitting diffusivity to

the early data once the K_d has been fixed and is the reason why data envelopes were used in the thesis.

The uncertainty in the observed values far outweighs any variation between the two degrees of discretisation and the 5 cell model is satisfactory.

The error bars are: vertical 90% confidence limits for the mean used (see response to 5. below for more details) and horizontal +/- 0.2 days.